0008-7114

Caryologia

International Journal of Cytology, Cytosystematics and Cytogenetics

2019
Vol. 72 - n. 4

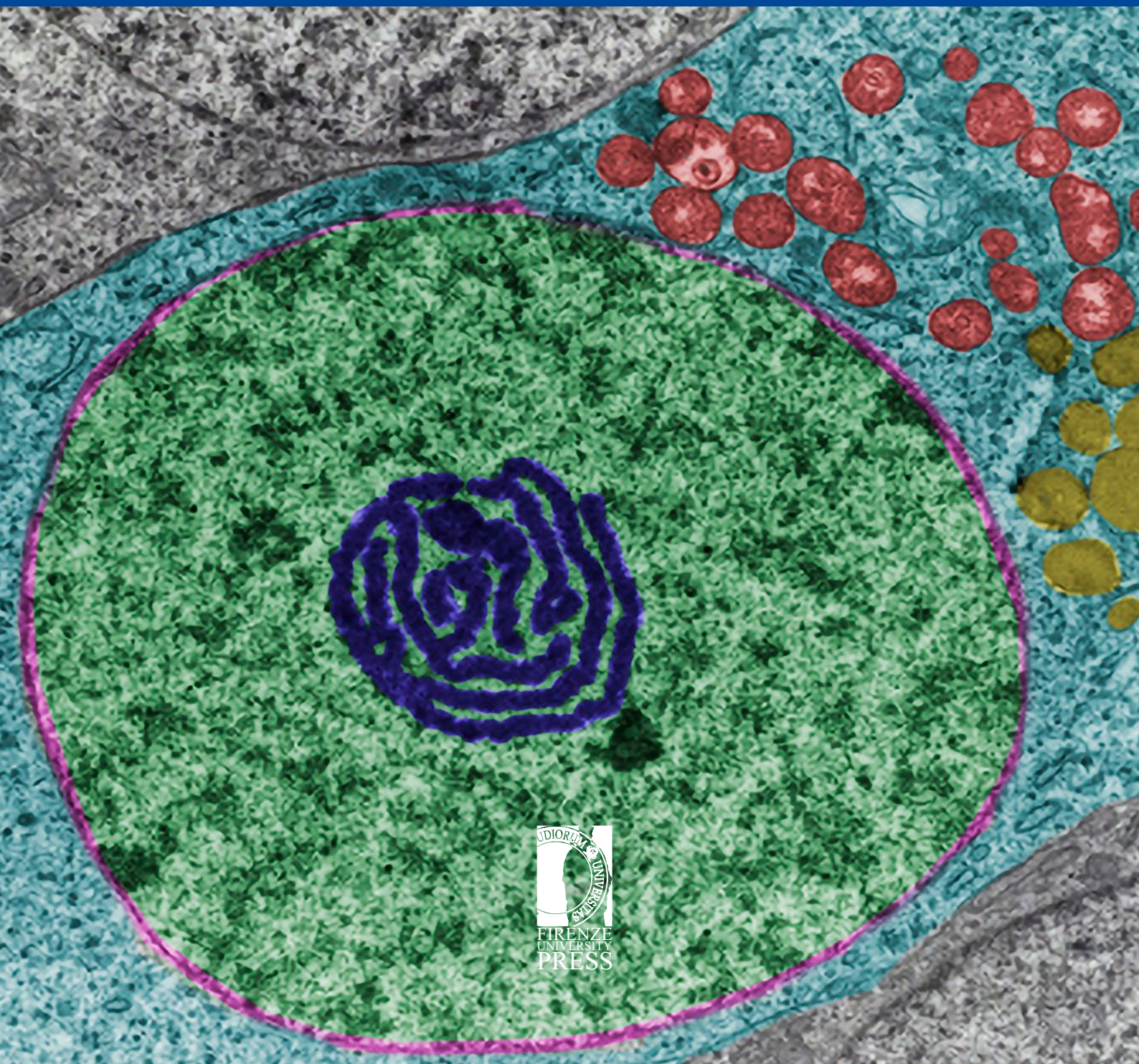

FIRENZE UNIVERSITY PRESS

Caryologia. International Journal of Cytology, Cytosystematics and Cytogenetics

Caryologia is devoted to the publication of original papers, and occasionally of reviews, about plant, animal and human karyological, cytological, cytogenetic, embryological and ultrastructural studies. Articles about the structure, the organization and the biological events relating to DNA and chromatin organization in eukaryotic cells are considered. *Caryologia* has a strong tradition in plant and animal cytosystematics and in cytotoxicology. Bioinformatics articles may be considered, but only if they have an emphasis on the relationship between the nucleus and cytoplasm and/or the structural organization of the eukaryotic cell.

Caryologia

International Journal of Cytology, Cytosystematics and Cytogenetics

Volume 72, Issue 4 - 2019

Firenze University Press

***Caryologia*. International Journal of Cytology, Cytosystematics and Cytogenetics**

Published by
Firenze University Press – University of Florence, Italy
Via Cittadella, 7 - 50144 Florence - Italy
http://www.fupress.com/caryologia

Caryologia
International Journal of Cytology, Cytosystematics and Cytogenetics

Firenze University Press
www.fupress.com/caryologia

OPEN ACCESS

Citation: A. Çetinbaş-Genç, F. Yanık, F. Vardar (2019) Histochemical and Biochemical Alterations in the Stigma of *Hibiscus syriacus* (Malvaceae) During Flower Development. *Caryologia* 72(4): 3-13. doi: 10.13128/cayologia-196

Published: December 23, 2019

Data Availability Statement: All relevant data are within the paper and its Supporting Information files.

Competing Interests: The Author(s) declare(s) no conflict of interest.

Histochemical and Biochemical Alterations in the Stigma of *Hibiscus syriacus* (Malvaceae) During Flower Development

Aslihan Çetinbaş-Genç*, Fatma Yanik, Filiz Vardar

Department of Biology, Marmara University, Istanbul, Turkey
*Corresponding author: aslihan.cetinbas@marmara.edu.tr

Abstract. The aim of this study is to determine the histochemical and biochemical changes that occurred during flower development in the stigmas of *Hibiscus syriacus*. The flower development of *H. syriacus* was divided into three successive stages; pre-anthesis, anthesis, post-anthesis, and stigma development was examined in parallel with these stages. At pre-anthesis, the stigmatic papillae cells covering the surface of the stigma were ovoid and their dense cytoplasm were rich in insoluble polysaccharide, protein and lipid. At anthesis, papillae cells grew and the pellicle layer becomes clear indicating dry-typed stigma. Meanwhile some sub-papillae cells, which accumulate dense organic matter from the beginning of development, began the process of autolysis and release their cellular content into the intercellular space. Whereas the organic matter content of papillae decreased at post-anthesis, it was still more than pre-anthesis stage. Similarly, peroxidase and non-specific esterase activity were very intensive at anthesis stage and activities were still remarkable at post-anthesis stage. The maximum CAT, SOD activity, H_2O_2 and MDA content were also determined at anthesis. Our results revealed that stigma of *H. syriacus* is receptive at anthesis and still conserve its receptivity at post anthesis assisting pollen germination and pollen tube growth.

Keywords. Anthesis, antioxidant enzyme, lipid peroxidation, papillae, stigma.

INTRODUCTION

Malvaceae family comprises 244 genera and more than 4225 species (Paoletti et al. 2009). Genus *Hibiscus* of Malvaceae has attracted considerable attention due to its large and attractive flowers. *Hibiscus syriacus* is the most popular species of this genus and has hermaphrodite flowers with white, pink, red, lavender, or purple color, depending on their cultivar (Punasiya and Pillai 2015). It consists of a tubular group of stamens surrounding the style which ends with the five branched stigma (Klips and Snow 1997; Çetinbaş-Genç and Ünal 2017).

Hibiscus syriacus has also a great social and economic importance whose flowers and seeds are frequently used in industry. It is mainly used in pharmaceutical products for the treatment of cardiovascular, urinary tract, skin,

and reproductive system diseases. Besides, it is often used in the production of hair-skin care products, perfumes, and used as a natural colorant in the beverage industry, and a source of fiber in the paper industry (Hsu et al. 2015).

To gain knowledge about the plant reproductive biology concerning pollination and fertilization helps to improve reproductive success which has direct effect on yield quality and economic benefits. Pollination involves a complex set of cell-cell communications that enable pollen-pistil interaction. This molecular interaction between the pollen wall and components of the stigmatic surface determines whether fertilization will take place (McInnis et al. 2006). Besides, stigma receptivity is one of the essential events for the start of pollen-pistil interaction. In many angiosperms, the stigma is receptive during anthesis but in some cases, the stigma may be still receptive after or even before anthesis (Brito et al. 2015). Therefore, the developmental characteristics of stigma are the focal point for pollination biology studies.

Despite their morphological diversity, the stigma of angiosperms is divided into two main groups: wet and dry typed. Although wet stigmas produce large surface secretions, dry stigmas are lack of secretions and its cuticle is coated with a proteinaceous surface layer. Despite these fundamental differences between wet and dry stigmas, high level of enzymatic activities indicates that stigmatic enzymes are essential for stigma function in both stigmatic types (Souza et al. 2016). Stigma includes heterogeneous components such as proteins, lipids, carbohydrates, amino acids and phenolic acids playing an important role in the pollen germination and tube growth on the stigma surface. These compounds present as a content of the exudate in wet stigmas, but in dry type stigmas they take place as a dry extracellular layer on the cuticle (Edlund et al. 2004).

The receptive surface of stigma is also characterized by the expression of biomolecules such as the peroxidases, esterases and reactive oxygen species (McInnis et al. 2006). It has been revealed that stigma shows high peroxidase and esterase activity in many plants when it gains receptivity for pollination (Hiscock et al. 2002). Besides, peroxidases and non-specific esterases are functional on the pollen-stigma interaction to loosen cell wall components of stigma cells with the aim of allowing pollen tubes to penetrate, and grow into the stigma (Hiscock et al. 2002; McInnis et al. 2006). Peroxidases generally catalyze the reduction of a wide range of organic substrates using hydrogen peroxide (H_2O_2) (McInnis et al. 2006). Stigmatic peroxidases and indirectly H_2O_2 metabolism form the components of signaling systems that mediate the identification of the proper pollens during pollen-stigma interaction (Cheong et al. 2002; Delannoy et al. 2003; Do et al. 2003).

In many cellular processes including development and tolerance to environmental stress, reactive oxygen species (ROS) also play a role as secondary messengers at low concentrations (Yanık et al. 2018). However, high concentrations of ROS cause harmful chain effects in the cell. Detoxification of ROS is carried out with antioxidant enzymes and non-enzymatic antioxidant systems. Superoxide dismutase, catalase, and peroxidase are some of the important antioxidant enzymes involved in the detoxification of ROS (Yanık et al. 2018). ROS have a role in signaling networks promoting pollen germination and pollen tube growth on stigma (McInnis et al. 2006; Hiscock and Allen 2008; Zafra et al. 2010). The concentration of ROS on the stigma affects the stigma receptivity, pollen germination and as a result the success of pollination. Therefore, in order to understand the pollination biology in detail, it is very important to examine the balance between production and detoxification of ROS during the development of the stigma.

The aim of the current study is to evaluate the histochemical and biochemical alterations of stigma in *H. syriacus* during the defined flowering stages; pre-anthesis (the period before anthesis), anthesis (the period in which flower is fully open and functional), and post-anthesis (the period after anthesis). Knowledge on stigmatic development will improve our information about the pollination success in plants as well as in *Hibiscus* varieties which have agronomic and ornamental potential.

MATERIAL AND METHODS

Flowers of *Hibiscus syriacus* L. were collected in June-August (2016-2018) in the vicinity of Göztepe-İstanbul (Turkey). Pistils at the different developmental stages were determined by stereomicroscope EZ4HD (Leica, Germany) and photographed by LAS EZ software.

Pistils were removed from flowers and fixed overnight in 3% (w/v) paraformaldehyde in 0.05 M sodium cacodylate buffer (pH 7.4) at 4 °C. After dehydration process with ethanol series and embedded in Epoxy resin using propylene oxide. Semi-thin sections (1-2 μm) were stained with Periodic Acid-Schiff (PAS) (Feder and O'Brien 1968) for insoluble polysaccharides, with Coomassie Brilliant Blue (CBB) (Fisher et al. 1968) for proteins and, with Sudan Black B (SBB) for lipids (Pearse 1961).

The optical density of organic content in papillae and sub-papillary cells was measured at different developmental stages according to Rodrigo et al. (1997).

Images were converted to 8-bit gray-scale and the optical density was quantized from black-and-white images using the Image J software. The mean and standard deviation of 5 images captured over an area of 300 μm² for papillae and 100 μm² for sub-papillary cells were computed.

For determination of qualitative peroxidase activity, fresh stigmatic tissue was incubated in sodium-phosphate buffer (PBS- 0.1 M, pH 5.8) containing 15 mM guaiacol and 5 mM H_2O_2 for 60 min (Birecka et al. 1973). To establish qualitative non-specific esterase activity, fresh stigmatic tissue was incubated in incubation buffer containing 1 mM α–naphthol acetate, 0.06 M Na_2PO_4, 0.01 M $NaNO_2$ and 2 M pararosaniline chloride for 10 min at 37 °C (Gomori 1950). After washing with dH_2O for 5 min, the stigmatic tissue squashed gently. All of the preparations were photographed with the KAMERAM software, assisted by a KAMERAM digital camera and an Olympus BX-51 microscope.

To evaluate the superoxide dismutase (SOD) and catalase (CAT) activity, 100 mg fresh stigmatic tissue were homogenized with 1 mL of cold PBS (50 mM, pH 7.0). After centrifugation at 14 000 rpm for 20 min at +4 °C, the supernatant was used as enzyme source. For CAT activity, 25 μL of the supernatant and 1 mL reaction mixture (20 mM PBS, pH 7.0 and 6 mM H_2O_2) were mixed and measured by the decrease in absorbance for 2 min at 240 nm, spectrophotometrically (Cho et al. 2000). For SOD activity, 2 μL of the supernatant and 2 mL reaction mixture (100 mM pH 7.0 PBS, 2 M Na_2CO_3, 0.5 M EDTA, 300 mM L-methionine, 7.5 mM nitro blue tetrazolium, 0.2 mM riboflavin) were mixed. After incubation under 15 W fluorescent lamps for 10 min, the mixture was measured at 560 nm, spectrophotometrically (Cakmak and Marschner 1992).

To measure the amount of hydrogen peroxide (H_2O_2) 300 mg fresh stigmatic tissue were homogenized with 2 mL extraction buffer (0.1% TCA, 1 M KI, 10 mM PBS) and centrifuged at 12 000 g for 15 min at 4 °C. After incubation in dark for 20 min, the supernatants were measured at 390 nm, spectrophotometrically (Junglee et al. 2014).

Lipid peroxidation (LPO) was determined by the production of malondialdehyde (MDA) level. 200 mg fresh stigmatic tissue were homogenized with 1 mL 0.1% TCA and centrifuged at 12 000 g for 20 min at +4 °C. 250 μL supernatant and 1 mL reaction mixture (0.6% TBA in 20% TCA) were mixed and incubated for 30 min at 95 °C. After cooling on ice, the mixture was centrifuged at 12 000 g for 10 min and the supernatant was measured at 532 and 600 nm, spectrophotometrically (Cakmak and Horst 1991).

All measurements and quantifications were repeated at least 3 times. Statistical analysis was performed using one-way analysis of variance (ANOVA), (SPSS 16.0 software). The significance of the applications was designated at the $P < 0.05$ level using the Tukey's test. All data presented are means ± SD.

RESULTS

In the current study, the stigma of *Hibiscus syriacus* analyzed in three successive stages (pre-anthesis, anthesis, and post-anthesis) correlated with some morphological markers such as color, the position of calyx and corolla, anther dehiscence, and the absence or presence of pollen on it.

In the stage of pre-anthesis, the flower buds of *H. syriacus* were ovoid with calyx covering half of the bud. Five stigmatic branches were very close to each other. There were no pollen grains on the stigma, because the anthers were still indehiscent (Figure 1 a,d,g). At anthesis stage, the flower was fully opened and their petals elongated. Stigma presented five distinctly separated branches with yellowish color. A lot of pollen grains were visible on the stigma due to anther dehiscence (Figure 1 b,e,h). At post-anthesis stage, the color of the petals began to fade and turned to brown, however a lot of pollen grains were still deposited on the stigma surface (Figure 1 c,f,i).

Hibiscus syriacus has capitate type stigma with five branches. The receptive surface of the stigma was covered with the tissue of unicellular papillae that are short, ovoid shaped, thin walled and tightly packed cells (Figure 2 a,f,k). Papillae cells lost their tight alignment with the increase of their width and length and their tips began to tape at anthesis. In the course of post-anthesis, papillae cells were much extended and thorn-shaped cells. At all stages of development, the dense cytoplasm of papillae cells was rich in insoluble polysaccharide, protein and lipids (Figure 2, Figure 3). The pellicle layer which was not very distinct at pre-anthesis became evident at anthesis (Figure 2 f). The papillae surfaces were covered with continuous pellicle and showed intense CBB staining indicating the dry-type stigma (Figure 2 g). The content of organic material in the papillae cells reached at maximum during anthesis (Figure 2 b,g,l). According to the optical density results, the insoluble polysaccharide content of papillae increased by 43 % (Figure 3 a), the protein content increased by 40 % (Figure 3 b), and lipid content increased by 77 % (Figure 3 c) at anthesis when compared to pre-anthesis. Besides, some of the sub-papillary cells accumulated a large

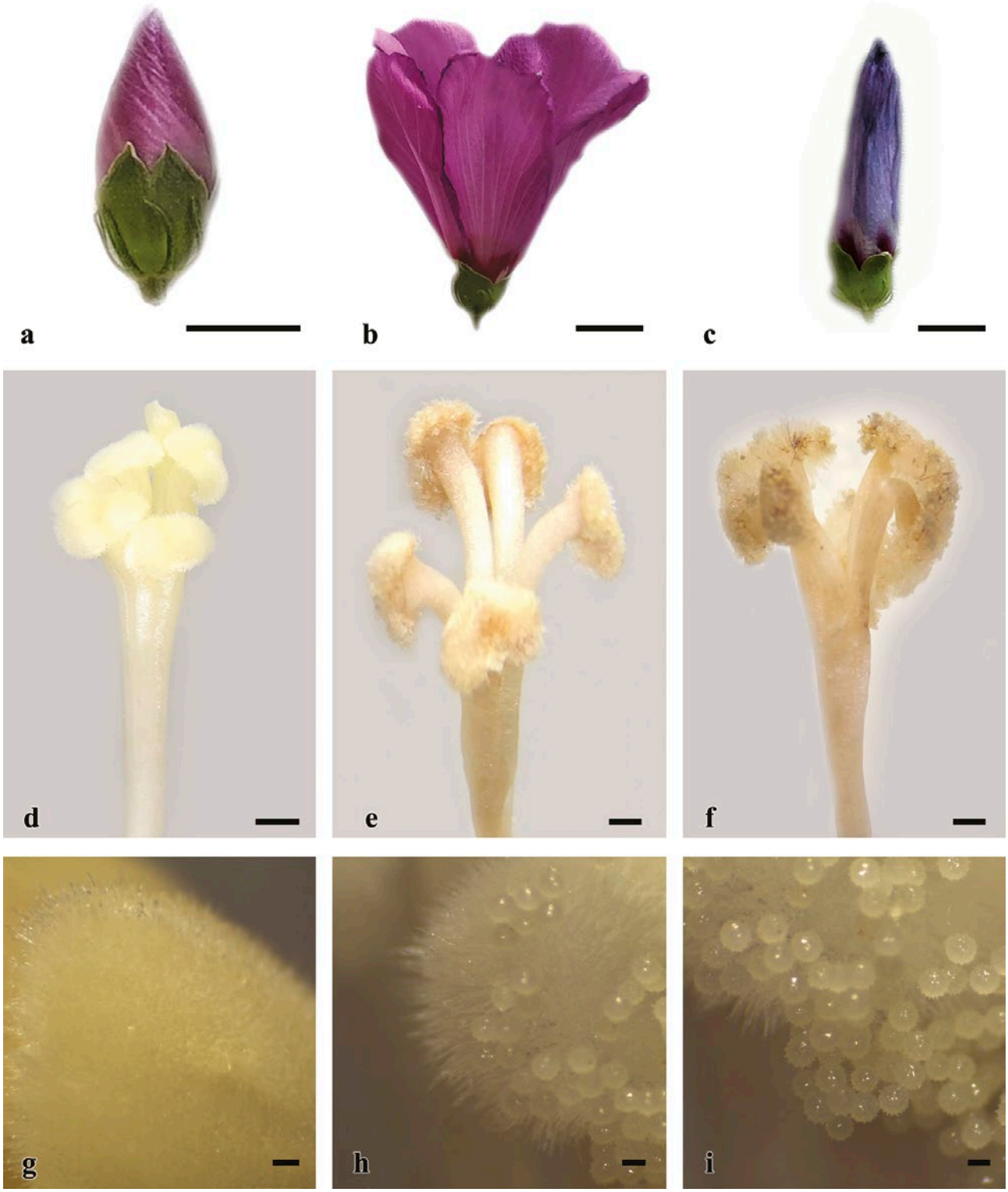

Figure 1. Determination of development stages of flower and stigma in *Hibiscus syriacus*. Flower morphology at pre-anthesis (a), anthesis (b), post-anthesis (c). Stigma morphology at pre-anthesis (d), anthesis (e), post-anthesis (f). Stigmatic surface at pre-anthesis (g), anthesis (h), post-anthesis (i). Scale: 1 cm in a-c, 1 mm in d-f and 100 μm in g-i.

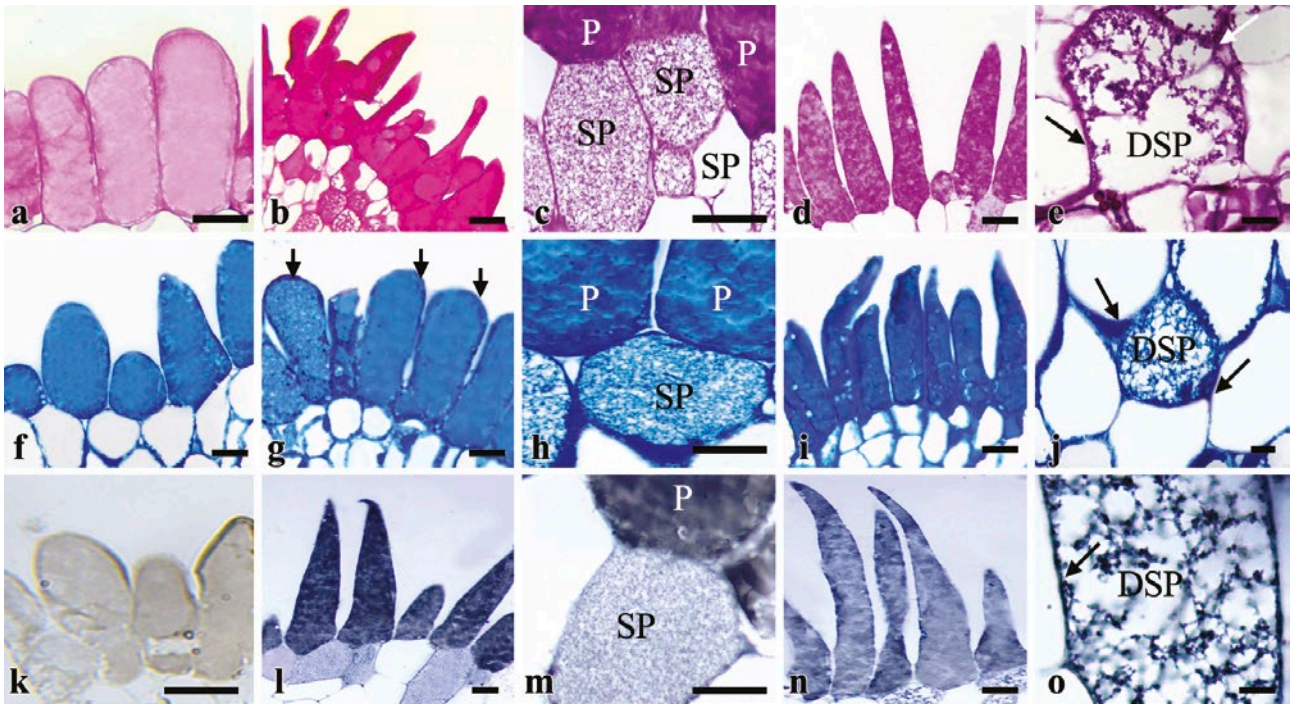

Figure 2. Semi-thin longitudinal sections of stigma of *Hibiscus syriacus* stained by PAS (a-e), CBB (f-j) and SBB (k-l). Short and ovoid papillae cells at anthesis (a, f, k). Papillae cells with dense organic material content and prominent pellicle layer (arrows) at anthesis (b, g, l). Sub-papillary cells that accumulate a large amount of organic material (c, h, m). Thorn shaped papillae with dense cytoplasm at post-anthesis (d, i, n). Degenerated subpapillary cells and their diffused contents to intercellular space (arrows) (e, j, o). P: Papillae cell, SP: Sub-papillary cell, DSP: Degenerated sub-papillary cell. Scale: 20 μm.

amount of organic matter during the transition from the pre-anthesis to anthesis. When sub-papillary cells started to degenerate at anthesis, their rich organic contents spread into the intercellular space indicating positive reaction with the PAS, CBB, and SBB staining (Figure 2 c,h,m)). At-post anthesis, the content of organic material papillae reduced in compare to anthesis (Figure 2 d,i,n)). The insoluble polysaccharide content of papillae was decreased by 10 % (Figure 3 a), the protein content was decreased by 18 % (Figure 3 b) and lipid content was decreased by 27 % (Figure 3 c) at post-anthesis with regard to anthesis. At this stage the pellicle got thinner (Figure 2 i). After the degeneration of sub-papillary cells, the accumulation of organic material at the intercellular space became more intense (Figure 2 e,j,o).

To measure the amount of starch granules in sub-papillary cells, the optical density of starch granules was measured after PAS staining. Although papillae cells had very few starch granules at all developmental stages, sub-papillary cells contained a large amount of dense starch granules representing a peak at anthesis (Figure 4 a-c). The starch content was increased by 109 % at anthesis (Figure 4 d) with regard to pre-anthesis. Despite the starch granule content decreased by 25 % at post-anthesis, it was still 55 % more than the pre-anthesis stage (Figure 4 c,d).

Based on our squash preparation results, non-specific esterase and peroxidase activity were not observed in stigmatic papillae cells at pre-anthesis (Figure 5 a,d). However, both enzyme activities gave progressive positive reaction at anthesis (Figure 5 b,e)). These positive activities indicated the stigma gains receptivity at this. Although the reduction of stigma receptivity at post-anthesis detected by poor reaction, it was still receptive in contrast to pre-anthesis (Figure 5 c,f)).

According to antioxidant enzyme activity results, the maximum CAT activity was determined at anthesis by 53 % while the minimum was observed at post-anthesis by 20 % in compare to pre-anthesis (Figure 5 g). Besides, the highest H_2O_2 production was observed at anthesis by 118 %, and lowest was observed at post anthesis by 6 % (Figure 5 h). Moreover, the SOD activity increased by 118 % at anthesis and 68 % at post-anthesis in compare to pre-anthesis (Figure 5 i). MDA one of the last products of lipid peroxidation was very high at anthesis and post-anthesis showing increase by 150 % and 116 %, respectively (Figure 5 j).

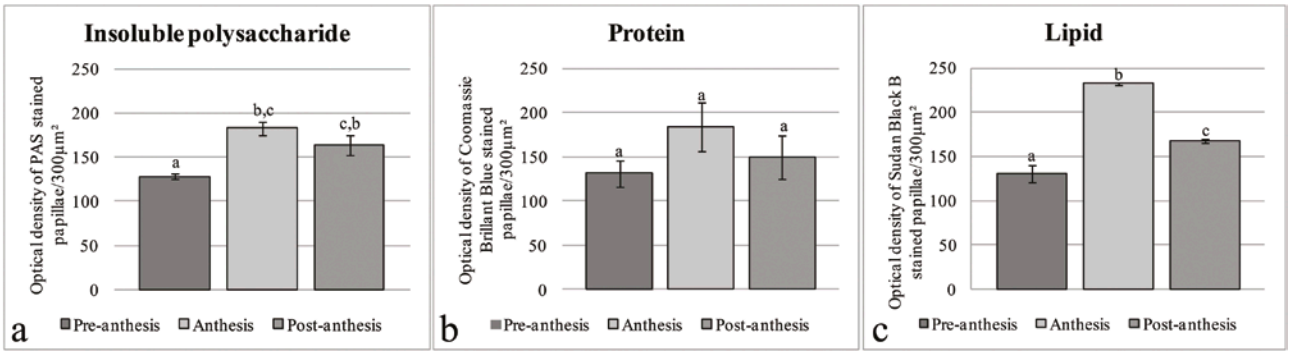

Figure 3. Organic material dynamics of papillae cells during stigma development of *Hibiscus syriacus*. a. Insoluble polysaccharide content, b. Protein content, c. Lipid content. Data are expressed as optical density per area unit (300 µm²). The data with different letters are significantly different according to Tukey's test at $P < 0.05$ for independent samples. Results are expressed as mean ± SD.

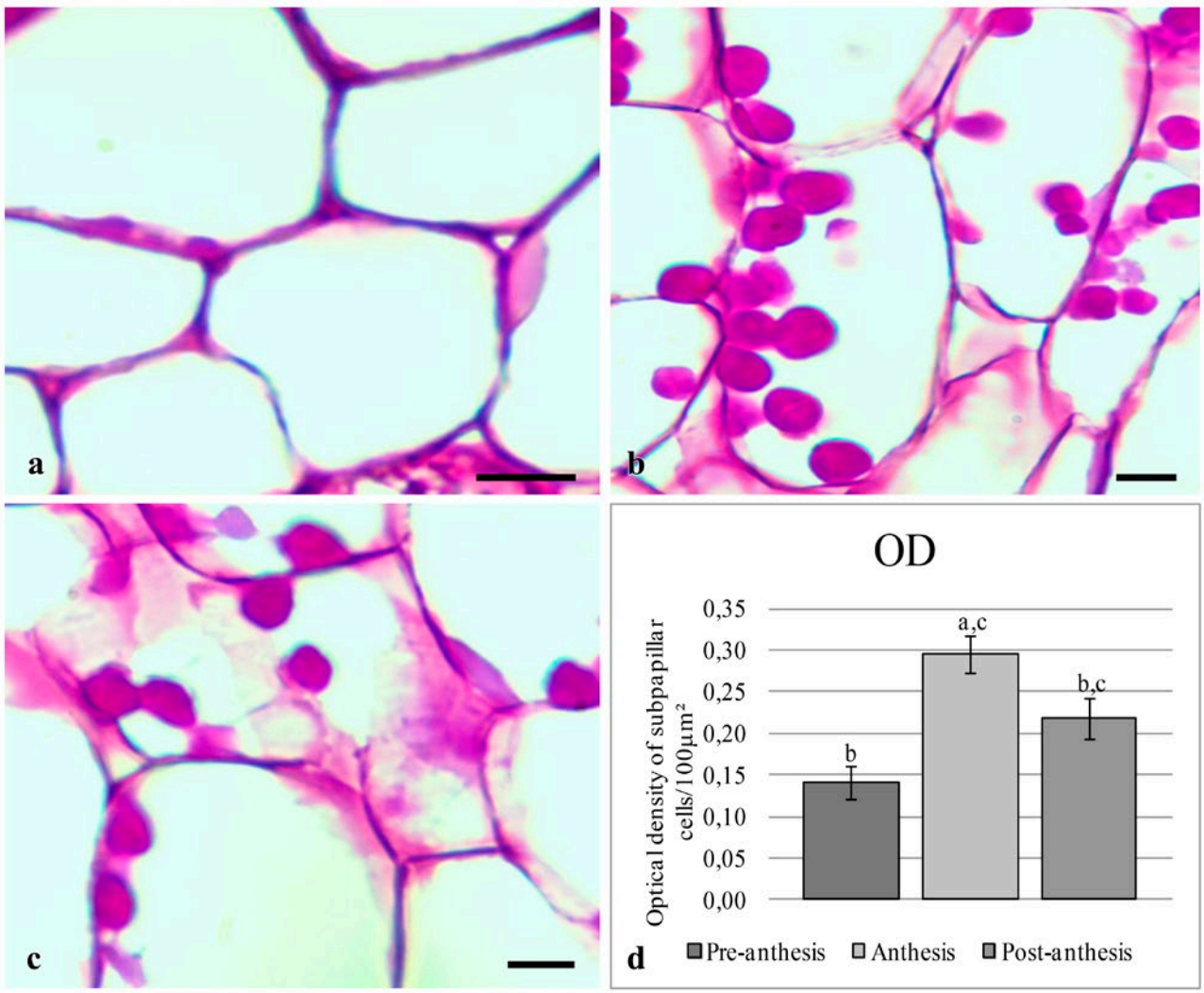

Figure 4. Starch dynamics at sub-papillary cells during stigma development of *Hibiscus syriacus*. a. Very few starch granules in sub-papillary cells at pre-anthesis, b. Large and dense starch granules in sub-papillary cells at anthesis, c. Starch granule content at post-anthesis (note the reduction in compare to anthesis), d. Starch synthesis/degradation pattern of sub-papillary cells, data are expressed as optical density per area unit (100 µm²). The data with different letters are significantly different according to Tukey's test at $P < 0.05$ for independent samples. Results are expressed as mean ± SD. Scale: 5 µm.

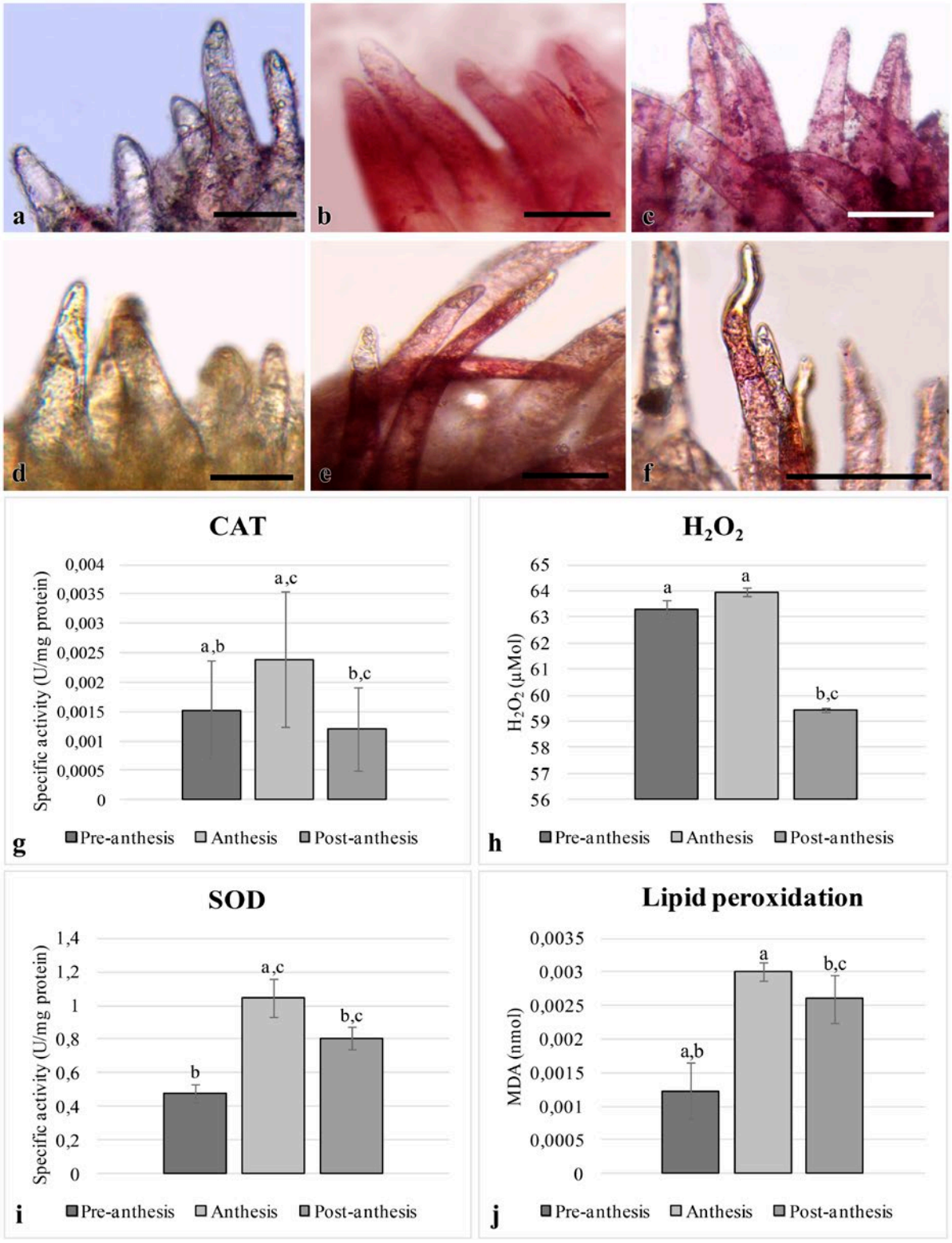

Figure 5. Enzymatic activities in stigma of *Hibiscus syriacus*. Non spesific esterase activity at pre-anthesis (a), anthesis (b), post-anthesis (c). Peroxidase activity at pre-anthesis (d), anthesis (e), post-anthesis (f), CAT activity (g), SOD activity (h), H_2O_2 content (i) and lipid peroxidation (j) of stigmas at different developmental stages. The data with different letters are significantly different according to Tukey's test at $P < 0.05$ for independent samples. Results are expressed as mean ± SD. Scale: 50 µm.

DISCUSSION

Flower development which is closely related to stigma differentiation may be categorized into different stages considering stigma (Suarez et al. 2012). Annahwi et al. (2017) previously defined the flower development stages of *Hibiscus rosa-sinensis* especially focusing on flower phenology. According to the researchers, we specified three stigma development stages in *Hibiscus syriacus* as a result of the examined morphological markers. *H. syriacus* and *H. rosa-sinensis* had similarities in flowering features. Calyx was longer than the corolla bud at pre-anthesis. Flowers were fully opened and anthers were dehiscent at anthesis. Annahwi et al. (2017) stated the last stage of flower development as fertilization, which was marked with the fall of the corolla, column, and pistil. But we preferred to name the last stage as post-anthesis, which was marked with shrinkage and discoloration of the corolla. The mature pistils of Malvaceae have been characterized as having five-branched and capitated stigma which was separated to each other during maturation in *H. syriacus* as it was in *H. rosa-sinensis* (Annahwi et al. 2017).

As a result of increased metabolic activity, it has been known that stigmatic papillae cells begin to accumulate polysaccharide, lipid, and protein throughout their development (Neil et al. 2002; Zafra et al. 2010). Lipids are reported to be effective in pollen hydration and growing pollen tube orientation. In addition, polysaccharides are known to form a suitable medium for pollen germination (Herrero and Dickinson 1979; Wolters-Arts et al. 1998). So, lipid and polysaccharides are found to be abundant on stigma, especially when it is ready for the pollination. Consistent with this, it was determined that stigmatic papillae cells of *H. syriacus* had an abundant polysaccharide, protein, and lipid content at all stages of development. However, their amounts were found to be at the maximum level at anthesis stage in which the stigma was the most receptive. Edlund et al. (2004) also stated that at the receptive stigma the formation of pellicle layer usually occurs. In *H. syriacus*, pellicle of papillae was formed at anthesis and it remained intact during the development. However, when stigma receptivity reduced at post-anthesis, the pellicle became thinner.

Degenerated sub-papillary cells were detected previously by Losada and Herrero (2012) in *Malus domestica* as it was in *H. syriacus*. The researcher stated that these cells contribute to the formation of stigmatic secretion. The release of their contents into the intercellular space provides the increment in the amount of secretion on the stigma surface and the intercellular space. Similar to *M. domestica*, organic material content in the intercellular space increased by degeneration of the sub-papillary cells in *H. syriacus*. However, there was no degeneration-based secretion on the stigmatic surface. Although degeneration-based organic material release started at post-anthesis, pellicle prevented the release of substances onto the stigma. According to the researchers the intercellular secretion has important roles in pollen recognition and germination (Heslop-Harrison 2000; McInnis et al. 2006). Besides, the accumulation of organic substances usually associated with stigma maturation and receptivity. It can be suggested that the accumulation of the substance in the intercellular space in *H. syriacus* was related to both maturity and receptivity at anthesis, however the continuation of the accumulation at post-anthesis may be associated with organ senescence rather than receptivity (Hiscock and Allen 2008).

Starch is principal storage carbohydrates having important roles on pollen tube growth, ovule and fruit formation and determination of flower quality in angiosperms (Chapin et al. 1990; Rodrigo et al. 2000; Reale et al. 2009; Alcaraz et al. 2010). Suarez et al. (2012) stated that the amount of starch increased in the sub-papillary cells and style channel during pollination in *Olea europaea*. In *H. syriacus*, whereas sub-papillary cells contained plenty of starch granules at pre-anthesis stage, along with pollination starch accumulation increased. At post-anthesis stage starch granules were still existed. Similarly, researchers noted that starches are reduced in stigmatic cells after pollination consuming as a source of energy for pollen tube growth (Rodriguez-Garcia et al. 2003).

Esterase and peroxidase are the major constituent of the stigma surface proteins. They are functional on the pollen-stigma interaction to loosen cell wall components of stigma cells with the aim of allowing pollen tubes to penetrate and grow into the stigma (Hiscock et al. 2002; McInnis et al. 2006). Their activity were determined on the surface of the receptive stigma in many species (Seymour and Blaylock 2000; Shakya and Bhatla 2010). In *H. syriacus*, the stigma exhibited poor non-specific esterase and peroxidase activity at pre-anthesis. But, intensive non-specific esterase and peroxidase activity detected at anthesis, indicating the stigma gained receptivity at this stage (Serrano and Olmedilla 2012). Although the expression of peroxidase decreased at post-anthesis with compare to the anthesis, it was more than pre-anthesis demonstrating that the stigma still continued to receptivity at post-anthesis. However, even in the case of a reduction in stigma receptivity, dense pollen grains, and continuing enzymatic activities represented that pollination still proceeds.

In recent years, many studies have reported that ROS function as signal molecules during the stigma - pollen interaction (McInnis et al. 2006; Zafra et al. 2010; Allen et al. 2011; Serrano and Olmedilla 2012). The most occurring ROS are superoxide anion ($O_2^{\cdot-}$), hydroxyl radical ($^{\cdot}OH$) and hydrogen peroxide (H_2O_2). Among them H_2O_2 which is produced by SOD from reduction of superoxide anions is the most stable ROS and it can cross the membranes. In angiosperm stigma, accumulation of H_2O_2 during the stigma receptivity is known to be a common feature. In parallel, H_2O_2 accumulation and SOD activity which is H_2O_2 catalyzer was at maximum level during the anthesis in *H. syriacus*. High concentrations of H_2O_2 may be involved in signaling networks that promote pollen germination and/or pollen tube growth on stigma as it was in *Arabidopsis thaliana* (McInnis et al. 2006). Furthermore, high levels of H_2O_2 can be produced as a result of increased metabolic activity in stigma papillae and surrounding tissues starting to collect pectin, arabinogalactan, proteins and other organic components, as well as starch and lipids (Neil et al. 2002; Zafra et al. 2010). It can be suggested that H_2O_2 concentration increased due to the accumulation of organic matter serving as a signal that promotes pollen germination and pollen tube entry at anthesis stage. It has been known that CAT breakdown H_2O_2 to H_2O and O_2 (Yanık et al. 2018). Although CAT activity increased at anthesis, H_2O_2 is still at high concentrations. This situation suggests that CAT activity is not sufficient to scavenge with over accumulated H_2O_2. ROS accumulation in papillae of *H. syriacus* indicates that stigma gains receptivity at anthesis. Supporting results were also stated in *Amygdalolia* and *O. europaea* cultivars (Aslmoshtaghi and Shahsavar 2016).

However, high concentrations of H_2O_2 cause oxidative stress resulting in biomolecular damage (Quan et al. 2008; Schieber and Chandel 2014). When the amount of ROS exceeds the threshold value, LPO occurs in both cell and organelle membranes and oxidative stress increases (Yanik et al. 2018). LPO can be monitored by the level of MDA that end product of LPO (Halliwell and Gutteridge 1989). Considering the highest H_2O_2 accumulation at anthesis, LPO was at highest level at anthesis in *H. syriacus* stigma. Furthermore, high MDA content may also relate to loosening of cell membrane components of papillae due to germinated pollen tubes at anthesis.

In conclusion, stigma of *H. syriacus* is receptive at anthesis stage and still receptive at post anthesis even its performance has fallen. At anthesis stage organic material synthesis, enzymatic activity, lipid peroxidation and H_2O_2 accumulation are very progressive assisting stigma receptivity, pollen germination and pollen tube growth. Our data will help improve our knowledge on pollination success in plants as well as in *Hibiscus*.

DISCLOSURE STATEMENT

No potential conflict of interest was reported by the authors.

REFERENCES

Alcaraz ML, Hormaza JI, Rodrigo J. 2010. Ovary starch reserves and pistil development in avocado (*Persea americana*). Physiol Plant. 140(4):395–404.

Allen AM, Thorogood CJ, Hegarty MJ, Lexer C, Hiscock SJ. 2011. Pollen–pistil interactions and self-incompatibility in the Asteraceae: new insights from studies of *Senecio Squalidus* (Oxford ragwort). Ann Bot. 108(4):687–698.

Annahwi D, Ratnawati R, Budiwati B. 2017. Flower and fruit development phenology and generative reproduction success of *Hibiscus rosa-sinensis* spp. YRU Journal of Science and Technology. 2(2):19–30.

Aslmoshtaghi E, Shahsavar AR. 2016. Biochemical changes involved in self-incompatibility in two cultivars of olive (*Olea europaea* L.) during flower development. J Hortic Sci Biotechnol. 91(2):189–195.

Birecka H, Briber KA, Catalfamo JL. 1973. Comparative studies on tobacco pith and sweet potato root isoperoxidases in relation to injury, indoleacetic acid, and ethylene effects. Plant Physiol. 52(1):43–49.

Brito MS, Bertolino LT, Cossalter V, Quiapim AC, Paoli HC, Goldman GH, Teixeira SP, Goldman MHS. 2015. Pollination triggers female gametophyte development in immature *Nicotiana tabacum* flowers. Front Plant Sci. 6:1–10.

Cakmak I, Horst JH. 1991. Effects of aluminum on lipid peroxidation, superoxide dismutase, catalase, and peroxidase activities in root tips of soybean (*Glycine max*). Physiol Plant. 83(3):463–468.

Cakmak I, Marschner H. 1992. Magnesium deficiency and high light intensity enhance activities of superoxide dismutase, ascorbate peroxidase, and glutathione reductase in bean leaves. Plant Physiol. 98(4):1222–1227.

Çetinbaş-Genç A, Ünal M. 2017. Timing of reproductive organs maturity in proterandrous *Malva sylvestris* L.. Not Sci Biol. 9(2):287–295.

Chapin III FS, Schulze ED, Mooney HA. 1990. The ecology and economics of storage in plants. Annu Rev Ecol Evol Syst. 21(1):423–447.

Cheong YH, Chang HS, Gupta R, Wang X, Zhu T, Luan S. 2002. Transcriptional profiling reveals novel interactions between wounding, pathogen, abiotic stress, and hormonal responses in Arabidopsis. Plant Physiol. 129(2):661–677.

Cho YW, Park EH, Lim CJ. 2000 Glutathione S-transferase activities of S-type and L-type thiol transferase from *Arabidopsis thaliana*. Biochem Mol Biol j. 33(2):179–183.

Delannoy E, Jalloul A, Assigbetse K, Marmey P, Geiger JP, Lherminier J, Daniel JF, Martinez C, Nicole M. 2003. Activity of class III peroxidases in the defense of cotton to bacterial blight. Mol Plant Microbe Interact. 16(11):1030–1038.

Do HM, Hong JK, Jung HW, Kim SH, Ham JH, Hwang BK. 2003. Expression of peroxidase-like genes, H2O2 production, and peroxidase activity during the hypersensitive response to *Xanthomonas campestris* pv. vesicatoria in *Capsicum annuum*. Mol Plant Microbe Interact. 16(3):196–205.

Edlund AF, Swanson R, Preuss D. 2004. Pollen and stigma structure and function: the role of diversity in pollination. Plant Cell. 16(1):84–97.

Feder N, O'Brien TP. 1968. Plant microtechnique: Some principles and new methods. Am J Bot. 55(1):123–142.

Fisher DB, Jensen WA, Ashton ME. 1968. Histochemical studies of pollen: Storage pockets in the endoplasmic reticulum. Histochemie. 13(2):169-182.

Gomori G. 1950. An improved histochemical technique for acid phosphatase. Stain Technol. 25(2):81–85.

Halliwell B, Gutteridge JM. 1989. 1 Iron toxicity and oxygen radicals. Baillieres Clin Haematol. 2(2), 195–256.

Herrero M, Dickinson HG. 1979. Pollen-pistil incompatibility in *Petunia hybrida*: changes in the pistil following compatible and incompatible intraspecific crosses. J Cell Sci. 36(1):1–18.

Heslop-Harrison Y. 2000. Control gates and micro-ecology: the pollen–stigma interaction in perspective. Ann Bot. 85(1):5–13.

Hiscock SJ, Hoedemaekers K, Friedman WE, Dickinson HG. 2002. The stigma surface and pollen-stigma interactions in *Senecio squalidus* L. (Asteraceae) following cross (compatible) and self (incompatible) pollinations. Int J Plant Sci.163(1):1–16.

Hiscock SJ, Allen AM. 2008. Diverse cell signalling pathways regulate pollen-stigma interactions: the search for consensus. New Phytol. 179(2):286–317.

Hsu RJ, Hsu YC, Chen SP, Fu CL, Yu JC, Chang FW, Chen YH, Liu JM, Ho JY, Yu CP. 2015. The triterpenoids of *Hibiscus syriacus* induce apoptosis and inhibit cell migration in breast cancer cells. BMC Complement Altern Med. 15(1):65–74.

Junglee S, Urban L, Sallanon H, Lopez-Lauri F. 2014. Optimized assay for hydrogen peroxide determination in plant tissue using potassium iodide. Am J Analyt Chem. 5(11):730–736.

Klips RA, Snow AA. 1997. Delayed autonomous self-pollination in *Hibiscus laevis* (Malvaceae). Am J Bot. 84(1):48–53.

Losada JM, Herrero M. 2012. Arabinogalactan-protein secretion is associated with the acquisition of stigmatic receptivity in the apple flower. Ann Bot. 110(3):573–584.

McInnis SM, Desikan R, Hancock JT, Hiscock SJ. 2006. Production of reactive oxygen species and reactive nitrogen species by angiosperm stigmas and pollen: potential signalling crosstalk?. New Phytol. 172(2):221–228.

Neill S, Desikan R, Hancock J. 2002. Hydrogen peroxide signalling. Curr Opin Plant Biol. 5(5):388–395.

Paoletti E, Ferrara AM, Calatayud V, Cervero J, Giannetti F, Sanz MJ, Manning WJ. 2009. Deciduous shrubs for ozone bioindication: *Hibiscus syriacus* as an example. Environ Pollut. 157(3):865–870.

Pearse AG. 1961. Histochemistry, theoretical and applied. Am J Med Sci. 241(1):136.

Punasiya R, Pillai S. 2015. In vitro, antioxidant activity of various leaves extract of *Hibiscus syriacus* L. J Pharmacogn Phytochem. 7(1):18–24.

Quan LJ, Zhang B, Shi WW, Li HY. 2008. Hydrogen peroxide in plants: A versatile molecule of the reactive oxygen species network. J Integr Plant Biol. 50(1):2–18.

Reale L, Sgromo C, Ederli L, Pasqualini S, Orlandi F, Fornaciari M, Ferranti F, Romano B. 2009. Morphological and cytological development and starch accumulation in hermaphrodite and staminate flowers of olive (*Olea europaea* L.). Sex Plant Reprod. 22(3):109–119.

Rodrigo J, Rivas E, Herrero M. 1997. Starch determination in plant tissues using a computerized image analysis system. Physiol Plant. 99(1):105–110.

Rodrigo J, Hormaza JI, Herrero M. 2000. Ovary starch reserves and flower development in apricot (*Prunus armeniaca*). Physiol Plant. 108(1):35–41.

Rodriguez-Garcia MI, M'Rani-Alaoui M, Fernandez MC (2003) Behavior of storage lipids during pollen development and pollen grain germination of olive (*Olea europaea* L.). Protoplasma. 221(3-4):237–244.

Schieber M, Chandel NS. 2014. ROS function in redox signaling and oxidative stress. Curr Biol. 24(10):453–462.

Serrano I, Olmedilla A. 2012. Histochemical location of key enzyme activities involved in receptivity and

self-incompatibility in the olive tree (*Olea europaea* L.). Plant Sci. 197:40–49.
Seymour RS, Blaylock AJ. 2000. Stigma peroxidase activity in association with thermogenesis in *Nelumbo nucifera*. Aquat Bot. 67(2):155–159.
Shakya R, Bhatla SC. 2010. A comparative analysis of the distribution and composition of lipidic constituents and associated enzymes in pollen and stigma of sunflower. Sex Plant Reprod. 23(2):163–172.
Souza EH, Carmello-Guerreiro SM, Souza FVD, Rossi ML, Martinelli AP. 2016. Stigma structure and receptivity in Bromeliaceae. Sci Hort. 203:118–125.
Suarez C, Castro AJ, Rapoport HF, Rodriguez-Garcia MI. 2012. Morphological, histological and ultrastructural changes in the olive pistil during flowering. Sexual Plant Reprod. 25(2):133–146.
Wolters-Arts M, Lush WM, Mariani C. 1998. Lipids are required for directional pollen-tube growth. Nature 392:818–821.
Yanik F, Aytürk Ö, Çetinbaş-Genç A, Vardar F. 2018. Salicylic acid-induced germination, biochemical and developmental alterations in rye (*Secale cereale* L.). Acta Bot Croat. 77(1):45–50.
Zafra A, Rodriguez-Garcia MI, Alche JD. 2010. Cellular localization of ROS and NO in olive reproductive tissues during flower development. BMC Plant Biol. 10(1):36–50.

Caryologia
International Journal of Cytology, Cytosystematics and Cytogenetics

Firenze University Press
www.fupress.com/caryologia

Citation: M. Han, F. Peng, P. Tan, Q. Deng (2019) Structure and development of male gametophyte in *Carya illinoensis* (Wangenh.) K. Koch. *Caryologia* 72(4): 15-27. doi: 10.13128/cayologia-152

Published: December 23, 2019

Data Availability Statement: All relevant data are within the paper and its Supporting Information files.

Competing Interests: The Author(s) declare(s) no conflict of interest.

Structure and development of male gametophyte in *Carya illinoensis* (Wangenh.) K. Koch

Minghui Han[1,2,*], Fangren Peng[1], Pengpeng Tan[1], Qiuju Deng[1]

[1] *Co-Innovation Center for the Sustainable Forestry in Southern China, Nanjing Forestry University, Nanjing 210037, P. R. China*
[2] *Forest Resources Management Dept., University of British Columbia, 2424 Main Mall, Vancouver, BC Canada, V6T 1Z4*
*Corresponding author: zhu4214536@qq.com

Abstract. In order to understand the differentiation of staminate flowers of pecans (*Carya illinoensis* (Wangenh.) K. Koch), we carried out an integrated study of staminate flower development in a protogynous cultivar, Mahan, by assessing changes in external morphology and microstructure at multiple levels. Results showed that the staminate inflorescence differentiation cycle for pecans was 1 year. Staminate inflorescence development was acropetal. When inflorescences developed to 5–8 cm, the microspore mother cells in the base florets of the inflorescences entered into meiosis prophase and the middle layer started to degrade. When inflorescences grew to 8–10 cm, the microspore mother cells in the based florets of the inflorescences were at the peak of meiosis and cytokinesis was synchronous. When bracts have opened to 15°, the microspore mother cells of the basal florets had undergone two divisions to form tetrads. When bracts have opened to 45°, the basal florets entered the mid-late uninucleate stage and the tapetum underwent degradation and autolysis. When bracts opened to >90°, mature pollen grains were 2-celled, with three germ pores and the middle layer tapetum completely degraded. Anther wall development followed the basic type, which was composed of an epidermal layer, an endothecial layer, middle layer (1–3 layers, fibrous thickening absent) and the tapetal layer (cell division was from uninucleate to an octonucleate cell). In summary, external morphology and gametophyte development in pecan staminate flowers were consistent to related; thus, the internal gamete development status can be determined from external morphological characteristics of the flower. This provided a sampling basis and theoretical foundation for *in vitro* culture of pollen grains and elucidation of flowering mechanisms.

Keywords. Microspores, male gametophytes, tapetum, pollen morphology.

The pecan (*Carya illinoinensis* anth; *Juglandaceae*) is a deciduous tree native to North America with pleasant flleasa and medicinal & nutritional properties, popular with Chinese consumers (Thompson and Conner 2012). The pecan was introduced to China more than 100 years ago and is now extensively cultivated in Jiangsu, Zhejiang, and Yunnan Provinces (Zhang Ret al. 2015). Among the pecan cultivars, the protogynous variety "Mahan"

has the best combined traits of any pecan grown in eastern China (Zhang R et al. 2013). The pecan industry is rapidly developing but progress on related basic research on flower and fruit development has been slow. Monoecious pecans are cross-pollinated and dichogamous. Pecans are classified as protoandrous and protogynous according to whether the male or female reproductive parts first to develop and mature. A combination of protogynous and protoandrous varieties is a prerequisitie for fruit setting in a pecan plantation (Zhang R etal. 2015). To date, local studies on flower development have mostly dealt with external morphology and flowering phenology (Xie J 2013; Li C 2012; Xie J. 2011.). This information is used to design varietal combination verities for pecan plantations.

As a wind-pollinated plant, pecan trees produce large amounts of mature pollen to guarantee pollination. Research on staminate flower development in pecans can provide a theoretical basis for controlling the amount of flowers, improving flower quality, promoting normal development of pollen, and decreasing pollen abortion in staminate flowers. A large number of studies on staminate flower development of pecans appeared at the end of the 20th century. Woodroof (1924) was the first person to use hand-drawn figures to describe flower development. Yates and Sparks (1992) used the angle between the bract and the inflorescence axis to divide staminate flower development into 5 stages. On this foundation, Yates described the external characteristics of staminate flower development in the protogynous "Stuart" variety and the protoandrous "Desirable" variety. He further demonstrated the internal development map of these varieties, such as microspore tetrads, free microspores, and binucleate pollen grains (Yates and Sparks 1992; Shuhart 1932). However, he did not carry out cytological validation of the detailed process of development of gametes. In China, only Yang (2014) described some of the anatomical structures involved in staminate flower development, specifically tetrads and bunucleate pollen grains, in fruit abscission research in pecans. However, the stage during which abortion occurs in staminate flowers (such as microspore mother cell meiosis) has not been fully described. There is also no systematic description of changes in the tapetum or middle layer that could ensure pollen maturation or provide large amounts of nutrients for pollen development (Yates and Sparks 1992). There was no discussion of the evolution of pollen morphology.

We used observations of external morphology and internal anatomy during staminate inflorescence development to determine stages of differentiation at the microscopic level to establish the relationship between internal and external development. This may help observers determine the internal cellular development status from external morphological characteristics of the flower and provide a sampling basis and theoretical foundation for *in vitro* pollen culture and elucidation of flowering mechanisms. Additionally, timely measures can be employed according to the development status of pecan staminate flowers in order to provide guidance for practical production, such as variety collocation, prediction of flowering period, and performance of artificial pollination and removal of staminate flowers at appropriate times and in appropriate quantities.

1. MATERIALS AND METHODS:

1.1 Experiment materials and study site

Materials were obtained from the pecan cultivation base (32°19'59.48"N, 118°52'22.37"E) at Shanbei Village, Xiongzhou Street, Luhe District, Nanjing City, Jiangsu Province. This site has a humid subtropical climate, with an average annual temperature of 20°C , annual precipitation of 800–1000 mm, thick soil with a pH of 6.5–7.5. This region is rich in pecan resources, with good population and individual phenotypes. The sampling points for this study were on the northern side of mountain at an altitude of 50–200 m. Five mature trees with strong tree vigor, free from diseases and pests, were randomly selected from the Mahan variety (currently, the only known dominant homozygote (pp or PP) protogynous variety, with protogynous progeny) (Thompson and Romberg 1985).

1.2 Experimental methods

1.2.1 External morphological observations of pecan staminate floral bud and staminate inflorescence development

Experimental observations and sampling were carried out from February 2014 to June 2015. For each sample tree, five measurable branches with terminal buds were selected and labeled. Observation, recording, and photography were carried out every morning and the morphological characteristics of floral buds were recorded. The observation period started from when brown scales of staminate floral buds fell off during spring until staminate inflorescences matured.

1.2.2 Collection of microspore samples and male gametophytes of pecans

Three trees with normal growth and free from diseases and pests were randomly selected for sampling.

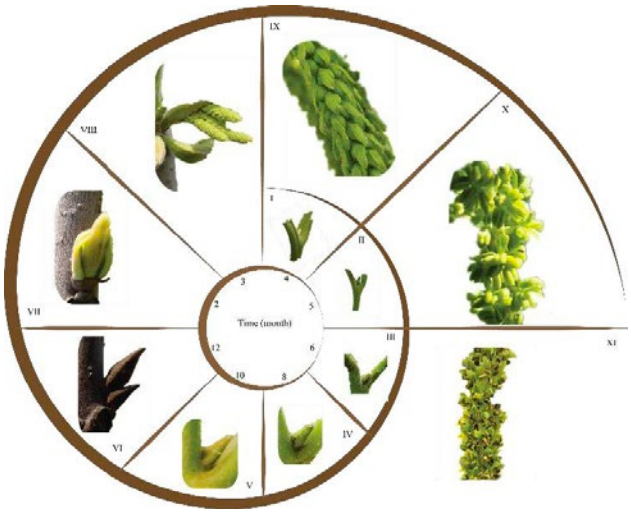

Figure 1. Cycle of pecan staminate flower differentiation over the course of one year.

The sampling time was determined according to the staminate flowering phenology of pecans (Figure 1, VII–XI). During late March of the second year, the leaves start to sprout and the brown scales on staminate floral buds abscise, taking on a broad ovate to triangular-ovate appearance, which is morphologically distinct from leaf buds. The first staminate inflorescence buds at the lower end of the main bearing branches were collected and sampling was carried out at 3-day intervals. Fifteen to twenty buds were collected during each sampling. Basal florets of staminate inflorescences from the sunward side of top and middle canopy layers were collected at 09:00–10:00 during the period from late March (when staminate flowers can be seen) to early May (when staminate flowers shed pollen). Collection was carried out according to different developmental stages (i.e. based on bract opening angle) since the flowering period of staminate flowers. The collected samples were immediately fixed and stored using FAA solution, then made into paraffin sections for microscopic observations and photography using an Olympus BX 60 microscope.

1.2.3 Sample preparation

Preparation of paraffin sections for optical microscopy: The sectioning technique was modified from Li (Li 1987). Flora buds were removed from fixation fluid and washed with distilled water. After cutting the buds in half along the middle axis, we used 10% ethylenediamine for 3–5 days of softening before dehydration using an alcohol gradient. Then, xylene was used for clearing and the plant tissue was embedded in paraffin for sectioning. The sections were 4–8 μm thick and were stained with safranin-Fast Green FCF and sealed in neutral resin. A LeicaDM-5000B microscope was used for observations and photography.

Sample preparation for scanning electron microscopy: One bunch of anthers which is goingto be shedding pollen were collected, fixed with glutaraldehyde, and washed 3–5 times with distilled water. A single pollen sac was cut transversely before dehydration using an ethanol gradient. Then it was dried to a critical point, placed on a platform, and sprayed with gold powder through ion spluttering. A FEI Quanta-200 scanning electron microscope was used for observations and photography.

DAPI fluorescence staining: Mature pollen grains were placed on glass slides and direct DAPI staining was carried out before the slides were sealed. Filter paper was used to absorb excess stain, nail polish was used to seal the sides, and the slides were stored at –20°C . The Olympus BH-2 epifluorescence microscope was used for observations, using a UGI (425 nm) excitation filter and an L420 (420 nm) emission filter.

1.2.4 Statistical analysis of pecan pollen morphology

By scanning electron microscopy, pole axis length (μm)/equator axis length (μm) and the number of particles per unit area (1 μm2) of 50 grains of pollen were measured using image processing software (Image J).

1.2.5 Image processing and data processing

All images were processed using Photoshop CS3 and Adobe Illustrator CS6.

2 RESULTS AND ANALYSIS

2.1 External morphology of pecan staminate flower development

As the bud scale abscise in late March, they expose the inner densely tomentose staminate floral buds and leaf primordia (Figure 2-1). The two lateral buds contain staminate inflorescences, which were tightly enclosed by large bracts and continue to differentiate. The floral axis continued to grow inside the bud and the bracts also continued to grow through early April(Figure 2-2). The middle bud contained unfolded new leaves that continued to grow. Inside, the new leaves started to uncurl (Figure 2-3). In mid-April, the staminate inflorescence extended and large bracts opened up (Figure 2-4). After large bracts had detached, the staminate inflorescence started to grow and

swell, taking on a slight curvature (Figure 2-9). The curved bracts were bound to the floral axis (Figure 2-10) and the pollen sacs were enlarged. The inflorescences continued to extend and swell, growing to around 5 cm. Slight separation of bracts and floral axis occurred (Figure 2-11).

In late April, the leaves had fully unfolded and the growth rate slowed down. The new shoot started to emerge slowly. The staminate inflorescence continued to differentiate and width was 2 cm. The perianth and anthers could be seen from outside the bud. Bracts started to straighten

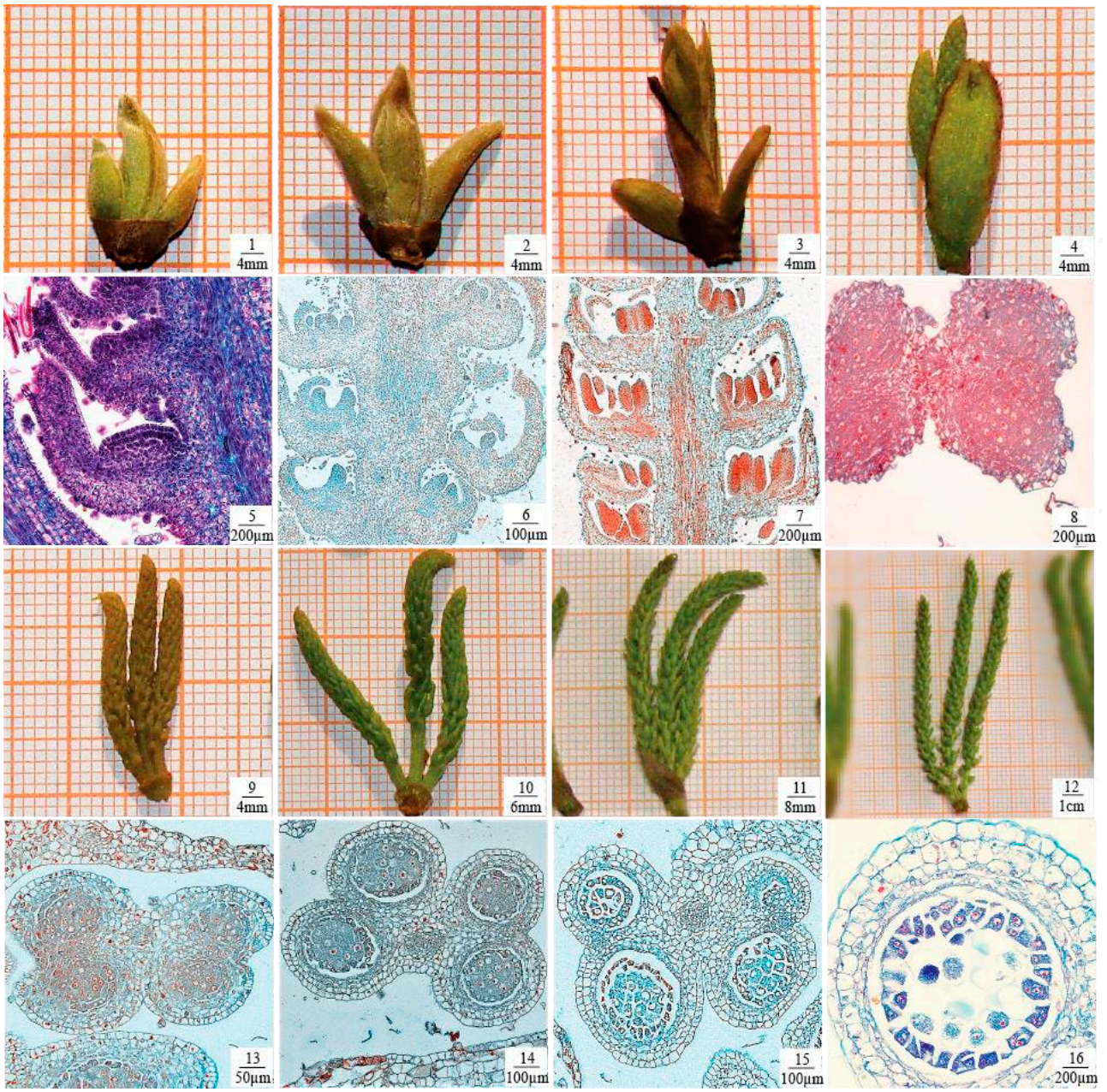

Figure 2. Internal and external structure of bud and staminate flower differentiation in pecan. 1) Staminate flower buds elongated and swollen. 2) Staminate flower buds elongating in bracts. 3) Leaves separation. 4) Side bracts cracking and staminate inflorescences extending. 5) Floret primordium expansion. 6) Bracteole differentiation. 7) Pollen sac elongation. 8) Secondary sporogenous cell differentiation. 9) Emergence of large deciduous bracts. 10) Inflorescence elongation and swelling. 11) Swelling of pollen sacs. 12) Visible pollen sacs. 13) Microspore mother cell differentiation. 14) Pollen sac: 4 chamber. 15) Microspore mother cells entering prophase. 16) Tapetum cell proliferation, microspore mother cell mitosis to dyad.

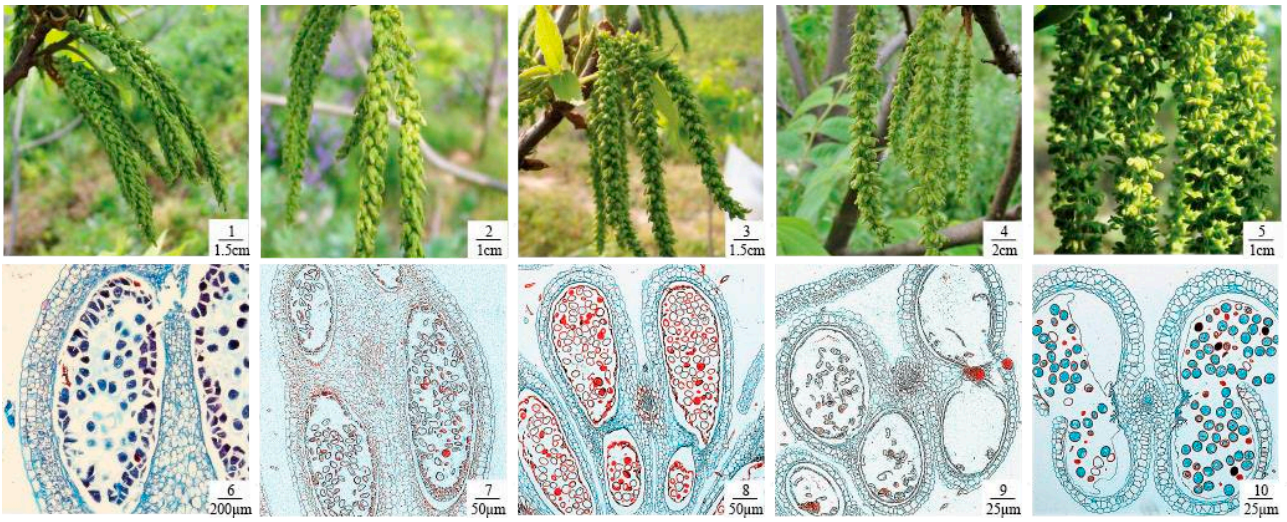

Figure 3. Internal and external structure of staminate flower differentiation in pecan. 1) Inflorescence elongated, angle between bracts and inflorescence axis around 5°. 2) Anthers dilated, bracts open, angle between bracts and inflorescence axis 10°. 3) Anther differentiation, angle between bracts and inflorescence axis 45°. 4) 4–6 anthers visible, angle between bracts and inflorescence axis 60°. 5) Anthers yellow-green, fully visible, turned outward, bracts open and inflorescence axis angle greater than 90°. 6) Microspore mother cells in metaphase nuclei and the nucleus polarized. 7-8) mononuclear microspores moved aside, and the tapetum degraded. 9) Microspore mother cells aborted, pollen wall degradation. 10) With the disintegration of the anther wall in each chamber, the pollen sac cracks and mature pollen was dispersed.

from a curved shape through extension and growth (Figure 2-10~Figure 2-12). The inflorescence grew until it reached a length of 9 cm, and bracts started to open (Figure 2-12). Bractlets gradually unfolded and their angle with the floral axis started to increase (Figure 3-1~Figure3–5). During the growth phase of the new shoots, leaves started to unfold and the tips of the leaves were reddish in color. In this period, staminate inflorescence length was around 5 cm and exhibited a cone shape. The anthers were enlarged and gradually changed from light green to emerald green before undergoing rapid enlargement. The four pollen sacs could be gradually seen and changed from green to yellow-green, and the texture of the pollen sacs changed from soft to hard, leathery, and reflective (Figure 3-5). In early May, when the staminate inflorescence stopped extending and bracts unfolded at an angle greater than 90°, unicellular pollen grains further developed into bicellular pollen grains until maturity, when anther dehiscence expose the yellow pollen. At the end of the pollen shedding period, the anthers shriveled, turned dark green, and gradually withered and fell off.

2.2 Primordium development and occurrence of microspores in staminate flowers

In late March, floret primordia protrusions appeared at the base of bract tissue and the top of the primordia became flatter and wider (Figure 2-5). Staminate inflorescences elongated and the number of bracts increasing. The bracts at the base of the inflorescence were relatively large while bracts at the top were smaller. The staminate flower primordia grow gradually and continue to differentiate into anthers. Column-shaped anthers became elongated and were arranged side by side within bracts (Figure 2-6).

In early April, archesporial cells appeared and underwent further periclinal division to form primary sporogenous cells. Then, the sporogenous cells differentiated into secondary sporogenous cells, forming young anthers that had a near-rectangular shape in longitudinal section (Figure 2- 7). Primary peripheral cells were formed by outward division, which then further differentiated into butterfly-shaped pollen sacs (Figure 2-8). Primary sporogenous cells continued to undergo mitosis to form several secondary sporogenous cells. These cells had a tight arrangement, thick cytoplasm, large nuclei, and polygonal shapes (Figure 2-8). Secondary sporogenous cells continued to undergo mitosis to form even more secondary sporogenous cells, which were arranged tightly inside the anther locule. The volume of the anther locule also increased. At the late stage of division of secondary sporogenous cells, cell-cell connections became weaker and large gaps appear. The cytoplasm became thinner while the nucleolus became apparent and was stained deeply (Figure 2-14). The secondary

sporogenous cell phase lasted 1 week, after which the nucleoplasm became thick again, the nucleolus ceased to be visible, microspore mother cells formed (Figure 2-15), and callose deposition began. Primary peripheral cells underwent periclinal division and were differentiated into an inner layer and outer layer of secondary peripheral cells (Figure 2-16). Cells actively differentiated inside the pollen sacs and both microspore mother cells and tapetal cells underwent vigorous division (Figure 2-16).

2.3 Microspore meiosis

After microspore mother cells became surrounded by callose they undergoes meiosis, the nuclear membrane and nucleolus disintegrated and microspore dyads formed (Figure 4-10). These dyads continued to divide into tetrads (Figure 4-12), which eventually formed pollen grains. Changes in chromosome behavior during meiosis of microspore mother cells were described as follows: (1) Prophase I: Chromosomes were extracted from the nucleolus (Figure 4-1~Figure 4- 2); the nucleolus became smaller (Figure 4-3) and gradually disintegrated (Figure 4-4) and disappeared. The chromosomes became short and thick (Figure 4-5). (2) Metaphase I: The spindle fibers were attached to the centromeres (Figure 4-6) and homologous chromosomes were pulled towards the two poles. Bivalent pairing could be observed at the polar view (Figure 4-7). From the lateral view, it can be seen that chromosomes were arranged on the equatorial plate (Figure 4-8). (3) Anaphase I: The nucleolus and nuclear membrane disappeared, homologous chromosomes that formed bivalents separated and continued to move towards the two poles (Figure 4-9). (4) Telophase I: The chromosomes that migrated to the poles disappeared and aggregated to form an irregular mass. Cytoplasm cleavage occurred and a binucleated cell was formed (Figure 4-10). Subsequently, the cell directly entered prophase II and stratification of anther wall cells was apparent (Figure 2-13). (5) Metaphase II: The nuclear membrane disappeared and chromosomes were arranged on two sides of the equatorial plate in the mother cell. The same anther locule exhibited synchronous progression (Figure 4-11). (6) Telophase II: cytoplasm cleavage occurred again and four cells surrounded by callose were formed, while the cell wall of each cell also took shape (Figure 4-12). Finally, the tetrad was formed.

2.4 Development of male gametophytes

At the end of April to early May, the staminate inflorescence grew rapidly. The four cells in the tetrad separated to form free microspores that were uninucleate. These microspores had thin walls and thick cytoplasm, and the nucleus was located in the center of the cell (Figure 5-1). Figure 5-2 shows a free microspore by fluorescent staining. The cells were red and slightly swollen. The uninucleate pollen grain absorbed nutrients from tapetal secretions or its degradation products and its volume increased. Cytoplasmic vacuolation was significant (Figure 5-3), forming a large central vacuole. The nucleus was compressed by the large vacuole and move close to the pollen wall (Figure 5-4). The free microspore entered the mid-late uninucleate stage (Figure 5-5) while cells became transparent (Figure 5-6). The nucleus underwent unequal division near the wall (Figure 5- 7) to form binucleate cells of different sizes. The vegetative cell near the vacuole was larger and the genital cell that was near the pollen wall was smaller. The cell plate disappeared and the large and small cells moved freely between the vacuole and the cell wall (Figure 5-8). With further development of the male gametophytes, the germ cells left the pollen wall and vacuolation decreased (Figure 5-9). They moved towards the center of the pollen grain and became separated from the vegetative cells (Figure 5-10). Figure 5-11 shows developing pollen grains. The genital cell gradually elongated and took on a crescent shape (Figure 5-12), then a spindle-shape (Figure 5-13) and the liquid-pattern nucleus (Figure 5-14) flew through the pollen tube through the germ pore (Figure 5-15).

2.5 Anther wall development

After one periclinal division and multiple anticlinal divisions, the primary peripheral cells differentiated into secondary peripheral cells (Figure 6-1). The two layers of cells divided, with the outer cells differentiating into the endothecium and middle layer while the inner cells developed into the middle layer and the tapetum (Figure 6-2). Cells in the middle layer of the anther locule and tapetal cells divided further, forming 1–3 layers of cells. Anther wall development was simulations with the occurrence of microspores and development of the male gametophytes. During meiosis of microspore mother cells, anther wall differentiated into an epidermal layer, endothecium, middle layer, and tapetum in the end (Figure 6-3).

Tapetal cells: The tapetal cells of the pecan anther wall belong to glandular tapetum type. During the initial phase of secondary sporogenous, it can be seen that the morphology of early tapetal cellswas similar to that of anther wall cells, with thick cytoplasm (Figure 6-4). Coincident with meiotic prophase in the microspore

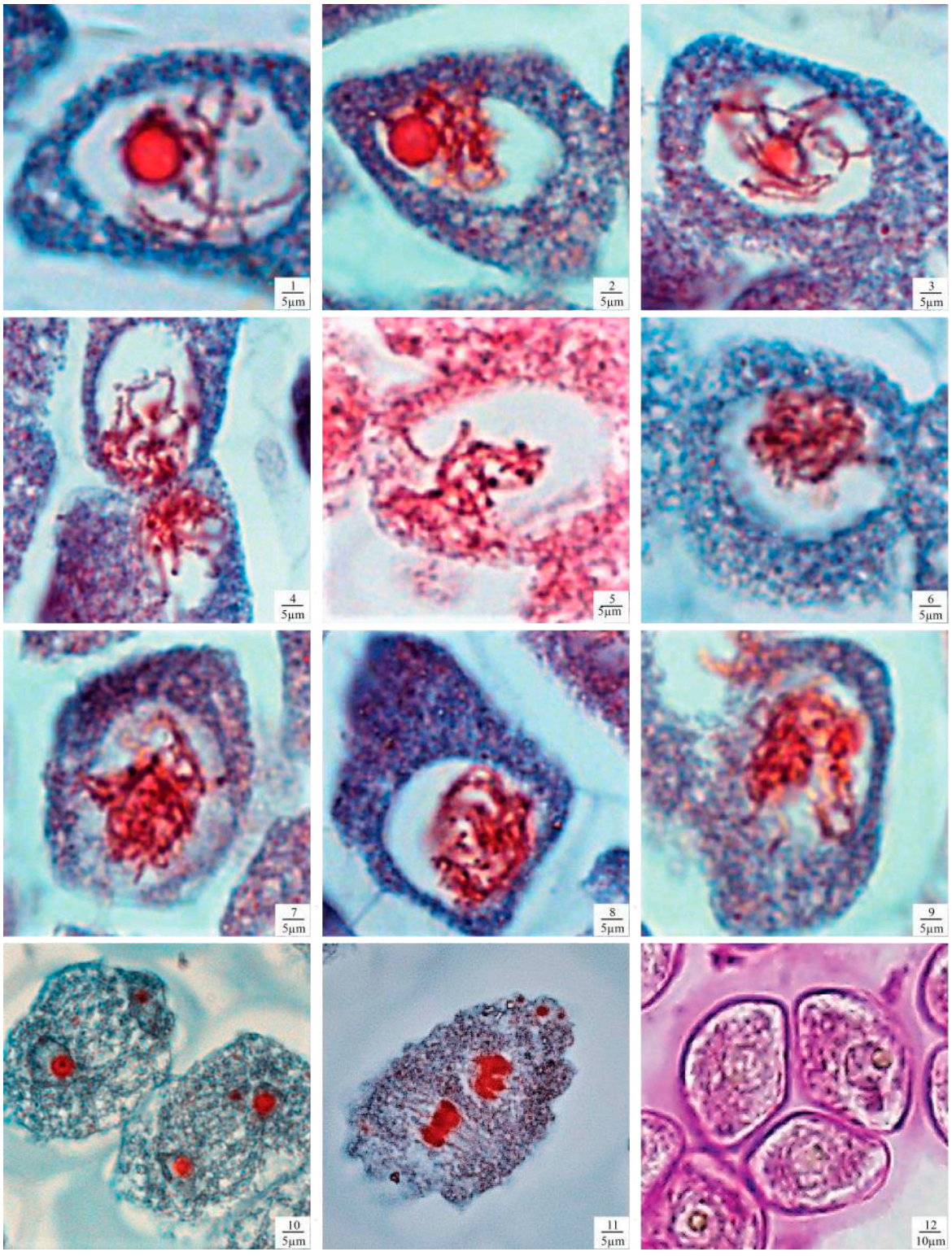

Figure 4. Male gametophyte development of pecan. 1) Microspore mother cells separating and detaching from each other. 2) Pre-prophase, leptonema I, chromosome extraction. 3) Zygotene I, nucleolus gradually disappearing. 4) Pachytene I, chromosomes shorter and thicker, relatively concentrated. 5) Diplotene I, chromosome pairing; Figure 4-6. Metaphase I (polar view). 7) Metaphase I (side view). 8-9) Anaphase I, chromosomes at poles. 10) Dyad, visible binucleated cells. 11) Metaphase II, spindle apparatus. 12) Tetrad stage of microspore development.

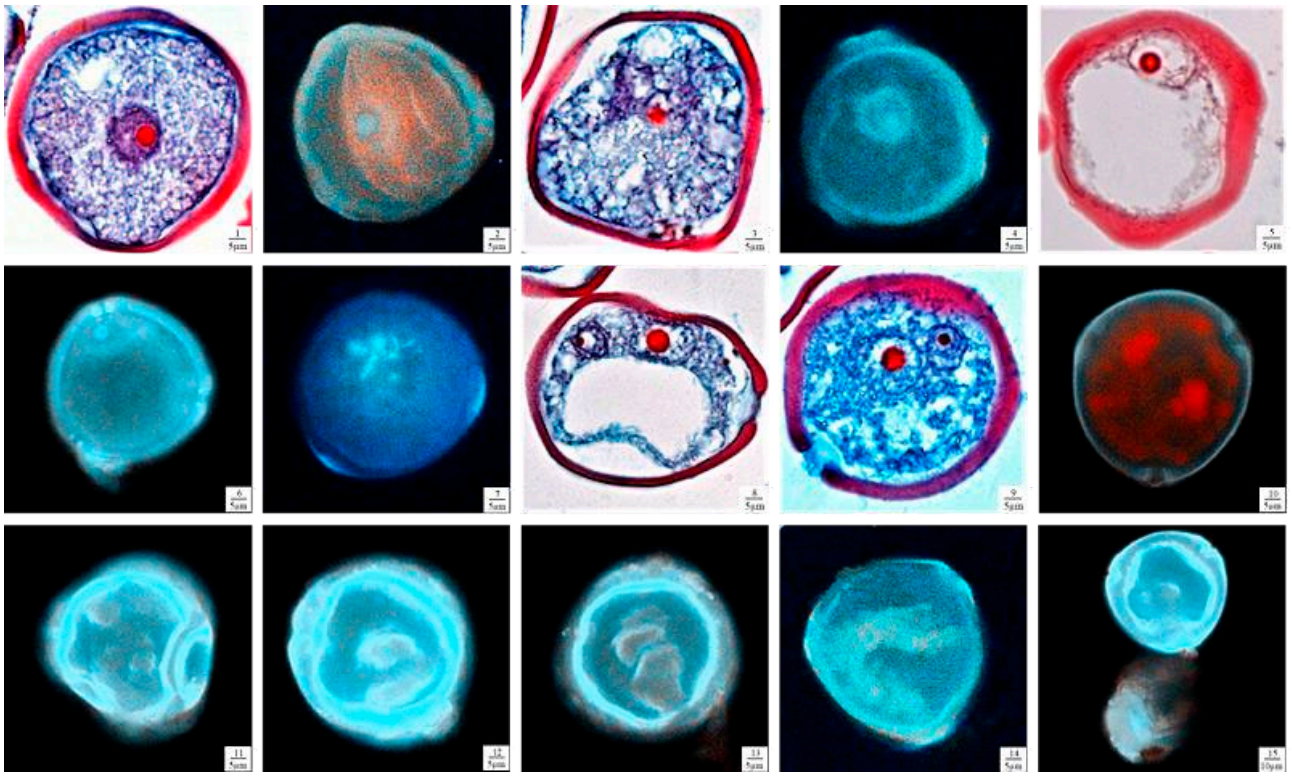

Figure 5. Observations of DAPI fluorescence staining of Microspore in *Carya illionensis*. 1-2) DAPI. Single isolated microspore. 3-4) DAPI. Central microspore. 5-6) DAPI. Uninucleate microspore in periphery stage. 7) Germ cell mitosis (DAPI). 8) Germ cells immersed in the cytoplasm of a vegetative cell and close to the cell wall. 9) Germ cells and vegetative cells free to the center of the nucleus. 10) Germ cells immersed in the cytoplasm of vegetative cells (DAPI). 11) Two-celled mature pollen (DAPI). 12) Differentiation of germ cells (DAPI). 13-14) Nucleus inclusions precipitated from the germination pore(DAPI). 15) Pollen germination(DAPI).

mother cells, the cytoplasm coincident with became thinner, and single nucleus could be seen. It then began to divide (Figure 6-5). Coincident with anaphase I of microspore mother cell meiosis, the tapetal cells were binucleated (Figure 6-6). The tapetal cells continued to divide and had a near-diamond shape, large nucleus, thick cytoplasm, small vacuole, and large volume. These cells are many times larger than other anther wall cells and had four, eight, or more nuclei (Figure 6-7). Tapetal cells divided into septal cells earlier than microspores (Figure 6-8). When microspore mother cells are at diakenesis I, the tapetum was formed (Figure 6-9). During the entire development process, the position of tapetal cells was unchanged and intracellular protoplastids provided nutrients and structural materials for microspore development through intracellular tangential surfaces. The tapetum underwent degradation and autolysis during the mid-late uninucleate stage of microsporogenesis. This was mainly manifested as cell wall degradation from the inner tangential wall towards the outer tangential wall (Figure 6-10). During the process of tapetum degradation, the tapetum provided nutrition for pollen grain elongation and structural materials (Figure 6-11~Figure 6-15). During the mid-late uninucleate stage, the tapetum underwent in situ disintegration and only a single layer of remnants was retained (Figure 6-16).

Middle layer: The 2–3 layers of cells were surrounded by the endothecium (Figure 6-6). During the formation of the microspore mother cell, the middle layer's second layer was compressed and degenerated to some degree (Figure 6-12~Figure 6-13). For example, three layers showed no sign of degeneration (Figure 6-14). The cells gradually atrophied and flattened, disintegrated, and were absorbed (Figure 6-17~Figure 6-18). When the pollen grain was mature and anthers underwent dehiscence, the middle layer of cells basically disintegrated and disappeared (Figure 6-18~Figure 6-19).

Endothecium: A layer of cells were near the epidermis (Figure 6-2). Cells were large and round during prophase (Figure 6-3). As the anther develops, the anther locule expanded, the diameter of inner wall cells

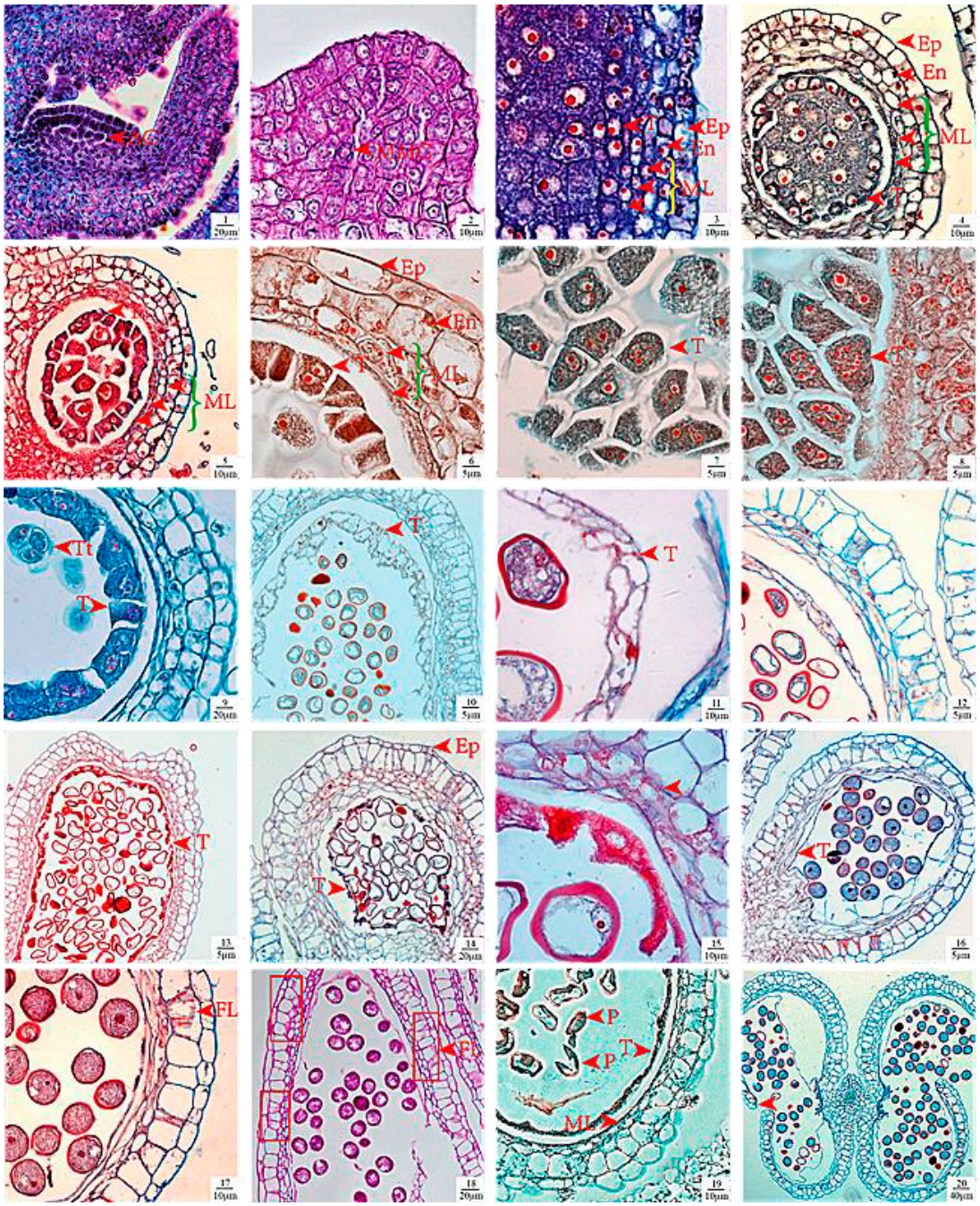

Figure 6. Development of male flower wall and tapetum of anther. Formation of the anther wall in *Carya illionensis*. AC, Archesporial cell; Ep, epidermis; En, endothecium; ML, middle layer, MMC. Microspore mother cell; Ta, Tapetum; FL, Fibrous layer, Tt, Tetrahedral tetrads; VC, vegetative cell; GC, generative cell. 1) Anther wall of primary sporogenous cell stage. 2) Anther wall of secondary sporogenous cells. 3) Anther wall of pollen mother cells: 6 layers, tapetum initial differentiation. 4) Pollen mother cells are separated from each other and differentiating tapetal cells are separated. 5) Microspore meiosis before the prophase, tapetum elongated and turn flattened. 6) Microspore meiosis I late, tapetal cell division. 7) Microspore meiosis I late transition period, heterotic tapetum division peak period. 8) Heterogeneous multicore tapetum; the middle containing starch granules and other nutrients. 9) Tetrad stage, epidermal expansion, the inner wall thickening, the middle 3 layers, glandular tapetum 2 to 3 layers. 10) Late uninucleate microspores: The tapetum wall beginning to disintegrate. 11) Tapetum showing disintegration and became thinning. 12) The inner layer of the tapetum was almost completely dissolved. 13) The tapetum had dissolved, leaving only a monolayer; the cell wall had dissolves, leaving the edge useless. 14) The tapetum was disintegrated outside the tangential wall and the middle layer was flattened. 15-16) The tapetum is almost completely dissolved. 17) The middle layer began to dissolve and banded; anther chamber wall showed fibrous thickening. 18) The cell walls of chamber showed fibrous thickening, and the middle layer had dissolved. 19) 2 nucleated stage, the middle layer is almost completely dissolved. 20) Interventricular rupture, pollen sac split.

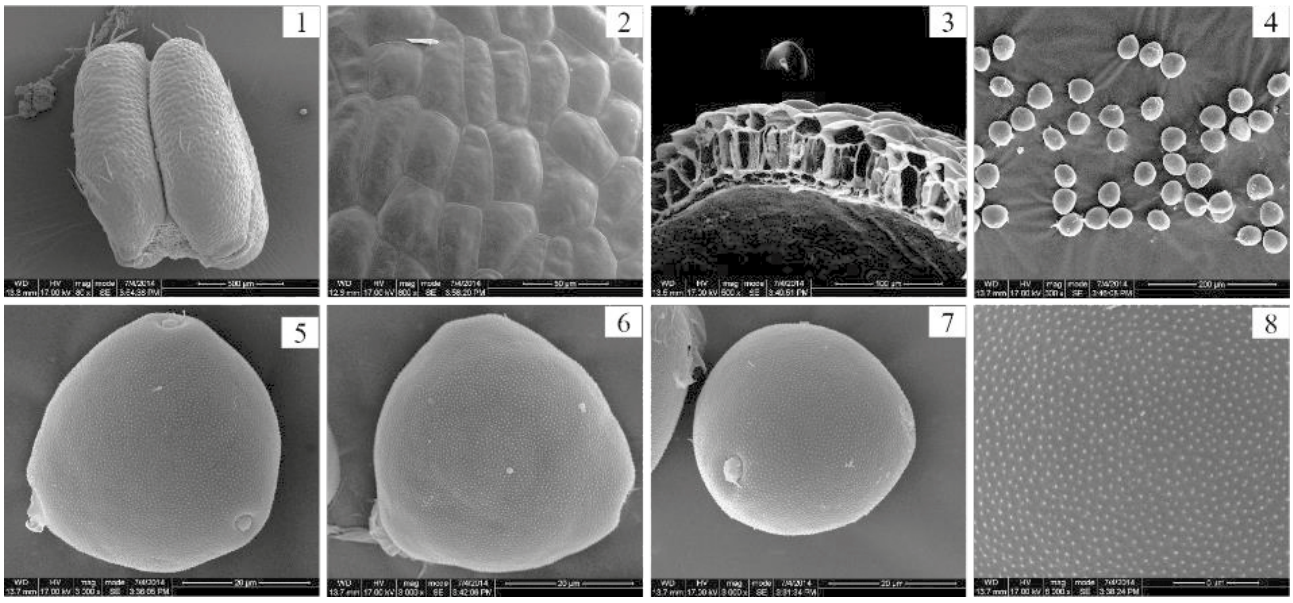

Figure 7. Scanning electron microscopic observation of pollen sac of pecan. 1) Overall appearance of anther. 2) Pollen sac surface. 3) Pollen sac wall anatomical structure when shedding pollen. 4) After pollen sac cracking, pollen group photo. 5) Pollen side view. 6) Pollen polar view. 7) Pollen equatorial plane view, showing micropyle. 8) Pollen surface ornamentation.

increased, and belt-like thickening took place outwards and upwards from the inner tangential wall (Figure 6-9). When the pollen grain was formed, the endothecium formed a fibrous bundle, also known as the fibrous layer (Figure 6-17~Figure 6-18). Secondary thickening did not occur in cells between two pollen sacs at one side of the butterfly-shaped pollen sac (Figure 6-14). During flowering, the entire pollen sac opened, shedding pollen (Figure 6-20), leaving the endothecium nearly empty (Figure 7-3).

Epidermis: Cross-sectional observations indicated that the epidermis exhibited a long rectangular shape, which then underwent anticlinal division in order to adapt to expansion caused by internal anther development. During meiosis of anther mother cells, the epidermis has a distinct cuticle that continued to thicken (Figure 6-6). When anthers were mature, the epidermis expanded and cells became flattened (Figure 6-10~Figure 6-13). Some of the cells disintegrated and only wavy residues were retained (Figure 6-18). The mature anthers contained hairs and the epidermal cells exhibited an irregular massive structure (Figure 7-1~Figure 7-2). Epidermal hairs decreased with anther development. Because anthers were exposed to the air, they underwent severe dehydration and the irregular magradually shrunk and protruded. Figure 7-3 shows the initiation of dehydration on the anther surface and severe dehydration caused the massive to shrink. The surface tension of the anther wall was increased, eventually causing dehiscence.

2.6 Pollen morphology

The pollen wall has three germ pores, which were distributed along the equatorial axis. The polar reveals a near-triangular shape. The proximal polar and distal polar morphological structures were generally similar, and the pollen was isopolar. The surface of the pollen exhibited densely distributed granular ornamentation. Upon measurement, we found the ornamentation density to be 8.9 um and the coefficient of variation to be 8%. The average length of the polar axis of pollen from the Mahan pecan was 39.92 μm and the equatorial axis was 35.66 μm. P/E value of Mahan is 1.119 and belongs to the spheroidal type.

2.7 Consistency between external morphology and anatomical structures during staminate flower development in pecans

Pecan staminate flowers take approximately 1 year from development of the inflorescence primordia to pollen grain maturation. Through observations of staminate floral bud and staminate flower differentiation in pecans, we summarized the correlation between external morphological and tissue structure during differentiation (Table 1). Descriptions of different stages, such as the length of the staminate inflorescence, whether bracts, perianth, or anthers are visible, color changes in bracts

Table 1. Relationship between the external morphology and anatomical structure on staminate flora-bud development of *Carya illinonensis*.

2012/date	2013/date	External morphology	Anatomical structure
03-07~03-13	03-08~03-15	Inflorescence extending out of bract	Archesporium formed
03-14~03-20	03-16~03-22	A cone shaped inflorescence	Archesporium periclinal division
03-21~03-27	03-23~03-27	Inflorescence thickened, elongated, globose	Primary sporulation cells and primary parietal cells are formed
03-28~04-10	03-28~04-14	Inflorescence axis elongation, morphological differentiation completed	Primary sporulation and primary parietal cells continue to differentiate
04-11~04-23	04-15~04-25	Inflorescence elongation, pollen sac enlargement	Secondary sporulation forms, and anther wall begins to divide
04-24~04-26	04-26~04-30	Angle between rachis and bract increased to 30	Formation of microspore mother cells and obvious stratification of pollen wall
04-27~05-03	04-31~05-05	Angle between rachis and bract increased to 45	Microspore enters tetrad period
05-04~05-11	05-06~05-10	Angle between rachis and bract increased to 90	Single cell pollen formation and degeneration of tapetum cells
05-12~05-15	05-11~05-13	Anthers dehiscence to release yellow pollen grains	2-cell pollen, pollen wall rupture, tapetum disappeared

and anthers can be used as indicators of structural changes in tissues.

3. CONCLUSION AND DISCUSSION

3.1 Developmental characteristics of pecan staminate flowers

In pecans, the developmental progress of different parts of the same tree can be different: The periphery of the canopy develops early while the core develops later. The upper parts of the tree develop early and the lower parts develop later. Healthy branches develop early while thin and weak branches develop later. In the same inflorescence, microspore mother cells at the base of the florets develop slightly earlier than florets at the top. Staminate inflorescence development is acropetal and undergoes basifugal growth and development; i.e., development and maturation gradually occur at the base of the floral axis towards the top. This is consistent with the development of *Cyclocarya paliurus* (Juglandaceae) (Fu et al. 2010) and *Carya cathayensi*s Sarg (Huang et al. 2006). Through observation of staminate flower development status at basal of staminate flowers to determine the development status of staminate flower, we found that the developmental stages of staminate inflorescence are consistent with that described by Yates (1992). During development of the external morphology of pecans, the inflorescence elongates, florets enlarge, bracts dehisce, and anthers turn yellow. At the corresponding internal anatomical development stage, the anthers and anther wall, microspores, and male gametophytes develop. Most protoandrous varieties enter into dormancy at the year when flower primordia are form. The protogynous "Mahan" variety forms flower primordia in the spring of the following year, which gradually differentiates into staminate flowers. The external morphological characteristics during staminate flower development can be used to evaluate the maturation stages of reproductive cells in the anthers of pecans.

3.2 Developmental characteristics of microspores and male gametophytes of pecans

Through combination with field observations, anther microscopic examination showed that the "Mahan" pecan variety enters into meiosis prophase when staminate inflorescences reach 4–8 cm. Microspore mother cell meiosis in pecans is classified as synchronous meiosis and division presentation is generally consistent, which is different from *Catalpa bungei* (Fan et al. 2011) and *Atractylodes japonica* (Cao et al. 2004). The microspore mother cell undergoes differentiation and two mitotic divisions to form microspores. The cytokinesis mode used by this plant is synchronous, which is consistent with cucumbers (Cao et al. 2004) and broccoli (Wan et al. 2006). Staminate inflorescences containing anthers and bractlets that are enclosed by large bracts do not get contain reproductive cells (i.e. mature microspores to male gametophytes) and only flower primordia and sporogenous cells are present. Subsequently, free microspores can be observed with the naked eye in bractlets and. After undergoing one mitotic division, microspores gradually form mature pollen grains,

which are binucleated pollen grains. The mature pollenhas three germ pores and the surface ornamentation is granular. Walker (Walker and Lee 1976) carried out a classification of pollen external morphology and proposed that plants with many germ pores belong to relatively evolved clades, with ornamentation changing from absent to present. In addition, there is an evolutionary trend of aperture appearance,granular protrusions,elongated shapte (rod shape), stripes. From this, we can deduce that pecans should be relatively primitive. The development of microspores and male gametophytes of pecans is similar to that of *Carya cathayensi*s Sarg. (Xie 2006) and *Cyclocarya paliurus* (Feng 2006), and other plants from the family Juglandaceae, which are species with primitive development (Luza and Polito 1988). According to the palynology criteria reported by Wang *et al*. (1983) Mahan pollen grains are medium-sized pollen grains. According to the classification criteria for pollen shapes by Punt *et al*. (2007), pollen grains with a polar axis to equatorial diameter ratio (P/E) between 1.10 and 1.14 are classified as spheroidal.

3.3 Developmental characteristics of anther wall of pecans

According to Davis's (1996) classification criteria for anther walls, the development of the anther wall of the pecan can be classified as basic, which is composed of an epidermal layer, an endothecial layer, middle layer (1–3 layers) and the tapetal layer. The epidermis is maintained until anther maturation to support anther structure and ensure that anaphase development in microspores is completed. The number of epidermal hairs decreases with anther development and aids in drying and dehiscence of the epidermis (Yates and Sparks 1992). Fibrous thickening of the endothecium and slight lignification when mature can aid in pollen sac dehiscence. There are 3 cell layers in the middle layer of pecans, which provide abundant starch and nutrients to microspore mother cells undergoing mitosis. The tapetum of pecan is a glandular tapetum.

ACKNOWLEDGEMENTS

We wish to thank the Priority Academic Program Development of Jiangsu Higher Education Institutions (PAPD) and the Special Fund for Forest Scientific Research in the Public Welfare (201304711) for financial assistance with this project.

REFERENCES

Cao QH, Chen JF, Qian CT, *et al*. 2004. Cytological studies on meiosis and male gametophyte development in cucumber. Acta Botanica Boreali-Occidentalia Sinica, 24(9):1721-1726. [In Chinese]

Davis G L. 1996. Systematic embryology of the angiosperms. New York: John Wiley and Sonc Inc., 1996: 6-27.

Fan LL, Peng FR, Zhou Qi, *et al*. 2011. Sporogenesis and Gametogenesis of *Catalpa bungei* (Bignoniaceae). Acta Botanica Boreali-Occidentalia Sinica, 31(3):431-438. [In Chinese]

Feng L. 2006. Preliminary examination of reproductive and developmental anatomy of *Cyclocarya paliurus*. Nanjing Forestry University. [In Chinese]

Fu XX, Feng L, Fang SZ, *et al*. 2010. Observation on flowering habits and anatomy of stamen development in *Cyclocarya paliurus*. Journal of Nanjing Forestry University (Natural Sciences Edition), 34(3):67-71. [In Chinese]

Huang YJ, Wang ZR, Zheng BS, *et al*. 2006. Anatomy of stamen development in *Carya cathayensis*. Journal of Zhejiang A&F University, 23(1):56-60. [In Chinese]

Li C. 2012. Study on flowering phenology and pollen characteristics of asexual pecan varieities. Southwest University. [In Chinese]

Li ZL. 1987. Techniques for making plant sections (2nd edition). China Science Publishing and Media Limited. [In Chinese]

Luza J G, Polito V S. 1988. Microsporogenesis and anther differentiation in *Juglansregia* L.: A developmental basis for heterodichogamy in walnut. Botanical Gazette, 149(*1*): 30-36.

Punt W, Hoen P, Blackmore S, *et al*. 2007. Glossary of pollen and spore terminology. Review of Palaeobotany and Palynology, 143(1-2):1-81.

Shuhart D V. 1932. Morphology and anatomy of the fruit of Hicoriapecan. Botanical Gazette, 93(1): 1-20.

Thompson T E, Conner P J. 2012. Pecan//Fruit Breeding. Springer, Boston, MA, 771-801.

Thompson T E, Romberg L D. 1985. Inheritance of heterodichogamy in pecan. Heredity, 13 76(6):456-458.

Walker G, Lee V E. 1976. Surface structures and sense organs of the cypris larva of Balanusbalanoides as seen by scanning and transmission electron microscopy. Journal of Zoology, 178(*2*): 161-172.

Wan SF, Zhang SN, Zhang J *et al*. 2006. Pollen mother cell mitosis and male gametophyte development in *Brassica oleracea* L. var. *italica* Plenckr. Acta Botanica Boreali-Occidentalia 19 Sinica, 26(5):970-975. [In Chinese]

Wang KF, Wang XZ. 1983. Introduction to palynology. Beijing: Peking University Press. [In Chinese]

Woodroof J G. 1924. Development of pecan buds and the quantitative production of pollen.

Xie G. 2006. Study of reproductive biology of pecans. Nanjing Forestry University. [In Chinese]

Xie J. 2011. Study of flowering phenology and pollen storage characteristics of pecans. Nanjing Forestry University. [In Chinese].

Xie J. 2013. Study of flowering biological characteristics of pecans. Nanjing Forestry University. [In Chinese]

Yang XY. 2014. Preliminary investigation of the biological causes of fruit abcission in pecan "Mahan" cultivars. Zhejiang A & F University. [In Chinese].

Yates I E, Sparks D. 1992. External morphological characteristics for histogenesis in pecan anthers . Journal of the American Society for Horticultural Science, 117(1): 1-17.

Zhang R, Li YR, Peng FR. 2013. Cultivation adaptability and evaluation of Mahan in *Carya illinoinensis*. Nonwood Forest Research, 31(2): 176-180. [In Chinese].

Zhang R, Peng F, Li Y. 2015. Pecan production in China. Scientia Horticulturae, 197(8): 719-727.

Zhang R, Peng F, Liang Y, *et al*. 2015. Flowering and pollination characteristics of Chinese-grown pecan (*Carya illinoinensis*). Acta Horticulturae, 1070(1070): 43-51.

Caryologia
International Journal of Cytology, Cytosystematics and Cytogenetics

Firenze University Press
www.fupress.com/caryologia

OPEN ACCESS

Citation: M.N. Moura, D.C. Cardoso, B.C.L. Baldez, M.P. Cristiano (2019) Genome size in ants: retrospect and prospect. *Caryologia* 72(4): 29-39. doi: 10.13128/cayologia-172

Published: December 23, 2019

Data Availability Statement: All relevant data are within the paper and its Supporting Information files.

Competing Interests: The Author(s) declare(s) no conflict of interest.

Genome size in ants: retrospect and prospect

Mariana Neves Moura[1,2], Danon Clemes Cardoso[2,*], Brenda Carla Lima Baldez[3], Maykon Passos Cristiano[2,*]

[1] *Programa de Pós- Graduação em Ecologia, , Universidade Federal de Viçosa, CEP: 36.570–000, Viçosa, Minas Gerais, Brazil*
[2] *Departamento de Biodiversidade, Evolução e Meio Ambiente, Universidade Federal Ouro Preiato – UFOP, CEP: 35.400–000, Ouro Preto, Minas Gerais, Brazil*
[3] *Programa de Pós- Graduação em Ecologia de Biomas Tropicais, Universidade Federal de Ouro Preto, CEP: 35.400–000, Ouro Preto, Minas Gerais, Brazil*
*Corresponding authors: danon@ufop.edu.br; maykon@ufop.edu.br

Abstract. Genome size is very useful in studies regarding taxonomy, evolution, and reproductive biology in many animal groups, including insects. Herein, we assembled the information about genome size in ants, compiling the DNA content estimated so far, in order to evaluate the methods, the tissues and the internal standard applied to estimate the genomes size. All values were placed in a phylogenetic tree to put it in an evolutionary context and the means of the subfamilies were further compared statistically to investigate changes and trends in the variation across *taxa*. The compiled data resulted in 86 specimens of ants, comprising 69 different species. This number represents 0.52% of the total number of 13,369 ant species described, covering only 40 from 333 valid extant genera. The average Formicidae genome size was 0.36 pg (± 0.13). Most of the estimates were obtained through flow cytometry (83.5%), commonly using brain tissues, with *Drosophila melanogaster* as internal standard (76%). Differences in DNA content of ant species may be related to differences in the amount of heterochromatin and is not related with chromosome number. The evaluation of the genome size estimations currently available for ants has highlighted their scarcity. Such information would be valuable as independent data for the study of ant diversity and evolutionary biology. Further, we conclude that the standardization of the techniques used and a large–scale study on ant genome size are urgently required, given the importance of this insect group and the needs for the improvement in our knowledge on ant genome.

Keywords. C-value, DNA content, Genetic diversity, Genome, Evolution, Phylogeny.

INTRODUCTION

Ants comprise a monophyletic group with approximately 13,369 valid species distributed throughout the planet, with exception of extreme northern and southern latitudes (Bolton, 2018). They are one of the largest groups among insects in species diversity and biomass and together with some wasps and bees, are known as eusocial insects and comprise the order Hymenoptera (Hölldobler and Wilson, 1990; Ardila–Garcia et al., 2010).

They represent an important insect group to investigate the relationship between the genealogical lineages and the distribution patterns of species, due to their occurrence in different habitats of the most diverse ecosystems (Goodisman et al., 2008). Currently, the family Formicidae is divided into 17 extant and 3 extinct subfamilies, spanning 333 valid extant genera and 154 extinct genera (Bolton, 2018). The subfamily Myrmicinae is the largest and most diverse subfamily worldwide, covering about 47% of all ant species (Françoso and Brandão, 1993; Brandão, 1999).

Genome size, also named DNA content, DNA amount, or DNA C–value, has been described as a trait that 'uniquely lies at the intersection of phenotype and genotype', and the genome size of eukaryotes varies over five orders of magnitude, with a distribution skewed toward small values, around 2 picograms (pg) (Oliver et al., 2007). This variation does not seem to be correlated with the complexity of the organism or with the number of genes in eukaryotes, leading to what is called the "C–value paradox" (Moore, 1984; Gregory, 2001, 2005a; Eddy, 2012). It has been questioned, for example, why similar organisms with similar amounts of coding sequence have different amounts of DNA. While changes in gene sequences are often slow and gradual, changes in genome size can be rapid and abrupt as a consequence of chromosomal rearrangements or duplications (Alberts et al., 2007).

The main methods used to estimate the total nuclear genome size are image cytometry, flow cytometry (FCM), and complete genome sequencing (Gregory, 2005b). Image cytometry was the first method used to determine genome size estimates. Basically, it operates by statically imaging a large number of cells stained with specific chemicals or fluorochromes, using optical microscopy (Torresan et al., 1994; Basiji et al., 2007). In contrast, flow cytometry evaluates the relative fluorescence intensity of suspended nuclei, also stained with specific fluorochromes, and presents the data in a typical histogram with a higher peak relative to the nuclei in the G0/G1 phase of cell cycle, and a lower peak, relative to the nuclei in G2 phase (Price et al., 2000; Dolezel and Bartos, 2005). The complete genome sequencing method, on the other hand, provides the complete DNA sequence of the genome of an organism at a single time with the precise order of the nucleotides and an estimate of the genome size after its assembly (Klug et al., 2014). A fourth less common technique known as biochemical analysis (BCA) was used during the early studies of genome size. It includes 'the chemical extraction and quantification of DNA combined with cell counts to give an average DNA amount per nucleus or the reassociation kinetics, in which the DNA molecule was denatured and then the time taken for the strands to renature is used to calculate the amount of DNA (Gregory, 2005b). Among the methods, flow cytometry has been shown to be the least cost and time expensive technique when compared to other molecular tools and provides rapid generation of accurate results (Merkel et al., 1987; Doležel et al., 2007).

According to Gregory (2018), haploid DNA contents (C–values, in picograms - pg) are currently available for 6,222 species of animals (3,793 vertebrates and 2,429 invertebrates), with insects representing 21.6% of this total. Li and Heinz (2000) performed the first DNA content estimation of an ant by mean of biochemical analysis (BCA), to quantify the genome of *Solenopsis invicta* Buren, 1972. Subsequently, Johnston et al. (2004) also estimated the genome size of *S. invicta* but now using flow cytometry. Yet, in 2008, Tsutsui et al. (2008) carried out the first comprehensive study regarding the evolution of the genome size in ants, reporting genome size estimates for 40 species from nine subfamilies. This was the last inclusion of a large number of ant species estimates to the genome size database that was followed by the study of Ardila–Garcia et al. (2010), which added a further 29 species. These two studies raised different questions about genome size, being the first a study of genome size evolution in Formicidae and the second a study of correlation between genome size with parasitism and eusociality in the order Hymenoptera as a whole. It is important to note that they applied different methodologies in genome size estimation: in Tsutsui et al. (2008) the DNA content was estimated by using only flow cytometry, while Ardila–Garcia et al. (2010) also performed the FIAD method (Feulgen image analysis densitometry) to estimate the DNA content, and then compared the results from both techniques.

Later, others studies explored the DNA content of ants, however in some cases covering only one species through complete genome sequencing (*e.g.* Nygaard et al., 2011) or, in other cases, considering specifically an ant genus through flow cytometry. The genome size of the genus *Mycetophylax* Emery, 1913 (*sensu* Klingenberg and Brandão, 2009) was estimated by Cardoso et al. (2012) that explored the data placing them in a phylogenetic context, also correlating it with chromosome number of fungus–growing ants; and Aguiar et al. (2016) that evaluated three *Camponotus* Mayr, 1861 species, exploring their correlation with the karyotype of the studied species.

Despite the importance of genome size, little is known about the ecological and evolutionary consequences of DNA amount in ants. Yet, the biological sig-

nificance and evolution of the genome size diversity in other groups has received much more attention over the last decades (Dufresne and Jeffery, 2011; Alfsnes et al., 2017; Pellicer et al., 2018). The diversity of genome size in plants has been shown to correlate with several phenotypic features of cells and ultimately the organisms. For instance, plant species with larger genomes are adapted to xeric and higher elevation environments (*e.g.* Bottini et al., 2000). Here, we evaluate the available information about the genome size of ants, assembling the DNA content estimated so far, in order to provide insights into the distribution, evolution and possible consequences of ant genome size diversity. We have also investigated and verified the needs of a re–evaluation in the genome size data (DNA C–value) for ants, as well the technique used in the estimation of the DNA content in respect of methodological issues such as: the internal standard and tissues used in the analysis. The basic information about ant genomes analyzed here may improve our knowledge about the evolution and diversification regarding this diverse group of insects and may help as a baseline and guidance for future studies about ant genome biology.

MATERIALS AND METHODS

To evaluate the knowledge about nuclear DNA content on ants, we compiled the haploid genome size estimates for ants and other insect groups from the Animal Genome Size Database (Gregory, 2018) and from the literature by searching in the publication databases Scopus® and ISI Web Science Knowledge™, by using the terms: "genome size", "DNA amount", "C–value" and "ants". Based on the seven manuscripts found on ant genome size, we evaluated the method used to measure genome size, the type of tissue and the internal standard used to obtain the total content of DNA.

To examine the genome size variation over Formicidae subfamilies we compiled the estimates in a Table of all the values available in the literature, expressed in picograms of DNA (pg) and mega base pairs (Mbp). Then we manually placed them in the phylogenetic tree proposed by Moreau and Bell (2013) by collapsing branches with equal names (same Operational Units - OTUs) and separating the subfamilies by color. General linear models were built to check for differences between the averaged genome sizes of the sampled subfamilies. The differences in genome size average for each subfamily were assessed by variance analysis of the GLM. When the *p*-value of ANOVA was significant ($p < 0.05$), a contrast analysis at 5% level was then performed to determine which mean was different. All the statistical analysis was performed in R v2.15.1 software (R Core Team, 2013) and GLM was submitted to residual analysis to evaluate adequacy of normal error distribution (Crawley, 2013).

RESULTS AND DISCUSSION

Overview: number of estimates, methods, tissues and internal standards used

The compiled data resulted in 86 specimens of ants whose genome size had been estimated, comprising 69 different species (Table 1). This number represents 0.52% of the total number of 13,369 ant species accepted until now, covering only 40 genera from 333 accepted (Bolton, 2018). From 17 existing subfamilies, we only found estimates for nine, with Myrmicinae having the largest number of species evaluated (32 spp.) (Figure 1). The number of estimates may reflect the richness of this subfamily that is the most diverse within Formicidae. Yet, Formicinae and Dolichoderinae together bear 20 spp. with DNA content estimates available. These three subfamilies represent 65% of DNA content estimates on ants.

The two main methods used to estimate DNA content in ants were FCM and FIAD. A third method, biochemical analysis (BCA), was used in a pioneering work from Li and Heinz (2000) in order to estimate the genome size sole for *Solenopsis invicta*. It is important to mention that *S. invicta* has the genome size estimates by all three methods listed above and different values were obtained in each estimate: 0.60 pg by BCA (Li and Heinz, 2000), 0.47 pg by FIAD (Ardila-Garcia et al., 2010) and 0.77 pg by flow cytometry (Johnston et al., 2004). Such huge variation in genome sizes may be explained by the occurrence of different ploidy levels in *S. invicta* or even outcomes due the different techniques employed in the studies. Cytogenetical evidence suggests that there may be different levels of ploidy in *S. invicta*.

All genome sizes are estimated by mean of comparison with nuclei of reference standard, whose genome size is known that is called the "internal standard". In the genome size estimation *Drosophila melanogaster* Meigen, 1830 (0.18 pg), *Scaptotrigona xantotricha* Moure, 1950 (0.43 pg) and *Tenebrio molitor* Linnaeus, 1758 (0.52 pg) are the internal standards most commonly used considering Hymenoptera as a whole. Most of the estimates were obtained using *D. melanogaster* as internal standard (76%), while FCM was the most common method used (83.5%). Generally, brain tissue is used to estimate nuclear genome size, but cells (hemocytes) obtained through hemolymph smears have also been tested (Ardi-

Table 1. Overview of the genome size data available in literature for Formicidae species.

Subfamily	Species	1C-value (pg)	1C-value (Mbp)	Method	Cell type	Standard	References
Amplyoponinae	*Amblyopone pallipes (Haldeman, 1844)**	0.34	332.52	FCM	BR	DM	Tsutsui et al., 2008
	*Amblyopone pallipes (Haldeman, 1844)**	0.37	361.86	FCM	BR	DM	Ardila-Garcia et al., 2010
Dolichoderinae	*Dolichoderus mariae* (Forel, 1885)	0.18	176.04	FCM	BR	DM	Ardila-Garcia et al., 2010
	Dolichoderus taschenbergi (Mayr, 1866)	0.23	224.94	FCM	BR	DM	Ardila-Garcia et al., 2010
	Dorymyrmex bicolor Wheeler, 1906	0.25	244.5	FCM	BR	DM	Tsutsui et al., 2008
	Dorymyrmex bureni (Trager, 1988)	0.18	176.04	FIAD	HE	TM	Ardila-Garcia et al., 2010
	Forelius pruinosus (Roger, 1863)	0.22	215.16	FIAD	HE	TM	Ardila-Garcia et al., 2010
	Linepithema humile (Mayr, 1868)	0.26	254.28	FCM	BR	DM	Tsutsui et al., 2008
	Linepithema humile (Mayr, 1868)	0.26	250.8	Genome sequencing	NS	NS	Smith et al., 2011
	Liometopum occidentale Emery, 1895	0.29	283.62	FCM	BR	DM	Tsutsui et al., 2008
	Tapinoma sessile (Say, 1836)	0.37	361.86	FCM	BR	DM	Ardila-Garcia et al., 2010
	Tapinoma sessile (Say, 1836) *A*	0.38	371.64	FCM	BR	DM	Tsutsui et al., 2008
	Tapinoma sessile (Say, 1836) *B*	0.61	596.58	FCM	BR	DM	Tsutsui et al., 2008
Dorylinae	*Cerapachys edentata*	0.22	215.16	FCM	BR	DM	Tsutsui et al., 2008
	Eciton burchelli (Westwood, 1842)	0.27	264.06	FCM	BR	DM	Tsutsui et al., 2008
	Labidus coecus (Latreille, 1802)	0.37	361.86	FCM	BR	DM	Tsutsui et al., 2008
Ectatomminae	*Ectatomma tuberculatum* (Olivier, 1792)	0.71	694.38	FCM	BR	DM	Tsutsui et al., 2008
Formicinae	*Camponotus castaneus* (Latreille, 1802)	0.31	303.18	FCM	BR	DM	Tsutsui et al., 2008
	Camponotus crassus Mayr, 1862	0.29	283.62	FCM	BR	SX	Aguiar et al., 2016
	Camponotus floridanus (Buckley, 1866)	0.23	224.94	FIAD	HE	TM	Ardila-Garcia et al., 2010
	Camponotus floridanus (Buckley, 1866)	0.245	240	Genome sequencing	NS	NS	Bonasio et al., 2010
	Camponotus pennsylvanicus (De Geer, 1773)	0.33	322.74	FCM	BR	DM	Tsutsui et al., 2008
	Camponotus renggeri Emery, 1894	0.29	283.62	FCM	BR	SX	Aguiar et al., 2016
	Camponotus rufipes (Fabricius, 1775)	0.29	283.62	FCM	BR	SX	Aguiar et al., 2016
	Formica pallidifulva Wheeler, 1913	0.39	381.42	FCM	BR	DM	Tsutsui et al., 2008
	Lasius (Acanthomyops) latipes (Walsh, 1863)	0.27	264.06	FCM	BR	DM	Ardila-Garcia et al., 2010
	Lasius alienus (Foerster, 1850)	0.31	303.18	FCM	BR	DM	Tsutsui et al., 2008
	Lasius minutus Emery, 1893	0.23	224.94	FCM	BR	DM	Ardila-Garcia et al., 2010
	Paratrechina longicornis (Latreille, 1802)	0.18	176.04	FIAD	HE	TM	Ardila-Garcia et al., 2010
	Prenolepis imparis (Say, 1836)	0.30	293.4	FCM	BR	DM	Tsutsui et al., 2008
Myrmeciinae	*Myrmecia varians* Mayr, 1876	0.28	273.84	FCM	BR	DM	Tsutsui et al., 2008
Myrmicinae	*Acromyrmex echinatior* (Forel, 1899)	0.36	335	FCM	BR	CRBC	Sïrvio et al., 2006
	Acromyrmex echinatior (Forel, 1899)	0.32	313	Genome sequencing	NS	NS	Nygaard et al., 2011
	Aphaenogaster rudis (texana group N16) Enzmann, 1947	0.43	420.54	FCM	BR	DM	Ardila-Garcia et al., 2010
	Aphaenogaster rudis (texana group N17) Enzmann, 1947	0.46	449.88	FCM	BR	DM	Ardila-Garcia et al., 2010
	Aphaenogaster rudis (texana group N22b) Enzmann, 1947	0.44	430.32	FCM	BR	DM	Ardila-Garcia et al., 2010
	Aphaenogaster fulva Roger, 1863	0.42	410.76	FCM	BR	DM	Ardila-Garcia et al., 2010
	Aphaenogaster treatae Forel, 1886	0.50	489	FCM	BR	DM	Ardila-Garcia et al., 2010
	Apterostigma dentigerum Wheeler, 1925	0.65	635.7	FCM	BR	DM	Tsutsui et al., 2008
	Atta cephalotes (Linnaeus, 1758)	0.31	303.18	FCM	BR	DM	Tsutsui et al., 2008
	Atta cephalotes (Linnaeus, 1758)	0.30	290	Genome sequencing	NS	NS	Suen et al., 2011
	Atta colombica Guérin-Méneville, 1844	0.31	303.18	FCM	BR	DM	Tsutsui et al., 2008
	Atta texana (Buckley, 1860)	0.27	264.06	FCM	BR	DM	Ardila-Garcia et al., 2010

Subfamily	Species	1C-value (pg)	1C-value (Mbp)	Method	Cell type	Standard	References
	Crematogaster hespera Buren, 1968*	0.28	273.84	FCM	BR	DM	Tsutsui et al., 2008
	Eurhopalothrix procera (Emery, 1897)	0.39	381.42	FCM	BR	DM	Tsutsui et al., 2008
	Messor andrei (Mayr, 1886)*	0.26	254.28	FCM	BR	DM	Tsutsui et al., 2008
	Monomorium viridum Brown, 1943	0.50	489	FIAD	HE	TM	Ardila-Garcia et al., 2010
	Mycetophylax conformis (Mayr, 1884)	0.32	312.96	FCM	BR	SX	Cardoso et al., 2012
	Mycetophylax morschi (Emery, 1888)	0.32	312.96	FCM	BR	SX	Cardoso et al., 2012
	Mycetophylax simplex (Emery, 1888)	0.39	381.42	FCM	BR	SX	Cardoso et al., 2012
	Myrmecina americana Emery, 1895 A	0.26	254.28	FCM	BR	DM	Tsutsui et al., 2008
	Myrmecina americana Emery, 1895 B	0.31	303.18	FCM	BR	DM	Tsutsui et al., 2008
	Pheidole dentata Mayr, 1886	0.24	234.72	FIAD	HE	TM	Ardila-Garcia et al., 2010
	Pheidole floridana Emery, 1895	0.21	205.38	FIAD	HE	TM	Ardila-Garcia et al., 2010
	Pheidole hyatti Emery, 1895	0.33	322.74	FCM	BR	DM	Tsutsui et al., 2008
	Pogonomyrmex badius (Latreille, 1802)	0.27	264.06	FCM	BR	DM	Tsutsui et al., 2008
	Pogonomyrmex barbatus (Smith, 1858)	0.24	235	Genome sequencing	NS	NS	Smith et al., 2011
	Pogonomyrmex californicus (Buckley, 1867)	0.25	244.5	FCM	BR	DM	Tsutsui et al., 2008
	Pogonomyrmex coarctatus Mayr, 1868	0.29	283.62	FCM	BR	DM	Tsutsui et al., 2008
	Pyramica rostrata (Emery, 1895)	0.28	273.84	FCM	BR	DM	Tsutsui et al., 2008
	Sericomyrmex amabilis Wheeler, 1925	0.45	440.1	FCM	BR	DM	Tsutsui et al., 2008
	Solenopsis invicta Buren, 1972	0.62	606.36	BCA	BR	NS	Li and Heinz 2000
	Solenopsis invicta Buren, 1972	0.77	753.06	FCM	BR	DM	Johnston et al., 2004
	Solenopsis invicta Buren, 1972	0.47	459.66	FIAD	HE	TM	Ardila-Garcia et al., 2010
	Solenopsis invicta Buren, 1972	0.49	482	Genome sequencing	NS	NS	Wurm et al., 2011
	Solenopsis molesta Emery, 1895	0.38	371.64	FCM	BR	DM	Ardila-Garcia et al., 2010
	Solenopsis xyloni McCook, 1880	0.48	469.44	FCM	BR	DM	Tsutsui et al., 2008
	Temnothorax ambiguus (Emery, 1895)	0.31	303.18	FCM	BR	DM	Ardila-Garcia et al., 2010
	Temnothorax texanus (Wheeler, 1903)	0.32	312.96	FCM	BR	DM	Ardila-Garcia et al., 2010
	Tetramorium caespitum	0.26	254.28	FCM	BR	DM	Tsutsui et al., 2008
	Tetramorium caespitum (Linnaeus, 1758)	0.27	264.06	FCM	BR	DM	Ardila-Garcia et al., 2010
	Trachymyrmex septentrionalis (McCook, 1881)	0.25	244.5	FIAD	HE	TM	Ardila-Garcia et al., 2010
Ponerinae	*Dinoponera australis* Emery, 1901	0.57	557.46	FCM	BR	DM	Tsutsui et al., 2008
	Harpegnathos saltator Jerdon, 1851	0.34	330	Genome sequencing	NS	NS	Bonasio et al., 2010
	Odontomachus bauri Emery, 1892	0.49	479.22	FCM	BR	DM	Tsutsui et al., 2008
	Odontomachus brunneus (Patton, 1894)	0.33	322.74	FIAD	HE	TM	Ardila-Garcia et al., 2010
	Odontomachus brunneus (Patton, 1894)	0.44	430.32	FCM	BR	DM	Tsutsui et al., 2008
	Odontomachus Cephalotes Smith, 1863	0.43	420.54	FCM	BR	DM	Tsutsui et al., 2008
	Odontomachus chelifer (Latreille, 1802)	0.54	528.12	FCM	BR	DM	Tsutsui et al., 2008
	Odontomachus clarus Wheeler, 1915	0.42	410.76	FCM	BR	DM	Tsutsui et al., 2008
	Odontomachus haematodus (Linnaeus, 1758)	0.51	498.78	FCM	BR	DM	Tsutsui et al., 2008
	Ponera pennsylvanica Buckley, 1866	0.55	537.9	FCM	BR	DM	Ardila-Garcia et al., 2010
	Ponera pennsylvanica Buckley, 1866	0.60	586.8	FCM	BR	DM	Tsutsui et al., 2008
Pseudomyrmicinae	*Pseudomyrmex ejectus* (Smith, 1858)	0.29	283.62	FIAD	HE	TM	Ardila-Garcia et al., 2010
	Pseudomyrmex gracilis (Fabricius, 1804)	0.35	342.3	FCM, FIAD	BR, HE	DM, TM	Ardila-Garcia et al., 2010
	Pseudomyrmex gracilis (Fabricius, 1804)	0.40	391.2	FCM	BR	DM	Tsutsui et al., 2008

Method: FCM = Flow cytometry, FIAD = Feulgen image analysis densitometry; Cell type: BR = Brain tissue, HE = Haemocyte; Standard: DM = *Drosophila melanogaster*, CRBC = Chicken Red Blood Cells, SX = *Scaptotrigona xantotricha*, TM = *Tenebrio molitor*, NS = not specified. *Valid names: *Stigmatomma pallipes* (Haldeman, 1844); *Crematogaster laeviuscula* Mayr, 1870; Veromessor andrei (Mayr, 1886), respectively.

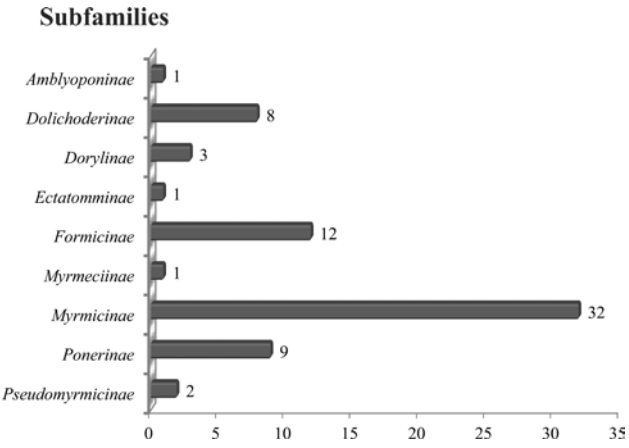

Figure 1. Distribution of the number of species across Formicidae subfamilies with published genome size estimates. The list of species is presented in Table 1.

la-Garcia et al., 2010). Considering *S. xantotricha*, this internal standard was started to be used in studies comprised stingless bees, and after with ants by the same research group (Tavares et al. 2010, Cardoso et al. 2012, Aguiar et al. 2016). Since no genome size histograms are available in either Ardila-Garcia et al. (2010) or Tsutsui et al. (2008), it is impossible to compare the usefulness of one or another internal standard considering the other two studies (Cardoso et al. 2012 and Aguiar et al. 2016) used *S. xantotricha*. In studies with plants, the choice of an appropriate internal standard considers the genome size magnitude of standard and studied group, mainly to avoid superposition of picks.

Concerning the methods employed in genome size estimation, the study from Ardila-Garcia et al. (2010) is the only one that multiple species in the same work had the genome measured by two methods. They evaluated by FIAD and FCM the genome size on *Odontomachus brunneus*, *Pseudomyrmex gracilis*, and *Solenopsis invicta* and showed that the estimates using the first method tended to be smaller. The authors argue that the values from both techniques do not differ statistically. However, it is difficult to say that this difference is solely due to the technique itself, since both the tissue and the internal standard used during the analysis were different.

The nuclear DNA content of some ants has also been measured using a fourth method, which utilized complete genome sequencing techniques in species such as *Acromyrmex echinatior* (Forel, 1899) (Nygaard et al., 2011), *Atta cephalotes* (Linnaeus, 1758) (Suen et al., 2011), *Camponotus floridanus* (Buckley, 1866) (Bonasio et al., 2010), *Harpegnathos saltator* Jerdon, 1851 (Bonasio et al., 2010), *Linepithema humile* (Mayr, 1868) (Smith et al., 2011), *Pogonomyrmex barbatus* (Smith, 1858) (Smith et al., 2011) and *Solenopsis invicta* (Wurm et al., 2011) (Table 1). The genome size of *Ac. echinatior* was 313 Mbp (or 0.32 pg considering 1 pg = 978 Mbp; (Doležel et al., 2003)) obtained with complete genome sequencing (Nygaard et al., 2011) and 335 Mbp (0.36 pg) by FCM (Sïrvio et al., 2006). This difference can be attributed to the loss of repetitive regions and some chromosomal regions, such as telomeres, through genome sequencing techniques (Gregory, 2005b). The same was observed in *A. cephalotes*, whose genome size estimated by complete genome sequencing was 290 Mbp (approximately 0.30 pg) (Suen et al., 2011) and by FCM was 303.18 Mbp (approximately 0.31 pg) (Tsutsui et al., 2008). The differences were greater in *S. invicta*, whose genome size was obtained with all four different techniques (BCA, FIAD, FCM, and Genome Sequencing): 606 Mbp (0.62 pg) (Li and Heinz, 2000) by BCA, 459 Mbp (0.47 pg) (Ardila-Garcia et al., 2010) by FIAD, 753 Mbp (0.77 pg) (Johnston et al., 2004) by FCM and 482 Mbp (0.49 pg) (Wurm et al., 2011) by genome sequencing. Values obtained with FIAD and genome sequencing are more similar. So, considering the loss of certain repetitive regions of DNA by the complete genome sequencing and the difficulties in using other techniques such as BCA and FIAD (mainly due to the low number of repetitions available to estimate de DNA amount) the use of FCM has proven to be the most efficient methodology to obtain accurately the total DNA content.

Genome size evolution

The reported DNA C–value of insects range from 0.07 pg (*Clunio tsushimensis* Tokunaga, 1933 – Diptera) to 16.93 pg (*Podisma pedestris* Linnaeus, 1758 – Orthoptera) and out of 1344 estimates found, 1224 (91%) were comprised of values between 0.07 to 2.00 pg (Gregory, 2018). From 27 orders of insects, 24 currently have estimates of genome size, with Diptera accounting for the largest number of measurements (386 specimens, 29% of the total), followed by Coleoptera (278 specimens, 21% of the total) and Hymenoptera (240 specimens, 18% of the total). The average genome size for the Formicidae (Hymenoptera) was 0.36 pg (± 0.13), with values ranging from 0.18 pg (the smallest value, found in Dolichoderinae and in Formicinae) to 0.77 pg in *S. invicta* (Myrmicinae) (Table 1; Figure 2), being always less than 1 pg. This is in accordance with the pattern already observed for others eukaryotes that most of the distribution of genome size is skewed towards smaller values (Oliver et al., 2007), since it is evident that the number of species declines as the genome doubles in size.

As can be seen in Figure 2 the variation of genome size among species of a subfamily is similar to the varia-

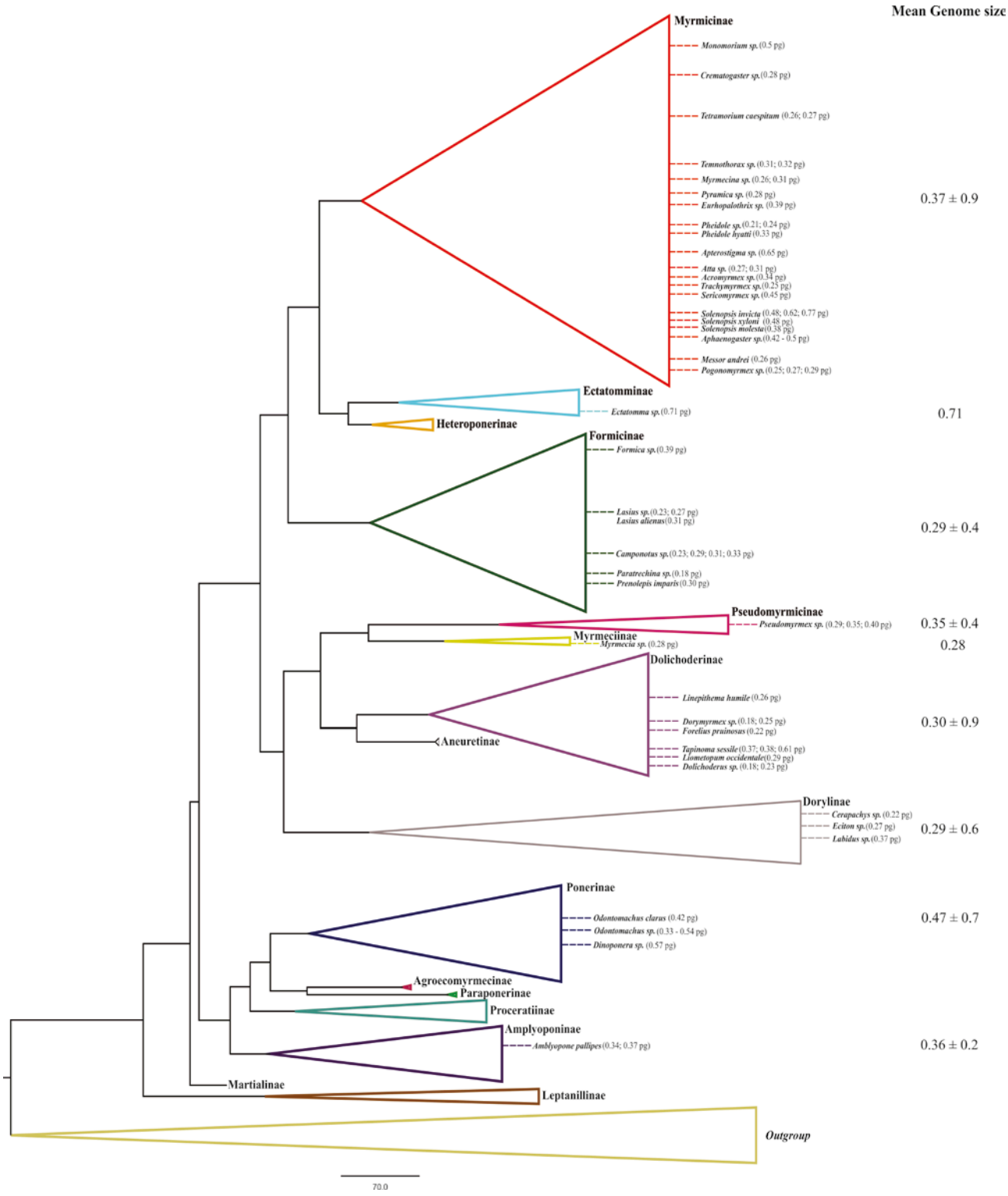

Figure 2. Phylogeny of the extant Formicidae. Phylogenetic tree redrawn from Moreau and Bell (2013). The figure highlights the subfamilies containing species with estimated genome size. Aside of each terminal on the tree the genome size is shown in picograms (pg) of DNA and also the mean genome size per Formicidae subfamilies.

tion found between subfamilies. Significant differences in genome size were observed between the subfamilies sampled (ANOVA, *p-value* < 0.01). Through contrast analysis, most of the subfamilies grouped statistically (group average = 0.34 pg, *p-value* > 0.05) except for Ponerinae, whose average was different from the others (average = 0.47, *p-value* < 0.01). The subfamilies Ectatomminae (*Ectatomma tuberculatum* (Olivier, 1792), 0.71 pg) and Myrmeciinae (*Myrmecia varians* Mayr, 1876, 0.28 pg) were not considered in the analysis because only one value for each was available, so it was not possible to calculate a mean for the comparison test (Figure 2). Differences in the genome size were also observed between genera within the sampled subfamilies and mainly between species of the same genus, as observed in *Atta* Fabricius, 1804 spp. (*e.g. Atta cephalotes* = 0.31 pg and *Atta texana* (Buckley, 1860) = 0.27 pg), *Camponotus* spp. (*e.g. Camponotus floridanus* = 0.23 pg and *Camponotus pennsylvanicus* (De Geer, 1773) = 0.33 pg) and *Odontomachus* spp. (*e.g. Odontomachus brunneus* (Patton, 1894) = 0.33 pg and *Odontomachus chelifer* (Latreille, 1802) = 0.54 pg) (Table 1, Figure 2). These differences in genome size among closely related species have been associated in several studies with the amount of heterochromatin in the chromosomes (Lopes et al., 2009; Tavares et al., 2010; Cardoso et al., 2012), transposable elements (Kidwell, 2002; Vieira et al., 2002) and other repetitive genome sequences (Gregory and Hebert, 1999; Petrov, 2001). In some species, as *Ectatomma tuberculatum* and *Apterostigma dentigerum* Wheeler, 1925 the differences in genome size was correlated with whole genome duplication events given the large genome size of this both species when compared with the others of Formicidae (0.71 pg and 0.65 pg, respectively) (Tsutsui et al., 2008).

The correlation between genome size and chromosome number has been reported in some studies for ants, for example, Cardoso et al. (2012) within fungus–growing ants. In their study, they found a relationship between these two characteristics being *Sericomyrmex amabilis* Wheeler, 1925 the species with the highest number of chromosomes and also the largest genome size and other two species with the lowest number of chromosomes also had the smallest genome size. Correlation between chromosome and genome size has been reported for some insects. For instance, Ardila–Garcia and Gregory (2009) also found this positive correlation among species of damselflies, but not in dragonflies (Insecta: Odonata). Lack of correlation between genome size and chromosome number has been shown in the highly eusocial stingless bees of Meliponini tribe (Hymenoptera: Apidae) (Tavares et al., 2012). Yet, body size was correlated with genome size among dragonflies and damselflies (Ardila–Garcia and Gregory, 2009), but not among stingless bees (Tavares et al., 2010) or ants (Tsutsui et al., 2008). These contradictory observations remain the issue whether genome size is shaped by neutral or natural selection.

It has been proven that changes in genome size are related to the addition and deletion of heterochromatin and that species with low amounts of heterochromatin also have lower DNA content per haploid nucleus, likewise the reverse is also true (Tavares et al., 2017). Although conclusion remarks still unlike due the limited availability of data and sampling representing more genera and species, important question could be addressed when more data became available. Considering the assembled data e evidences from other social insects, as bees, we propose that the differences in DNA content among ant species may also be related to the different amount of heterochromatin in the chromosomes. Nevertheless, we emphasize that this can only be confirmed after a detailed study of chromosomal structure and chromosome counts across genera and subfamilies.

CONCLUSIONS AND PERSPECTIVES

The compilation of the genome size data currently available in the literature for ants has highlighted the scarcity of estimates for this hyper–diverse family (with only 0.52% of known species having been estimated). Little is known about the methodologies employed and the lack of standardization of the works makes it problematic to compare the different estimates (Ardila–Garcia et al., 2010; Doležel and Greilhuber, 2010), especially regarding the buffer to isolate the nuclei, tissue and internal standard used. Also, the mechanisms involved in the evolution of the genome in ants are still unknown, especially those related to the total amount of heterochromatin in chromosomes and their relationship with genome size; the whole–genome duplication events, which could explain the large variation of the genome of some species, such as *Ectatoma tuberculatum* and *Apterostigma dentigerum* (Tsutsui et al., 2008); and polyploidy events as in *Solenopsis invicta* males (Glancey et al., 1976; Lorite and Palomeque, 2010). Our analysis highlight the importance and accuracy of the use of FCM to estimate the genome size of species and the possibility of obtaining robust results, since a large number of nuclei (10.000 or more per sample) are analyzed to determine the DNA content. Therefore, the standardization of the techniques used and a large–scale study of the ant genome size are urgently required, given the ecological and economic importance of this group contributing to

our knowledge on ant evolution by using another genetic diversity and independent dataset.

CONFLICT OF INTEREST

The authors declare that they have no conflict of interest.

ACKNOWLEDGMENTS

This study was carried out as part of the PhD thesis of the first author. Author is grateful to CAPES for the scholarship. The authors thanks FAPEMIG (Fundação de Amparo à Pesquisa de Minas Gerais), CNPq (Conselho Nacional de Desenvolvimento Científico e Tecnológico) and UFOP (Universidade Federal de Ouro Preto) for their financial support. Author received a Research Productivity Fellowship from FAPEMIG (PPM–00126–15).

REFERENCES

Aguiar HJAC Barros LAC Soares FAF Carvalho CR Pompolo SG (2016) Estimation of nuclear genome size of three species of *Camponotus* (Mayr 1861) (Hymenoptera: Formicidae: Formicinae) and their cytogenetic relationship. Sociobiology 63: 777–782. http://dxdoiorg/1013102/sociobiologyv63i2948

Alberts B, Johnson A, Lewis J, Raff M, Roberts K, Walter P (2007) Molecular biology of the cell fifth ed. Garland Science New York.

Alfsnes K, Leinaas HP, Hessen DO (2017) Genome size in arthropods, different roles of phylogeny habitat and life history in insects and crustaceans. Ecology and Evolution 7: 5939–5947. https://doi.org/10.1002/ece3.3163

Ardila–Garcia AM, Gregory TR (2009) An exploration of genome size diversity in dragonflies and damselflies (Insecta: Odonata). Journal of Zoology 278: 163–173. https://doi.org/10.1111/j.1469-7998.2009.00557.x

Ardila–Garcia AM, Umphrey GJ, Gregory TR (2010) An expansion of the genome size dataset for the insect order Hymenoptera with a first test of parasitism and eusociality as possible constraints. Insect Molecular Biology 19: 337–346. https://doi.org/10.1111/j.1365-2583.2010.00992.x

Basiji DA, Ortyn WE, Liang L, Venkatachalam V, Morrissey P (2007) Cellular image analysis and imaging by flow cytometry. Clinics in Laboratory Medicine 27: 653–70. https://doi.org/10.1016/j.cll.2007.05.008

Bolton, B. 2018. An online catalog of the ants of the world. Available from http://antcat.org. [accessed 04 March 2018].

Bonasio R, Zhang G Ye C, Mutti NS, Fang X, Qin N, Donahue G, Yang P, Li Q, Li C, Zhang P, Huang Z, Berger SL, Reinberg D, Wang J, Liebig J (2010) Genomic comparison of the ants *Camponotus floridanus* and *Harpegnathos saltator*. Science 329: 1068–1071. https://doi.org/10.1126/science.1192428

Brandão CRF (1999) Família Formicidae in: Brandão CRF, Cancello EM (Eds) Invertebrados terrestres. ed. Biodiversidade do Estado de São Paulo: síntese do conhecimento ao final do século XX. (Joly CA Bicudo CEM (orgs)) FAPESP São Paulo pp 215–223.

Cardoso DC, Carvalho CR, Cristiano MP, Soares FAF, Tavares MG (2012) Estimation of nuclear genome size of the genus *Mycetophylax* Emery 1913: evidence of no whole–genome duplication in Neoattini. Comptes Rendus Biologies 335: 619–624. http://dx.doi.org/10.1016/j.rvi.2012.09.012

Crawley MJ (2013) The R Book second ed. John Wiley & Sons Ltd. London.

Doležel J, Bartoš J (2005) Plant DNA flow cytometry and estimation of nuclear genome size. Annals of Botany 95: 99–110. https://doi.org/10.1093/aob/mci005

Doležel J, Bartoš J, Voglmayr H, Greilhuber J (2003) Nuclear DNA content and genome size of trout and human. Cytometry. Part A 51: 127–128. https://doi.org/10.1002/cyto.a.10013

Doležel J, Greilhuber J (2010) Nuclear genome size: are we getting closer? Cytometry. Part A 77A: 635–642. https://doi.org/10.1002/cyto.a.20915

Doležel J, Greilhuber J, Suda J (2007) Estimation of nuclear DNA content in plants using flow cytometry. Nature Protocols 2 2233–2244. https://doi.org/10.1038/nprot.2007.310

Dufresne F, Jeffery N (2011) A guided tour of large genome size in animals: what we know and where we are heading. Chromosome Research 19: 925–938. https://doi.org/10.1007/s10577-011-9248-x

Eddy SR (2012) The C–value paradox junk DNA and ENCODE. Current Biology 22: 898–899. https://doi.org/10.1016/j.cub.2012.10.002

Françoso ML, Brandão CRF (1993) Classificação superior dos Formicidae. Biotemas 6: 121–132. https://doi.org/10.5007/%25x

Glancey BM, Romain MKS, Crozier RH (1976) Chromosome numbers of the red and the black imported fire ants *Solenopsis invicta* and *S. richteri*. Annals of the Entomological Society of America 69: 469–470. https://doi.org/10.1093/aesa/69.3.469

Goodisman MAD, Kovacs JL, Hunt BG (2008) Functional genetics and genomics in ants (Hymenoptera: Formicidae): The interplay of genes and social life. Myrmecological News 11: 107–117.

Gregory TR (2001) Coincidence coevolution or causation? DNA content cell size and the C–value enigma. Biological Reviews 76: 65–101. https://doi.org/10.1111/j.1469-185X.2000.tb00059.x

Gregory TR (2005a) The C–value enigma in plants and animals: a review of parallels and an appeal for partnership. Annals of Botany 95: 133–146. https://dx.doi.org/10.1093%2Faob%2Fmci009

Gregory TR (2005b) Genome Size Evolution in Animals in: Gregory TR (Ed) The Evolution of the Genome. Elsevier San Diego pp 3–87.

Gregory TR (2018) Animal genome size database. Available online: http://wwwgenomesizecom. [accessed 04 March 2018].

Gregory TR, Hebert PDN (1999) The modulation of DNA content: proximate causes and ultimate consequences. Genome Research 9: 317–324. https://doi.org/10.1101/gr.9.4.317

Hölldobler B, Wilson EO (1990) The ants. Harvard University Press Cambridge.

Johnston JS, Ross LD, Beani L, Hughes DP, Kathirithamby J (2004) Tiny genomes and endoreduplication in Strepsiptera. Insect Molecular Biology 13: 581–585. https://doi.org/10.1111/j.0962-1075.2004.00514.x

Kidwell MG (2002) Transposable elements and the evolution of genome size in eukaryotes. Genetica 115: 49–63. https://doi.org/10.1023/A:1016072014259

Klingenberg C, Brandão CRF (2009) Revision of the fungus–growing ant genera *Mycetophylax* Emery and *Paramycetophylax* Kusnezov rev stat and description of *Kalathomyrmex* n gen (Formicidae: Myrmicinae: Attini). Zootaxa 2052: 1–31.

Klug WS, Cummings MR, Spencer CA, Palladino MA (2014) Concepts of genetics eleventh. Ed. Pearson. New Jersey

Li J, Heinz KM (2000) Genome complexity and organization in the red imported fire ant *Solenopsis invicta* Buren. Genetical Research 75: 129–135

Lopes DM, Carvalho CR, Clarindo WR, Praça MM, Tavares MG (2009) Genome size estimation of three stingless bee species (Hymenoptera: Meliponinae) by flow cytometry. Apidologie 40: 517–523. https://doi.org/10.1051/apido/2009030

Lorite P, Palomeque T (2010) Karyotype evolution in ants (Hymenoptera: Formicidae) with a review of the known ant chromosome numbers. Myrmecological News 13: 89–102.

Merkel DE, Dressler LG, McGuire WL (1987) Flow cytometry cellular DNA content and prognosis in human malignancy. Journal of Clinical Oncology 5: 1690–1703. https://doi.org/10.1200/JCO.1987.5.10.1690

Moore GP (1984) The C–value paradox. BioScience 34: 425–429. https://doi.org/10.2307/1309631

Moreau CS, Bell CD (2013) Testing the museum versus cradle biological diversity hypothesis: Phylogeny diversification and ancestral biogeographic range evolution of the ants. Evolution 67: 2240–2257. https://doi.org/10.1111/evo.12105

Nygaard S, Zhang G, Schiøtt M, Li C, Wurm Y, Hu H, Zhou J, Ji L, Qiu F, Rasmussen M, Pan H, Hauser F, Krogh A, Grimmelikhuijzen CJP, Wang J, Boomsma JJ (2011) The genome of the leaf–cutting ant *Acromyrmex echinatior* suggests key adaptations to advanced social life and fungus farming. Genome Research 21: 1339–1348. https://dx.doi.org/10.1101%2Fgr.121392.111

Oliver MJ, Petrov D, Ackerly D, Falkowski P, Schofield OM (2007) The mode and tempo of genome size evolution in eukaryotes. Genome Research 17: 594–601. https://dx.doi.org/10.1101%2Fgr.6096207

Pellicer J, Hidalgo O, Dodsworth S, Leitch IJ (2018) Genome Size Diversity and Its Impact on the Evolution of Land Plants. Genes 9: 88. https://doi.org/10.3390/genes9020088

Petrov DA (2001) Evolution of genome size: new approaches to an old problem. Trends in Genetics 17: 23–28. https://doi.org/10.1016/S0168-9525(00)02157-0

Price HJ, Hodnett G, Johnston S (2000) Sunflower (*Helianthus annus*) leaves contain compounds that reduce nuclear propidium iodide fluorescence. Annals of Botany 86: 929–934. https://doi.org/10.1006/anbo.2000.1255

R Core Team (2013) R Foundation for statistical computing. R: a language and environment for statistical computing. http://wwwR–projectorg [accessed 15 May 2017].

Sirviö A, Gadau J, Rueppell O, Lamatsch D, Boomsma JJ, Pamilo P, Page RE Jr (2006) High recombination frequency creates genotypic diversity in colonies of the leaf–cutting ant *Acromyrmex echinatior.* Journal of Evolutionary Biology 19: 1475–1485.

Smith CD, Zimin A, Holt C, Abouheif E, Benton R, Cash E, Croset V, Currie CR, Elhaik E, Elsik CG, Fave M-J, Fernandes V, Gadau J, Gibson JD, Graur D, Grubbs KJ, Hagen DE, Helmkampf M, Holley JA, Hu H, Viniegra ASI, Johnson BR, Johnson RM, Khila A, Kim JW, Laird J, Mathis KA, Moeller JA, Muñoz-Torres MC, Murphy MC, Nakamura R, Nigam S, Overson

RP, Placek JE, Rajakumar R, Reese JT, Robertson HM, Smith CR, Suarez AV, Suen G, Suhr EL, Tao S, Torres CW, Wilgenburg EV, Viljakainen L, Walden KKO, Wild AL, Yandell M, Yorke JA Tsutsui ND (2011) Draft genome of the globally widespread and invasive Argentine ant (*Linepithema humile*). Proceedings of the National Academy of Sciences of the United States of America 108: 5673–5678. https://doi.org/10.1073/pnas.1008617108

Smith CR, Smith CD, Robertson HM, Helmkampf M, Zimin A, Yandell M, Holt C, Hu H, Abouheif E, Benton R, Cash E, Croset V, Currie CR, Elhaik E, Elsik CG, Favé M-J, Fernandes V, Gibson JD, Graur D, Gronenberg W, Grubbs KJ, Hagen DE, Viniegra ASI, Johnson BR, Johnson RM, Khila A, Kim JW, Mathis KA, Munoz-Torres MC, Murphy MC, Mustard JA, Nakamura R, Niehuis O, Nigam S, Overson RP, Placek JE, Rajakumar R, Reese JT, Suen G, Tao S, Torres CW, Tsutsui ND, Viljakainen L, Wolschin F, Gadau J (2011) Draft genome of the red harvester ant *Pogonomyrmex barbatus.* Proceedings of the National Academy of Sciences of the United States of America 108: 5667–5672. https://doi.org/10.1073/pnas.1007901108

Suen G, Teiling C, Li L, Holt C, Abouheif E, Bornberg–Bauer E, Bouffard P, Caldera EJ, Cash E, Cavanaugh A, Denas O, Elhaik E, Favé MJ, Gadau J, Gibson JD, Graur D, Grubbs KJ, Hagen DE, Harkins TT, Helmkampf M, Hu H, Johnson BR, Kim J, Marsh SE, Moeller JA, Muñoz–Torres MC, Murphy MC, Naughton MC, Nigam S, Overson R, Rajakumar R, Reese JT, Scott JJ, Smith CR, Tao S, Tsutsui ND, Viljakainen L, Wissler L, Yandell MD, Zimmer F, Taylor J, Slater SC, Clifton SW, Warren WC, Elsik CG, Smith CD, Weinstock GM, Gerardo NM, Currie CR (2011) The genome sequence of the leaf–cutter ant *Atta cephalotes* reveals insights into its obligate symbiotic lifestyle. PLoS Genetics 7: e1002007. https://doi.org/10.1371/journal.pgen.1002007

Tavares MG, Carvalho CR, Soares FAF (2010) Genome size variation in *Melipona* species (Hymenoptera: Apidae) and sub–grouping by their DNA content. Apidologie 41: 636–642. https://doi.org/10.1051/apido/20010023

Tavares MG, Carvalho CR, Soares FAF, Campos LAO (2012) Genome size diversity in stingless bees (Hymenoptera: Apidae, Meliponini). Apidologie 43: 731–736. https://doi.org/10.1007/s13592-012-0145-x

Tavares MG, Lopes DM, Campos LAO (2017) An overview of cytogenetics of the tribe Meliponini (Hymenoptera: Apidae). Genetica 145 241–258. https://doi.org/10.1007/s10709-017-9961-2

Torresan F, Zanella L, Mattarozzi A, Quiroga A, Bacchini P, Bertoni F, Gandolfi L (1994) DNA analysis with flow cytometry and image cytometry in colorectal polyps. Surgical Endoscopy 8: 1412–1416.

Tsutsui ND, Suarez AV, Spagna JC, Johnston JS (2008) The evolution of genome size in ants. BMC Evolutionary Biology 8: 64. https://doi.org/10.1186/1471-2148-8-64

Vieira C, Nardon C, Arpin C, Lepetit D, Biémont C (2002) Evolution of genome size in *Drosophila* Is the invader's genome being invaded by transposable elements? Molecular Biology and Evolution 19: 1154–1161. https://doi.org/10.1093/oxfordjournals.molbev.a004173

Wurm Y, Wang J, Riba–Grognuz O, Corona M, Nygaard S, Hunt BG, Ingram KK, Falquet L, Nipitwattanaphon M, Gotzek D, Dijkstra MB, Oettler J, Comtesse F, Shih CJ, Wu WJ, Yang CC, Thomas J, Beaudoing E, Pradervand S, Flegel V, Cook ED, Fabbretti R, Stockinger H, Long L, Farmerie WG, Oakey J, Boomsma JJ, Pamilo P, Yi SV, Heinze J, Goodisman MAD, Farinelli L, Harshman K, Hulo N, Cerutti L, Xenarios I, Shoemaker DW, Keller L. (2011) The genome of the fire ant *Solenopsis invicta.* Proceedings of the National Academy of Sciences of the United States of America 108: 5679–5684.

Caryologia
International Journal of Cytology, Cytosystematics and Cytogenetics

Firenze University Press
www.fupress.com/caryologia

OPEN ACCESS

Citation: A.R. Andrada, V. de los Á. Páez, M.S. Caro, P. Kumar (2019) Meiotic irregularities associated to cytomixis in *Buddleja iresinoides* (Griseb.) Hosseus. (Buddlejaceae) and *Castilleja arvensis* Schltdl. & Cham. (Orobanchaceae). *Caryologia* 72(4): 41-49. doi: 10.13128/caryologia-298

Published: December 23, 2019

Data Availability Statement: All relevant data are within the paper and its Supporting Information files.

Competing Interests: The Author(s) declare(s) no conflict of interest.

Meiotic irregularities associated to cytomixis in *Buddleja iresinoides* (Griseb.) Hosseus. (Buddlejaceae) and *Castilleja arvensis* Schltdl. & Cham. (Orobanchaceae)

Aldo Ruben Andrada[1,*], Valeria de los Ángeles Páez[1], M.S. Caro[1,2], P. Kumar[3]

[1] *Fundación Miguel Lillo. Miguel Lillo 251, San Miguel de Tucumán, Tucumán, Argentina*
[2] *Facultad de Ciencias Naturales e Instituto Miguel Lillo. Miguel Lillo 205, San Miguel de Tucumán, Tucumán, Argentina*
[3] *Botanical Survey of India, Northern Regional Centre, Dehradun - 248 195, Uttarakhand, India*
*Corresponding author: arandrada@lillo.org.ar

Abstract. The current paper analyzes the male meiotic behavior in wild populations of *Buddleja iresinoides* and *Castilleja arvensis* from Piedmont areas of the Northwest Region of Argentina. *Castilleja arvensis* showed tetraploid number of chromosome of $2n = 24$. Our results are not in agreement with the previously reported base number $x = 19$ for *Buddleja* and the chromosome number $n = 28$ found for *B. iresinoides* is atypical in the genus. Around 7 % pollen mother cells were aneuploid as they showed meiotic chromosome count of n = 20-21 bivalents. Possible origin for such atypical chromosome number has been discussed in this paper. During the cytological studies we also came across pollen mother cells showing meiotic abnormalities such as cytomixis, chromatin stickiness and anaphase bridges with lagging chromatin. Consequently microsporogenesis was also irregular showing dyads and triads. However, the percentage of these irregularities during meiosis and microsporogenesis was not higher, and pollen fertility was not affected to a great extent. Cytomixis and other meiotic abnormalities in these species are reported here for the first time.

Keywords. *Buddleja iresinoides*, *Castilleja arvensis,* Chromatin, pollen mother cells, cytomixis, chromosome numbers.

INTRODUCTION

The migration of chromatin from the nucleus of one pollen mother cell (PMC) through specialized channels (named cytomictic channels) into an adjacent PMC was observed by Gates (1911) who called it cytomixis. Subsequently, Risueno *et al.* (1969) during their investigations noticed that these intercellular channels were sufficiently large to permit the migration of chro-

Figure 1. Morphological overview of the studied plants, A) General appearance of *Buddleja iresinoides*, and B) inflorescence detail; C) General appearance of *Castilleja arvensis*.

matin/chromsomes and other cytoplasmic organelles. In addition, the studies of Mursalimov et al. (2018) have established that plastids can pass into another cell through cytomictic channels.

Cytomictic connections were observed for the first time Körnicke (1901) in PMCs of *Crocus sativus*, but as the cytogenetic studies in plants advanced this phenomenon was also reported in meristematic, tapetal, integumental, nucellar and ovary cells in both Angiosperms and Gymnosperms (Cooper, 1952; Koul, 1990; Guzicka & Wozny, 2005; Wang *et al*., 2004; Oliveira-Pierre & Sousa, 2011; Kumar et al., 2015; Kumar & Chaudhary, 2016; Kumar & Singhal, 2016; Reis et al., 2016; Mursalimov & Deineko, 2017; Mursalimov & Deineko, 2018). As the cytogenetic analysis in higher plants expanded, cases of cytomixis were observed more frequently in accessions of cultured or natural plants populations. During our previous investigations, we observed the presence of cytomixis in different families of Angiosperms such as Pipperaceae, Cuscutaceae, Ranunculaceae and Cactaceae from the Northwest of Argentina (NOA) (Andrada *et al*., 2009; Lozzia *et al*., 2009; Páez *et al*., 2013 a, b). We also investigated *Buddleja iresinoides* (Griseb.) Hosseus. (Buddlejaceae) and *Castilleja arvensis* Schltdl. & Cham. (Orobanchaceae) for male meiosis and pollen fertility and we observed cytomixis and meiotic irregularities.

The genus *Buddleja* consist of ca. 100 species and cultivars that occur in warm, tropical, and subtropical climates from the Americas, Africa and Asia (Tallent-Halsell & Watt, 2009). *Buddleja iresinoides* is a shrubby plant, native to South America, distributed from Bolivia to the Northwest of Argentina were it is found in Catamarca, Jujuy, Salta and Tucumán provinces. It is a dioecious plant with quadrangular stems and ovate-lanceolate leaves, tomentose flowers with a bell-shaped calyx and corolla, the latter of white or yellow color (Fig.1A and B) (Carrizo & Isasmendi, 1994).

Castilleja Mutis ex L. f. comprises approximately 200 species native from western North to South America (González, 2013). *Castilleja arvensis* is an annual hemiparasitic herb, growing on humid soils from Mexico to the central region of Argentina. This species is characterized by its erect, simple, hispid, leafy stems (Fig. 1C). The leaves at the top of the stem are bract-like, gradually become smaller than the lower ones, and generally are red or purple colored (Botta & Cabrera, 1993).

For *Buddleja* chromosome numbers of 18 species are listed in IPCN (Index to plant chromosome numbers) (Goldblatt & Johnson, 1979+). The basic chromosome number $x = 19$ is accepted and the majority of species present this number or higher ploidy levels as gametophytic number (Norman, 2000; Tallent-Halsell & Watt, 2009).

Chromosome numbers of 54 species are listed in IPCN for the genus *Castilleja* (Goldblatt & Johnson, *op. cit*.). Based on the published literature the basic chromosome number of x = 12 and one or more polyploid levels have been suggested (Heckard, 1968; Heckard & Chuang, 1977; Chuang & Heckard, 1982; Tank & Olmstead, 2008; Tank *et al*., 2009).

The aim of the current paper is to analyze the male meiotic behavior in wild populations of *B. iresinoides* and *C. arvensis* in order to establish that meiotic irregularities are related to the phenomenon of cytomixis and, furthmore, to evaluate if they influence pollen fertility.

MATERIALS AND METHODS

Analyzed materials

All the material studied in this investigation was collected from natural populations of *Buddleja iresinoides* (Figure 1A-B) and *Castilleja arvensis* (Figure 1C) in Tucumán province. Voucher samples were deposited at the phanerogamic herbarium of Miguel Lillo Foundation (LIL).

Buddleja iresinoides: ARGENTINA, Prov. Tucumán, Dpto. Concepción, Loc. Cochuna, 27°10'20" S, 65°55'39" W, alt. 1160 m, *Andrada R.* S/N (LIL 610862).

Castilleja arvensis: ARGENTINA, Prov. Tucumán, Dpto. Tafí Viejo, Loc. Camino a la Toma, 26°43'05,122" S, 65°17'45.53" W, alt. 878 m, 29-lX-2007, *Andrada R.* S/N (LIL610759).

Analysis of meiosis

The material used consisted of flower buds from 5 randomly selected plants which were fixed in Farmer solution (3 ethanol : 1 glacial acetic acid) for one day, immediately transferred to 70% ethanol and stored at 4 °C. Anthers were first hydrolyzed in 1 N HCl at 60 °C for 20 minutes and then washed in distilled water. Pollen mother cells were prepared by the squash technique and stained with a drop of hematoxylin propionic with ferric citrate (Sáez, 1960; Núnez, 1968). 100 PMCs at each stage of the meiosis were observed.

Size and fertility of pollen grains

Fixed flowers immediately after anthesis were selected in order to estimate pollen fertility rates. At least 100 pollen grains of each species were measured to determine the typical pollen size range. Pollen grains were stained using Müntzing solution (glycerin-acetic carmin 1:1) (Sharma & Sharma, 1965). Well-filled pollen grains with uniformly stained cytoplasm were scored as apparently fertile/viable while the shrivelled/flaccid ones with unstained or poorly stained cytoplasm were counted as apparently sterile/unviable. At least 1000 pollen grains were analyzed for each taxon.

Photomicrographs were taken using a Nikon Eclipse E-200 microscope equipped with a Moticam 1000 digital camera (1.3 MP). The graphics were designed with the software CorelDRAW X3.

RESULTS

Analysis of meiosis:

Buddleja iresinoides: Generally the meiosis at prometaphase I started totally normal (97%) with the presence of 28 bivalents at diakinesis (Fig. 2A and B). Cytomixis was a common phenomenon in different stages of meiosis. About 2% of the PMCs of telophase I (TI) showed simple cytomictic channels indicating transfer of chromatin and cytoplasmic material among proximate PMCs (Fig. 2C), simple cytomictic channels connecting two or more cells were observed in 25% of MII (Fig. 2D). Furthermore, at TII cytomixis consisting of 1-2 channels between two cells were found in 45% of PMCs (Fig. 2E). Different kinds of irregularities were observed (Table 1). At diakinesis, 7% of PMCs were aneuploid, and showed 20-21 bivalents. At metaphase I (MI), irregularities such as out of plate bivalents were observed in 9% of the PMCs (Fig. 2F). In addition, 8% of the PMCs at TI stage were found to show anaphase bridges with lagging chromatin between two nuclei (Fig. 2G). At MII and AII, respectively 6% and 4% of PMCs exhibited chromatin stickiness between contiguous nuclei. (Figs. 2H-I). At the end of meiosis, abnormal sporads such as dyads and triads were present. (Fig. 2J). The mean diameter for *B. iresinoides* pollen, as determined by light microscopy, was 13.3 µm (range of 12.9 to 13.6 µm) (Table 1). Pollen viability rates in *B. iresinoides* was 89 % (Fig. 4A).

Castilleja arvensis: Chromosome numbers in PMCs were not constant. The diakinesis showed 78% regular PMCs with a gametophytic number of $n = 12$ (Fig. 3A). Cytomixis was revealed to be a very frequent phenomenon during pachytene, and 92% of the PMCs were con-

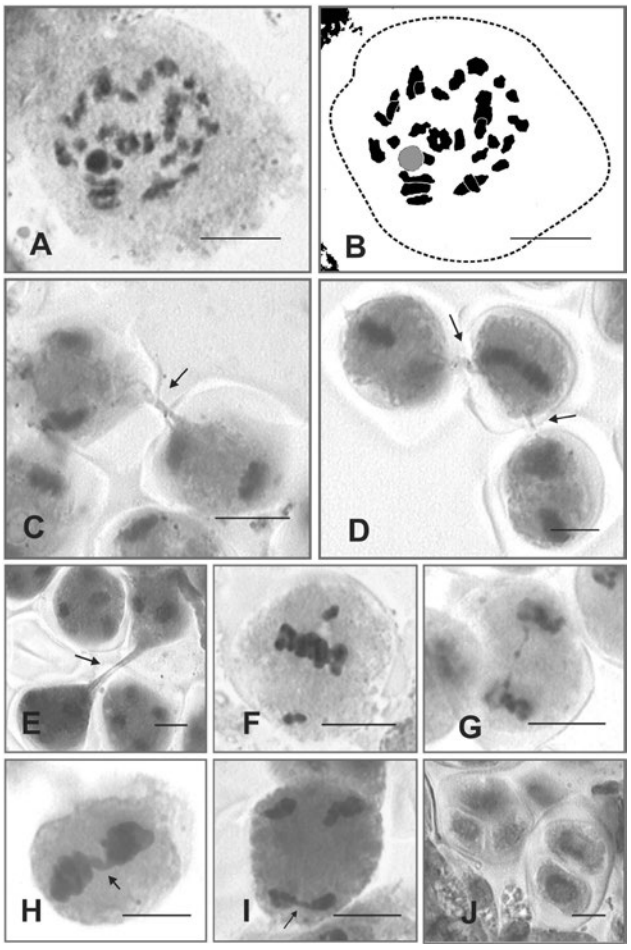

Figure 2. Meiosis in *Buddleja iresinoides*. A) Diakinesis with $n = 28$, B) Graphic representation of figure A; C) cytomictic channel in TI connecting 2 cells; D) MII with cytomictic channels connecting 3 cells; E) Cytomixis between tetrads; F) MI with two chromosomes away from the equatorial plate; G) TI showing anaphase bridges with lagging chromatin; H) MII with chromatin stickiness between two equatorial plates; I) AII with chromatin stickiness connecting 2 neighbour poles; J) Dyad and triad. Scale = 10 μm.

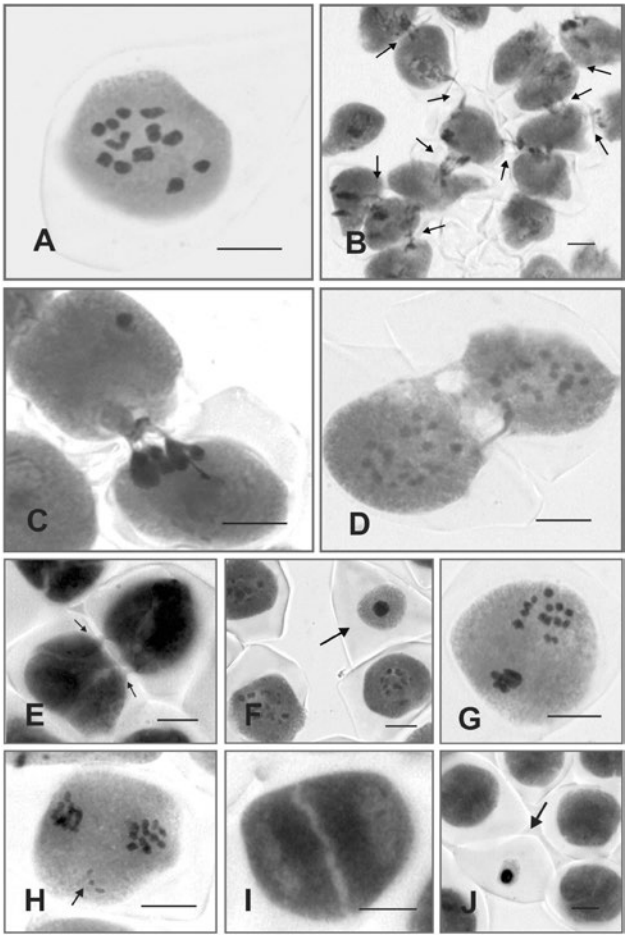

Figure 3. Meiosis in *Castilleja arvensis*. A) Diakinesis with 12 bivalents; B) Cells with multiple cytomictic channels in pachytene; C) Donor PMC transferring almost all the chromatin to a neighbor PMC; D) Two cells in diakinesis connected by 3 cytomictic channels; E) Cytomictic channels between tetrads; F) Small-sized meiocytes with a small nucleus during the division I; G) MII showing a plate with 14 chromosomes; H) MII showing chromosomes disconnected from equatorial plate; I) Dyad; J) small-sized meiocytes with a small nucleus at the end of the division II. Scale = 10 μm.

nected by 1-5 cytomictic channels linking two or more adjacent meiocytes (Fig. 3B). To a great extent, these channels were filled by chromatin strands indicaticating material transfer from one PMC to another. The donor cell sometimes transferred almost the whole of its chromosome complement to a recipient meiocyte leaving only a chromosome-like heteropycnotic body beside the nucleolus; the recipient meiocytes had bigger agglomerations of chromatin material (Fig. 3C). At diakinesis, 22% meiocytes showed 1-5 cytomictic channels (Fig. 3D). In 8.5% of PMCs, 1 or 2 cytomictic channels were found between the neighbour tetrads at the end of second division (Fig. 3E). Irregularities observed in this species occurred in different stages (Table 1). During diakinesis there were present hyperploid PMCs with up to $n = 20$ (Fig. 3D). During this stage, small-sized meiocytes with only a small nucleus were found. These small sized cells were covered by thick callose walls giving them an aspect of monads (Fig. 3F). Subsequent stages of first meiotic division (MI, AI and TI) were not observed in the preserved material. In MII, up to 7% of meiocytes were found to possess the hyperploid chromosome number of 14 at one pole (Fig. 3G). In 5% PMCs at metaphase II, it was found that chromosomes do not align on the metaphase plate and tend to lie towards the periphery of the cell wall (Fig. 3H). Dyads were also observed in 3%

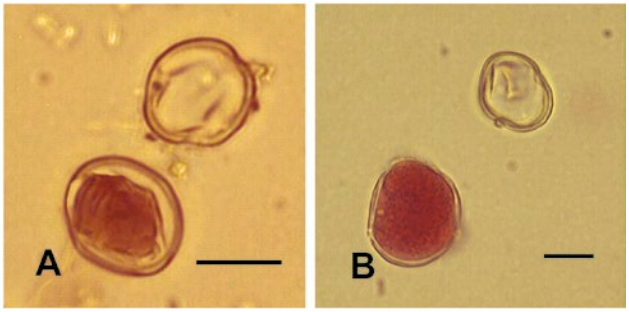

Figure 4. A-J: Fertile/stained and Sterile/unstained pollen grains in; A) *Buddleja iresinoides* and, B) *Castilleja arvensis*. Scale = 10 µm.

cases (Fig. 3I). Interestingly, 2% of PMCs were of small sizes and small nuclei (Fig. 3J).

Pollen size of *Castilleja arvensis* was observed to range from 20.1 µm to 20.8 µm (the mean diameter was 20.5 µm) (Table 1). Pollen viability rates in *Castilleja arvensis* was 95%, (Fig. 4B).

DISCUSSION

Our results are not in agreement with the base number $x = 19$ previously reported for *Buddleja* (Norman, 2000; Tallent-Halsell & Watt, 2009) and the chromosome number $n = 28$ found for *B. iresinoides* is atypical in the genus. However, Gadella (1980) suggested that $x = 19$ may have been derived from ancestral hybridization between two basic stocks with $x = 12$ and 7 (Norman, 2000; Oxelman *et al*., 2004). Our results suggested that *B. iresinoides* could be an octoploid with a putative basic number $x = 7$ or its chromosome number, $n = 28$ may have derived through secondary aneuploidy from a diploid parent having $n = 36$.

Another hypothesis is that the unusual chromosome number $n = 28$ ($2n = 56$) in this population may have derived by fusion of an unreduced gamete $n = 36$ from a putative parent and another normal gamete $n = 19$ (total $2n = 55$) followed by a chromosome gain (e.g. through cytomixis) to reach 2n = 56. Similarly, the rest of irregular gametes found $n = 20$-21 could have increased their chromosome number by cytomixis; this is after normal gametes $n = 19$ "acted" like recipient cells increasing their chromosome complement in 1 or 2 additional chromosomes.

The chromosome number of $x = 12$ had been suggested for the genus *Castilleja* (Heckard, 1968; Heckard & Chuang, 1977; Chuang & Heckard, 1982; Tank & Olmstead, 2008; Tank *et al*., 2009) and *C. arvensis* showed tetraploid number of chromosome of $2n = 24$.

The phenomenon of cytomixis as well as dyads and chromosomes that didn't attach to the equatorial plate were observed in both analyzed species. These latter kinds of meiotic irregularities could be caused by the cytomixis (Kumar, 2010; Kumar *et al*., 2010; Kumar *et al*., 2013).

The origin of cytomixis is still not clear and different opinions exist with respect to its causes and permanence during meiosis. Oliveira-Pierre & Sousa (2011) concluded that the cytomixis could have multiple origins. However, these authors have cited relatively recent investigations which show that cytomictic channels always structurally occur in the same way: 1) in the beginning, plasmodesms loss their connections with smooth endoplasmic reticulum (desmotubules) and then starts the intrusion of cytoplasmic material into the plasmodesms that inncrease their size forming cytomictic channels (Wei-cheng *et al*.,1988; Oliveira-Pierre & Sousa, *op. cit*.); 2) During the cytomixis process both cellulase and pectinase enzymes are presented as playing a role in digesting the cell walls of PMCs involved in this phenomenon (Wang *et al*.,1998); 3) in cells of germinal tissues of anthers during callose depositions that should block up the plamodesms occur disturbances, the connector channels increase their size and in this way facilitate the formation of cytomictic channels (Falistocco *et al*., 1995; Sheidai & Fadaei, 2005; Sheidai *et al*. 2006; Sidorchuk *et al*., 2007).

Some authors argued that cytomixis is a process that occur in the early stages of meiotic division (at prophase I generally) supporting the idea that after passage of chromatin from one PMC to another, cells which acquired or donated chromatinic material tend to degenerate. This kind of result was obtained by Koul (1990) through investigations carried out in *Alopecurus rundinaceus* Poir. On the other hand, there are authors that state that cytomixis could develop in all stages of meiosis (Basavaiah & Murthy, 1987 in *Urochloa panicoides* P. Beauv.; Bellucci *et al*., 2003 in *Medicago sativa* L.; Malallah & Attia, 2003 in *Diplotaxis harra* Boiss.; Singhal & Kumar, 2008 in *Meconopsis aculeata* Royle; Singhal *et al*., 2009 in *Anemone rivularis* Buch.-Ham. ex DC.). Authors have different positions regarding the transfer of cell components through cytomixis. During cell division, Heslop-Harrison (1966) suggested that intercellular connections occur to foment the synchrony between meiocytes allowing homogeneity of organelles and cytoplasmic components among them. However, Guanq-Qin & Gou-Chang (2004) refused this hypothesis because they considered it inconsistent, being that in plants the tapetal cells are responsible for providing nutrients to the PMCs (not the passage from one PMC to another),

between the last cells never has hitherto been observed cytoplasmic connections together the meiocytes. These authors attributed to cytomixis a more general function such as the mechanism that allows share regulatory and structural genetic products (e.g., mRNAs, oragnelles, etc.) between connected cells, favoring thus a necessary homogenization of cytoplasmatic restructural events occurred during prophase I which could cause heterogeneity in the meiocytes and consequently could lead to loss of their quality (generating more abnormal but less normal gametes).

During the pachytene stage, we have never observed cytomixis in PMCs of *B. iresinoides* but these started from telophase I. Our observations are not in agreement with Koul's hypothesis (1990) according to which the cytomixis occurs in first stages of meiotic division. However, in *C. arvensis* cytomictic channels were present in prophase I in most of the meiocytes (92% of PMCs) suggesting that absence or presence of cytomixis does not essentially depend on the stage of cell division. Participation of other factors that may play some role in cytomixis is still not clear. It is evident that the cytomixis can occur in different stages of meiosis from prophase I to tetrad formation as revealed in our results. Our findings agree with Guanq-Qin & Gou-Chang (2004) who reported that cytomictic channels always are formed among cells at the same division stage.

Nevertheless, the above cited authors mentioned that cytomixis promote homogeneity between meiocytes, observations that contradict our results because we observed in *C. arvensis* pachytene the transfer of almost all the chromatin from donor cell to recipient cell and the presence of hypoploid and hyperploid PMCs. Altogether, these irregularities (heterogeneity), probably produced by cytomixis, made up more than 30% of the observed cells.

According to morphological characteristics, the small-sized meiocytes with a little nucleus observed in both the division I and the division II correspond to apoptotic cells similar to the ones cited by different authors in both plants and animals (Fuzinatto et al., 2007; Kravets, 2013; Andrada et al., 2016). The abnormal cells could be degraded by means of apoptosis, thus explaining the high percentage of pollen grains viability observed in *C. arvensis*. In this species this phenomenon occured two times: after pachytene at diakinesis and between the tetrads at the end of TII (both in division I and division II after or during the two stages with major percentage of cytomixis). Although this kind of abnormal cell was not observed in *B. iresinoides* it is possible that some similar mechanism could occur and the abnormal cells would be eliminated. By removing the abnormal pollen grains these plants ensure that gametes transferred being viable.

In *B. iresinoides* transfer of chromatin from a donor cell to a recipient cell is not limited only to neighbouring meiocytes but also occurs between PMCs at same stage of division. According to Ortíz *et al.* (2006) and Andrada & Páez (2014), this kind of connections could disturb the normal development of the phragmoplast during cytokinesis causing irregularities which could finish as unbalanced gametes and give rise to dyads as it was observed in *B. iresinoides*. Although in *C. arvensis* connections among meiocytes from the same PMC was not observed, these were present in dyads once meiosis had been completed.

In both species chromosomes which did not align to metaphase plate and stood near cell wall were found but in different stages in the two species examined. In *B. iresinoides* they occured during MI, whereas in *C. arvensis* this kind of irregularite was observed at MII even at the hyperploid cells. These chromosomes could occur due to transfer from a PMC to other neighbouring PMC through cytomixis channels during the early metaphase.

In *Buddleja iresinoides*, during the división II the 57% of PMCs showed irregularities (stickness, cytomixis and bad debelop phragmoplast that finished in dyads and triads). This percentage is far to the 11% of irregular and inviable pollen grains revealed by Münting's stain, however, before start the division II the regulatory mechanism that controls the normal course of the meiosis or the method to eliminate irregular PMCs still remains unknown. In addition, in *B. iresinoides* it is evident that the cytomixis (reaching the maximum value of 45% at TII) does not have a large impact on the development of non-viable pollen grains. Gernand *et al.* analyzed the mechanisms underlying selective elimination of the paternal chromosomes during the development of wheat × pearl millet hybrid embryos and found that chromosome elimination frequently took place during meiosis. These cytological observations showed that parental genomes were spatially separated within the hybrid nucleus, and the pearl millet chromatin destined for elimination occupied peripheral positions. A similar phenomenon was found in this study; chromosomes were spatially separated within the PMCs where the chromatin occupied a predominantly peripheral position at metaphase I from *B. iresinoides* and at pachitene and MII from *C. arvensis*. In addition, given that the *B. iresinoides* and *B. stachyoides* Cham. & Schltdl. (chromosome number unknown) grow together, it is likely that the taxon studied contain chromosomes from *B. stachyoides*. This would have given rise to populations of hybrids with this atypical gametophytic number (n = 28).

In *Castilleja arvensis*, among the frequent abnormalities (as stickness, cytomixis and bad debelop phragmoplast that finished in dyads and triads) the cytomictic channels at pachitene (Table 1 and Figure 3B) were salient. However, the cytomixis does not seem to be the main cause of pollen inviability. In this species, the apoptosis which was observed in both prophase and TII where occur the most of irregularities could regulate the number of abnormal PMCs during the meiosis and the non viable pollen grains would be obtained when simply some PMCs with different type of irregularities add together up to reach 5%.

Buddleja iresinoides and Castilleja arvensis have high percentages of pollen grains stained (viables) close to 90% and small ranges of variation of size close to 0,7 µm. This fact suggest that polyploid cells (produced through of dyads and triads) which should develop giant pollen grains or "Jumbo grains" were eliminated during the last steps of microsporogenesis. On the other hand, the limit size values of stained pollen grains may mask hyperploids and hypoploid cells as apparently normal and fertile pollen grains. Future studies related to germinabaility of pollen grains could clarify the strange behavior of these species that show high percentages of irregularities during the meiosis and low production of sterile pollen grains.

CONCLUSIONS

Castilleja arvensis is a diploid taxon with $n = 12$ while the unusual number $n = 28$ from *B. iresinoides* suggest that the basic chromosome number for this genus could be less than $x = 19$. However, that this atypical number could have originated through passage of additional chromosomes from a donor cell to recipient cell by cytomixis or through hybridization process is possible too. In the present study, we have found that cytomixis is a process which is not stage specific and its frequency may vary from species to species which is evident from our results in *B. iresinoides* where maximum percentage of cytomixis occur during TII, whereas in *C. arvensis* it is more frequent in pachytene. In addition, this process could cause numerous irregularities that would result in (at the end of meiosis) genetically unbalanced gametes. Furthermore depending upon the severity of meiotic irregularities it may hamper the reproductive success of species. Cytomixis has been reported here for the first time from both Buddlejaceae and Orobanchaceae families.

ACKNOWLEDGEMENTS

This work was made possible by the financial support of Fundacaión Miguel Lillo (Proyecto B-0013/1). We are grateful to the Director of the Genetic Institute of Miguel Lillo Foundation, G. E. Ruiz de Bigliardo for her critical reading of the manuscript. The authors are also very grateful to the Director of the Botanical Survey of India, Kolkata for necessary internet and library facilities.

REFERENCES

Andrada AR, Lozzia ME, Cristóbal ME (2009) Cytological studies in *Piper tucumanum* C. DC. and *Piper hieronymi* C. DC. Lilloa 46: 3–9. (in Spanish)

Andrada AR, Páez VA (2014) Meiotic studies and pollen viability of three species of *Tibouchina* (Melastomataceae). Lilloa 51: 131–140. (in Spanish)

Andrada AR, Silenzi Usandivaras GM, Bigliardo GE, Romero M, Dode M (2016) Citogenetic studies in two natural populations of *Doru lineare* (Dermaptera, Forficulidae). Acta Zool Lilloana 60: 3–9. (in Spanish)

Basavaiah D, Murthy TCS (1987) Cytomixis in pollen mother cells of *Urochloa panicoides* P. Beauv. (Poaceae). Cytologia 52: 69–74.

Bellucci M, Roscini C, Mariani A (2003) Cytomixis in Pollen Mother Cells of *Medicago sativa* L. J Hered 94: 512–516.

Botta SM, Cabrera AL (1993) Scrophulariaceae. In: Cabrera AL (ed) Flora of the Province of Jujuy. Scientific Collection INTA 13: 155–226.

Carrizo J, Isasmendi S (1994) Buddlejaceae. In: Flora of the Lerma Valley. Botanical Contributions of Salta. Flora Series: 1–10.

Cooper DC (1952) The transfer of deoxyribose nucleic acid from the tapetum to the microsporocytes at the onset of meiosis. Am Nat 86: 219–229.

Chuang TI, Heckard LR (1982) Chromosome numbers of *Orthocarpus* and related monotypic genera (Scrophulariaceae: Subtribe Castillejinae). Brittonia 34: 89-101

Falistocco E, Tosti N, Falcinelli M (1995) Cytomixis in pollen mother cells of diploid *Dactylis*, one of the origins of 2n gametes. J Hered 86: 448–453.

Fuzinatto VA, Pagliarini MS and Valle CB (2007) Evidence of programmed cell death during microsporogenesis in an interspecific *Brachiaria* (Poaceae: Panicoideae: Paniceae) hybrid. Genet. Mol. Res. 6: 308-315.

Gadella TWJ (1980) Cytology. In: Leeuwenberg AJM *(*ed*),* Engler and Prantl's 'Die natürlichen Pflanzen-

familien', Fam. Loganiaceae, vol. 28b (1), Duncker& Humblot, Berlin, pp 202–210.

Gates RR (1911) Pollen formation in *Oenothra gigas*. Ann Bot 25. 909–940.

Gernand D, Rutten T, Varshney A, Rubtsova M, Prodanovic S, Brüß C, Kumlehn J, Matzk F, and Houben A. (2005) Uniparental chromosome elimination at mitosis and interphase in wheat and pearl millet crosses involves micronucleus formation, progressive heterochromatinization, and DNA fragmentation. The Plant Cell 17(9): 2431–2438..

González F (2013). A new species of *castilleja* (Orobanchaceae) from the Páramos of the colombian eastern cordillera, with comments on its association with *Plantago rigida* (Plantaginaceae). Caldasia 35: 261–262.

Guanq-Qin G, Gou-Chang Z (2004) Hypotheses for the functions of intercellular bridges in male germ cell development and its cellular mechanisms. J Theor Biol 229: 139–146.

Guzicka M, Wozny A (2005) Cytomixis in shoot apex of Norway spruce [Picea abies (L.) Karst.]. Trees 18: 722–724.

Heckard LR (1968) Chromosome numbers and polyploidy in *Castilleja* (Scrophulariaceae). Brittonia 20: 112–126.

Heckard LR, Chuang TI (1977) Chromosome numbers, polyploidy, and hybridization in *Castilleja* (scrophulariaceae) of the Great Basin and Rocky Mountains. Brittonia 29: 159–172.

Heslop-Harrison J (1966) Cytoplasmic connections between angiosperm meiocytes. Ann Bot 30: 221–30.

Körnicke M (1901) Uber Ortsveränderung von Zallkarnern. Sitzgsber. Niederrhein. Ges. Natur-U Heilk. zu. Bonn A., 14–25.

Koul KK (1990) Cytomixis in Pollen Mother Cells of *Alopecurus arundinaceus* Poir. Cytologia 55: 169–173.

Kravets EA (2013) Cytomixis and Its Role in the Regulation of Plant Fertility. Russ. J. Dev. Biol. 44: 113–128.

Kumar P (2010) Exploration of cytomorphological diversity in the members of Polypetalae from Lahaul-Spiti and adjoining areas. Ph.D thesis, Punjabi University, Patiala, Punjab, India. http://hdl.handle.net/10603/2872.

Kumar G, Chaudhary N (2016) Induced cytomixis and syncyte formation during microsporogenesis in *Phaseolus vulgaris* L. Cytol Genet 50: 121–127.

Kumar R, Rana PK, Himshikha S, Kaur D, Kaur M, Singhal VK, Gupta RC, Kumar P (2015) Structural heterozygosity and cytomixis driven pollen sterility in *Anemone rivularis* Buch.-Ham. ex DC. from Western Himalayas (India). Caryologia 68: 246–253.

Kumar P, Rana PK, Himshikha S, Singhal VK, Gupta RC (2013) Cytogeography and phenomenon of cytomixis in *Silene vulgaris* from cold regions of Northwest Himalayas (India). Plant Syst Evol 300: 831–842.

Kumar P, Singhal VK (2016) Nucleoli migration coupled with cytomixis. Biologia 71: 651–659.

Kumar P, Singhal VK, Kaur D, Kaur S (2010) Cytomixis and associated meiotic abnormalities affecting pollen fertility in *Clematis orientalis*. Biol Plantarum 54: 181–184.

Lozzia ME, Páez VA, Toranzo MI, Cristóbal ME (2009) Cytological Studies on *Anemone decapetala* Ard., *Thalictrum decipiens* Boivin and *Thalictrum venturii* Boivin (Ranunculaceae). Lilloa 46: 72–76.

Malallah GA, Attia TA (2003) Cytomixis its possible evolutionary role in a Kuwaiti population of *Diplotaxis harra* (Brassicaceae). Bot J Linn Soc 143: 169–175.

Mursalimov SR, Deineko EV (2017) Cytomixis in tobacco microsporogenesis: are there any genome parts predisposed to migration?. Protoplasma 254:1379–1384.

Mursalimov SR, Deineko, EV (2018) Cytomixis in plants: facts and doubts. Protoplasma 255:719–731.

Mursalimov SR, Sidorchuk YV, Zagorskaya AA, Deineko EV (2018) Migration of DNA-Containing Organelles between Tobacco Microsporocytes during Cytomixis. Russ. J. Dev. Biol. 49: 159–165.

Norman EM (2000) Buddlejaceae. Flora Neotropica Monograph 81, New York Botanical Garden, New York, USA, pp 225.

Núñez O (1968) An acetic-haematoxylin squash method for small chromosomes. Caryologia 21: 115–119.

Oliveira-Pierre PM, Sousa SM (2011) Cytomixis in plants: causes, mechanisms and consequences. Rev Bras Biocienc. 9: 231–240.

Ortíz AM, Seijo JG, Lavia GI (2006) Meiotic mechanisms involved in the reduction of the viability and in the variation of the morphology of the pollen grains of *Arachis glabrata* Benth. (Rhizomatosae section). Scientific and Technological Communications, Universidad Nacional del Nordeste, Summary, B–043.

Oxelman B, Kornhall P, Norman EM (2004) Buddlejaceae. In: K. Kubitzki (ed) The families and genera of vascular plants. vol. 7, Berlin/Heidelberg/New York, pp 39–44.

Páez V.A, Andrada AR, Muruaga NB (2013) Cytogenetic analysis and pollen viability in *Rhipsalis lumbricoides* (Cactaceae). Succulents 10: 16–20.

Páez VA, Andrada AR, Lozzia ME (2013) Meiotic analysis of two species of *Cuscuta* subgenera *Grammica* (Convolvulaceae). Lilloa 50: 59–64.

Reis A, Sousa S, Viccini L (2016) High frequency of cytomixis observed at zygotene in tetraploid *Lippia alba*. Plant Syst Evol 302: 121–127.

Risueno MC, Gimenez-Martín G, Lopéz-Saez JF, Garcia MIR (1969) Connexions between meiocytes in plants. Cytologia 34: 262–272.

Sáez FA (1960) The use of acetic or propionic hematoxylin for the study of chromosomes with the technique of crushing. Communication from the Biological Society. Montevideo. Mimeographed.

Sharma AK, Sharma A (1965) Chromosome techniques, theory and practice. Butteworth & Co., London. pp 474.

Sheidai M, Fadaei F (2005) Cytogenetic studies in some species of *Bromus* L., section Genea Dum. J Genet 84: 189–194.

Sheidai M, Attaei S, Khosravi-Reineh M (2006) Cytology of some Iranian *Stipa* (Poaceae) species and populations. Acta Bot Croat 65: 1–11.

Sidorchuk YV, Deineko EV, Shumny VK (2007) Role of microtubular cytoskeleton and callose walls in the manifestation of cytomixis in pollen mother cells of tobacco *Nicotiana tabacum* L. Cell Tissue Biol 1: 577–581.

Singhal VK, Kumar P (2008) Impact of cytomixis on meiosis, pollen viability and pollen size in wild populations of Himalayan poppy (*Meconopsis aculeata* Royle). J Biosci 33: 371-380.

Singhal VK, Kumar P, Kaur D, Rana PK (2009) Chromatin transfer during male meiosis resulted into heterogeneous sized pollen grains in *Anemone rivularis* Buch.-Ham. ex DC. from Indian cold Deserts. Cytologia 74: 229–234.

Tallent-Halsell NG, Watt MS (2009) The invasive *Buddleja davidii* (Butterfly Bush). Bot Rev 75: 292–325.

Tank DC, Egger JM, Olmstead RC (2009) Phylogenetic classification of Subtribe Castillejinae (Orobanchaceae). Syst Bot 34: 182-197.

Tank DC, Olmstead RC (2008) From annuals to perennials: phylogeny of subtribe Castillejinae (Orobanchaceae). Am J Bot 95: 608–625.

Wang XY, Yu, CH, Li X, Wang CY, Zheng GC (2004) Ultrastructural aspects and possible origin of cytomictic channels providing intercellular connection in vegetative tissues of anthers. Russ J Plant Physiol 51:110-120.

Wei-cheng Z, Wen-mei Y, Cheng-hou L (1988) The structural changes during the degeneration process of antipodal complex and its function to endosperm formation in wheat caryopsis. Acta Bot Sin 30: 457-462.

Caryologia
International Journal of Cytology, Cytosystematics and Cytogenetics

Firenze University Press
www.fupress.com/caryologia

OPEN ACCESS

Citation: F. Farahani, A. Sedighzadegan, M. Sheidai, F. Koohdar (2019) Population Genetic Studies in *Ziziphus jujuba* Mill.: Multiple Molecular Markers (ISSR, SRAP, ITS, Cp-DNA). *Caryologia* 72(4): 51-60. doi: 10.13128/caryologia-390

Published: December 23, 2019

Data Availability Statement: All relevant data are within the paper and its Supporting Information files.

Competing Interests: The Author(s) declare(s) no conflict of interest.

Population Genetic Studies in *Ziziphus jujuba* Mill.: Multiple Molecular Markers (ISSR, SRAP, ITS, Cp-DNA)

Farah Farahani[1], Atieh Sedighzadegan[2], Masoud Sheidai[2], Fahimeh Koohdar[2]

[1] *Department of Microbiology, Qom Branch, Islamic Azad University, Qom, Iran*
[2] *Faculty of Life Sciences and Biotechnology, Shahid Beheshti University, Tehran, Iran*
*Corresponding authors: farahfarahani2000@yahoo.com, asedighzadegan@yahoo.com, msheidai@yahoo.com, f_koohdar@yahoo.com

Abstract. *Ziziphus jujuba* (jujube) is an important horticultural crop with medicinal value. It is under cultivation in many areas of Iran and also grows as wild in several geographical populations throughout the country. We have no information on genetic variability and population structure of this important plant species in our country. Therefore, the aim of the present study was to perform genetic fingerprinting of 13 geographical populations of jujuba for the first time and provide data on population genetic structure, admixture versus genetic fragmentation of this important crop. We used multilocus molecular markers (ISSRs and SRAPs) for genetic fingerprinting and also compared the results with bioinformatics investigation results we did on jujuba cultivars by using nuclear r-DNA and chloroplast inter-genetic cp-DNA sequences. Genetic diversity parameters and AMOVA test as well as Ivanno test support some kind of genetic distinctness of the jujuba populations studied. We found that cp-DNA inter-genic sequences can also discriminate jujuba cultivars as efficient as multilocus molecular markers and therefore, a multiple molecular approaches may be used for genetic fingerprinting of jujuba. The present study revealed good level of genetic diversity among wild/ uncultivated populations of jujuba which can be used in conservation and breeding of this important horticultural crop plant within the country. As this crop has several wild geographical populations throughout the country, we plan to continue our quest to investigate many more populations in nearby future and try to utilize cp-DNA inter-genic sequences along with multilocus molecular markers for genetic discrimination of wild populations.

Keyword. Cp-DNA, ISSR, ITS, SRAP, *Ziziphus jujube*.

INTRODUCTION

The genus *Ziziphus* Mill. belongs to the buckthorn family Rhamnaceae. It is contains about 40 species that are deciduous evergreen trees or shrubs distributed in the tropical and subtropical regions of the world (Sing et al. 2007). The wide geographical and climatic distribution makes it interesting

for genetic diversity investigations and gene pool identification.

South and Southeast Asia is the center of both evolution and distribution of the genus *Ziziphus* (Sing et al. 2007). Tow fossil species are known for *Ziziphus* in Eocene era (US Govt. Printing Office 1982).

Ziziphus species are of medicinal value and are known to be self-incompatible and have synchronous protandrous dichogamy and produce viable inter-specific hybrids (Asatryan and Tel-Zur, 2013). Among *Ziziphus* species, few are well known like: *Z. jujuba* (jujuba), and *Z. spina-christi* (L.)Desf. that grow in south-western Asia, *Z. lotus* in Mediterranean region, ber (*Z. mauritiana*), that is found in western Africa to India and *Z. joazeiro* Mill. that grows in the Caatinga of Brazil (Gupta et al. 2004; Jiang et al. 2007; Vahedi et al. 2008).

Traditional use of jujuba dates back 2,500 years ago in original Chinese material medical records. The fruit, seed, and bark of jujuba are also described in Korean, Indian, and Japanese traditional writings. They are used to alleviate stress and insomnia and as appetite stimulants, digestive aids, anti-arrhythmic, and contraceptives. The sweet smell of the fruit is said to make teenagers fall in love. The fruit is eaten fresh or dried and made into candy; tea, syrup, and wine are also made from the berries (Gupta et al. 2004; Jiang et al. 2007; Vahedi et al. 2008).

The fruit is energy-rich because of the large amount of sugar it contains. It is cultivated and eaten fresh, dry, and in jam. It is also added as a base in meals and in the manufacture of candy. The leaves can be either deciduous or evergreen depending on species, and are aromatic.

The seeds, fruit, and bark of jujuba have been used in traditional medicine for anxiety and insomnia, and as an appetite stimulant or digestive aid. Experiments in animals support the presence of anxiolytic and sedative properties. However, clinical trials are lacking (Gupta et al. 2004; Jiang et al. 2007; Vahedi et al. 2008). Some specific saponins, as well as ethyl acetate and water extracts of the fruit and bark, have explored the potential cytotoxicity of jujuba. Apoptosis and differential cell cycle arrest are suggested to be responsible for the dose-dependent reduction in cell viability. Activity against certain human cancer cell lines has been demonstrated in vitro (Lee et al. 2004; Huang et al. 2007; Vahedi et al. 2008).

Jujuba is one of the important horticultural crops in Iran and about with annual production of 4980 Kg that is about 14.7% of total cold region fruit production (34000 Tones) (Hosseinpour et al. 2016). It has been cultivated in several regions of the country and also is grown wild in several areas throughout Iran.

Different molecular markers have been used for population genetic investigation and phylogenetic studies in *Ziziphus* species. For example, Islam and Simmons (2006) performed an intra-generic classification of 19 *Ziziphus* species by using morphological characteristics and nuclear rDNA internal transcribed spacers, 26S rDNA, and the plastid trnL-F intergenic spacer. Similarly, the genetic relationships between different *Z. jujuba* cultivars and/ or wild jujuba individuals was studied by using random amplified polymorphic DNA (RAPD), amplified fragment length polymorphisms (AFLP), sequence-related amplified polymorphisms (SRAP), simple sequence repeats (SSR), inter-simple sequence repeats (ISSR), and chloroplast microsatellite (Cp-SSR) markers (see for example, Peng et al. 2000; Liu et al. 2005; Wang et al. 2007; Singh et al. 2007; Wang et al. 2014; Zhang et al. 2014; Huang et al. 2015).

Population genetic study is an important step for genetic evaluation of medicinally important species as it provides insight on the genetic structure, genetic diversity and gene flow versus genetic fragmentation of these plant species. It also produces data on the number of potential gene pools for conservation and breeding strategies for the studied taxa (Sheidai et al. 2013, 2014, 2016).

The aims of present study are: 1- Produce data on population genetic structure of *Ziziphus jujuba* of Iran for the first time and 2- Investigate the discrimination power of ISSR and SRAP molecular markers in *Ziziphus jujuba* populations and compare them with sequencing data like nuclear r-DNA sequences (ITS = Internal transcribed spacer DNA) and chloroplast gene sequences.

We used ISSR (Inter simple sequence repeats) and SRAP (Sequence related amplified polymorphism) molecular markers, as these markers are very useful tool to detect genetic polymorphism, are inexpensive and readily adaptable technique for routine germplasm fingerprinting and evaluation of genetic relationship between accessions or genotypes and construction of genetic linkage maps (Sheidai et al. 2013, 2014, 2016). Moreover, SRAP markers target the open reading frames (ORFs).

MATERIAL AND METHODS

Plant Materials

In total 130 plants were studied in 13 geographical populations of *Ziziphus jujuba* (Table 1). Ten plants were randomly selected in each population and used for molecular studied (ISSR and SRAP).

Table 1. *Ziziphus jujuba* population in ISSR and SRAP studies.

	Province	Locality	Longitude	Latitude
1	Qom	Kalaghneshin	50. 2536 °	34.4122°
2	Qom	Ghaziolia	50.2850°	34.3222°
3	Qom	Dolatabad	50.3032°	34.1258°
4	Qom	Jafarieh	50.3429°	34.4722°
5	Qom	Khalajestan	50.3844°	34.2852°
6	Markazi	Aveh	50.2523°	34.4732°
7	Markazi	Delijan	50.4102°	33.5926°
8	Markazi	Saveh	50.2124°	35.0117°
9	Esfahan	Kashan niasar	51.0856°	33.5822°
10	Esfahan	Koohpayeh	52.2623°	32.4249°
11	Esfahan	Shahreza	51.5200°	32.0032°
12	Esfahan	Dehaghan	51.3916°	31.5612°
13	Esfahan	Ardestan	52.2238°	33.232.07°

DNA Extraction

For molecular studies, the fresh leaves were randomly collected from 53 randomly selected plants in the studied area and were dried in silica gel powder. The genomic DNA was extracted using CTAB-activated charcoal protocol (Križ man et al. 2006). The extraction procedure was based on activated charcoal and poly vinyl pyrrolidone (PVP) for binding of polyphenolics during extraction and under mild extraction and precipitation conditions. This promoted high-molecular-weight DNA isolation without interfering contaminants. Quality of extracted DNA was examined by running on 0.8% agarose gel.

ISSR Assay

Ten ISSR primers, UBC 807, UBC 810, UBC 811, UBC 834, CAG(GA)7, (CA)7AC, (CA)7AT, (CA)7GT (GA)9A, and (GA)9T, commercialized by the University of British Columbia, were used.

PCR reactions were performed in a 25-µL volume containing 10 mM Tris-HCl buff er at pH 8, 50 mM KCl, 1.5 mM MgCl2 , 0.2 mM of each dNTP (Bioron, Germany), 0.2 µM of a single primer, 20 ng of genomic DNA, and 3 U of Taq DNA polymerase (Bioron).

Amplification reactions were performed in a Techne thermocycler (Germany) with the following program: 5 min for initial denaturation step at 94 °C, 30 s at 94 °C, 1 min at 52 °C, and 1 min at 72 °C. Th e reaction was completed by a final extension step of 7 min at 72 °C. The amplification products were visualized by running on 2% agarose gel, followed by ethidium bromide staining. The fragments size was estimated by using a 100-bp molecular size ladder (Fermentas, Germany). The experiment was replicated 3 times and constant ISSR bands were used for further analyses.

SRAP Assay

Five sequences related amplified polymorphism (SRAP) primer pairs including forward primers: Me1, Me2, Me3, Me4, Me5 and reverse primers: Em1, Em2, Em3, Em4, Em5 were used (Feng et al. 2014).

PCR reactions were carried in a 25µl volume containing 10 mM Tris-HCl buffer at pH 8; 50 mM KCl; 1.5 mM MgCl2; 0.2 mM of each dNTP (Bioron, Germany); 0.2 µM of a single primer; 20 ng genomic DNA and 1 U of *Taq* DNA polymerase (Bioron, Germany).

The amplifications, reactions were performed in Techne thermocycler (Germany) with the following program: 5Min initial denaturation step 94°C, followed by five cycles of 94°C for 1min, 35°C for 45 sec, and 72°C for 1 min; followed by 35 cycles of 94°C for 1min, 50°C for 45 sec, and ITC for 1 min; followed by 7 min at 72°C. The amplification products were observed by running on 1% agarose gel, followed by the ethidium bromide staining. The fragment size was estimated by using a 100 bp molecular size ladder (Fermentas, Germany).

ITS and cp-DNA Inter-Genic Sequences Analyses

cp-DNA and nuclear-DNA ITS sequences of 11 jujuba cultivars were obtained from NCBI(National Center for Bioinformatic Information) and used to differentiate the studied cultivars. The cultivars accession numbers have been provided in tables 2 and 3.

Data Analyses

The ISSR and SRAP bands obtained were treated as binary characters and coded accordingly (presence = 1, absence = 0). The number of private bands versus common bands was determined. Genetic diversity parameters like: The percentage of allelic polymorphism, allele diversity (Weising, 2005), Nei's gene diversity (He), and Shannon information index (I) (Weising, 2005), were determined. We used GenAlex 6.4 for these analyses (Peakall and Smouse 2006).

The Nei genetic distance (Weising 2005) was determined among the studied populations and was used for the grouping of the genotypes. Genetic differentiation of the studied populations was studied by AMOVA with 1000 permutations as performed in GenAlex 6.4 (Peakall and Smouse 2006).

Table 2. The accession numbers of taxa in cp-DNA studies.

No	Species	accession number
1	*Ziziphus jujuba*	HG765030.1
2	*Ziziphus jujuba*	HG765029.1
3	*Ziziphus jujuba*	HG765028.1
4	*Ziziphus jujuba*	GQ435353.1
5	*Ziziphus jujuba*	EU075109.1

Table 3. The accession numbers of taxa in ITS studies.

No	Species	accession number
1	*Ziziphus jujuba*	DQ146578.1
2	*Ziziphus jujuba*	DQ146577.1
3	*Ziziphus jujuba*	DQ146576.1
4	*Ziziphus jujuba*	DQ146575.1
5	*Ziziphus jujuba*	DQ146574.1
6	*Ziziphus jujuba*	DQ146573.1
7	*Ziziphus jujuba*	FJ593183.1
8	*Ziziphus jujuba*	EU075088.1
9	*Ziziphus jujuba*	KF241298.1
10	*Ziziphus jujuba*	KF241297.1
11	*Ziziphus jujuba*	KF186458.1

The Mantel test (Podani 2000) was performed to study the association between genetic distance and geographical distance of the studied populations. We also used Mantel test to investigate the agreement of results between ISSR and SRAP data. PAST ver. 3.14 (Hammer et al. 2001).

Genetic structure of the populations was studied by model-based clustering as performed by STRUCTURE software ver. 2.3 (Pritchard et al. 2000). We used the admixture ancestry model under the correlated allele frequency model. A Markov chain Monte Carlo simulation was run 20 times for each value of K (1-13) after a burn-in period of 10^5 . Data were scored as dominant markers and analysis followed the method suggested by Falush et al. (2007).

For the optimal value of K in the studied populations we used the STRUCTURE Harvester website (Earl and von Holdt 2012) to perform the Evanno method (Evanno et al. 2005). The choice of the most likely number of clusters (K) was carried out by calculating an ad hoc statistic ΔK based on the rate of change in the log probability of data between successive K values, as described by Evanno et al. (2005).

For ITS and cp-DNA the sequences were aligned by MUSCLE program as implemented in MEGA 7. NJ and Maximum likelihood phylogenetic trees were constructed by MEGA7 software (Tamura et al. 2012). Kimura distance was determined for jujuba cultivars based on ITS and cp-DNA sequences by MEGA ver.7.

RESULTS

ISSR assay

We obtained 40 ISSR bands (Loci) in total (Table 4). The highest Number of bands (27 bands) occurred in population 9 (Neyasar), followed by population 7 (Delijan) (23 bands). Some of the populations had private bands with population 9 having the highest number (6 private bands). Few common bands occurred in the population too. These are shared alleles among these populations.

Genetic diversity parameters determined in *Z. jujuba* populations are presented in Table 5. The percentage of genetic polymorphisma obtained ranged from 7.50 in population 2 (Ghazi-Olya) to 52.50 in population 7 (Delijan). A good level of genetic polymorphism (37.50%) also occurred in three populations 3, 4, and 5 (Doolatabad, Jafariyeh, and Dastjerd, respectively). The same populations had higher value of gene diversity (He).

AMOVA revealed that these populations differ significantly in their genetic content (PhiPT = 0.54, P = 0.001). AMOVA identified that 72% of total genetic variability occurred among populations while, 28% of genetic variability was due to within population difference. Paired-sample AMOVA also produced significant difference among the studied populations.

NJ clustering (Figure 1) revealed that most of the samples in the studied populations are grouped together and are almost separated from the other populations (For example, samples in populations 1, 2, 7, 8, 9, 11, 12, and 13).

Nei, genetic distance and genetic identity determined among *Ziziphus jujuba* populations (Table 6) revealed that genetic similarity among populations ranged from 0.58 between populations 9 and 13, to 0.93 between populations 3 and 5.

Table 4. Details of ISSR bands obtained in the studied populations of *Ziziphus jujuba* (populations numbers are according to Table 1).

Population	1	2	3	4	5	6	7	8	9	10	11	12	13
No. Bands	21	14	20	21	18	16	23	10	27	16	14	15	15
No. Private Bands.	0	1	0	0	0	1	2	0	6	0	0	0	1
No. LComm Bands (<=25%)	1	0	1	1	0	0	1	0	3	1	0	0	1
No. LComm Bands (<=50%)	5	2	4	3	2	2	6	2	6	3	4	3	1

Table 5. Genetic variability parameters determined in *Ziziphus jujube* populations based on ISSR markers (pop ulations numbers are according to Table 1).

Pop	Na	Ne	I	He	uHe	%P
Pop 1	0.800	10157	0.146	0.097	0.116	%27.50
Pop 2	0.425	1.045	0.041	0.027	0.033	%7.50
Pop 3	0.875	1.251	0.209	0.142	0.157	%27.50
Pop 4	0.900	1.283	0.232	0.154	0.176	37.50%
Pop 5	0.825	1.302	0.231	0.161	0.179	%37.50
Pop 6	0.575	1.101	0.092	0.061	0.070	%17.50
Pop 7	1.100	1.352	0.292	0.189	0.220	%52.50
Pop 8	0.425	1.125	0.102	0.070	0.080	%17.50
Pop 9	0.975	1.194	0.169	0.113	0.136	%30
Pop 10	0.550	1.077	0.072	0.047	0.052	%15
Pop 11	0.525	1.131	0.105	0.072	0.080	%17.50
Pop 12	0.600	1.136	0.123	0.082	0.098	%22.50
Pop 13	0.550	1.115	0.097	0.065	0.075	%17.50

N = No. plants, Na = No. alleles, Ne = No. effective alleles, I = Shanon Information Index, He = Nei gene diversity, UHe = Unbiased gene diversity, %P = Percentage of genetic polymorphism

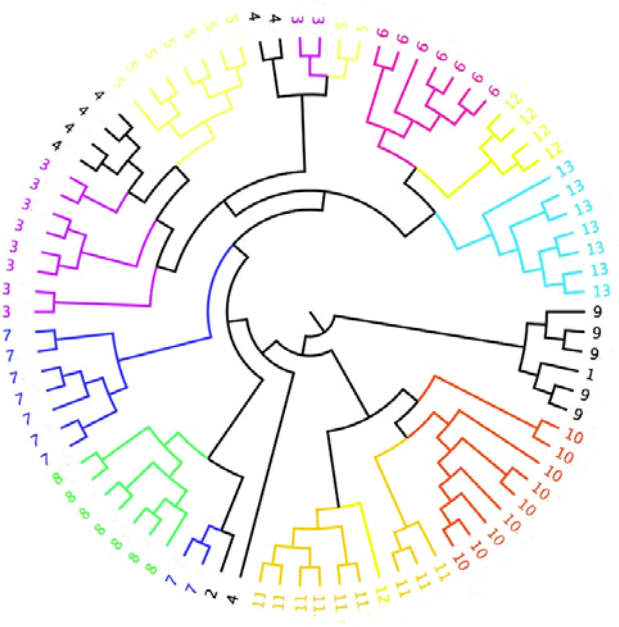

Figure 1. NJ dendrogram of *Ziziphus jujuba* specimens showing genetic differences of the studied populations.

Mantel test between geographical distance and genetic distance produced significant correlation ($P<0.01$). Therefore, with increase in geographical distance, genetic difference of the populations increased and isolation by distance (IBD) occurred in *Z. jujuba* populations studied.

The genetic structure of the studied populations and degree of gene flow/ or shared common alleles were determined by STRUCTURE analysis. The STRUCTURE plot (Figure 2) revealed presence of different allele combinations (differently coloured segments) in the *Z. jujuba* populations. However, some degree of shared common alleles was observed between populations 3 and 4, and to lesser extent population 5. Similarly, populations 10 and 11 had genetic similarity. The other populations had unique allele combinations (specific coloured segment) as well as some degree of shared alleles.

Evanno test produced optimal number of genetic group k = 8. Therefore, 13 studied Ziziphus jujuba populations studied could be grouped in 8 genetic groups.

SRAP Markers Assay

We obtained 42 SRAP bands (Loci) in total (Table 7). The highest Number of bands (26 bands) occurred in population 13, while the lowest number of SRAP bands occurred in population 4 (14 bands). Populations 1, 4, 8 and 13 had private bands. Few common bands occurred in the population too. These are shared alleles among the studied populations.

Genetic diversity parameters determined based on SRAP molecular markers in *Z. jujuba* populations are presented in Table 8. The percentage of genetic polymorphisma obtained ranged from 7.14 in population 8 to 38.10 in populations 3 and 13. These two populations had higher value of gene diversity (He).

AMOVA revealed that the studied *Ziziphus jujuba* populations differ significantly in their genetic content (PhiPT = 0.65, P = 0.001). AMOVA identified that 66% of total genetic variability occurred among populations while, 34% of genetic variability was due to within population difference. Paired-sample AMOVA also produced significant difference among the studied populations. NJ distance clustering (Figure 3) revealed that most of the samples in the studied populations are grouped together and are almost separated from the other populations (For example, samples in populations 1, 9, 12 and 13). This indicates that SRAP molecular markers can efficiently differentiate jujube populations and may be used in germplasm diversity evaluation.

PCoA plot of the studied populations (Figure 4) obtained after 99 permutations, almost separated the studied populations in two major groups (with populations 1 and 9 somewhere in the middle).

The populations 2-7 formed the first group, while populations 8, 10-13, comprised the second group. Therefore, *Zizphus jujuba* populations can be genetically discriminated by ISSR markers.

Table 6. Nei genetic distance and genetic identity (populations numbers are according to Table1).

Pop ID	1	2	3	4	5	6	7	8	9	10	11	12	13
1	****	0.7857	0.7781	0.7202	0.7947	0.7194	0.8011	0.7576	0.8117	0.7012	0.7697	0.7462	0.7660
2	0.2412	****	0.7929	0.7385	0.8074	0.6631	0.7905	0.7260	0.6737	0.7130	0.6715	0.6947	0.7035
3	0.2509	0.2321	****	0.9339	0.9511	0.8575	0.9064	0.8043	0.7280	0.7418	0.7362	0.8516	0.8704
4	0.3282	0.3031	0.0684	****	0.9309	0.8262	0.8844	0.7837	0.6696	0.7370	0.6891	0.8023	0.7803
5	0.2298	0.2139	0.0502	0.0716	****	0.8507	0.9397	0.8183	0.6888	0.7431	0.7417	0.8282	0.8274
6	0.3294	0.4109	0.1537	0.1909	0.1617	****	0.8230	0.7832	0.5932	0.7619	0.7230	0.8882	0.8224
7	0.2218	0.2351	0.0982	0.1228	0.0622	0.1948	****	0.8516	0.6906	0.7853	0.8219	0.8283	0.8054
8	0.2776	0.3202	0.2178	0.2437	0.2006	0.2443	0.1606	****	0.6428	0.7891	0.7644	0.7943	0.7376
9	0.2086	0.3950	0.3175	0.4011	0.3728	0.5222	0.3703	0.4419	****	0.5813	0.6721	0.6473	0.7684
10	0.3549	0.3383	0.2986	0.3052	0.2970	0.2719	0.2416	0.2369	0.5425	****	0.8698	0.7940	0.7124
11	0.2617	0.3983	0.3062	0.3724	0.2988	0.3244	0.1961	0.2686	0.3973	0.1395	****	0.8327	0.6940
12	0.2928	0.3643	0.1606	0.2203	0.1886	0.1186	0.1883	0.2303	0.4350	0.2307	0.1831	****	0.8511
13	0.2666	0.3517	0.1388	0.2481	0.1895	0.1956	0.2164	0.3043	0.2634	0.3392	0.3653	0.1613	****

Table 7. Details of SRAP bands obtained in the studied populations of *Ziziphus jujuba* (populations numbers are according to Table 1).

Population	Pop1	Pop2	Pop3	Pop4	Pop5	Pop6	Pop7	Pop8	Pop9	Pop10	Pop11	Pop12	Pop13
No. Bands	21	21	20	14	18	17	21	16	17	20	19	20	26
No. Bands Freq. >= 5%	21	21	20	14	18	17	21	16	17	20	19	20	26
No. Private Bands	1	0	0	1	0	0	0	1	1	0	0	0	2
No. LComm Bands (<=25%)	3	0	0	0	2	1	1	0	2	1	1	1	1
No. LComm Bands (<=50%)	8	7	7	4	5	5	8	1	5	6	7	8	11

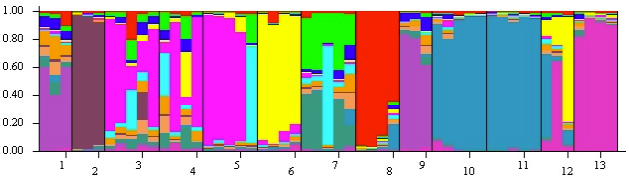

Figure 2. STRUCTURE plot of *Ziziphus jujuba* populations studied (populations numbers are according to Table1).

Table 8. Genetic distance among jujube cultivars based on cp-DNA PSBA sequences (populations numbers are according to Table 2).

	1	2	3	4
2	0			
3	0	0		
4	0.58	0.58	0.58	
5	0.58	0.58	0.58	0

STRUCTURE plot of SRAP molecular markers (Figure 5) revealed more detailed information on the genetic affinity of the studied populations. It also revealed the presence of specific allele combinations (differently coloured segments) versus available common shared alleles (similarly coloured segments) in these populations. For example, close affinity between populations 1 and 9 that were identified by PCoA plot seems to be due to some low degree of shared common alleles between these populations. The same is true for the other studied populations.

Evanno test produced delta k = 2 as the optimal genetic groups. Therefore, the studied jujuba populations can be differentiated in two broader and distinct genetic groups. The populations 1-7 form the first group, while populations 8-13 comprise the second group.

Mantel test performed between ISSR and SRAP data produced significant correlation (P = 0005). Therefore, both types of molecular markers efficiently differentiate jujuba populations and also show similar genetic grouping.

Similarly, Mantel test produced significant correlation (P = 0.001) between the studied molecular markers with geographical distance of the populations. Therefore, with increase in geographical distance among jujube populations, the genetic difference of these populations also increases. This indicates the occurrence of IBD (Isolation by distance) in the studied jujuba populations.

Table 9. Genetic distance among jujube cultivars based on nuclear DNA (ITS sequences) (populations numbers are according to Table 2).

	1	2	3	4	5	6	7	8	9	10
2	0									
3	0	0								
4	0	0.003	0.003							
5	0	0.003	0.003	0						
6	0	0.003	0.003	0	0					
7	0	0.003	0.003	0	0	0				
8	0	0.007	0.007	0.003	0.003	0.003	0.003			
9	0	0.007	0.007	0.003	0.0037	0.003	0.003	0		
10	0	0.007	0.007	0.003	0.0037	0.003	0.003	0	0	
11	0	0.007	0.007	0.0037	0.0037	0.003	0.003	0	0	0

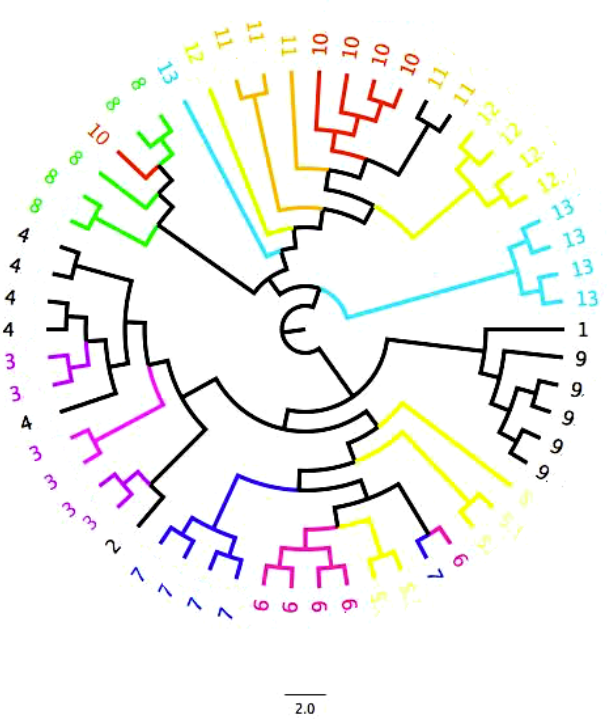

Figure 3. NJ dendrogram of the studied *Ziziphus jujube* populations based on SRAP molecular markers. (Populations 1-13 are according to Table 1).

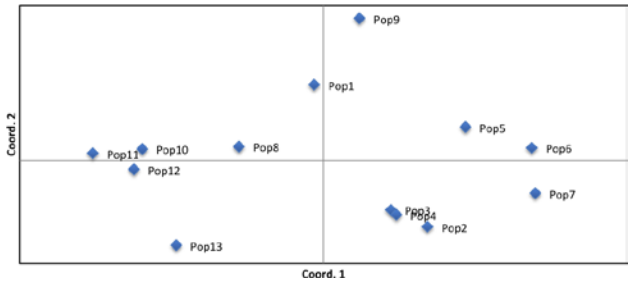

Figure 4. PCoA plot of *Ziziphus jujube* populations based on SRAP molecular markers. (Populations 1-13 are according to Table 1).

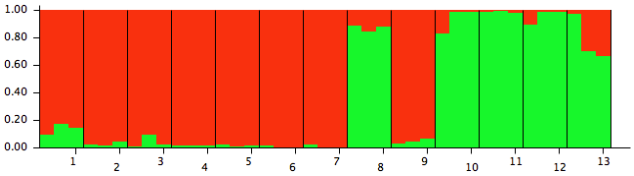

Figure 5. Top: STRUCTURE plot of *Ziziphus jujuba* populations based on SRAP data. Bottom: STRUCTURE plot based on k = 2 (Populations 1-13 are according to Table 1).

ITS and cp- DNA Sequences

Nuclear r-DNA (ITS) and chloroplast inter-genic region of trnH-psbA sequence data were obtained for few jujuba cultivars. Phylogenetic tree based on these sequences (Figures 6 and 7) differentiated the studied cultivars in three clusters with high bootstrap values. Therefore, we can also apply these sequence-based molecular markers in future studies to investigate jujuba cultivar discrimination, the methods that have not been utilized in genetic finger printing of this important horticultural plant species.

Pair-wise genetic distances in the studied jujube cultivars are provided in Tables 9 and 10. In case of trnH-psbA, we obtained the mean genetic distance of 0.58 which is comparable to the genetic distance obtained for ISSR and SRAP molecular markers. However, in case of ITS sequences, we obtained much lower genetic distance value (0.003-0.007). This is probably due to much more conservative nature of ITS sequences compared to that of cp-DNA inter-genic sequences. Therefore, we may suggest using cp-DNA inter-genetic sequences for future

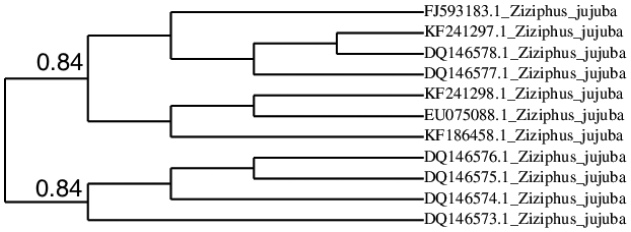

Figure 6. Maximum parsimony phylogenetic tree of jujube cultivars based on ITS sequences (Numbers above branches are bootstrap value).

Table 9. Genetic distance among jujube cultivars based on cp-DNA PSBA sequences (populations numbers are according to Table 2).

	1	2	3	4
2	0			
3	0	0		
4	0.58	0.58	0.58	
5	0.58	0.58	0.58	0

genetic finger printing of jujube cultivars and populations, but also keeping in mind that using multilocus molecular markers (ISSRs and SRAPs) are more cost-benefit approaches.

DISCUSSION

Population genetic study provides valuable information on genetic structure of plants, the stratification versus gene flow among the species populations, genetic divergence of the populations, etc. (Sheidai et al. 2014). These information have different applications, and from pure understanding of biology of the species to conservation of endangered species, choosing of proper parents

Figure 7. Maximum parsimony phylogenetic tree of jujube cultivars based on trnH-psbA sequences (Numbers above branches are bootstrap value).

for hybridization and breeding and phylogeography and mechanism of invasion (Freeland et al. 2011). *Ziziphus jububa* is of wide spread in our country and it has several medicinal applications (Vahedi et al. 2008), however we had no information on its genetic structure. The present study revealed interesting data about its genetic variability, and genetic stratification of this medicinally important species in the country.

Assessment of the genetic variation within collections of *Ziziphus jujuba* genetic resources is crucial for the effective conservation and utilization of these resources in breeding programs, and could be dramatically enhanced by using molecular genotyping tools. The present study revealed that multilocus molecular markers like ISSRs and SRAPs are powerful technique for the assessment of genetic variability among *Ziziphus jujuba* collections. Moreover, we can also use cp-DNA inter-genic sequences for genetic finger printing and discriminating jujuba cultivars and populations. For

Table 10. Genetic distance among jujube cultivars based on nuclear DNA (ITS sequences) (populations numbers are according to Table 2).

	1	2	3	4	5	6	7	8	9	10
2	0									
3	0	0								
4	0	0.003	0.003							
5	0	0.003	0.003	0						
6	0	0.003	0.003	0	0					
7	0	0.003	0.003	0	0	0				
8	0	0.007	0.007	0.003	0.003	0.003	0.003			
9	0	0.007	0.007	0.003	0.0037	0.003	0.003	0		
10	0	0.007	0.007	0.003	0.0037	0.003	0.003	0	0	
11	0	0.007	0.007	0.0037	0.0037	0.003	0.003	0	0	0

grouping of the cultivars we can also utilizenuclear r-DNS sequences.

We obtained about 40 bands for either of ISSR and SRAP molecular markers and almost good level of genetic variability within each population (ranging from 17 to 35%). These markers have good discriminating power to differentiated jujuba populations. Cp-DNA inter-genic sequences also revealed high degree of genetic difference among jujuba cultivars (0.58).

Saleh et al. (2016), studied genetic diversity in populations of *Ziziphus spina-christi* (L.) Willd. By using 11 ISSR markers and reported the occurrence of 105 scorable loci, of which 93.4% were found to be polymorphic. They obtained genetic diversity value of 0.26, and total genetic diversity Ht = 0.266, as well as intra-population genetic diversity, Hs = 0.22.

These values are in good agreement with genetic variability obtained here by both multilocus molecular markers (ISSRs and SRAPs) as well as cp-DNA sequences.

The genetic variability within the studied populations is of fundamental importance in the continuity of a species as it is used to bring about the necessary adaptation to the cope with changes in the environment (Sheidai et al. 2013, 2014). This is particularly expected in *Ziziphus jujuba* as it forms several geographical populations throughout the country.

Degree of genetic variability within a species is highly correlated with its reproductive mode, the higher degree of open pollination/ cross breeding brings about higher level of genetic variability in the studied taxon (Freeland et al. 2011). *Ziziphus jujuba* is a self-incompatible species (Asatryan and Tel-Zur 2013) and therefore, moderate genetic variability in these populations may be related to the open pollination nature of this species.

AMOVA revealed significant genetic difference among the studied populations of jujube, while Ivanno test identified 8 genetic groups within these populations. Moreover, Mantel test showed positive significant correlation between genetic distance and geographical distance. All these data support some kind of genetic distinctness of the jujuba populations studied. Different mechanisms like isolation, drift, founder effects and local selection may act to bring about among population differentiation (Jolivet and Bernasconi 2007; Sheidai et al. 2014).

In conclusion, the present study revealed good level of genetic diversity among wild/ uncultivated populations of jujube which can be used in conservation and breeding of this important horticultural crop plant within the country. As this crop has several wild geographical populations throughout the country, we plan to continue our quest to investigate many more populations in nearby future and try to utilize cp-DNA inter-genic sequences along with multilocus molecular markers for genetic discrimination of wild populations.

REFERENCES

Alake CO, Alake OO. 2016. Genetic diversity for agro-nutritional traits in African landraces of Vigna subterranean Germplasm. Journal of Crop Improvement. 30(4):378–398.

Alansi S, Tarroum M, Al-Qurainy F, Khan S, Nadeem M. 2016. Use of ISSR markers to assess the genetic diversity in wild medicinal *Ziziphus spina-christi* (L.) Willd. collected from different regions of Saudi Arabia. *Biotechnology & Biotechnological Equipment* 30: 942- 947.

Asatryan A, Tel-Zur N. 2013. Pollen tube growth and self-incompatibility in three *Ziziphus* species (Rhamnaceae). Flora. 208:390-399.

Evanno G, Regnaut S, Goudet J. 2005. Detecting the number of clusters of individuals using the software STRUCTURE: a simulation study. Molecular Ecology.14: 2611-2620.

Earl DA, Von Holdt Bm . 2012. STRUCTURE HARVESTER: a website and program for visualizing STRUCTURE output and implementing the Evanno method. Conservation Genetics Resources 4: 359–361.

Falush D, Stephens M, Pritchard JK. 2007. Inference of population structure using multilocus genotype data: dominant markers and null alleles. Molecular Ecology Notes. 7:574-578.

Feng SG, Lu JJ, Gao L, Liu JJ, Wang HZ .2014. Molecular Phylogeny Analysis and Species Identification of *Dendrobium* (Orchidaceae) in China. Biochemical Genetics. 52:127–136.

Freeland J R, Kirk H, Petersen S. 2011. Molecular Genetics in Ecology. Molecular Ecology Notes . 2: 1-34.

Gupta M, Mazumder UK, Vamsi ML, Sivakumar T, Kandar CC. 2004. Anti-steroidogenic activity of the two Indian medicinal plants in mice. Journal of Ethnopharmacology. 90(1):21-25.

Huang X, Kojima-Yuasa A, Norikura T, Kennedy Do, Hasuma T, Matsui-Yuasa I. 2007. Mechanism of the anti-cancer activity of *Zizyphus jujuba* in HepG2 cells. The American Journal of Chinese Medicine. 35:517-532.

Huang J, Yang X, Zhang C, Yin X, Liu S, Li X . 2015. Development of Chloroplast Microsatellite Markers and Analysis of Chloroplast Diversity in Chinese Jujube (*Ziziphus jujuba* Mill.) and Wild

Jujube (*Ziziphus acidojujuba* Mill.). PLoS ONE 10: e0134519.

Islam MB, Simmons MP.2006. A Thorny Dilemma: Testing Alternative Intrageneric Classifications within *Ziziphus* (Rhamnaceae). Systematic Biology 31: 826–842.

Jiang, J.G., Huang, X.J., Chen, J, Lin, Q.S. 2007. Comparison of the sedative and hypnotic effects of flavonoids, saponins, and polysaccharides extracted from Semen *Ziziphus jujuba* . Natural Product Research. 21:310-320.

Hosseinpour R, Ahmadi K, Ebaddzadeh H, Mohammadnia Afroozi SH , Abbastaghani R. 2016. Exoports and Imports agronomical section. Jihad -Keshavarzi Ministry, Planning and Economic section, Data and Comunation center. Tehran, Iran, PP. 107.

Jolivet C, Bernasconi G. 2007. Molecular and quantitative genetic differentiation in European populations of *Silene latifolia* (Caryophyllaceae). Journal of Human Genetics.177:1239-1247.

Križman M, Jakše J, Baričevič D, Javornik B , Prošek M. 2006. Robust CTAB-activated charcoal protocol for plant DNA extraction. Acta Agriculturae Slovenica. 87:427- 433.

Lee SM, Park JG, Lee YH. 2004. Anti-complementary activity of triterpenoides from fruits of *Zizyphus jujuba* . Biological and Pharmaceutical Bulletin. 27:1883-1886.

Liu P, Peng JY, Peng SQ, Zhou JY, Dai L. 2005. Study on Systematic Relationships of *Ziziphus jujuba* using RAPD technique. Scientia Sinica. 41:182-185.

Peakall R, Smouse PE. 2006. GENALEX 6: genetic analysis in Excel. Population genetic software for teaching and research. Molecular Ecology Notes. 6: 288-295.

Peng JY, Shu HR, Sun ZX, Peng SQ .2000. RAPD Analysis of germplasm resources on Chinese date. Acta Chimica Sinica 27: 171–176.

Podani J. 2000. Introduction to the Exploration of Multivariate Data. Backhuyes, Leiden, 407 pp.

Singh A, Sharma P, Singh R.2007. Assessment of genetic diversity in *Ziziphus mauritiana* using inter-simple sequence repeat markers. Journal of Plant Biochemistry and Biotechnology. 16:35- 40.

Sheidai M, Zanganeh S, Haji-Ramezanali R, Nouroozi M, Noormohammadi Z, Ghsemzadeh-Baraki S. 2013. Genetic diversity and population structure in four *Cirsium* (Asteraceae) species. Biologia. 68: 384-397.

Sheidai M, Ziaee S, Farahani F, Talebi Sm, Noormohammadi Z, Hasheminejad Ahangarani Farahani Y . 2014. Infra-specific genetic and morphological diversityin *Linum album* (Linaceae). Biologia. 69: 32e39

Sheidai M, Taban F, Talebi Sm, Noormohammadi Z. 2016. Genetic And morphological diversity in *Stachys lavandulifolia* (Lamiaceae) populations. Biologija. 62(1) : 9-24.

Tamura K, Peterson D, Peterson N, Stecher G, Nei M, Kumar S. 2012. MEGA5: molecular evolutionary genetics analysis using maximum likelihood,evolutionary distance, and maximum parsimony methods. Molecular Biology and Evolution. 28:2731e2739.

Vahedi F, Fathi Najafi M, Bozari K. 2008. Evaluation of inhibitory effect and apoptosis induction of *Zizyphus jujuba* on tumor cell lines, an in vitro preliminary study. Cytotechnology. 56:105-111.

Wang S, Liu Y, Ma L, Liu H, Tang Y, Wu L. 2014. Isolation and characterization of microsatellite markers and analysis of genetic diversity in Chinese jujuba (*Ziziphus jujuba* Mill.). Plos One. 9: e99842.

Wang YK, Tian JB, Wang YQ, Sui Cl, Li Dk, Huang Cl. 2007. AFLP analysis of jujuba cultivars and strain. Journal of Fruit Science. 242: 146–150.

Zhang C, Huang J, Yin X, Lian C, Li X. 2014. Genetic diversity and population structure of sour jujuba, *Ziziphus acidojujuba*. Tree Genetics & Genomes. 11:809.

Caryologia
International Journal of Cytology, Cytosystematics and Cytogenetics

Firenze University Press
www.fupress.com/caryologia

Citation: M. Alemdag, R.C. Ozturk, S.A. Sahin, I. Altinok (2019) Karyotypes of Danubian lineage brown trout and their hybrids. *Caryologia* 72(4): 61-67. doi: 10.13128/caryologia-160

Published: December 23, 2019

Data Availability Statement: All relevant data are within the paper and its Supporting Information files.

Competing Interests: The Author(s) declare(s) no conflict of interest.

Karyotypes of Danubian lineage brown trout and their hybrids

Melike Alemdag, Rafet Cagri Ozturk, Sebnem Atasaral Sahin, Ilhan Altinok*

Department of Fisheries Technology Engineering, Surmene Faculty of Marine Sciences, Karadeniz Technical University, 61530 Surmene, Trabzon, Turkey
*Corresponding author: ialtinok@ktu.edu.tr

Abstract. Cytogenetic analysis of brown trout, *Salmo trutta*, have been described for different populations and morphs; however, cytogenetic analysis of interspecific brown trout hybrids is unknown. Cultured kidney cells from four brown trout subspecies (*Salmo trutta abanticus*, *S.t. caspius*, *S.t. fario* and *S.t. labrax*) and their reciprocal hybrids were karyotyped using conventional staining, C-banding and Ag-NOR staining techniques. Chromosome number (2N) and chromosome arm number (NF) ranged from76 to 80 and 98 to 102, respectively. Silver staining revealed the presence of NOR sites on the short arm of the submetacentric chromosome. The size and number of NOR sites showed uniformity. The presence of heterochromatin on different chromosome arms was confirmed by C-banding. The presence and position of constitutive heterochromatin showed variability among individuals. Chromosome structures of purebred brown trout subspecies belonging to the Danubian linage and their hybrids were similar, and no distinctive characteristics were observed in any of the species. The results of this study are applicable to the development of improved conservation and management strategies for brown trout.

Keywords. Cytogenetic, Karyotype, *Salmo trutta*, Ag-NOR, C-banding.

INTRODUCTION

Brown trout, *Salmo trutta* (Linnaeus, 1758), is a polymorphic and widespread species. Its historic geographic range covers Europe, Western Asia and Northern Africa. During the past century, *Salmo trutta* have been introduced to different parts of the world, and the range of brown trout has been extended to all continents except Antarctica (Elliott, 1989). The systematic classification of *Salmo trutta* is plagued by many nomenclatural issues. *Salmo trutta* was once recognized as a polymorphic species with three morphs based on life-history variation: resident trout, lake trout and river trout (Ferguson, 2004). Mitochondrial DNA (mtDNA) sequence variation analysis revealed the existence of five major phylogenetic groups, which are believed to have been separated for some 500,000 to 2 million years (Bernatchez, 1995). Over the years, distinct species or nominal subspecies have

been described based on morphological and molecular analysis (Kottelat & Freyhof, 2007; Turan, Kottelat, & Engin, 2014). However, *S. trutta* subspecies such as *S.t. abanticus*, *S.t. caspius*, *S.t. fario* and *S.t. labrax* belonging to Danubian lineage have been proved to be a single biological species called *Salmo trutta*. Thus, it was recommended that strains should be named according to location, such as Abant, Caspian, Anatolian and Black Sea (Kalayci et al., 2018).

Inter- and intraspecific hybridization experiments in fish are often less concerned with identification of the genomic composition than with the evolution of performance and survival (Johnson & Wright, 1986). Morphology and variation in chromosome number have been proven useful in identifying fish populations (Phillips, 2005). Cytogenetically, the *Salmo trutta* complex is one of the best analyzed salmonid. The karyotype of *Salmo trutta* consists of 80 chromosomes with a fundamental arm number (NF) ranging from 98 to 102 (Amaro, Abuin, & Sanchez, 1996; Woznicki, Jankun, & Luczynski, 1998; Woznicki, Sanchez, Martinez, Pardo, & Jankun, 2000). Although *Salmo trutta* have been subjected to numerous cytogenetic analyses, and karyotypes have been described for different populations and morphs, (Caputo, Giovannotti, Cerioni, Splendiani, & Olmo, 2009; Jankun, 2000; Kalbassi, Dorafshan, Tavakolian, Khazab, & Abdolhay, 2006; Northland-Leppe, Lam, Jara-Seguel, & Capetillo-Arcos, 2009; Woznicki, Jankun, & Luczynski, 1997; Woznicki et al., 1998), the chromosome complement of interspecific brown trout hybrids seems to be comparatively less studied (Polonis, Fujimoto, Dobosz, Zalewski, & Ocalewicz, 2018; Ziomek, Debowska, Hliwa, & Ocalewicz, 2016). A cytogenetic characterization of hybrids and parental species would aid in a better understanding of their species status. Therefore, the aim of the present study was 1) to determine the chromosomal characteristics of Abant trout (*S.t. abanticus*), Black Sea trout (*S.t. labrax*), Caspian trout (*S.t. caspius*), Anatolian trout (*S.t. fario*) and their reciprocal hybrids and 2) to determine if the NF of chromosomes varies among purebred and hybrid trout.

MATERIALS AND METHODS

Fish

Abant, Anatolian, Black Sea and Caspian trout were crossed to each other to produce the F1 generation of all possible reciprocal crossing combinations (16 cross-types) (Table 1). After fertilization, each family was separately incubated in a vertical incubator and transferred to a separate flow-through indoor tank after hatching. This study was approved by the Institutional Animal Care and Use Committee at Karadeniz Technical University (approval #14/2013).

Chromosome Preparation

Five fish from each cross-type were used in chromosome analysis (Table 1). Fish were anaesthetized with ice, and their anterior kidney tissue was sampled on ice. Tissue was cut into small pieces and incubated in 1.5 ml of RPMI media supplemented with penicillin G (75 U/ml), fungizone (1.5 µg/ml), gentamycin sulphate (30 µg/ml) and streptomycin sulphate (75 µg/ml) for 24 h at room temperature. Supplementing the culture media with antibiotics eliminated any growth of fungi, yeasts, mycoplasma and Gram-positive and Gram-negative bacteria. After incubation of the tissue with colchicine (0.1%) for 1 h, samples were centrifuged at 1000 x *g* for 10 min, and the supernatant was removed. Pellets were resuspended in 3 ml ice-cold 0.075 mol/l KCl solution, incubated at 4°C for 30 min and then four drops of ice-cold Carnoy fixative (methanol: acetic acid, 3:1) were added. Samples were centrifuged at 1000 x *g* for 10 min, and the supernatant was removed. After that, 5 ml of fixative was added to the sample, which was then centrifuged at 1000 x *g* for 10 min. This step was repeated three times to wash the cells. Tissues were transferred to a petri dish with one milliliter of fixative and then cut into small pieces with a surgery blade. Slides were placed over boiled

Table 1. Cross-types of fish and their abbreviation, mean length and weight.

Crosses (female X male)	Family Abbreviation	Mean Length (cm)	Mean Weight (gr)
S.t labrax X *S.t. labrax*	LL	18.63±1.41	69.18±5.25
S.t. labrax X *S.t. abanticus*	LA	19.70±1.50	71.51±5.31
S.t. labrax X *S.t. caspius*	LC	24.36±1.81	156.0±10.12
S.t. abanticus X *S.t. abanticus*	AA	17.37±1.28	38.84±3.00
S.t. abanticus X *S.t. labrax*	LL	16.45±1.11	48.58±3.41
S.t. abanticus X *S.t. caspius*	LA	15.20±1.08	34.78±2.04
S.t. caspius X *S.t. labrax*	LC	15.88±1.12	41.70±3.06
S.t. caspius X *S.t. abanticus*	AA	11.62±0.84	13.67±0.07
S.t. caspius X *S.t. caspius*	LL	12.54±0.92	18.30±1.025
S.t. fario X *S.t. fario*	FF	7.15±0.41	5.11±1.01
S.t. fario X *S.t. abanticus*	FA	6.01±0.28	5.09±0.09
S.t. fario X *S.t. caspius*	FC	5.12±0.17	4.81±0.41
S.t. fario X *S.t. labrax*	FL	6.57±0.65	4.51±0.46
S.t. abanticus X *S.t. fario*	AF	7.24±0.47	5.11±1.06
S.t. caspius X *S.t. fario*	CF	5.03±0.21	4.24±0.38
S.t. labrax X *S.t. fario*	LF	7.31±0.58	5.19±0.91

water steam, and three drops of cell suspension were dropped onto slides from a height of 30–40 cm. For each fish species, a total of 15 slides were prepared and air dried, and 5 of them were stained with 10% Giemsa. The remaining 10 were used for C-banding (5 slides) and Ag-NORs analysis as explained below.

C-banding was performed according to the method described by Sumner (1972), with slight modifications. Slides containing the chromosome preparation were treated with 0.2 mol/l HCl solution at 37°C for 1 h and rinsed with distilled water. Washed slides were incubated in 2X SSC (pH 7.0) at 60°C for 1 h, rinsed with distilled water and finally stained with 10% Giemsa for 20 min.

Silver staining of nucleus organizer regions (Ag-NORs) were performed according to the method described by Howell and Black (1980). Two drops of colloidal developer and a single drop of aqueous silver nitrate were dropped onto a slide on which the chromosome preparation was mounted and covered with a cover glass. The slide was incubated at 70°C until the silver-staining mixture turned a golden-brownish color. The slides were then rinsed with distilled water, air dried and stained with 10% Giemsa.

Metaphase cells were screened with a fully automated karyotyping software system (CytoVision ver. 3.92) connected to an Olympus light microscope. Metaphase cell photos were captured at 100x magnification for further analysis. Ten high-quality metaphase spreads from each slide were used in chromosome analysis. Image-Pro Premier (Media Cybernetics), SmartType 3.1.0.43 (Digital Scientific, Cambridge, UK) and tpsDig2 v2.26 (New York State University, Stony Brook, USA) were used in karyotyping. The NF value was estimated by counting biarmed (metacentric and submetacentric) and unarmed (acrocentric and subtelocentric) chromosomes and calculated according to the formula given by Naran (1997).

RESULTS

The chromosome numbers and structures of four subspecies of brown trout and their cross-types (n = 16) were successfully determined. Furthermore, karyogram and chromosome measurement tables were generated. About 500 metaphase plates from 80 individuals were examined. Cross-types were karyotyped based on the representative chromosome image (Fig. 1) and chromosome arm scale (Table 2). Diploid chromosome numbers (2N) of all examined cross-types ranged from 76 to 80, but the majority of cross-types had 2N = 80 chromosomes (Table 3). The pure breed LL (see Table 1 for abbreviation) and the hybrid CA had 76 chromosomes, while CL had 78 chromosomes The NF varied from 96 to 102, the lowest being obtained from CL (96) followed by CC, LL and CA (98) (Table 3). Metacentric (M), submetacentric (SM) and acrocentric/telocentric (A/T) chromosome numbers varied from 14 to 18, 4 to 8, 2 to 14 and 46 to 56, respectively, among cross-types (Table 3).

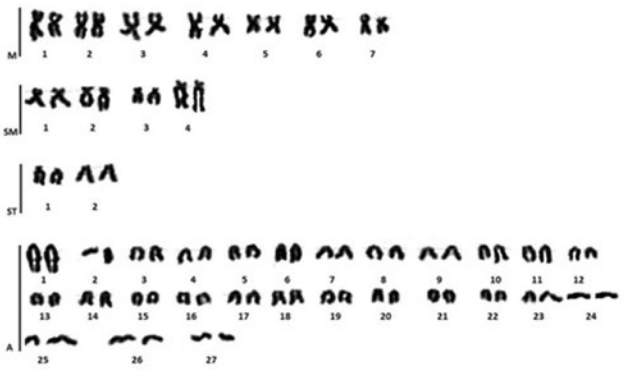

Figure 1. Karyotype of Abant trout *Salmo t. abanticus (2N=80)* stained conventionally with Giemsa. Metacentric (M), submetacentric (SM), subtelocentric (ST), acrocentric and telocentric chromosome (A/T) of cross-types.

Ag-NOR staining revealed the presence of one pair of NOR sites on the short arm of the SM chromosome in all the analyzed specimens (Fig 2). C-banding showed constitutive heterochromatin at the centromeres and arms of most of the chromosomes (Fig. 3) and the presence and position of constitutive heterochromatin within cross-types were variable even in pure breeds (Fig. 3). C-banding was not discriminative for brown trout subspecies.

DISCUSSION

Several cytogenetic methods of chromosome isolation have been developed. The main objective of all such methods is to obtain cells at the metaphase stage by disrupting the cell spindle (Pack, 2002). Solid tissues and cultured cells, together with colchicine treatment, are the most common sources of samples for the preparation of slides of fish chromosomes. Spleen, kidney, liver, gills and scales are the preferred sources of chromosomes. To prepare chromosomes, we first used the solid-tissue technique by harvesting various fish tissues and then empirically tested the colchicine concentration, exposure method (injection and bath) and fixation duration to obtain the most efficient means of chromosome preparation. Despite our efforts, we were unable to prepare metaphase plates for all but a couple of samples. With

Table 2. Relative arm lenght (μ), total lenght (μ), arm ratio (p/q) and chromosome type of Abant trout.

Chromosome number (2n)	Short arm length (p)	Long arm length(q)	Total Lenght	Arm ratio (q/p)	Chromosome Type
1	0.12	0.12	0.24	1.00	M
2	0.12	0.12	0.24	1.00	M
3	0.12	0.12	0.24	1.00	M
4	0.12	0.12	0.24	1.00	M
5	0.90	0.90	1.80	1.00	M
6	0.10	0.10	0.20	1.00	M
7	0.80	0.80	1.70	0.89	M
8	0.05	0.12	0.17	2.40	SM
9	0.07	0.13	0.20	1.86	SM
10	0.05	0.10	0.15	2.00	SM
11	0.03	0.12	0.15	4.00	ST
12	0.06	0.19	0.25	3.17	ST
13	0.02	0.13	0.15	6.50	ST
14	0.00	0.22	0.22	∞	A
15	0.00	0.09	0.09	∞	A
16	0.00	0.14	0.14	∞	A
17	0.00	0.12	0.12	∞	A
18	0.00	0.14	0.14	∞	A
19	0.00	0.15	0.15	∞	A
20	0.00	0.11	0.11	∞	A
21	0.00	0.11	0.11	∞	A
22	0.00	0.11	0.11	∞	A
23	0.00	0.11	0.11	∞	A
24	0.00	0.11	0.11	∞	A
25	0.00	0.12	0.12	∞	A
26	0.00	0.10	0.10	∞	A
27	0.00	0.11	0.11	∞	A
28	0.00	0.10	0.10	∞	A
29	0.00	0.08	0.08	∞	A
30	0.00	0.10	0.10	∞	A
31	0.00	0.12	0.12	∞	A
32	0.00	0.12	0.12	∞	A
33	0.00	0.11	0.11	∞	A
34	0.00	0.11	0.11	∞	A
35	0.00	0.07	0.07	∞	A
36	0.00	0.08	0.08	∞	A
37	0.00	0.08	0.08	∞	A
38	0.00	0.10	0.10	∞	A
39	0.00	0.08	0.08	∞	A
40	0.00	0.13	0.13	∞	A

Table 3. Chromosome number (N) fundamental number (NF) and structure [metacentric (M), submetacentric (SM), subtelocentric (ST), acrocentric and telocentric chromosome (A/T)] of cross-types.

Cross-type	M	SM	ST	A/T	N	NF
AA	14	8	2	56	80	102
CC	14	4	4	58	80	98
LL	16	6	4	50	76	98
FF	14	6	4	56	80	100
AC	16	4	8	52	80	100
AL	16	6	2	56	80	102
CA	16	6	6	48	76	98
CL	14	4	8	52	78	96
LA	16	4	14	46	80	100
LC	18	4	2	56	80	102
AF	18	4	2	56	80	102
FA	16	4	4	56	80	100
FC	18	4	4	54	80	102
CF	16	4	6	54	80	100
LF	16	6	4	54	80	102
FL	16	4	6	54	80	100

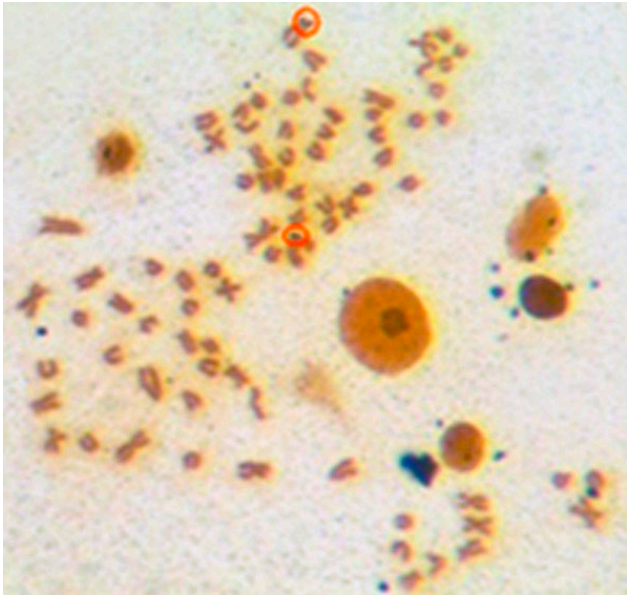

Figure 2. Karyotype of Abant trout *Salmo t. abanticus* with silver staining. Presence of NOR sites on the short arm of the submetacentric chromosome indicated with red ring.

the cell culture technique as described in the Materials and Methods section, we were able to obtain numerous well-spread metaphase chromosomes. The solid-tissue technique is applicable to various eukaryotic organisms (Kligerman & Bloom, 1977), but we favor the culture technique when working with salmonid fish, especially *Salmo trutta*.

The typical karyotypes of all three ecological forms of *Salmo trutta* (2N = 80 and NF = 100 – 102) were found, in agreement with numerous other studies

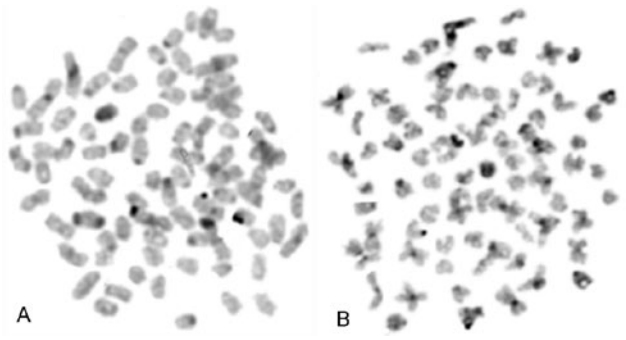

Figure 3. C-banded karyotype of Abant trout *Salmo t. abanticus.* Constitutive heterochromatin at the centromeres and arms of most of the chromosomes.

(Woznicki et al., 1998). This study documented slight karyotype variation among cross-types, with a diploid chromosome number and NF ranging from 76 to 80 and 98 to 102, respectively, while the majority of the cross-types exhibited 2N = 80, in agreement with previous reports (Woznicki et al., 1998). Intra-specific variation in both chromosome number and NF was previously documented among different fish species, including brown trout (Gjedrem, Eggum, & Refstie, 1977). Intra-specific variation in chromosome numbers in these trout forms and their hybrids suggest centric fusion between acrocentric chromosome pairs during the karyotype evolution of Robertsonian translocation. Loss of chromosome number due to counting errors and chromosome loss during preparation of slides is within the bounds of possibility (Gold & Gall, 1975; Zenzes & Voiculescu, 1975). Allopolyploids have genomes from different species; therefore, it is associated with hybridization. Allopolyploidy can be occurred in the nature as a results of interspecific or intergeneric hybridizations and offspring holds two different diploid chromosome sets (Zhou & Gui, 2017). Consequence of interhomolog recombination in genomic rearrangements can cause gene losses, and gametic aneuploidy (Hollister, 2015).

Polymorphic NOR size is common in fish and particularly in salmonids (Gold, 1984; Woznicki & Jankun, 1994). The NORs are commonly located on chromosome pair number 11 in *Salmo trutta,* but multichromosomal NOR-site polymorphism and variation in NOR size has also been reported (Sanchez, Martinez, Vinas, & Bouza, 1990; Schmid et al., 1995; Zhuo, Reed, & Phillips, 1995). In our study, the positions of NORs showed remarkable uniformity among individuals and cross-types. We could not detect any variation in the size and number of NORs.

Chromosomal characteristics of brown trout hybrids were studied for the first time in the present study. Chromosome structures of purebred brown trout subspecies (*S.t. abanticus*, *S.t. caspius*, *S.t. fario* and *S.t. labrax*) belonging to the Danubian linage and their hybrids were similar, and no distinctive characteristic was observed in any of the species. Therefore, they should be the same species but different strains. This statement was confirmed by Kalayci et al. (2018). They found that *S.t. abanticus*, *S.t. caspius*, *S.t. fario* and *S.t. labrax* are single biological species which should be called *Salmo trutta*. The results of this study are applicable to the development of improved conservation and management strategies for brown trout. Brown trout population in the nature is very low and governmental fisheries agencies are releasing hatchery reared brown trout to the stream or rivers to restore the population. Therefore, extra precaution should be should be taken in order to protect local brown trout population genetics

ACKNOWLEDGEMENTS

This study was funded by the Scientific and Technological Research Council of Turkey (TUBITAK: 214O595).

DISCLOSURE STATEMENT

The authors declare that they have no conflict of interest

REFERENCES

Amaro, R., Abuin, M., & Sanchez, L. (1996). Chromosomal evolution in salmonids: A comparison of Atlantic salmon, brown trout, and rainbow trout R-band chromosomes. *Genetica, 98*(3), 297-302. doi:10.1007/Bf00057594

Bernatchez, L. (1995). A role for molecular systematics in defining evolutionarily significant units in fishes. *Evolution and the Aquatic Ecosystem: Defining Unique Units in Population Conservation, 17*, 114-132.

Caputo, V., Giovannotti, M., Cerioni, P. N., Splendiani, A., & Olmo, E. (2009). Chromosomal study of native and hatchery trouts from Italy (Salmo trutta complex, Salmonidae): conventional and FISH analysis. *Cytogenetic and Genome Research, 124*(1), 51-62. doi: 10.1159/000200088

Elliott, J. M. (1989). Wild Brown Trout Salmo-Trutta - an Important National and International Resource. *Freshwater Biology, 21*(1), 1-5. doi: 10.1111/j.1365-2427.1989.tb01343.x

Ferguson, A. (2004). *Brown trout genetic diversity: origins, importance and impacts of supplemental stocking.* Paper presented at the Proceedings of the Institute of Fisheries Management 34th Annual Study Course.

Gjedrem, T., Eggum, A., & Refstie, T. (1977). Chromosomes of Some Salmonids and Salmonid Hybrids. *Aquaculture, 11*(4), 335-348. doi: 10.1016/0044-8486(77)90083-7

Gold, J. R. (1984). Silver-Staining and Heteromorphism of Chromosomal Nucleolus Organizer Regions in North-American Cyprinid Fishes. *Copeia*(1), 133-139. doi: 10.2307/1445043

Gold, J. R., & Gall, A. E. (1975). Chromosome cytology and polymorphism in the Californian high sierra golden trout (*Salmo aguabonita*). *Canadian Journal of Genetics and Cytology, 17*, 41-53.

Hollister, J.D. 2015. Polyploidy: adaptation to the genomic environment. *New Phytologist* (2015) 205: 1034–1039. doi: 10.1111/nph.12939

Howell, W. M., & Black, D. A. (1980). Controlled Silver-Staining of Nucleolus Organizer Regions with a Protective Colloidal Developer - a 1-Step Method. *Experientia, 36*(8), 1014-1015. doi: 10.1007/Bf01953855

Jankun, M. (2000). Standard karyotype of sea trout (Salmo trutta morpha trutta) based on replication banding patterns. *Cytobios, 103*(403), 79-89.

Johnson, K. R., & Wright, J. E. (1986). Female Brown Trout X Atlantic Salmon Hybrids Produce Gynogens and Triploids When Backcrossed to Male Atlantic Salmon. *Aquaculture, 57*(1-4), 345-358. doi: 10.1016/0044-8486(86)90213-9

Kalayci, G., Ozturk, R. C., Capkin, E., & Altinok, I. 2018. Genetic and molecular evidence that brown trout *Salmo trutta* belonging to the Danubian lineage are a single biological species. *Journal of Fish Biology, 93,* 792-804. doi: 10.1111/jfb.13777

Kalbassi, M. R., Dorafshan, S., Tavakolian, T., Khazab, M., & Abdolhay, H. (2006). Karyological analysis of endangered Caspian salmon, *Salmo trutta caspius* (Kessler, 1877). *Aquaculture Research, 37*(13), 1341-1347. doi: 10.1111/j.1365-2109.2006.01560.x

Kligerman, A. D., & Bloom, S. E. (1977). Rapid Chromosome Preparations from Solid Tissues of Fishes. *Journal of the Fisheries Research Board of Canada, 34*(2), 266-269. doi: 10.1139/f77-039

Kottelat, M., & Freyhof, J. (2007). *Handbook of European Freshwater Fishes*. Cornol, Switzerland

Naran, D. (1997). *Cytogenetic studies of Pseudobarbus and selected Barbus (Pısces: Cyprinidae) of Southern Afrıca.* (Master of Science), Rhodes University, Grahamstown, South Africa.

Northland-Leppe, I., Lam, N., Jara-Seguel, P., & Capetillo-Arcos, J. (2009). Chromosomes And Ag-Nor Location in Fluviate Populations of *Salmo trutta fario* L. 1758 (Salmoniformes: *Salmonidae*) From Atacama Desert, Chile. *Gayana, 73*(1), 45-48.

Pack, S. D., Stratakis, C.A. (2002). Chromosomes: MEthod for preperation *Encyclopedia of life sciences*. New Jersey: John Wiley and Sons.

Phillips, R. (2005). Chromosome morphology. In F. K. Cadrin SX, Waldman JR (Ed.), *Stock Identification Methods* (pp. 273-294). Amsterdam: Elsevier Academic Press.

Polonis, M., Fujimoto, T., Dobosz, S., Zalewski, T., & Ocalewicz, K. (2018). Genome incompatibility between rainbow trout (*Oncorhynchus mykiss*) and sea trout (*Salmo trutta*) and induction of the interspecies gynogenesis. *Journal of Applied Genetics, 59*(1), 91-97. doi: 10.1007/s13353-017-0425-2

Sanchez, L., Martinez, P., Vinas, A., & Bouza, C. (1990). Analysis of the Structure and Variability of Nucleolar Organizer Regions of Salmo-Trutta by C-, Ag-, and Restriction Endonuclease Banding. *Cytogenetics and Cell Genetics, 54*(1-2), 6-9. doi: 10.1159/000132944

Schmid, M., Feichtinger, W., Weimer, R., Mais, C., Bolanos, F., & Leon, P. (1995). Chromosome-Banding in Amphibia .21. Inversion Polymorphism and Multiple Nucleolus Organizer Regions in Agalychnis-Callidryas (Anura, Hylidae). *Cytogenetics and Cell Genetics, 69*(1-2), 18-26. doi: 10.1159/000133929

Sumner, A. T. (1972). Simple Technique for Demonstrating Centromeric Heterochromatin. *Experimental Cell Research, 75*(1), 304-&. doi: 10.1016/0014-4827(72)90558-7

Turan, D., Kottelat, M., & Engin, S. (2014). Two new species of trouts from the Euphrates drainage, Turkey (Teleostei: Salmonidae). *Ichthyological Exploration of Freshwaters, 24*(3), 275-287.

Woznicki, P., & Jankun, M. (1994). Chromosome Polymorphism of Atlantic Salmon (Salmo-Salar) from the River Dzwina, Baltic Sea Basin - Arm Length and nor Location Variation of the 8th Chromosome. *Canadian Journal of Zoology-Revue Canadienne De Zoologie, 72*(2), 364-367. doi: 10.1139/z94-050

Woznicki, P., Jankun, M., & Luczynski, M. (1997). Chromosome studies in brown trout (Salmo trutta m. fario) from Poland: hypothetical evolution of the 11th, 12th and 14th chromosome pairs in the Salmo karyotype. *Cytobios, 91*(366-67), 207-214.

Woznicki, P., Jankun, M., & Luczynski, M. (1998). Chromosome polymorphism in Salmo trutta morpha lacustris from Poland, Wdzydze Lake population: Variation in the short arm length of chromosome eleven. *Aquatic Sciences, 60*(4), 367-375. doi: 10.1007/s000270050047

Woznicki, P., Sanchez, L., Martinez, P., Pardo, B. G., & Jankun, M. (2000). A population analysis of the structure and variability of NOR in Salmo trutta by Ag, CMA(3) and ISH. *Genetica, 108*(2), 113-118. doi: 10.1023/A:1004055125295

Zenzes, M. T., & Voiculescu, I. (1975). C-Banding Patterns in Salmo-Trutta, a Species of Tetraploid Origin. *Genetica, 45*(4), 531-536. doi: 10.1007/Bf01772875

Zhuo, L., Reed, K. M., & Phillips, R. B. (1995). Hypervariability of Ribosomal DNA at Multiple Chromosomal Sites in Lake Trout (Salvelinus-Namaycush). *Genome, 38*(3), 487-496. doi: 10.1139/g95-064

Zhou, L., & Gui, J. 2017. Natural and artificial polyploids in aquaculture. *Aquaculture and Fisheries 2*, 103-111. doi: 10.1016/j.aaf.2017.04.003

Ziomek, E., Debowska, M., Hliwa, P., & Ocalewicz, K. (2016). Impaired gonadal development in the sea trout (*Salmo trutta*) x Atlantic salmon (*Salmo salar*) F1 hybrid females. *Oceanological and Hydrobiological Studies, 45*(3), 337-343. doi: 10.1515/ohs-2016-0028

Caryologia
International Journal of Cytology, Cytosystematics and Cytogenetics

Firenze University Press
www.fupress.com/caryologia

OPEN ACCESS

Citation: S. Heneidak, E. Martin, F. Altinordu, A. Badr, H.E. Eroğlu (2019) Chromosome counts and karyotype analysis of species of family Apocynaceae from Egypt. *Caryologia* 72(4): 69-78. doi: 10.13128/cayologia-192

Published: December 23, 2019

Data Availability Statement: All relevant data are within the paper and its Supporting Information files.

Competing Interests: The Author(s) declare(s) no conflict of interest.

Chromosome counts and karyotype analysis of species of family Apocynaceae from Egypt

Samia Heneidak[1,*], Esra Martin[2], Fahim Altinordu[2], Abdelfattah Badr[3], Halil Erhan Eroğlu[4]

[1] *Department of Botany, Faculty of Science, Suez University, Suez, Egypt*
[2] *Department of Biotechnology, Faculty of Science, Necmettin Erbakan University, Konya, Turkey*
[3] *Department of Botany and Microbiology, Faculty of Science, Helwan University, Egypt*
[4] *Department of Biology, Faculty of Science and Art, Bozok University, Yozgat, Turkey*
*Correspondence: sheneidak2000@yahoo.com

Abstract. The chromosome counts of 13 species of family Apocynaceae in the flora of Egypt have been reported; one species from subfamily Periplocoideae and the other 12 species from subfamily Asclepiadoideae. The chromosome numbers are $2n = 22$ for *Periploca angustifolia*, *Glossonema boveanum*, *Pentatropis nivalis*, *Cynanchum acutum*, *Calotropis procera*, *Gomphocarpus sinaicus*, *Pergularia daemia* and *Pergularia tomentosa*; $2n = 24$ for *Leptadenia arborea* and *Solenostemma arghel*; $2n = 22, 44$ for *Caudanthera edulis*, *Caudanthera sinaica* and *Desmidorchis acutangulus*. The chromosome numbers and karyotype analyses were firstly reported in *Leptadenia arborea* ($2n = 24$). The polyploid nature was demonstrated by the prevalence of cells with $2n = 4x = 44$ chromosomes in *Caudanthera edulis*, *Caudanthera sinaica* and *Desmidorchis acutangulus*. The chromosomes are median and submedian as most species in the Apocynaceae. The intrachromosomal asymmetry and interchromosomal asymmetry were estimated with M_{CA} and CV_{CL} values. In intrachromosomal asymmetry, *Desmidorchis acutangulus* is the most symmetrical karyotype, while *Pergularia tomentosa* is the most asymmetrical karyotype. In interchromosomal asymmetry, *Glossonema boveanum* is the most symmetrical karyotype, while *Cynanchum acutum* is the most asymmetrical karyotype.

Keywords. Apocynaceae, chromosome number, Egyptian flora, karyotype asymmetry.

INTRODUCTION

The family Apocynaceae comprises 366 genera and *ca*. 5100 species (Meve, 2002; Endress et al., 2014). This family is currently divided into five subfamilies; Periplocoideae, Asclepiadoideae, Apocynoideae, Rauvolfioideae, Secamonoideae (Endress and Bruyns, 2000; Endress et al., 2014). The majority of species represented in the Egyptian flora are classified in the two subfamilies Periplocoideae and Asclepiadoideae. The subfamily Periplocoideae is a small group of species comprising only *ca*. 195 species in 33 genera (Heneidak and Naidoo, 2015). On the other hand, Asclepiadoideae is the largest

subfamily of the Apocynaceae and contains about 3000 species in 164 genera of five tribes. The tribes are divided into 15 subtribes (Meve, 2002; Endress et al., 2014).

Chromosome data have been constantly used for systematic purposes but chromosome number alone is not sufficient to exactly trace the evolutionary history of taxonomic groups. However, comparative karyotype analysis of related species has traditionally been used to describe patterns and directions of chromosomal evolution within plant groups and to infer the evolutionary role of chromosomal changes in plant evolution (Stebbins, 1971; Badr et al, 1997; 2009; Eroğlu et al., 2013; Kamel et al. 2014). More detailed information about the karyotype has been found necessary in order to provide diagnostics criteria for the systematics and phylogeny of plants (Altay et al., 2017). In fact, karyological features are evaluated as important taxonomic characters only when provide additional information and allow conclusions about evolutionary events in the group of interest (Badr and Elkington, 1977; Peruzzi and Eroğlu, 2013).

Survey of chromosome counts in the Apocynaceae in chromosome count reports, particularly the *Index to Plant Chromosome Numbers of the Missouri Botanical Garden* (http://www.tropicos.org/Project/IPCN) and the Chromosome Counts Database (CCDB) (http://ccdb.tau.ac.il) which is a community resource of plant chromosome numbers (New Phytol. 206(1): 19-26) as well as the old counts reported in Federov (1969) as well as the chromosome count reports that was frequenty published in the Journal Taxon indicated thatseveral authors have reported chromosome numbers of many species of the Apocynaceae. Several authors have reported chromosome numbers of many species of the Apocynaceae (Francini, 1927; Mitra and Datta, 1967; Fedorov, 1969; Arrigoni and Mori, 1976; Albers and Delfs, 1983; Albers and Austmann, 1987; Khatoon and Ali 1993; Liede 1996; Albers et al., 1993; Albers and Meve, 2001; Kamel et al., 2014). These studies showed that the family is karyologically almost entirely homogenous, especially subfamilies Asclepiadoideae and Periplocoideae, with nearly 96% of the taxa investigated so far having chromosome complements in multiples of a basic number of $x = 11$, with a few deviating numbers.

Deviating chromosome numbers were reported with $2n = 18, 24$ in *Funastrum clausum* (Jacq.) Schulr. and *Funastrum cynanchoides* (Decne.) Schulr. (tribe Asclepiadeae) (Albers et al., 1993), $2n = 20$ in *Microloma incanum* Decne. *Microloma calycinum* E. Mey., *Microloma sagittatum* (L.) R. Br. and *Microloma tenuifolium* (L.) K. Schum. (tribe Asclepiadeae) (Albers et al., 1993) and $2n = 24$ in *Periploca graeca* L. (subfamily Periplocoideae) (Pesci, 1971). In literature, $x = 9$ was only reported in *Cynanchum acutum* L. and *Pergularia tomentosa* L. (Fedorov, 1969). The deviating chromosome numbers, i.e. $2n = 24$ and $x = 9$ that were found previously and in the present work were reported a deviating base chromosome numbers in the genera *Cynanchum, Microloma*, and *Sarcostemma* (Albers et al. 1993). These authors gave an account of previously published deviating chromosome numbers in the Asclepiadaceae.

In subfamily Asclepiadoideae, the polyploidy rate is approximately 6%. The polyploid species are mostly tetraploid (85%) with $2n = 44$ and only a few are hexaploid with $2n = 66$ (Albers and Meve, 2001). Albers (1983) reported the polyploid taxa in most of the genera of tribe Ceropegieae. Albers and Meve (1991) observed that the proportion of polyploid cells in the meristems of adventives roots is significantly higher than in the meristems of primary and secondary roots in genera *Duvalia* Haw., *Hoodia* Sweet ex Decne., *Orbea* Haw., *Pectinaria* Haw., *Stapelia*, *Trichocaulon* N.E.Br. and *Tridentea* Haw. High ploidy levels were recorded in *Tylophora anomala* N. E. Br.; for example the decatetraploid ($2n = 132$-154) and the hexaploid ($2n = 66$) (Meve, 1999).

In Apocynaceae, the counting and measuring of small size of the chromosomes is difficult. The chromosomes form a graded series with only very slight differences in morphology (Albers, 1983). Within a single karyotype the chromosomes are comparatively similar in size. The heterogeneous karyotypes were only found where chromosome sizes varied considerably in the subfamilies Periplocoideae, Asclepiadoideae and Secamonoide (Albers and Meve, 2001).

In the present study, 13 species of the family Apocynaceae were investigated karyologically to determine the chromosome numbers and to compare with earlier results. In addition, the karyotype of the examined species growing in Egypt has been analysed using a number of chromosome characterizing parameters such as varaitions in length, arm ration and centromeric asymmetry indices in order to gather more information that might help a better understanding of the taxonomic treatment of the species of Apocynaceae in the Egyptian flora.

MATERIALS AND METHODS

Plant materials

Seeds of 13 species of Apocynaceae were collected from mature flowers from sites in their natural habitats as given in Table 1 and mapped as in Figure 1. Voucher specimens of the examined species are kept at Suez University Herbarium. In the two succulent species (*Caudanthera edulis* and *Desmidorchis acutangulus*),

Table 1. List of species examined and the localities from which plants used for chromosome counts were collected and date of collection.

Taxa	Date	Locality
1. *Periploca angustifolia* Labillardiere	12.06.2009	El-Salûm: Wadi Salufa, 31°37'24"N–25°09'00" E, Morsy et al. s.n.
2. *Caudanthera edulis* (Edgew) Meve & Liede	27.01.2009	Gebel Elba: Wadi Yahameib, 22°25'18"N–36°18'33"E, Morsy et al. s.n.
3. *Caudanthera sinaica* (Decne.) Plowes	10.05.2009	North Sinai: Gidda Pass, 30°13'06"N–33°03'04"E, Heneidak s.n.
4. *Desmidorchis acutangulus* Decne.	23.08.2009	Gebel Elba: Wadi Aideib, 22°15'00"N–36°26'12"E, Morsy et al. s.n.
5. *Leptadenia arborea* (ForssK.) Schweinf.	17.02.2009	Aswan: 24°05'00"N–32°54'18"E, Heneidak s.n.
6. *Glossonema boveanum* (Decne.) Decne.	09.04. 2009	Sharm El Sheikh: Nabq protectorate, South Sinai, 28°07'00"N–34°25'00"E, Heneidak s.n.
7. *Solenostemma arghel* (Delile) Hayne	25.11. 2009	Dahab: South Sinai, 28°29'05"N–34°31'18"E, Heneidak s.n.
8. *Pentatropis nivalis* (J. F. Gmel.) D. V. Field & J. R. I. Wood	30.05.2009	Gebel Elba: Abu Ramad, 22°20'00"N–36°34'00"E, Morsy et al. s.n.
9. *Cynanchum acutum* L.	07.10. 2009	Suez: Shalufa, 30°07'03"N–32°32'27"E, Heneidak s.n.
10. *Calotropis procera* (Willd.) R. Br.	06.10. 2009	Ismailia: 30°64'00"N–32°27'00"E, 06.10.2009, Heneidak s.n.
11. *Gomphocarpus sinaicus* Boiss.	15.04. 2009	Saint Catherine: Wadi El Arbeen, South Sinai, 28°32'12"N–33°95'00"E, Heneidak s.n.
12. *Pergularia daemia* (Forssk.) Chiov.	25.10. 2009	Gebel Elba: Wadi Acaw, 22°15'31"N–36°21'00"E, Morsy et al. s.n.
13. *Pergularia tomentosa* L.	13.12. 2009	Ismailia: Suez desert road, 29°38'33"N–32°16'32"E, Heneidak s.n.

the root tips of adventitious roots were collected from plants, except *Caudanthera sinaica* from seedlings.

Cytogenetic procedure

For cytological preparations, seeds were germinated on moist Whatman paper and actively–growing root tips were pre-treated in saturated aqueous α-bromonaphthalene at 4°C for 24 hours, or in a solution of 0.002 M 8-hydroxyquinoline at 18°C for 5-6 hours. They were fixed in absolute ethanol:acetic acid (3:1) for at least one hour, hydrolysed in 1N HCl at 60°C for 8 minutes and stained in Feulgen staining solution. The slides were mounted in Euparal for long-term storage (Martin et al., 2011). Photographs of chromosome spreads were taken using a Carl Zeiss Axiostar Plus microscope fitted with a Canon (Pc 1200 Power shoot A641) digital camera.

The number of somatic chromosomes was carefully counted in five slides for each species. Karyotype analyses were made by using Bs200Pro Image Analysis Software. Homologous pairs of somatic chromosomes were determined according to their total and relative lengths for each species.

The following parameters were used to characterize the chromosomes: long arm (LA), short arm (SA), total length (TL = LA + SA) and arm ratio (LA / SA). Total haploid lengths and mean haploid lengths were calculated. For the karyotype formula, chromosomes were classified using the nomenclature of Levan et al. (1964).

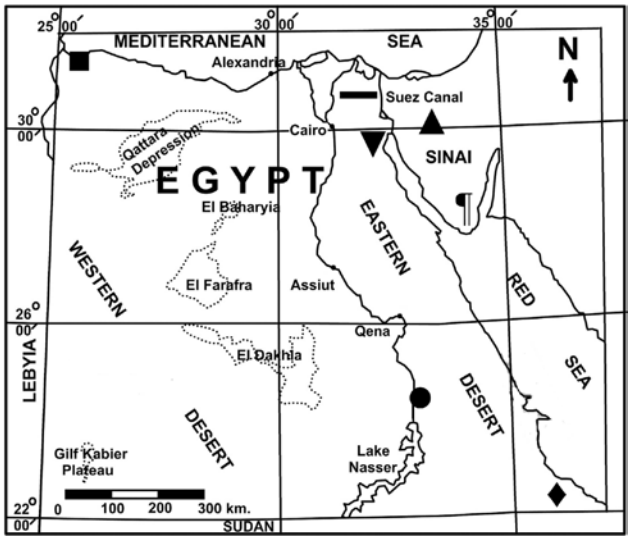

Figure 1. The distribution map of the studied species in Egypt. *Periploca angustifolia* (▪); *Caudanthera edulis*, *Desmidorchis acutangulus*, *Pentatropis nivalis*, *Pergularia daemia* (♦); *Caudanthera sinaica* (▲); *Leptadenia arborea* (●); *Glossonema boveanum*, *Solenostemma arghel*, *Gomphocarpus sinaicus* (¶); *Cynanchum acutum* (▼); *Calotropis procera*, *Pergularia tomentosa* (▬).

Several karyotype symmetry indices have been applied to express the asymmetry of the karyotype. Karyotype asymmetries were estimated by mean centromeric asymmetry (M_{CA}) (Peruzzi and Eroğlu, 2013) and coefficient of variation of chromosome length (CV_{CL}) (Paszko, 2006). The intrachromosomal asymmetry was

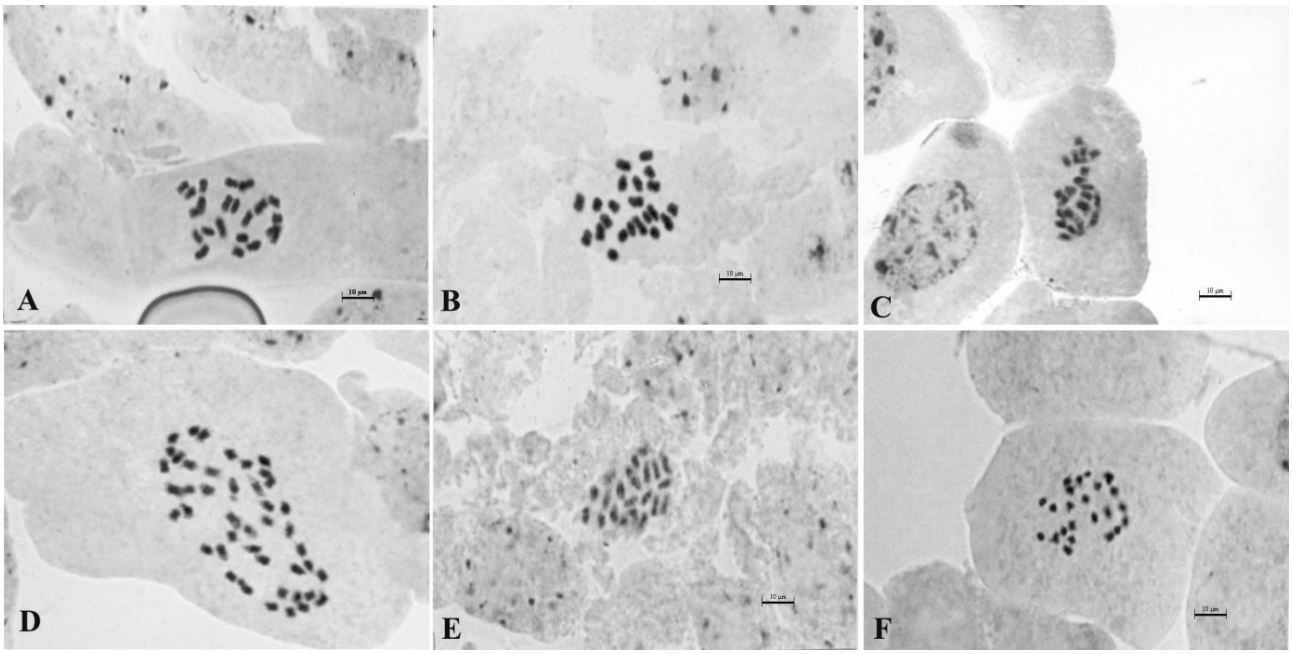

Figure 2. Photomicrographs of somatic metaphase chromosomes in root tip cells: *Periploca angustifolia* (A), *Caudanthera sinaica* (B), diploid *Caudanthera edulis* (C), tetraploid *Caudanthera edulis* (D), *Desmidorchis acutangulus* (E), *Leptadenia arborea* (F). Scale bar = 10 µm.

calculated with M_{CA} = [mean (L – S) / (L + S)] × 100. The formula contains the length of long arm (L) and short arm (S) of each chromosome. The interchromosomal asymmetry was calculated with CV_{CL} = [standard deviation / mean chromosome length] × 100. Finally, a scatter diagram between intrachromosomal asymmetry (M_{CA}) and interchromosomal asymmetry (CV_{CL}) was drawn.

RESULTS AND DISCUSSION

The subfamily Periplocoideae is represented with one species in tribe Periploceae. The subfamily Asclepiadoideae is represented with 12 species in tribe Ceropegieae and Asclepiadeae. The photographs illustrating the chromosomes of the studied species are shown in Figures 2 and 3. The ideograms are given in Figure 4.

The gametic and somatic chromosome counts of the investigated species in present and previous studies are given in Table 2. Detailed chromosomal data are given in Table 3.

Chromosome numbers

Table 2 summarizes the chromosome number and the previous counts for the studied species of Apocynaceae. Eleven of the 13 species examined here have $2n$ = 22, based on a basic number of x = 11. These results confirmed previous records for other species, and therefore, it is clear that the dominance of a basic number of x = 11 and a majority of 2n = 22 is the base in the subfamilies Periplocoideae and Asclepiadoideae. It is the first time to count the chromosomes of *Leptadenia arborea* ($2n$ = 24); (Figure 2F).

Both diploid chromosome number ($2n$ = 22) and tetraploid chromosome number ($2n$ = 44) cells were scored in the three succulent species, which belong to tribe Ceropegieae; i.e. *Caudanthera sinaica*, *C. edulis* (Figures 2C, 2D) and *Desmidorchis acutangulus*. Diploid number ($2n$ = 22) is reported also in *Caudanthera edulis* by Albers and Meve (2001), in *Caudanthera sinaica* by Albers and Meve (2001), Kamel et al. (2014), and in *Desmidorchis acutangulus* by Albers and Delfs (1983), Albers and Meve (2001). However, tetraploid number ($2n$ = 44) is recorded also in *Caudanthera edulis* by Albers and Austmann (1987), in *Desmidorchis acutangulus* by Kamel et al. (2014), while in *Caudanthera sinaica* recorded in the present study only). Polyploidy is known to occur in 11 genera of subfamily Asclepiadoideae with eight genera belonging to tribe Ceropegieae (Albers and Meve, 2001). There are different patterns (mixoploidy) in terms of the number of chromosomes. This is probably the state of the endopolyploidy that is the result of enderoduplication. No odd-number polyploidy was

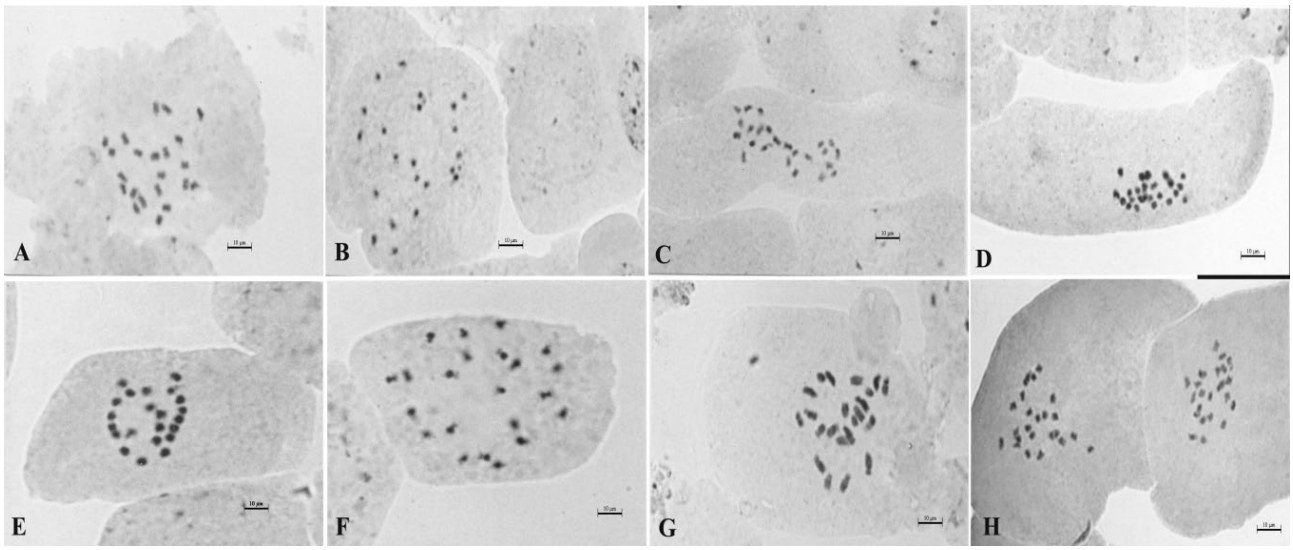

Figure 3. Photomicrographs of somatic metaphase chromosomes in root tip cells: *Pentatropis nivalis* (A), *Glossonema boveanum* (B), *Solenostemma arghel* (C), *Cynanchum acutum* (D), *Pergularia tomentosa* (E), *Pergularia daemia* (F), *Gomphocarpus sinaicus* (G), *Calotropis procera* (H). Scale bar = 10 μm.

found. The diploid count supports the findings of Albers and Meve (2001); while the tetraploid count in this study supports the findings of Albers and Austmann (1987). Albers and Meve (1991) reported that the frequency of tetraploid cells in the adventitious roots is higher than in the primary and the secondary roots. This phenomenon may lead to a complete polyploidization of adventitious roots, and can be ascribed to ecological rather than morphological or genetic factors (Albers and Meve, 1991).

Diploid chromosome number ($2n$ = 22) is recorded in *Periploca angustifolia* in this study and by Arrigoni and Mori (1976). Deviations from this number are absent in this species as reported before in subfamily Periplocoideae by Albers and Meve (2001). In the current study, three species; *Glossonema boveanum*, *Pentatropis nivalis* and *Gomphocarpus sinaicus* was also found to have a diploid chromosome number of $2n$ = 22 as scored by Albers and Meve (2001), Kamel et al. (2014) and other four *Gomphocarpus* species examined by Albers and Meve (2001). The same for *Cynanchum acutum* was also found to have a diploid chromosome number of $2x$ = 22 as recorded by Kamel et al. (2014) and in other 25 *Cynanchum* species examined by Albers and Meve (2001). The old records of earlier numbers of n = 9 and $2n$ = 18 in *Cynanchum acutum* quoted in Francini (1927) and Federov (1969) as well as the count of $2n$ = 24 in *Cynanchum virens* (Albers et al., 1993) may be regarded as deviating numbers as argued by Albers et al. (1993).

Calotropis procera was also found to have a diploid chromosome number of $2n$ = 22 as recorded by Fedorov (1969), Albers and Meve (2001) and Kamel et al. (2014). The other number of $2n$ = 26 recorded for this species by Bramwell et al. (1972) may be regarded as deviating number as argued by Albers et al. (1993). The two *Pergularia* species were also found to have a diploid chromosome number of $2n$ = 22 as recorded by Albers and Meve (2001) and Kamel et al. (2014) in *Pergularia daemia* or by Albers and Meve (2001) in *Pergularia tomentosa*. The old records of earlier numbers of n = 9 in *Pergularia tomentosa* quoted in Federov (1969) as well as the count of $2n$ = 24 in *Pergularia daemia* (Mitra and Datta, 967) may be regarded as deviating numbers as argued by Albers et al. (1993).

Chromosome number of *Leptadenia arborea* was $2n$ = 24 in this report, while Albers and Meve (2001) found $2n$ = 22 in two *Leptadenia* species (*L. pyrotechnica* Decne. and *L. hastata* (Pers.) Decne.). This may be regarded as deviating number as argued by Albers et al. (1993). The same for *Solenostemma arghel* was also found to have a diploid chromosome number of $2n$ = 24 in this study, while Kamel et al. (2014) found $2n$ = 22 in this species.

Karyotype analyses

The chromosomes of the examined species are all small with slight morphological differences among the complements of the studied samples. When compared the chromosome morphology among the species, the smallest mean chromosome length (2.60 μm)

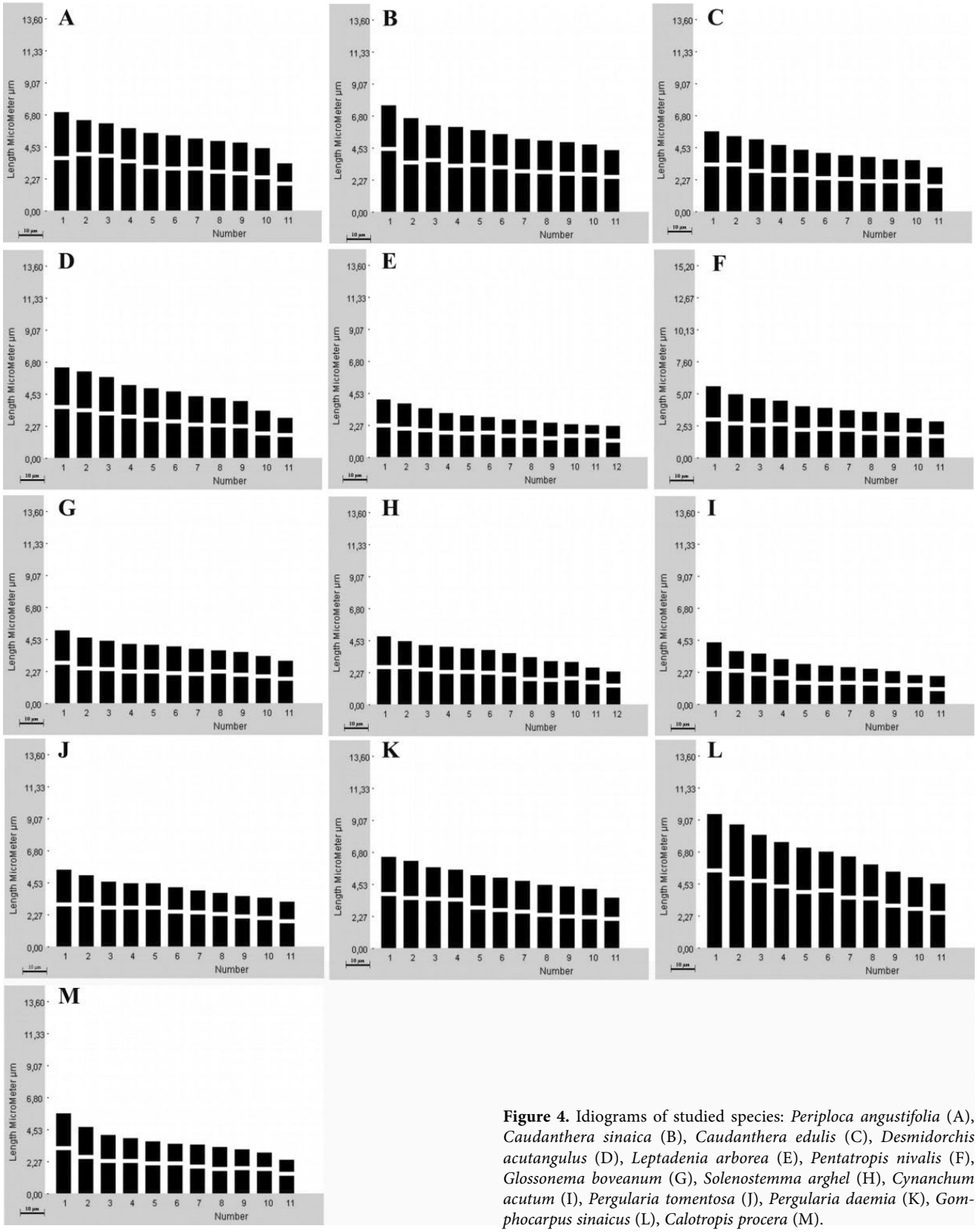

Figure 4. Idiograms of studied species: *Periploca angustifolia* (A), *Caudanthera sinaica* (B), *Caudanthera edulis* (C), *Desmidorchis acutangulus* (D), *Leptadenia arborea* (E), *Pentatropis nivalis* (F), *Glossonema boveanum* (G), *Solenostemma arghel* (H), *Cynanchum acutum* (I), *Pergularia tomentosa* (J), *Pergularia daemia* (K), *Gomphocarpus sinaicus* (L), *Calotropis procera* (M).

Table 2. The gametic and somatic chromosome counts of the investigated species in present and previous studies.

Subfamily, Tribe, Subtribe	Species	Previous results		Reference	Present counts	Explanation
		n	2*n*		2*n*	
Subfamily Periplocoideae Tribe Periploceae	*Periploca angustifolia*	—	22	Arrigoni and Mori (1976)	22	Detailed measurements
Subfamily Asclepiadoideae Tribe Ceropegieae						
Subtribe Stapeliinae	*Caudanthera edulis*	— —	22 44	Albers and Meve (2001) Albers and Austmann (1987)	22 44	Detailed measurements
	Caudanthera sinaica	—	22	Albers and Meve (2001), Kamel et al. (2014)	22 & 44	New count & detailed measurements
	Desmidorchis acutangulus	— —	22 44	Albers and Delfs (1983), Albers and Meve (2001) Kamel et al. (2014)	22 44	Detailed measurements
Subtribe Leptadeniinae Tribe Asclepiadeae	*Leptadenia arborea*	—	—	—	24	First report
Subtribe Asclepiadinae	*Calotropis procera*	11 — — —	— 22 26 44	Fedorov (1969) Albers and Meve (2001), Kamel et al. (2014) Bramwell et al. (1972) Kamel et al. (2014)	22	Detailed measurements
	Gomphocarpus sinaicus	—	22	Kamel et al. (2014)	22	Detailed measurements
	Pergularia daemia	— —	22 24	Albers and Meve (2001), Kamel et al. (2014) Mitra and Datta (1967)	22	Detailed measurements
	Pergularia tomentosa	9 — —	— 22 44	Fedorov (1969) Albers and Meve (2001) Kamel et al. (2014)	22	Detailed measurements
	Solenostemma arghel	—	22	Kamel et al. (2014)	24	New count
Subtribe Cynanchinae	*Cynanchum acutum*	9 — —	— 18 22	Fedorov (1969) Francini (1927) Kamel et al. (2014)	22	Detailed measurements
	Glossonema boveanum	—	22	Albers and Meve (2001), Kamel et al. (2014)	22	Detailed measurements
Subtribe Tylophorinae	*Pentatropis nivalis*	—	22	Albers and Meve (2001), Kamel et al. (2014)	22	Detailed measurements

was observed in *Cynanchum acutum* of tribe Asclepiadeae. In contrast the largest mean length (6.51µm) was observed in *Gomphocarpus sinaicus* of tribe Asclepiadeae. Albers and Meve (2001) concluded that the average karyotype size diminished from rather large chromosomes in the Periplocoideae to the smallest karyotype length in the presumed most advanced tribe of the Asclepidoideae, the Asclepiadeae.

The mean chromosomes length in *Leptadenia arborea* is 2.61µm, whereas Albers and Meve (2001) noticed an average length of 0.72 µm in two *Leptadenia* species (*L. pyrotechnica* and *L. hastate*). In this study, mean chromosome lengths in *Caudanthera sinaica*, *Desmidorchis acutangulus* and *Caudanthera edulis* were relatively larger (7.25, 6.14 and 5.38 µm, respectively). These three species also express evolutionarily basic morphological characters (Albers and Meve, 2001). Meve and Heneidak (2005) reported that the average mean chromosome length is (1.06-1.38 µm) in *Apteranthes europaea* of tribe Ceropegieae. The chromosomes of the three polyploid species studied here are usually smaller than those of diploid ones as reported before in polyploidy taxa by Albers and Meve (2001). A general tendency of size reduction can be seen starting with the presumably most primitive subfamily Periplocoideae to the more evolved Asclepiadoideae, and within the latter subfamily starting

Table 3. The measurement data of the studied Apocynaceae species.

Species	KF	SC (μm)	LC (μm)	RL (%) SC-LC	THL (μm)	MCL (μm)	CV_{CL}	M_{CA}
Periploca angustifolia	20m + 2sm	3.08	6.68	5.52-11.99	55.73	5.06	19.87	15.37
Caudanthera edulis	20m + 2sm	2.84	5.38	6.37-12.07	44.55	4.05	19.34	16.45
Caudanthera sinaica	22m	4.08	7.25	6.95-12.37	58.61	5.33	17.35	13.01
Desmidorchis acutangulus	22m	2.59	6.14	5.31-12.59	48.74	4,43	25.05	10.81
Leptadenia arborea	20m + 4sm	1.88	3.80	5.99-12.11	31.35	2.61	23.20	16.29
Glossonema boveanum	22m	2.70	4.88	6.59-11.92	40.97	3.72	16.63	11.20
Solenostemma arghel	24m	2.04	4.54	5.11-11.34	40.00	3.33	22.57	17.71
Pentatropis nivalis	22m	2.52	5.32	6.13-12.93	41.17	3.74	21.85	12.07
Cynanchum acutum	18m + 4sm	1.67	4.10	5.82-14.31	28.63	2.60	29.16	16.98
Calotropis procera	22m	2.08	5.37	5.53-14.26	37.67	3.42	26.27	15.19
Gomphocarpus sinaicus	22m	4.20	9.20	5.86-12.83	71.71	6.51	23.94	14.42
Pergularia daemia	22m	3.30	6.19	6.31-11.83	52.36	4.76	18.65	12.82
Pergularia tomentosa	22m	2.88	5.12	6.71-11.92	42.94	3.90	17.72	19.94

Abbreviations: karyotype formula (KF), shortest chromosome length (SC), longest chromosome length (LC), relative length (RL), total haploid chromosome length (THL), mean chromosome length (MCL).

with the most primitive Fockeeae to the most advanced Asclepiadeae, a decrease in chromosome size has taken place (Albers and Meve, 2001).

The chromosomes of most karyotypes are comparatively similar in size. Only rarely were heterogeneous karyotypes found where chromosome size varied considerably (Albers and Meve, 2001). The smallest arm ratio was observed in *Desmidorchis acutangulus* (1.06) and the highest one was observed in *Leptadenia arborea* (2.12). *Cynanchum acutum* has the smallest chromosome length as 1.67 μm and the biggest chromosome length is measured in *Gomphocarpus sinaicus* as 9.20 μm. Liede et al. (2002) also found that the chromosomes are generally short and varying in length, one pair of the large sized chromosomes in *Glossonema boveanum*. In Apocynaceae, chromosomes are typically submetacentric, rarely acrocentric with one pair of chromosomes possessing secondary constrictions with satellites (Albers, 1983; Albers and Meve, 2001). Albers and Meve (2001) found the smaller chromosomes in tribe Asclepiadeae, in particular the subtribes Asclepiadinae, Astephaninae and Metastelminae where mean length ranges from 0.70 to 1.15 μm.

In tribe Ceropegieae, the M_{CA} values indicated that *Desmidorchis acutangulus* is the most symmetrical karyotype, while *Caudanthera edulis* is the most asymmetrical karyotype. Whereas, the CV_{CL} values indicated that the most homogeneous centromere position is observed in *Caudanthera sinaica*. On the other hand the most heterogeneous centromere position is observed in *Desmidorchis acutangulus*.

In tribe Asclepiadeae, the M_{CA} values indicated that *Glossonema boveanum* is the most symmetrical karyotype, while *Pergularia tomentosa* is the most asymmetrical karyotype. The CV_{CL} values indicated that the most homogeneous centromere position is observed in *Glossonema boveanum*. On the other hand the most heterogeneous centromere position is observed in *Cynanchum acutum*.

In all tribe, the symmetrical and asymmetrical karyotypes are quite different. In parallel, a weak positive correlation is determined between M_{CA} and CV_{CL} ($r = 0.120$) (Figure 5). In Figure 5, three tribes of family Apocynaceae have different karyotypes in terms of asymmetry degrees: tribe Asclepiadeae with higher intrachromosomal asymmetry and interchromosomal asymmetry, tribe Ceropegieae with lower intrachromosomal asymmetry and interchromosomal asymmetry, one species of tribe Periploceae with relatively average intrachromosomal and interchromosomal asymmetry. On the other hand the results need to be supported by data from more species, because the species number investigated (per tribe) is much too low.

The possible origin of deviating chromosome numbers called numerical aneuploidy are defects in cell division as anaphase lagging, nondisjunction or presence of B-chromosomes. B-chromosomes, which are also known as supernumerary chromosomes, are a major source of intraspecific variation in nuclear DNA (Jones et al., 2008). The general consideration is that B-chromosomes are derived from the A-chromosomes. Probably, a B-chromosome may have originated from paracentro-

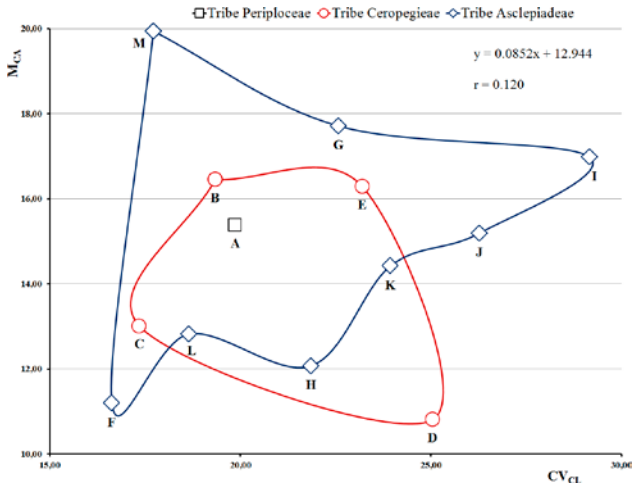

Figure 5. Scatter diagram between M_{CA} and CV_{CL}: *Periploca angustifolia* (A), *Caudanthera edulis* (B), *Caudanthera sinaica* (C), *Desmidorchis acutangulus* (D), *Leptadenia arborea* (E), *Glossonema boveanum* (F), *Solenostemma arghel* (G), *Pentatropis nivalis* (H), *Cynanchum acutum* (I), *Calotropis procera* (J), *Gomphocarpus sinaicus* (K), *Pergularia daemia* (L), *Pergularia tomentosa* (M).

meric region amplication of a fragmented A chromosome or from A chromosome fusions.

CONCLUSION

With this study, new chromosome data were given for 13 taxa of family Apocynaceae. More karyological data are needed to understand the phylogeny of Apocynaceae. In conclusion, some intrageneric relationships within Apocynaceae will clarify with comparative chromosomal analysis. Also, additional comparative high-resolution molecular cytogenetic studies will be necessary to clarify phylogenetic relationships between genera or species.

ACKNOWLEDGEMENTS

We would like to thank Prof. Dr. Ahmed Mursi Ahmed for collecting *Caudanthera edulis*, *Desmidorchis acutangulus*, *Pentatropis nivalis* and *Pergularia daemia* from Gebel Elba, in south east area of Egypt.

REFERENCES

Albers F (1983). Cytotaxonomic studies in African Asclepiadaceae. Bothalia 14: 795-798.

Albers F, Austmann M (1987). Chromosome number reports XCV. Taxon 36: 494-496.

Albers F, Delfs W (1983). In IOPB chromosome number reports LXXXI. Taxon 32: 667-668.

Albers F, Liede S, Meve U (1993). Deviating chromosome numbers in Asclepiadaceae. Nord J Bot 13: 37-39.

Albers F, Meve U (1991). Mixoploidy and cytotypes: A study of possible vegetative species differentiation in stapeliads (Asclepiadaceae). Bothalia 21: 67-72.

Albers F, Meve U (2001). A karyological survey of Asclepiadoideae, Periplocoideae, and Secamonoideae, and evolutionary considerations within Apocynaceae s.l. Ann Missouri Bot Gard 88: 624-656.

Altay D, Eroğlu HE, Hamzaoğlu E, Koç M (2017). Karyotype analysis of some taxa of *Dianthus* section *Verruculosi* (Caryophyllaceae, Sileneae). Turk J Bot 41: 367-374.

Arrigoni PV, Mori B (1976). Numeri cromosomici per la flora Italiana: 366-374. Inform Bot Ital 10: 46-55.

Badr A, Elkington TT (1977). Variation of Giemsa C-band and fluorochromes banded karyotypes and relationships in *Allium* subgenus *Molium*. Plant Syst Evol 128: 23-35.

Badr, A, Kamel, EA, Garcia-Jacas, N (1997). Chromosomal studies in the Egyptian flora. VI. Karyotype features of species in subfamily Asteroideae (Asteraceae). Compositae Newsletter 30: 15-28.

Badr, A, El-Shazly, HAH, Kamel, EA (2009). Chromosomal studies in the Egyptian flora. VII. Karyotype analysis of species in the two tribes Chicorieae and Cardueae of Asteraceae. Egypt. J. Bot. 49: 71-86.

Bramwell D, Humphries CJ, Murray BG, Owens SJ (1972). Chromosome studies in the flora of Macaronesia. Bot Notiser 125: 139-152.

Endress ME, Bruyns PV (2000). A revised classification of the Apocynaceae s.l. Bot Rev 66: 1-56.

Endress ME, Liede-Schumann S, Meve U (2014). An updated classification for Apocynaceae. Phytotaxa 159: 175-194.

Eroğlu HE, Şimşek N, Koç M, Hamzaoğlu E (2013). Karyotype analysis of some *Minuartia* L. (Caryophyllaceae) taxa. Plant Syst Evol 299: 67-73.

Fedorov AA (1969). Chromosome numbers of flowering plants. Leningrad: Academy of Science of the USSR, Komarov Botanical Institute.

Francini E (1927). L'embriologia del *Cynanchum acutum* L. Nuovo Giorn Bot Ital 34: 381-395.

Heneidak S, Naidoo Y. (2015). Floral function in relation to floral structure in two *Periploca* species (Periplocoideae) Apocynaceae. Turk J Bot 39: 653-663.

Jones RN, Viegas W, Houben A (2008). A century of B chromosomes in plants: so what? Ann Bot 101: 767-775.

Kamel EAR, Sharawy SM, Karakish EAK (2014). Cytotaxonomical investigations of the tribes Asclepiadeae

and Ceropegieae of the subfamily Asclepiadoideae-Apocynaceae. Pak J Bot 46: 1351-1361.
Khatoon, S and Ali, SI (1993). Chromosome Atlas of the Angiosperms of Pakistan. Department of Botany, University of Karachi, Karachi.
Liede, S (1996) A Revision of Cynanchum (Asclepiadaceae) in Africa. Ann Missouri Bot Gard 83(3): 283.
Levan A, Fredga K, Sandberg AA (1964). Nomenclature for centromeric position on chromosomes. Hereditas 52: 201-220.
Liede S, Meve U, Täuber A (2002). What is the subtribe Glossonematinae (Apocynaceae: Asclepiadoideae)? A phylogenetic study based on cpDNA spacer. Bot J Linn Soc 139: 145-158.
Martin E, Çetin Ö, Akçiçek E, Dirmenci T (2011). New chromosome counts of genus *Stachys* (Lamiaceae) from Turkey. Turk J Bot 35: 671-680.
Meve U (1999). *Tylophora anomala* (Asclepiadaceae) - a cytologically anomalous species. Syst Geogr Pl 68: 255-263.
Meve U (2002). Species numbers and progress in asclepiad taxonomy. Kew Bull 57: 459-464.
Meve U, Heneidak S (2005). A morphological, karyological and chemical study of the *Apteranthes* (*Caralluma*) *europaea* complex. Bot J Linn Soc 149: 419-432.
Mitra K, Datta N (1967). In IOPB chromosome number reports XIII. Taxon 16: 445-461.
Paszko B (2006). A critical review and a new proposal of karyotype asymmetry indices. Plant Syst Evol 258: 39-48.
Peruzzi L, Eroğlu HE (2013). Karyotype asymmetry: again, how to measure and what to measure? Comp Cytogen 7: 1-9.
Pesci G (1971). In numeri cromosomici per la flora Italiana. Inf Bot Italiano 3: 124-157.
Stebbins GL (1971). Chromosomal evolution in higher plants. London: Edward Arnold Ltd.

Caryologia
International Journal of Cytology, Cytosystematics and Cytogenetics

Firenze University Press
www.fupress.com/caryologia

Citation: Z.A. Hamad, A. Kaya, Y. Coşkun (2019) Geographical distribution and karyotype of *Nannospalax ehrenbergi* (Nehring 1898) (Rodentia, Spalacidae) in Iraq. *Caryologia* 72(4): 79-83. doi: 10.13128/caryologia-318

Published: December 23, 2019

Data Availability Statement: All relevant data are within the paper and its Supporting Information files.

Competing Interests: The Author(s) declare(s) no conflict of interest.

Geographical distribution and karyotype of *Nannospalax ehrenbergi* (Nehring 1898) (Rodentia, Spalacidae) in Iraq

Zaitoon Ahmed Hamad[1], Alaettin Kaya[2], Yüksel Coşkun[2,*]

[1] *Dicle University Institute of Science Biology Section, Diyarbakır /Turkey*
[2] *Dicle University Science Faculty, Department of Biology, Diyarbakır/Turkey*
*Corresponding author: yukselc@dicle.edu.tr

Abstract. This paper concerns the karyological analysis of fourteen mole rats collected in four different localities of North-Iraq (Kurdistan Region). The result showed that they belong to the following cytotypes of *Nannospalax ehrenbergi:* «Duhok-Bardarash Population» 2n = 52, NF = 76, and NFa = 72 and «Arbil-Sulaimania-Kirkuk populations» 2n = 52, NF = 80 and NFa = 76. The karyotypes of the Duhok population are similar to those from Mosul, but the Arbil-Sulaimania-Kirkuk populations' karyotype represents a new chromosomal form. Their distribution extends from North Iraq to Sulaimania.

Keywords. Rodentia, Spalacidae, Nannospalax ehrenbergi, Karyology, Iraq.

1. INTRODUCTION

Scientific research on mammals in Iraq is scarce in the country and requires special attention in order to determine the mammalian fauna of Iraq. Amr (2009), Garstecki & Amr (2011) noted that the mammalian fauna of Iraq consists of 74 species, including insectivores (6), bats (15), and carnivores (19) as well as extinct species such as the leopard (*Panthera pardus)*, artiodactyls (8). Rodents constituted the largest mammalian group in Iraq with 25 species. Recently, an updated checklist of the mammals of Iraq was published by Al-Sheikhly et al. (2015). The checklist takes into account 93 mammalian species of Iraq and listed the mole rats under the name *Nannospalax ehrenbergi*.

The Palearctic rodent blind mole rats (Rodentia: Spalacidae) are subterranean mammals and the chromosomally diverse and they are difficult to distinguish based on phenotype, whose phylogenetic relationships are problematic, resulting in taxonomic uncertainties at every level from species to higher taxa (Savic & Nevo 1990; Musser & Carleton 2005). Fossil, morphological, chromosomal and molecular evidence suggest that Spalacidae have two distinct genera *Spalax* and *Nannospalax* (Topachevski 1969, Lyapunova et al. 1974, Hadid et al. 2012). Morphologically *Nannospalax* differs from *Spalax*

by the presence of supracondyloid foramina and two longitudinal ridges anterior surface of the upper incisors (Topachevski 1969). Karyologically, *Nannospalax* has both low diploid (2n) and fundamental (NF) numbers and acrocentric chromosomes (Lyapunova et al. 1974).

The species *Nannospalax ehrenbergi* is the south eastern representative of the genus – initially described by Nehring (1898) on specimens, who were collected from Yafa-Israel – also occurs in the Middle East, Egypt, and Southeast Anatolia of Turkey (Lay & Nadler 1972; Musser & Carleton 2005; Coşkun et al. 2006). *Nannospalax ehrenbergi* exhibits great diversity in both diploid number of chromosomes (2n= 48-62) and the number of chromosome arms (NF= 62-90) (Wahrman et al. 1969; Ivanitskaya et al. 1997; 1998; Coşkun et al. 2006 and reference therein).

The distribution of *Nannospalax ehrenbergi* in Iraq has been known mainly from morphological studies, which have not been extensive (Cheesman 1920; Reed 1958; Harrison 1956; Hatt 1959; Turnbull & Reed 1974; Harrison & Bates 1991). Recently, spalacids from the Hawraman Mountains were identified as *Spalax leucodon* by Lahony et al. (2013). The old records and distribution of the species in Iraq were previously summarized in detail by Coşkun et al. (2012). The cytogenetic information, which was available for this mole rat (*N. ehrenbergi*) and the existing data, were restricted to conventional stained karyotypes or reports of the diploid chromosome number (Coşkun et al. 2012; 2014). The geographical distribution and karyological peculiarities have not yet been documented in detail.

The aim of the present work is to verify the distribution and the karyotype characteristics of several *Nannospalax* populations from Iraq to fill the gap in our knowledge about karyological forms as well as their distributional areas in the north of Iraq.

2. MATERIAL AND METHODS

The territory of Iraq is lies between latitudes 29° to 38° N and longitudes 39° to 49° E and the landscape includes high mountains in the North (Kurdistan), desert, arid lands and sandy steppes in the western and south-western plateau (Al-Badiyah), and the Mesopotamian marshlands in the southern alluvial plain (Zohayr 1973).

The study was conducted on four populations of blind mole rats from Duhok- Bardarash, Arbil-New Arbil, Sulaimania-Mughagh and Kirkuk-Shwan in the Kurdistan Province of Iraq (Fig. 1). In total, fourteen specimens (4 males, 10 females) of blind mole rats were studied. The sampled localities, the number of individuals analyzed, and karyological results are presented in Table 1.

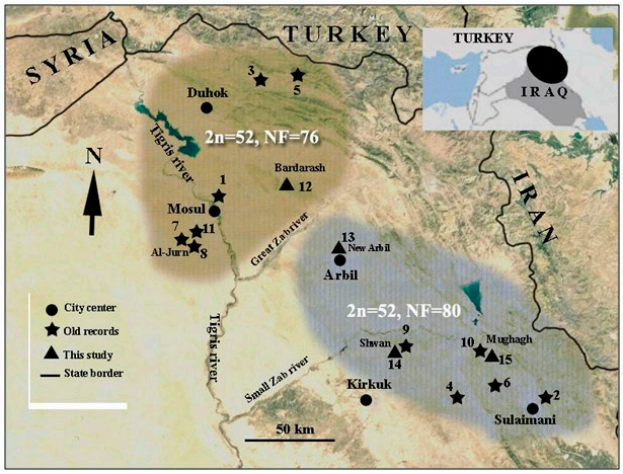

Figure 1. Sampling localities and geographical distribution of chromosomal forms of *Nannospalax ehrenbergi* in the Kurdistan region-Iraq (∗: Old records) 1- Near Mosul (Cheesman 1920); 2- Near Sulaimania (Bate 1930); 3- Sarsank (Hatt 1959); 4- Jarmo, Chemchamal Valley (Reed 1958); 5- Ser ʻAmadia and Tinn (Harrison 1956); 6- Jarmo, Palegawra Cave (Turnbull and Reed 1974); 7-Al-Jurn (Coşkun et al. 2012); 8- Al-Jurn (Coşkun et al. 2014); 9- Kirkuk-Shwan (Coşkun et al. 2014);10- Sulaimania- Mughagh (Coşkun et al. 2014); 11- Al-Jurn (Coşkun et al. 2016); (▲: This study) 12- Duhok-Bardarash; 13- Arbil-New Arbil; 14- Kirkuk-Shwan; 15- Sulaimania- Mughagh.

Direct chromosome preparations were made from bone marrow (Hsu 1969) and about 25-30 metaphase cells, which were well stained, and whose chromosomes were separately examined. The diploid number of chromosomes (2n), the number of autosomal arms (NFa), the total number of chromosomal arms (NF), and the sex chromosomes were determined from photos of the metaphase plates according to the centromere position. The karyotype preparations and animals examined were deposited in the Department of Biology, the Faculty of Sciences at Dicle University.

3. RESULTS AND DISCUSSION

Morphological peculiarities of the mole rats of Iraq were documented in detail by Coşkun et al. (2016). They conclude that morphologically all studied populations in North Iraq show great similarities and can be morphologically classified as *Nannospalax ehrenbergi*. The approximate geographic area of each chromosomal form is shown in Fig. 1.

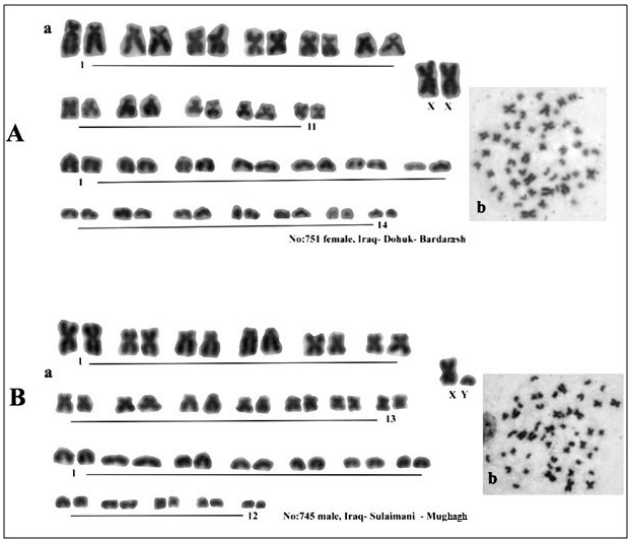

Figure 2. The karyotype *Nannospalax ehrenbergi:* A. Duhok-Bardarash population, B. Arbil population. (**a:** karyotype, **b:** metaphase plate).

3.1. Duhok Population

The karyotype of individuals from Duhok (Bardarash locality) was 2n = 52, NF = 76, NFa =72, which consists of 11 pairs of metacentric/submetacentric autosomes, and 14 pairs of acrocentric autosomes. The X chromosomes were large metacentrics (Fig. 2A). This cytotype is similar to that observed in the previously studied individuals ascribed to *Nannospalax ehrenbergi* from Al-Jurn (Mosul) by Coşkun et al. (2012). Mole rats of this locality (Duhok populations) inhabit the north of the Great Zab River (Tab.1).

3.2. Arbil Population

The samples from Arbil (New Arbil), Kirkuk (Shwan; 50 km north Kirkuk) and Sulaimania (Mughagh; 55 km west Sulaimania) possessed karyotypes of 2n=52, NF=80, NFa=76 and consists of 13 pairs meta /submetacentric 12 pairs acrocentric autosomes. The X chromosome was large metacentrics and the Y chromosome was small acrocentric (Fig. 2B and Tab. 1). The karyotypes of these three populations which is newly described here, are similar with each other's and they are located on the south side of the Great Zab river,in Iraq.

According to Gromov & Baranova (1981), Spalacidae has two distinct genera, *Nannospalax* and *Spalax*, and Turkish spalacids belong to the genus *Nannospalax*. Iraqi populations also belong to the genus *Nannospalax*. Reed (1958), Hatt (1959), Turnbull & Reed (1974), Harrison & Bates (1991), Lahony et al. (2013) have stated that mole rat samples in all Iraq are *S. leucodon* but our results show that all samples across Iraq are *N. ehrenbergi.*

Mole rat, belonging to the *N. ehrenbergi* exhibits two chromosomal forms that are widely distributed across north Iraq. One chromosomal form is 2n= 52 and NF= 76, NFa= 72. This chromosomal form (Duhok populations) is found north of the Great Zab river and is similar to the Mosul-Al Jurn (Coşkun et al. 2012) and Turkish Diyarbakır (Coşkun et al, 2006) populations. The other form, 2n= 52 and NF= 80, NFa= 76 (Arbil, Kirkuk-Sulaimania populations) in the south of the Great Zab river is a new chromosomal form that has not been previously described. Each of the karyotype forms exhibits an allopatric distribution, separated mostly by the Great Zab river or some ecological barriers, which may limit their dispersal (Fig. 2).

Chromosomal differences are frequently associated with taxonomic differences at the species level (Patton & Sherwood 1983). Chromosomal change has been implicated as a primary isolating mechanism in speciation. Chromosomal divergence is considered an indication of speciation events (Nevo et al. 2001).

This study filled the gaps in the knowledge of distribution of blind mole rat chromosomal forms in the north of Iraq. According to the results *N.ehrenbergi* are distributed in all parts of North Iraq, and it forms a potential species complex of *N. ehrenbergi*.

Table 1. The localities of samples that chromosomal analysis was performed in Iraq (**N:** sample size,**2n:** diploid chromosome numbers, **NF:** chromosomal arm numbers, **NFa:** autosomal arm number, **m**: metacentrics, **sm**: submetacentrics, **a:** acrocentric).

Locations			N	2n	Autosomes		NF	NFa	Gonosomes		Reference
City	Town	Village			m/sm	a			X	Y	
Kirkuk	Shwan	---	4♀	52	13	12	80	76	Sm	.	This study
Sulaimania	Dukan	Mughagh	2♂, 2♀	52	13	12	80	76	Sm	a	
Arbil	NewArbil	----	2♂, 3♀	52	13	12	80	76	Sm	a	
Duhok	Bardarash	Zamzamok	1♀	52	11	14	76	72	Sm	-	
Mosul	Al Jurn	----	3♂	52	11	14	76	72	Sm	a	Coşkun et al. (2012)

In order to fully understand the distribution and karyology of blind mole rats in Iraq, we need more information on hybrid zones in the territory, population structure and population size. There is a real necessity to establish long-term cytogenetic studies for this rodent. It is indeed very important to pay more attention to the role of natural barriers such as the Great Zab river and other ecological factors on speciation of Iraqi mole rats.

ACKNOWLEDGEMENT

We would like to thank Ms Yazgülü Zeybek of the Bergische University Wuppertal for English editing. Our gratitude and thanks are also extended to the anonymous reviewers for their valuable comments and input which greatly improved the manuscript. This study was supported by the Dicle University Research Fund (BAP, Project number 15 FF 010).

STATEMENT OF CONFLICT OF INTEREST

The authors declare that there is no any conflict ofinterests regarding the publication of this article.

REFERENCES

Al-Sheikhly O. F., M. K. Haba, F. Barbanera, G. Csorba, and D. L Harrison 2015. Checklist of the Mammals of Iraq (Chordata: Mammalia). - *Bonn Zool. Bull*., 64 (1): 33–58.

Amr Z. 2009. Mammals of Iraq. Publication No.NI-0209-002, Nature Iraq.Sulaimania, Kurdistan Iraq.

Bate D. M. A. 1930. Animal Remains from Dark Cave, Hazar Merd. -*Bull. Amer. School Prehist. Res*. 6: 38–41.

Cheesman R.E. 1920. Report on the mammals of Mesopotamia collected by members of the Mesopotamian Expeditionary Force, 1915 to 1919. - *J. Bombay Nat. Hist. Soc*. 27: 323–346.

CoşkunY., S. Ulutürk, and G. Yürümez 2006. Chromosomal diversity in mole-rats of the species *Nannospalaxehrenbergi*(Rodentia: Spalacidae) from South Anatolia, Turkey. - *Mamm. Bio. - Z. Saugetierkd.* 71(4): 244–250.

Coşkun Y., A. Namee, A. Kaya, and Z. I. F. Rahemo 2012. - Karyotype of *Nannospalax ehrenbergi* (Nehring 1898) (Rodentia: Spalacidae) in the Mosul Province, Iraq. - *Hystrix, It. J. Mamm*. 23(2): 72-75.

Coşkun Y., N. Aşan Baydemir, A. Kaya and A. Karöz 2014.Nucleolar organizer region distribution in *Nannospalax ehrenbergi* (Nehring, 1898) (Rodentia: Spalacidae) from Iraq. - *Turk. J. Zool*. 38: 250- 253.

Coşkun Y., Hamad Z. A. and Kaya A. 2016. Morphological properties of *Nannospalax* (Rodentia: Spalacidae) distributed in North-Iraq. - *Hacettepe J. Bio. & Chem*. 44 (2): 173-179.

Garstecki, T. and Z. Amr 2011.Biodiversity and Ecosystem Management in the Iraqi Marshlands – IUCN Screening Study on Potential World Heritage Nomination. Amman, Jordan.

Gromov I. M., and G. I. Baranova1981. Catalogue of Mammals in USSR.Nauka, Leningrad.

Hadid, Y., Németh, A., Snir, S., Pavlíček, T., Csorba, G., Kázmér, M., Major, Á.,Mezhzherin, S., Rusin, M., Çoşkun, Y. and Nevo, E., 2012. Is evolution of blind mole rats determined by climate oscillations? *PLoS One,* **7**: e30043. https://doi.org/10.1371/journal.pone.0030043.

Harrison D. L. 1956. Mammals from Kurdistan, Iraq, with description of a new bat. *J. Mamm*. **37**: 257–263.

Harrison D. L. and P. J. J. Bates 1991. The Mammals of Arabia. 2nd Edition. Harrison Zoological Museum Publication.262–301.

Hatt, R.T. 1959. The Mammals of Iraq. - *Misc. Publ. Mus. Zool., Univ. Michigan*, No. 106: 1-113.

Hsu T. C. 1969.-Direct bone marrow preparations for karyotyping. *Mamm.Chrom. Newsletter*, 10: 99-101.

Ivanitskaya E., Coşkun Y. and E. Nevo 1997. Banded karyotypes of mole rats (*Spalax*, Spalacidae, Rodentia) from Turkey: a comparative analysis. - *J. Zool. Syst. Evol. Res.* **35**(4): 171-177.

Ivanitskaya E. and E. Nevo 1998. Cytogenetics of mole rats of the *Spalax ehrenbergi* superspecies from Jordan (Spalacidae, Rodentia). - *Zeits. Saug*. 63(6): pp.336

Lahony S.R.A., M. K. Mohammad, H. H. Ali, A. A. Al-Moussawi, and M. S. A. Al-Rasul 2013. Hawraman Lowest Zone, Kurdistan Province North East Of Iraq. - *Bull. Iraq nat. Hist. Mus.* **12**(4): 7-34.

Lay D. M., and Nadler C. F. 1972.Cytogenetics and origin of North African *Spalax* (Rodentia: Spalacidae). - *Cyt. Gen. Res.* 11(4): 279-285.

Lyapunova, E.A., Vorontsov, N.N. and , L. Martynova 1974. Cytological differentiation of burrowing mammals in the Palaearctic. In: *Symposium Theriologicum II* (eds. J. Kratochvíl and R. Obrtel). Proc. Int. Symp. on Species and Zoogeography of European Mammals. Academia, Prague, pp. 203-215.

Musser G. G. and M. D. Carleton 2005. Superfamily Muroidae. p. 894-1531. In: D. E. Wılson and D. A.

M. Reeder (Eds), Mammal species of the World: A taxonomic and geographic reference. 3rd ed., Vol. 2. – Baltimore.

Nehring A. 1898. Über mehrere neue *Spalax* Arten. - *Sitzungberichte der Berlinischen Gesellschaft Naturforschender Freunde* 10: 163-183.

Nevo E., E. Ivanitskaya and A. Beiles 2001. Adaptive radiation of blind subterranean mole rats: Naming and revisiting the four sibling species of *Spalax ehrenbergi* superspecies in Israel: *Spalax galili* (2n = 52), *S. golani* (2n = 54), *S. carmeli* (2n = 58) and *S. judaei* (2n = 60). – Leiden, 195 pp.

Patton J. L. and S.W. Sherwood 1983. Chromosome evolution and speciation in Rodents. *Ann. Rev. Ecol. Syst*. 14:139-158.

Reed C. A. 1958. Observations on the burrowing rodent *Spalax* in Iraq. - *J. Mamm*. 39: 386-389.

Savic I. and Nevo E. 1990. The Spalacidae: Evolutionary history, speciation and population biology. In: Evolution of Subterranean Mammals at the Organismal and Molecular Levels, Ed. by O. REIG. New York: Alan R. Liss, Inc.pp. 129–153.

Topachevskii V.A., 1969. *Fauna of the USSR. Mammals: Mole rats, Spalacidae*, Vol. 3, No. 3.Academia Nauka, Leningrad.

Turnbull, P. F., and C. A. Reed 1974. The Fauna from the Terminal Pleistocene of Palegawra Cave, A Zarzian Occupation Site in Northeastern Iraq. – *Fieldiana Anthropol*. 63(3): 81–146.

Wahrman J., R. Goitin, and Nevo E. 1969. Geographic variation of chromosome forms in *Spalax*, a subterranean rodent of restricted mobility. In: Benirschke E. (ed.), *Comp. Mamm. Cyt.* Springer Verlag. New York: 30–48.

Zohary M. 1973. Geobotanical foundations of the Middle East. Fischer Verlage, Stuttgart.V,1

Caryologia
International Journal of Cytology, Cytosystematics and Cytogenetics

Firenze University Press
www.fupress.com/caryologia

Citation: S.T. Nabavi, F. Farahan, M. Sheidai, K. Poursakhi, M.R. Naeini (2019) Population genetic study of *Ziziphus jujuba* Mill.: Insight in to wild and cultivated plants genetic structure. *Caryologia* 72(4): 85-92. doi: 10.13128/caryologia-405

Published: December 23, 2019

Data Availability Statement: All relevant data are within the paper and its Supporting Information files.

Competing Interests: The Author(s) declare(s) no conflict of interest.

Population genetic study of *Ziziphus jujuba* Mill.: Insight in to wild and cultivated plants genetic structure

Seyyedeh Tahereh Nabavi[1], Farah Farahan[2], Masoud Sheidai[3,*], Katayoun Poursakhi[1], Mohammad Reza Naeini[4]

[1] *Department of Horticulture Science, Isfahan (Khorasgan) Branch, Islamic Azad University, Isfahan, Iran*
[2] *Department of Microbiology, Qom Branch, Islamic Azad University, Qom, Iran*
[3] *Faculty of Life Sciences and Biotechnology, Shahid Beheshti University, Tehran, Iran*
[4] *Department of Horticulture Crops Research, Qom Agricultural and Natural Resources Research and Education Center,AREEO, Qom, Iran*
*Corresponding author: msheidai@yahoo.com

Abstract. *Ziziphus jujuba* (jujube) of buckthorn family (Rhamnaceae) is an important medicinal crop plant cultivated in different provinces of Iran. It has also wild populations in some geographical areas. We carried out population genetic study on 8 populations of cultivated versus wild jujuba by using ISSR molecular markers to produce data on population genetic structure, gene flow, and genetic variability in the studied populations. We also aimed to investigate genetic differentiation between wild and cultivated plants and identify the potential gene pools of this medicinal plant species. The studied populations had a moderate genetic variability and were grouped in two major groups by PCoA plot. AMOVA revealed significant genetic difference among these cultivars. Mantel test showed significant correlation between genetic distance and geographical distance in the studied populations. PCoA analysis showed genetic differentiation between wild and cultivated plants within each province. STRUCTURE analysis identified two potential gene pools for jujube cultivars. Data obtained may be used in genetic conservation and future breeding programs of this medicinal plant species in the country.

Keyword. *Ziziphus jujube*, ISSR, STRUCTURE.

INTRODUCTION

The genus *Ziziphus* Mill. of the buckthorn family (Rhamnaceae), contains about 40 species that are deciduous evergreen trees or shrubs and are distributed in the tropical and subtropical regions of the world (Sing et al. 2007). South and Southeast Asia are considered to be the center of both evolution and distribution of *Ziziphus* species (Sing et al. 2007). These plant species are of medicinal value and are known to be self-incompatible and produce inter-specific hybrids (Asatryan and Tel-Zur 2013, 2014).

Z. jujuba (jujube) is one of the well known species of the genus with great medicinal value. It is mainly distributed in southwestern Asia. Traditional use of the species dates back to 2,500 years ago, as revealed in the original Chinese materia medica records. The fruit, seed, and bark are used to alleviate stress and insomnia and as appetite stimulants, digestive aids, antiarrhythmics, and contraceptives (Vahedi et al. 2008).

The fruit is eaten fresh or dried and made into candy; tea, or syrup (Gupta et al. 2004; Jiang et al. 2007). Moreover, some specific saponins, as well as ethyl acetate and water extracts of the fruit and bark, have explored the potential cytotoxicity of jujube. These extracts bring about apoptosis and differential cell cycle arrest, moreover, activity against certain human cancer cell lines has been demonstrated in vitro (Lee et al. 2004; Huang et al. 2007;Vahedi et al. 2008).

Ziziphus jujube is an important plant species to the mankind, due to which its cultivation and conservation gained high importance within recent years. Moreover, as jujube has wide geographical distribution and forms many local populations, it is important to be studied from population genetic point of view.

The species with extensive geographical distribution can be adapted to adverse environmental conditions and harbor different gene content that may be used in future breeding programs and establishing genetic-rich germ plasm collections (Sheidai et al. 2013, 2014, 2016).

Different molecular markers were used to investigate the genetic diversity in *Z. jujuba* cultivars or wild individuals. For instance, random amplified polymorphic DNA (RAPD), amplified fragment length polymorphisms (AFLP), sequence-related amplified polymorphisms (SRAP), simple sequence repeats (SSR), inter-simple sequence repeats (ISSR), and chloroplast microsatellite (Cp-SSR) markers were used to study cultivar relationships and genetic variability (see for example, Zhao and Liu 2003; Peng et al. 2000; Liu et al.2005; Wang et al. 2007; Singh et al. 2007; Wang et al. 2014; Zhang et al. 2014; Huang et al. 2015).

Population genetic study is an important step for genetic evaluation of medicinally important species as it gives insight on the genetic structure, genetic diversity and gene flow versus genetic fragmentation of these plant species. It also produces data on the number of potential gene pools for conservation and breeding strategies (Sheidai et al. 2013, 2014, 2016). Therefore, the aim of present study was to produce data on genetic diversity, population genetic structure and to compare the cultivars and wild populations of *Ziziphus jujuba* of Iran. We investigated 150 plants of both cultivated as well as wild jujube growing in 23 localities within 8 provinces.

For genetic study we used ISSR molecular markers, as these markers are very useful tool to detect genetic polymorphism, are inexpensive and readily adaptable technique for routine germplasm fingerprinting. They can be used to illustrate genetic relationship between accessions or genotypes and construction of genetic linkage maps (Sheidai et al. 2013, 2014, 2016). The suitability of ISSRs was reported by Alansi et al. (2016), who studied genetic diversity in populations of *Ziziphus spina-christi* (L.) Willd.

MATERIAL AND METHODS

Plant materials

In total 80 plants were studied in 8 provinces (Fig. 1). Ten plants were randomly selected in each population and used for molecular studied.

ISSR assay

For molecular studies, the fresh leaves were randomly collected from 53 randomly selected plants in the studied area and were dried in silica gel powder. The genomic DNA was extracted using CTAB-activated charcoal protocol (Križ man et al., 2006). The extraction procedure was based on activated charcoal and polyvi-

Figure 1. Distribution map of *Zizphus jujube* populations studied.

nylpyrrolidone (PVP) for binding of polyphenolics during extraction and under mild extraction and precipitation conditions. This promoted high-molecularweight DNA isolation without interfering contaminants. Quality of extracted DNA was examined by running on 0.8% agarose gel.

Ten ISSR primers, UBC 807, UBC 810, UBC 811, UBC 834,CAG(GA)7, (CA)7AC, (CA)7AT, (CA)7GT (GA)9A, and (GA)9T, commercialized by the University of British Columbia, were used. PCR reactions were performed in a 25-µL volume containing 10 mMTris-HCl buff er at pH 8, 50 mM KCl, 1.5 mM MgCl2 , 0.2 mM of each dNTP (Bioron, Germany), 0.2 µM of a single primer, 20 ng of genomic DNA, and 3 U of Taq DNA polymerase (Bioron). Amplification reactions were performed in a Techne thermocycler (Germany) with the following program: 5 min for initial denaturation step at 94 °C, 30 s at 94 °C, 1 min at 55 °C, and 1 min at 72 °C. Th e reaction was completed by a fi nal extension step of 7 min at 72 °C. The amplification products were visualized by running on 2% agarose gel, followed by ethidium bromide staining. The fragment sizes were estimated using a 100-bp molecular size ladder (Fermentas, Germany). The experiment was replicated 3 times and constant ISSR bands were used for further analyses.

Data analyses

The ISSR bands obtained were treated as binary characters and coded accordingly (presence = 1, absence = 0). The numbers of private versus common alleles were determined. The shared loci among populations were determined by POPGENE ver. 1.3 (2000). Genetic diversity parameters like, New gene diversity (He), Shannon information index (I), the number of effective alleles, and percentage of polymorphism (Weising 2005), were determined by using GenAlex 6.4 (Peakall and Smouse, 2006).

For genetic grouping of the studied cultivated and wild plants, Nei genetic distance was determined (Weising, 2005), and used in clustering as well as ordination methods (Podani 2000). Genetic differentiation of the studied populations was determined by AMOVA after 1000 permutations as performed in GenAlex 6.4 (Peakall and Smouse, 2006). The Mantel test (Podani, 2000) after 5000 permutation was performed to study the association between genetic distance and geographical distance of the studied populations.

Genetic structure of the populations was studied by model-based clustering as performed by STRUCTURE software ver. 2.3 (Pritchard et al., 2000). We used the admixture ancestry model under the correlated allele frequency model. A Markov chain Monte Carlo simulation was run

20 times for each value of K (1-8) after a burn-in period of 10 5. Data were scored as dominant markers and analysis followed the method suggested by Falush et al. (2007). For the optimal value of K in the population studied, we used The STRUCTURE Harvester website (Earl and von Holdt, 2012) was used to perform the Evanno method to identify the proper value of K (Evanno et al., 2005). To study genetic differentiation between wild and cultivated plants, we performed PCoA (Principal coordinate analysis) analysis within each province.

RESULTS

We obtained 31 ISSR bands (Loci) in total (Table 1). The highest number of bands (17 bands) occurred in population 1 (Soth Khorasan), and 2 (Fars) (16 bands), respectively. Some of the populations had private bands with population 4 (Sistan-o-Baloochestan) having the highest number (4 private bands). Few common bands occurred in the studied populations too. These are shared alleles among these populations.

Genetic diversity parameters determined in *Z. jujuba* populations are presented in Table 3. The percentage of genetic polymorphism obtained ranged from 3.25 in population 7 (Golestan) to 51.61 in population 2 Fars). A moderate level of genetic polymorphism (>30%) also occurred in populations 3, and 4 (DNorth-Khorasan, andSistan-o-Baloochestan, respectively). The highest mean value of New gene diversity (He) occurred in populations 1 to 4 (0.10-0.16, Table 2).

Table 1. Details of ISSR bands in *Z. Jujube* populations.

Population	Pop1	Pop2	Pop3	Pop4	Pop5	Pop6	Pop7	Pop8
No. Bands	16	17	13	15	12	10	8	13
No. Bands Freq. >= 5%	16	17	13	15	12	10	8	13
No. Private Bands	1	2	0	4	0	1	0	1
No. LComm Bands (<=50%)	6	7	6	5	4	3	3	5

Table 2. Genetic variability parameters determined in *Ziziphus jujube* populations based on ISSR markers (populations numbers are according to Fig. 1).

Pop	N	Na	Ne	I	He	uHe	P%
Pop1	10.000	0.968	1.240	0.223	0.146	0.154	45.16%
Pop2	10.000	1.065	1.262	0.252	0.164	0.172	51.61%
Pop3	10.000	0.742	1.180	0.161	0.107	0.112	32.26%
Pop4	10.000	0.871	1.193	0.177	0.115	0.121	38.71%
Pop5	10.000	0.613	1.141	0.125	0.084	0.088	22.58%
Pop6	10.000	0.484	1.105	0.091	0.061	0.065	16.13%
Pop7	10.000	0.290	1.028	0.021	0.015	0.016	3.23%
Pop8	10.000	0.710	1.167	0.145	0.097	0.102	29.03%

N = No. Of studied plants, Na = No. Of polymorphic alleles, Ne = Effective No. of alleles, He = New gene diversity, uHe = Unbiassed gene diversity, and P% = Percentage of polymorphism.

Detailed analysis of ISSR loci revealed that 16 ISSR loci (50% of all ISSR loci), have high Gst value I.e. >0.50 (equivalent of Fst). This indicates that, these loci are different in the studied populations and lead to population genetic differentiation. This ISSR locus had a low value of Nm and therefore, they are not shared by all the populations. On the contrary, 14 ISSR loci had Nm value >1, and low Get value. They are the common alleles shared by the studied populations. The mean Nm value of the studied populations was 0.38, which is very low and indicates lack of extensive gene flow among the studied populations.

The Nei's genetic identity and genetic distance of the studied populations are provided in Table 3. Genetic similarities between 0.70 to 0.96% were observed in the studied populations. The highest genetic identity occurred between populations 1 and 2 (0.96%).

Table 3. Nei genetic identity versus genetic distance in the *Z. Jujube* populations (populations numbers are according to Fig1. Nei's genetic identity (above diagonal) and genetic distance (below diagonal).

pop ID	1	2	3	4	5	6	7	8
1	****	0.9609	0.8920	0.8411	0.8574	0.8735	0.8445	0.9128
2	0.0399	****	0.9189	0.8675	0.8526	0.8032	0.7677	0.8477
3	0.1143	0.0846	****	0.9076	0.8505	0.7602	0.7187	0.7955
4	0.1731	0.1422	0.0969	****	0.8741	0.7263	0.6824	0.7415
5	0.1538	0.1595	0.1619	0.1345	****	0.8011	0.7621	0.7748
6	0.1353	0.2192	0.2742	0.3198	0.2218	****	0.9434	0.9539
7	0.1691	0.2644	0.3303	0.3821	0.2717	0.0583	****	0.9548
8	0.0913	0.1652	0.2288	0.2991	0.2552	0.0472	0.0462	****

Genetic differential of Z. Jujube *populations*

Based on Nei genetic distance, PCoA plot was constructed for the studied cultivars and wild populations, separately (Fig. 2). The plot constructed for the cultivars, placed *Z. Jujube* populations in two main groups. Populations 2, 3 and 4 formed the first main group, while populations 1, 6, 7, and 8, comprised the second major group. Some trees in population1 and 5 were intermixed in both groups. This is due to within population genetic variability and the common shared alleys in these two populations.

Similarly, PCoA analysis of the wild populations revealed that these populations differ genetically from each other as they are placed in separate groups (Fig. 3).

Therefore, both cultivated and wild plants of the studied provinces are genetically differentiated from each other. Moreover, AMOVA produced significant genetic difference among *Z. Jujube* populations (PhiPT = 0.57, P = 0.001). AMOVA revealed that 57% of total genetic variability occurred among populations while, 43% of genetic variability was due to within population difference. Paired-sample AMOVA also produced significant difference among the studied populations. These results indicate that although the studied *Z. jujube* cul-

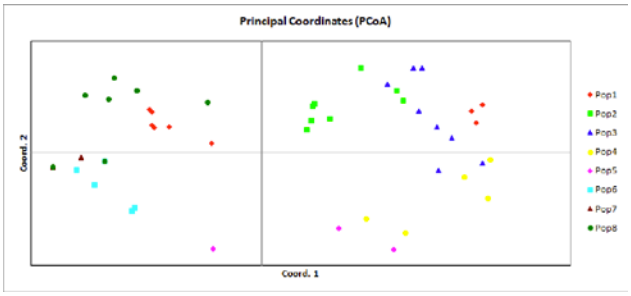

Figure 2. PCoA plot of ISSR data in *Z. Jujube* populations.

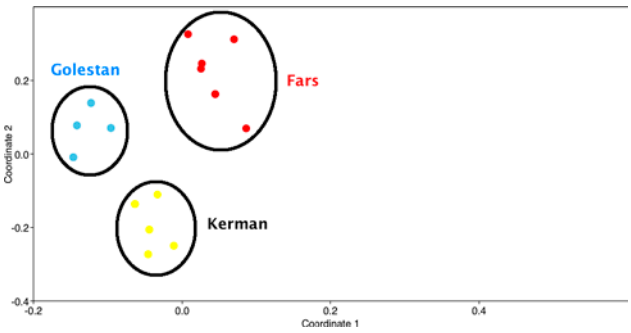

Figure 3. PCoA plot of *Z. Jujube* wild populations based on ISSR data.

tivars and wild populations differ genetically from each other, but also some degree of within population of genetic variability do occur in each population.

Wild versus cultivated Z. Jujuba *plants*

In the other attempt, we investigated the genetic differentiation of wild versus cultivated plants within each locality. In three provinces namely, 1- Fare, 2- Golestan, and 3-Kerman, both cultivated and wild plants were present. The comparison of ISSR bands in these plants revealed almost complete genetic differentiation of wild and cultivated plants in Fars province, while in two other provinces, they were genetically differentiated to some degree (Fig. 4). This indicates that these two types of *Z. jujube*, are not genetically alike and we may have still novel genes in wild plants that can be introduced in to cultivated plants genome. These genetic variability are of high importance in medicinal plant conservation and breeding.

Assocition between genetic diversity and geographical features

Correlation analysis performed did not show significant association between gene diversity with either altitude or latitude in the studied populations (Fig. 5). The same hold true for percentage of genetic polymorphism. This may happen due to cultivation practice and selection made by local gardeners which interfere with local natural adaptation.

However, Mantel test (Fig. 6) between geographical distance (combined distance of longitude and altitude)

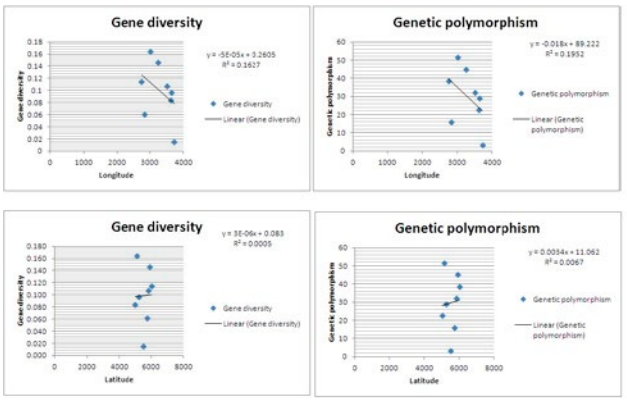

Figure 5. Correlation analysis of genetic diversity and genetic polymorphism with geographical features in *Z. Jujube* populations.

and genetic distance produced significant correlation ($P<0.01$). Therefore, with increase in geographical distance, an increase in genetic difference of the populations occurred. This is called isolation by distance (IBD). This indicates that the combined effect of geographical features as well as genetic background of the studied cultivars bring about significant genetic differentiation among *Z. Jujube* populations.

Genetic structure of Z. Jujube *populations*

The genetic structure of the studied populations and degree of genetic admixture among populations were determined by STRUCTURE analysis. The STRUCTURE plot (Fig. 7) revealed presence of different allele combinations (differently colored segments) in the *Z. Jujube* populations. However, some degree of shared common alleles (similarly colored segments) was observed in populations 1, 2 and 3, and also in populations 6, 7, and 8. Populations 4 and 5 contained distinct allele combinations.

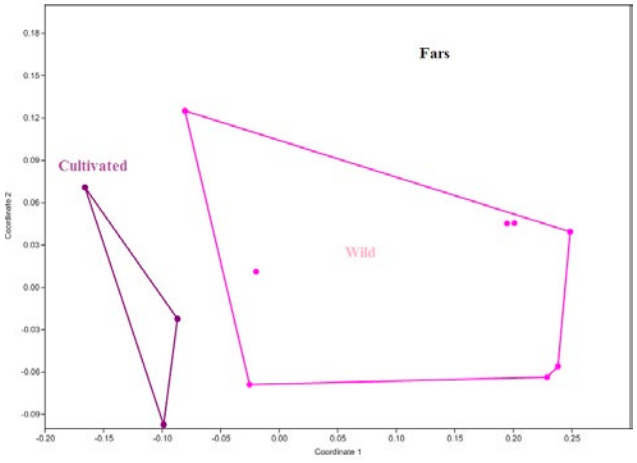

Figure 4. PCoA plot of wild versus cultivated *Z. Jujube* plants within Fars province.

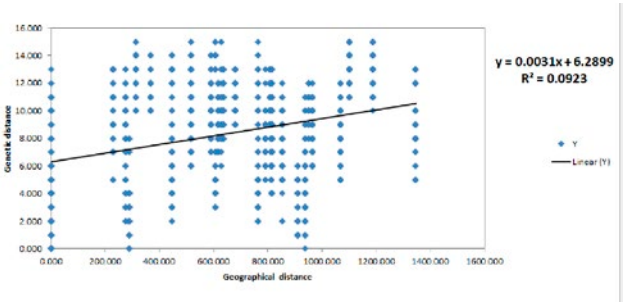

Figuse 6. Mantel test plot between genetic distance and geographical distance of *Z. Jujube* populations.

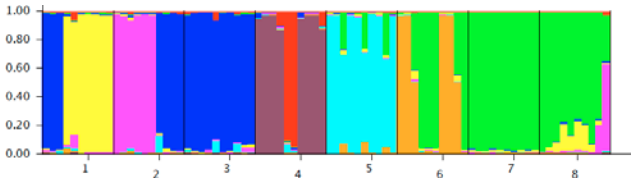

Figure 7. STRUCTURE plot of *Z. Jujube* populations based on k = 8.

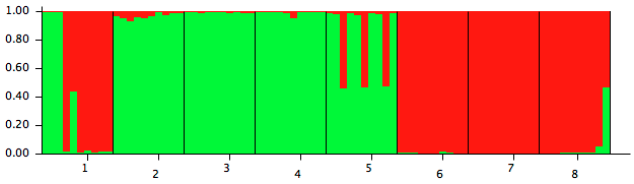

Figure 8. STRUCTURE plot of *Z. Jujube* populations based on k = 2.

Evanno test produced optimal number of genetic group k = 2. Therefore, 13 studied *Ziziphus jujube* populations studied could be grouped in 2 genetic groups. STRUCTURE plot based on k = 2 (Fig. 8), revealed that populations 2-4 comprise the first genetic group, while populations 6-8 comprise the second genetic group. Moreover, populations 1 and 5 stands somewhere in between these two groups. This is in complete agreement with PCoA plot results presented before.

DISCUSSION

In spite of medicinal importance (Vahedi et al. 2008) and wide geographical distribution of *Ziziphus jububa* in our country, we had no detailed information on its genetic variability and structure.The present study revealed the presence of a moderate genetic variability in the cultivated populations. It also showed genetic differentiation between wild versus cultivated plants within each province. Therefore, we can use these plants in a core germ plasm collection of Z. Jujube for conservation and breeding purpose (Sheidai et al. 2013, 2014, 2016).

Alansi et al. (2016), studied genetic diversity in populations of *Ziziphus spina-christi* (L.) Willd. By using ISSR markers and reported the genetic diversity value of 0.26, total genetic diversity Ht = 0.266, and intra-population genetic diversity, Hs = 0.2199.

In present study, AMOVA revealed significant genetic difference among *Z. jujube* cultivars, and also identified a good level of genetic variability within studied population. Moreover, Gst and Nm results revealed that about 50% of ISSR loci was either private on not shared by all populations, and 50% were exchange in populations via gene flow. This may be to some degree related to out-crossing nature of *Z. jujube*.

Zhang et al. (2015) studied genetic variability and differentiation in cultivated jujube and wild jujube by using SSR molecular markers. They reported high levels of genetic diversity (HE=0.659 and HS=0.674) within populations, and moderate differentiation among studied populations (FST=0.091, RST= 0.068, GST=0.271). They also reported a high degree of gene flow (Nm=6.572) and weak correlation between genetic and geographical distances (r 2 =0.026, P>0.05), and suggested that gene flow occurred frequently among populations. AMOVA showed that most of the existing genetic diversity was distributed within populations (88 %), and only 12 % occurred among populations, therefore, the studied populations were not differentiated.

On the other hand, Singh et al. (2017) investigated genetic variation and relationships among cultivars of *Ziziphus mauritiana* (Lamk.) native of India by using start codon targeted (SCoT), ISSR, and ribosomal DNA (rDNA) markers. They reported high level of polymorphism among SCoT (61.6%) and ISSR (61%) markers. SCoT and ISSR dendrograms delineated all the cultivars of Z. *mauritiana* into well-supported distinct clusters. These populations were genetically differentiated as also was indicated with high Get values.

Difference in the results of these studies is probably due to difference in geographical isolation of the studied populations. In present study, the distance between populations is great as they are located in different provinces ranging from south to north of the country with no intermediately plant populations among them (Fig. 1). Genetic differentiation of the studied populations may be attributed to a combination of adaptation to different environmental conditions and limited capacity for long-distance dispersal (Zhang et al. 2015). However, we also noticed good genetic differentiation within each province between wild and cultivated Z. Jujube plants; this is probably due to effects of cultivation practice and artificial selection made by jujube growers in the gardens. Such selection pressure is absent in wild plants.

In conclusion, we have presented data on genetic variability and genetic structure of both *Z. Jujube* cultivars and wild plants in the country. Two main gene pools were identified for jujube cultivars which may be used in future genetic conservation and hybridization programs of this important medicinal plant.

REFERENCES

Asatryan A, Tel-Zur N. 2014. Intraspecific and interspecific crossability in three *Ziziphus* species (Rhamnaceae). Genetic Resources and Crop Evolution. 208:390–399.

Asatryan A, Tel-Zur N. 2013. Pollen tube growth and self-incompatibility in three *Ziziphus* species (Rhamnaceae). Flora. 208:390–399.

Earl DA, Von Holdt Bm . 2012. STRUCTURE HARVESTER: a website and program for visualizing STRUCTURE output and implementing the Evanno method. Conservation Genetics Resources 4: 359–361.

Evanno G, Regnaut S, Goudet J. 2005. Detecting the number of clusters of individuals using the software STRUCTURE: a simulation study. Molecular Ecology.14: 2611–2620.

Gupta M, Mazumder UK, Vamsi ML, Sivakumar T, Kandar CC. 2004. Anti-steroidogenic activity of the two Indian medicinal plants in mice. Journal of Ethnopharmacology. 90(1):21–25.

Križman M, Jakše J, Baričevič D, Javornik B , Prošek M. 2006. Robust CTAB-activated charcoal protocol for plant DNA extraction. Acta Agriculturae Slovenica. 87:427–433.

Lee SM, Park JG, Lee YH. 2004. Anti-complementary activity of triterpenoides from fruits of *Zizyphus jujuba* . Biological and Pharmaceutical Bulletin. 27:1883–1886.

Peakall R, Smouse PE. 2006. GENALEX 6: genetic analysis in Excel. Population genetic software for teaching and research. Molecular Ecology Notes. 6: 288–295.

Sheidai M, Zanganeh S, Haji-Ramezanali R, Nouroozi M, Noormohammadi Z, Ghsemzadeh-Baraki S. 2013. Genetic diversity and population structure in four *Cirsium* (Asteraceae) species. Biologia. 68: 384–397.

Sheidai M, Ziaee S, Farahani F, Talebi Sm, Noormohammadi Z, Hasheminejad Ahangarani Farahani Y .2014. Infra-specific genetic and morphological diversityin *Linum album* (Linaceae). Biologia. 69: 32e39

Sheidai M, Taban F, Talebi Sm, Noormohammadi Z. 2016. Genetic And morphological diversity in *Stachys lavandulifolia* (Lamiaceae) populations. Biologija. 62(1): 9-24.

Singh A, Sharma P, Singh R. 2007. Assessment of genetic diversity in *Ziziphus mauritiana* using inter-simple sequence repeat markers. Journal of Plant Biochemistry and Biotechnology. 16:35–40.

Singh, S. K., Chhajer, S., Pathak, R., Bhatt, R. K.,Kalia, R. K. 2017. Genetic diversity of Indian jujube cultivars using SCoT, ISSR, and rDNA markers. Tree Genetics & Genomes. 13: 12 DOI 10.1007/s11295–016-1092-x.

Vahedi F, Fathi Najafi M, Bozari K. 2008. Evaluation of inhibitory effect and apoptosis induction of *Zizyphus jujuba* on tumor cell lines, an in vitro preliminary study. Cytotechnology. 56:105–111.

Weising K, Nybom H, Wolff K, Kahl G.2005. DNA Fingerprinting in Plants. in: Principles, Methods, and Applications. (2nd ed.), Boca Rayton, Fl., USA: CRC Press, p. 472.

Zhao J, Liu MJ. 2003. RAPD Analysis on the cultivars, strains and related species of Chinese jujube (Ziziphus jujuba Mill.). Scientia Agricultura Sinica. 36(5), 590–594.

Falush D, Stephens M, Pritchard JK. 2007. Inference of population structure using multilocus genotype data: dominant markers and null alleles. Molecular Ecology Notes. 7:574–578.

Huang X, Kojima-Yuasa A, Norikura T, Kennedy Do, Hasuma T, Matsui-Yuasa I. 2007. Mechanism of the anti-cancer activity of *Zizyphus jujuba* in HepG2 cells. The American Journal of Chinese Medicine. 35:517–532.

Huang J, Yang X, Zhang C, Yin X, Liu S, Li X . 2015. Development of Chloroplast Microsatellite Markers and Analysis of Chloroplast Diversity in Chinese Jujube (*Ziziphus jujuba* Mill.) and Wild Jujube (*Ziziphus acidojujuba* Mill.). PLoS ONE 10: e0134519.

Jiang, J.G., Huang, X.J., Chen, J, Lin, Q.S. 2007. Comparison of the sedative and hypnotic effects of flavonoids, saponins, and polysaccharides extracted from Semen *Ziziphus jujuba* . Natural Product Research. 21:310–320.

Liu P, Peng JY, Peng SQ, Zhou JY, Dai L. 2005. Study on Systematic Relationships of *Ziziphus jujuba* using RAPD technique. Scientia Sinica. 41:182–185.

Peng JY, Shu HR, Sun ZX, Peng SQ .2000. RAPD Analysis of germplasm resources on Chinese date. Acta Chimica Sinica 27: 171–176.

Pritchard JK, Stephens M, Donnelly P. 2000. Inference of population structure using multilocus genotype Data. Genetics. 155: 945–959.

Alansi S, Tarroum M, Fahad A.Q, Khan S, Nadeem M. 2016. Use of ISSR markers to assess the genetic diversity in wild medicinal Ziziphus spina-christi (L.) Willd. collected from different regions of Saudi Arabia. Biotechnology & Biotechnological Equipment. 30(5): 942–947

Singh S. K., Chhajer, S., Pathak, R., Bhatt, R. K.,Kalia, R. K. 2017. Genetic diversity of Indian jujube cultivars using SCoT, ISSR, and rDNA markers. Tree Genetics & Genomes 13: 12 DOI 10.1007/s11295–016-1092-x

Singh A, Sharma P, Singh R.2007. Assessment of genetic diversity in *Ziziphus mauritiana* using inter-simple sequence repeat markers. Journal of Plant Biochemistry and Biotechnology. 16:35–40.

Wang YK, Tian JB, Wang YQ, Sui Cl, Li Dk, Huang Cl. 2007. AFLP analysis of jujuba cultivars and strain. Journal of Fruit Science. 242: 146–150.

Wang S, Liu Y, Ma L, Liu H, Tang Y, Wu L. 2014. Isolation and characterization of microsatellite markers and analysis of genetic diversity in Chinese jujuba (*Ziziphus jujuba* Mill.). Plos One. 9: e99842.

Zhang, Ch., Huang, J., Yin, X., Lian, Ch., Li, X. 2015. Genetic diversity and population structure of sour jujube, *Ziziphus acidojujuba*. Tree Genetics & Genomes 11: 809.

Zhang C, Huang J, Yin X, Lian C, Li X. 2014. Genetic diversity and population structure of sour jujuba, *Ziziphus acidojujuba*. Tree Genetics & Genomes. 11:809.

Caryologia
International Journal of Cytology, Cytosystematics and Cytogenetics

Firenze University Press
www.fupress.com/caryologia

OPEN ACCESS

Citation: Z. Bouziane, R. Issolah, A. Tahar (2019) Analysis of the chromosome variation within some natural populations of subterranean clover (*Trifolium subterraneum* L., Fabaceae) in Algeria. *Caryologia* 72(4): 93-104. doi: 10.13128/caryologia-164

Published: December 23, 2019

Data Availability Statement: All relevant data are within the paper and its Supporting Information files.

Competing Interests: The Author(s) declare(s) no conflict of interest.

Analysis of the chromosome variation within some natural populations of subterranean clover (*Trifolium subterraneum* L., *Fabaceae*) in Algeria

Zahira Bouziane[1,3], Rachida Issolah[2,*], Ali Tahar[3]

[1] *Université Abbès Laghrour, Khenchela, Algérie*
[2] *INRAA, CRP Mehdi Boualem, Division de Recherche sur les ressources phytogénétiques, BP 37, Baraki, Alger, Algérie*
[3] *Université Badji Mokhtar, Laboratoire de Biologie végétale et de l'environnement, Annaba, Algérie*
*Corresponding author: rachida.issolah@yahoo.com

Abstract. Nine natural populations of subterranean clover (*Trifolium subterraneum* L.) coming from different eco-geographical sites of the North-East Algeria, have been studied for their chromosome number and karyotype features. The study is part of the evaluation and valorization of plant genetic resources of fodder and pastoral interest in Algeria. The results of mitosis detect two groups of populations, and reveal diversity in the number among and within populations. The Algerian populations of *T. subterraneum* are characterized by two chromosomic formulas. The first formula (2n=2x=16m) (median), more common in most of the studied populations, is in conformity with previous reports in this species. The karyotype of these populations is symmetrical for size and form. The second (2n=2x= 18m), is detected for the first time and described as a new chromosomal formula in *T. subterraneum*. The latter is relatively more frequent than the first one and characterizes the populations coming from high altitude areas. The karyotype (2n=2x=18m) is relatively symmetrical. At the level of the two established Karyotypes, satellites are highlighted at the first pair. A variation in the size and frequency of these satellites is observed. The species exhibits regular meiotic behaviour, confirming the presence of two basic chromosome numbers (x=8 and 9). The study also highlights the role of ecological factors (Altitude and Rainfall) of the originating environment of Algerian populations in the variation and evolution of chromosome numbers in *T. subterraneum.* The new cytogenetic data can be exploited in the taxonomy of the species in Algeria in order to select and develop this plant genetic resource in the agricultural field.

Keywords. Chromosomes, Intraspecific variability, Karyotype, Subterranean clover, *Trifolium subterraneum* L.

INTRODUCTION

The genus *Trifolium* is one of the largest genera of the *Fabaceae* family (sub-family, *Papilionoideae*). It has more than 255 annual and perennial spe-

cies (Zohary and Heller 1984; Gillet and Taylor 2001). Most of them are of great agricultural importance and widely grown as fodder and green manure (Ellison et al. 2006). The genus *Trifolium* is originating from Mediterranean, because of the greatest diversity of numbers and chromosome forms have been found in this region (Taylor 1985). It has been subdivised into eight sections: *Lotoidea*, *Paramesus*, *Mystillus*, *Vesicaria*, *Chronosemium*, *Trifolium*, *Trichocephalum* and *Involucrarium* (Zohary and Heller 1984). The principal geographical centers of diversity of *Trifolium* are the Mediterranean basin, the West of North America, and the highlands of Eastern Africa (Ellison et al. 2006). The cytotaxonomic studies carried out on *Trifolium* have shown that it presents a surprising variety of chromosome numbers, and the changes in the number of chromosomes have played a large part in its evolution (Falistocco et al. 2013). Britten (1963) and Pritchard (1969) have shown that an aneuploid series of basic numbers x=5, 6, 7 and 8 are found in this genus. The presence of x=8 in about 80% of the species suggests that x=8 is the ancestral number of the genus (Senn 1938; Pritchard 1969; Zohary and Heller 1984; Ellison et al. 2006), from which the numbers x = 7, 6 and 5 are derived. Polyploidy is more common in perennial species (Kiran et al. 2010; Falistocco et al. 2013).

Subterranean clover (*Trifolium subterraneum* L., sect *Trichocephalum*), commonly known as the burrowing clover or sower, is a winter annual species, native to the Mediterranean Basin, West Asia and the Atlantic coast of Western Europe (Gladstones and Collins 1983 ; Zohary and Heller 1984). The plant of subterranean clover is autogamous, characterized by mechanisms of burial of reproductive structures, ensuring thus, its own self-regenerating (Masson 1997). The species constitutes an heterogenous complexesis, divided into three subspecies: *subterraneum*, *brachycalycinum* and *yanninicum* (Katznelson 1984), identifiable enough by their morpho-physiology, karyotypes, isozymes and polymorphisms for molecular markers (Piluzza et al. 2005). In Algeria, the subterranean clover is very common in the Tell and the mountain meadows (Quezel and Santa 1962), adapted to different ecological conditions (Issolah et al. 2015). This species is represented by three varieties belonging to the *subterraneum* subspecies (Subsp. *subterraneum* Var. *subterraneum*, Var. *brachycladum*, Var. *flagelliforme*) on the eight varieties described in Algeria (Zohary and Heller 1984). Despite the agronomic importance of the species in the world, as cattle feed and soil improvement, its cytological characterization remains very restricted.

This is because of the small size of chromosomes like all the other species of *Trifolium* (Zohary and Heller 1984).

The first investigations on *T. subterraneum* focused only on the determination of the chromosome number (2n=16), but without establishing the karyotype (Weselxen 1928; Yates and Brittan 1952; Brock 1953; Hutton and Peak 1954; Zohary and Katznelson 1958; Kliphuis 1962; Britten 1963; Katznelson and Morley 1965a). Later, some karyotype studies were performed in Spain (Angelo et al. 1975, 1977, 1983), Iran (Hezamzadeh Hijazi and Ziaeinasab 2006) and Italy (Falistocco et al. 1987; Falistocco et al. 2013).

The present study is interested in the evaluation and the valorization of the phytogenetic resources of fodder and ¦pastoral¦ interest in Algeria.

Its aim is the analysis of the chromosomal diversity presents in the natural populations of *Trifolium subterraneum* L., and the establishment of its karyotype.

It follows the different studies carried out on natural fodder legumes (Issolah and Abdelguerfi 1999a; Issolah and Khalfallah 2007; Issolah et al. 2006, 2012, 2015, 2016).

MATERIAL AND METHODS

Plant materials

The *Trifolium subterraneum* specimens were collected by INRAA (National Institute of Agronomic Research of Algeria), in July 2010. Nine natural populations sampled from North-East Algeria (Issolah et al. 2015), were the subject of a karyological study (Table 1).

Chromosome counting

The seeds belonging to the nine studied populations, were scarified to remove in tegumentary hardness, and then germinated on wet filter paper in Petri dishes at room temperature. The root tips meristems (1 to 1.5 cm in length) were excised in the morning between 8 am- 8.30 am and pretreated with α-bromonaphthalene (1%) at room temperature for 2h45mn. The use of this pretreatment increases the number of metaphase mitotic cells, allows the chromosomes to be well spread in the cell, straightens the chromatids, and contracts the chromosomes, which makes primary and secondary constrictions very noticeable (Singh 2018). For chromosomes analysis, root tips were hydrolyzed in 1N HCl and stained in lactopropionic orcein (Dyer 1963). The chromosomic observations were repeated several times. For each population, five plates of chromosomes were selected from at least 30 individuals (seeds). Then, they were observed and photographed using a Primo Star Zeiss

microscope. Chromosome counts were performed on metaphase plates with well individualized chromosomes.

Karyotype analysis

The karyomorphological analysis was carried out according to the following parameters: the lenght of long arm (L), short arm (S), the total length of the chromosome (LT = L + S), the difference between arms (d = L-S), and the relative length (LR (‰) = 1000 x TL/ ΣTL). Centromere position and chromosome types were determined from the two parameters: arm ratio (r= L/S), and centromeric index (CI % = S/LT x100) according to the nomenclature of Levan et al. (1964). For determining the asymmetry of the karyotype, three parameters were estimed: [(Ias. K% = (Σ L/Σ LT) x100 (Aran and Saito 1980)], the ratio between the longest and the shortest chromosome pairs (R), and the inter-chromosomal asymmetry coefficient (A2) (standard deviation of chromosome length / mean chromosome length) (Romeo Zarco 1986). Chromosome measurements, based on five plates per population, were performed using the Axiovision software (1999-2009). The different karyotype calculations were made thanks to Excel (2007).

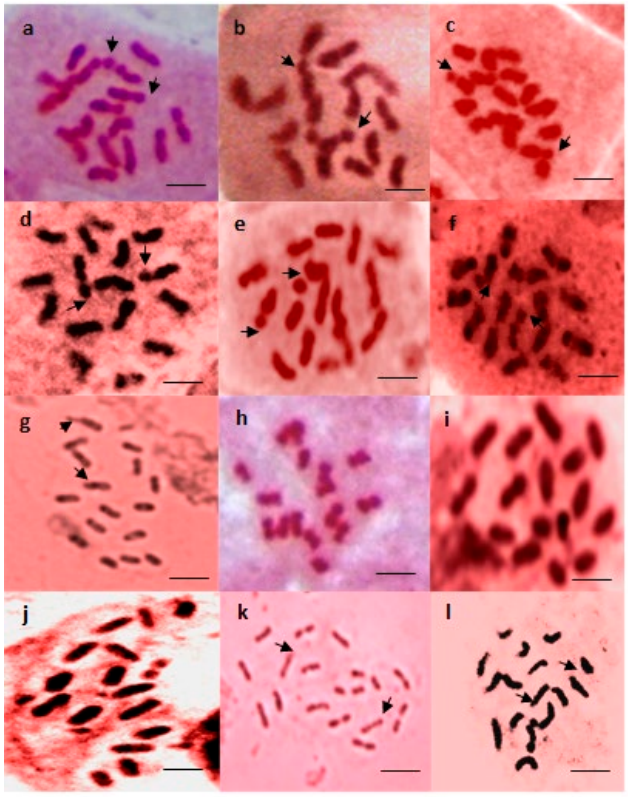

Figure 1. Mitotic metaphases of Algerian natural populations of *Trifolium subterraneum* L. with two chromosomes numbers 2n=16 and 2n=18 respectively: (a) population 12/10; (b) population 13/10; (c) population 19/10; (d) population 20/10; (e) population 22/10; (f) population 23/10; (g) population 25/10; (h) population 26/10; (i) population 33/10; (j) population 22/10 (2n=18); (k) population 25/10 (2n=18); (l) population 26/10(2n=18) . Arrows: satellites. Bar: 2.5µm.

Meiosis

To confirm the results corresponding to the numbers found by mitosis (presence of supernumerary chromosome pair for certain populations), the meiotic behaviour of the nine populations was also analysed. For this purpose, a trial has been conducted at the experimental station of INRAA (November 2014). Each population was represented by twenty individuals (seeds) and sowed in total randomization (field) for identifying the different phases of meiosis (laboratory). The flower buds collect period was spread over a month before flowering (recovering flower buds of variable size). For each plant, at least five flower buds were collected (April 2015) in the early morning (from 8h), then fixed in Carnoy solution (Ethanol-acetic acid 3 : 1, v/v) for at least 48 h at 4C°. After dissection of the anthers, the pollen mother cells (PMC) were crushed in an acetic carmine drop 1% (Jahier et al. 1992). Observations and photographs at different phases were performed using a Primo Star Zeiss microscope.

RESULTS

Chromosome counting

All mitotic metaphase plates of investigated populations of the species *Trifolium subterraneum* L. showed a diploid number of chromosomes (2n = 16) (Figure 1). This number is frequently observed in individuals of the populations 12/10; 13/10; 19/10; 20/10 and 33/10. However, the somatic metaphases of the four populations 22/10; 23/10; 25/10; 26/10, have presented along with the characteristic number of the species (2n = 16), a second and new number of chromosomes (2n = 18), often encountered during this study in these later populations (Figure 1). The two chromosome numbers (2n = 16 and 18) are observed within the cells of the same individual, and also in different individuals of the same population. This indicates a chromosomical variation within and between the populations of *Trifolium subterraneum*.

The analysis of 15 individuals per population, indicated that the variation of the chromosome numbers (2n = 16 and 18) was not in the same frequency in these

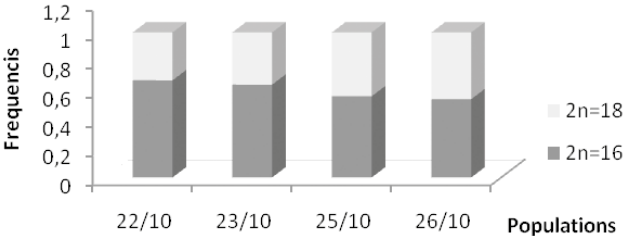

Figure 2. Frequencies of the two chromosomes numbers (2n=16 and 18) in the four populations of *Trifolium subterraneum* L. (15 individuals / population).

latter populations (Figure 2). Indeed, within the populations (22/10 and 23/10), the frequency of the number (2n = 16) represents twice the frequency of the number (2n=18) (0.67 and 0.33; 0.64 and 0.36, respectively). However, very similar frequency values are shown in the other two populations (25/10 and 26/10) (0.56 and 0.44; 0.5 and 0.46 respectively) (Figure 2).

Karyotype analysis

In all investigated populations, the morphology and chromosome structure are almost identical (Table 2-5). Our results showed that the chromosomes of the Algerian population of the species *Trifolium subterraneum* L. are small. The size of the chromosomes varies from 1.02 µm (Table 3) to 3.01 µm (Table 2). The total lengths of diploid chromosome set are comprised between 12.82 µm (Table 4) and 18.87 µm (Table 2). The mean value of the total length (TLG) of all studied populations is 1.92µm. The results of this study indicate also that the population 22/10 (2n =16) is characterized by the highest values for the selected parameters, like the mean value of chromosome length, which gives an estimated size of the genome (18.87 µm) and the largest first pair and eighth pair (3.01µm-1.72µm) (Table 2). Thus, we note that the two additional chromosomes present in the populations (2n = 18), have the same form, with a mean size of 1.09 µm (Figure 1, Table 3 and 5). The results of this study indicated also that satellites are located at the first chromosome pair within all investigated populations. A variation of the size and an abundance of these satellites are noticed. Thus, the metaphase plates of the populations characterized by (2n= 16), present a considerable size of these satellites compared to that noted on the plates of the populations characterized by (2n=18) with 0.25 µm ± 0.022; 0.18 µm ± 0.025, respectively.

These satellites are more abundant in the metaphases of populations with 2n = 18 compared to those with 2n = 16. Their frequencies are 0.70 and 0.44, respectively (Figure 1). Otherwise, the results of the centromeric index (Ic) and the ratio between the long arm and the short arm (r) allowed us to determine the homologous chromosomes and to classify the different chromosomal types. Therefore, all the studied populations are characterized by the karyograms, presenting median chromosomes (Figure 3b).

Table 1. Geographical origin and ecological characteristics of the sampling sites of nine populations of *Trifolium subterraneum* L. in Algeria

N° of populations	Origin	Altitude (m)	Rainfall (mm)
12/10	Guelma	170	600
13/10	Guelma	200	558
19/10	Tarf	665	661
20/10	Tarf	555	661
22/10	Souk Ahras	950	800
23/10	Souk Ahras	1040	700
25/10	Souk Ahras	800	900
26/10	Souk Ahras	1110	700
33/10	Skikda	110	562

Source (Issolah et al. 2015)

Table 2. Morphometric data within the population 22/10 (2n=16) of *Trifolium subterraneum* L. in Algeria.

Ch p	L (µm) (±SD)	S (µm) (±SD)	TL (µm)	RL ‰	d	r	Ci %	Ct
1	1.69 (0.41)	1.32 (0.26)	3.01	159.36	0.37	1.28	43.90	m-sat
2	1.42 (0.31)	1.26 (0.43)	2.68	141.96	0.17	1.13	46.86	M
3	1.53 (0.38)	1.08 (0.35)	2.61	138.52	0.45	1.42	41.33	M
4	1.26 (0.50)	1.09 (0.40)	2.35	124.38	0.17	1.15	46.45	M
5	1.23 (0.50)	1.05 (0.43)	2.28	120.85	0.18	1.17	45.98	M
6	1.18 (0.40)	1.05 (0.31)	2.23	118.11	0.13	1.12	47.12	M
7	1.05 (0.29)	0.94 (0.32)	1.99	105.65	0.11	1.12	47.16	M
8	0.92 (0.31)	0.80 (0.19)	1.72	91. 17	0.12	1.15	46.61	M
	I1as% =54.48	ΣTL=18.87	TLG=2.36	R1=1.75	$A_{2(1)}$=0.14			

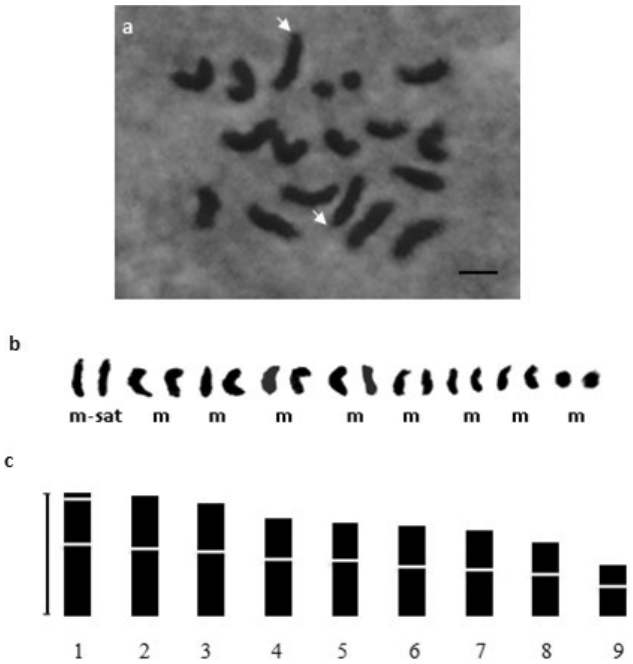

Figure 3. Karyotype of *Trifolium subterraneum* L. in Algeria. (a) Somatic metaphasis (2n=18, population 23/10); (b) Karyogram; (c) Idiogram; arrow (satellites). Bar: 2µm.

The values of the asymmetry index Ias% (Arano and Saito, 1980), the ratio between the largest and the smallest chromosome pairs (R), and the interchromosomal index A2 (Romero Zarko 2006) gives indications on the evolution of chromosomes in plants. The results of the three parameters [(R1: 1.75, R3 =1.78), (I1as% = 54.48, I3as% = 55.81), and (A2 (1) = 0.14, A2(3) = 0.19)] (Table 2 and 4) are weak and indicate that the karyotype (2n=16m) is very symmetrical for the size and the form. It is therefore primitive. Nevertheless, although the asymmetry indices are low (I2as%: 56.69, I4as% 55.07) in the populations (2n = 18), they showed a karyotype with more or less uniform sizes except for the ninth pair. This is reflected by relatively high values of the ratio (R) and interchromosomal asymmetry A2, compared to those found for the karyotype (2n = 16) (Table 3 and 5).

Meiosis analysis

The study of meiotic behaviour showed that the nine natural populations of the species *Trifolium subterraneum* exhibit normal and regular meiosis, with dominance of bivalents at the diakinesis, metaphases I and

Table 3. Morphometric data within the population 23/10 (2n=18) of *Trifolium subterraneum* L. in Algeria.

Ch p	L (µm) (±SD)	S (µm) (±SD)	TL (µm)	RL ‰	d	r	Ci %	Ct
1	1.45 (0.17)	1.05 (0.14)	2.50	146.23	0.40	1,38	42.06	m-sat
2	1.39 (0.13)	1.02 (0.16)	2.41	140.86	0.37	1,37	42.27	M
3	1.33 (0.11)	0.93 (0.08)	2.26	132.46	0.39	1,42	41.31	M
4	1.09 (0.32)	0.89 (0.08)	1.98	116.14	0.20	1,23	44.84	M
5	1.07 (0.25)	0.80 (0.22)	1.87	109.50	0.27	1,33	42.97	M
6	1,01 (0.24)	0.81 (0.19)	1.82	106.51	0.21	1,26	44.30	M
7	0.92 (0.25)	0.81 (0.19)	1.73	101.41	0.11	1,13	46.86	M
8	0.85 (0.30)	0.63 (0.04)	1.48	86.93	0,21	1,34	42.77	M
9	0.57 (0.24)	0.45 (0.15)	1.02	59.96	0.11	1,25	44.42	M
	I2as%=56.69	ΣTL=17.08	TLG=1.90	R2=2.45	$A_{2(2)}$=0.25			

Table 4. Morphometric data within the population 25/10 (2n=16) of *Trifolium subterraneum* L. in Algeria.

Ch p	L (µm) (±SD)	S (µm) (±SD)	TL (µm)	RL ‰	d	r	Ci %	Ct
1	1.14 (0.23)	0.91 (0.02)	2.05	159.96	0.22	1.24	44.57	m-sat
2	1.12 (0.10)	0.82 (0.01)	1.94	151.56	0.31	1.37	42.14	M
3	0.96 (0.09)	0.80 (0.01)	1.76	137.50	0.16	1.20	45.60	M
4	0.99 (0.01)	0.73 (0.02)	1.72	134.38	0.26	1.35	42.30	M
5	0.83 (0.06)	0.67 (0.02)	1.50	117.00	0.16	1.24	44.50	M
6	0.80 (0.02)	0.61 (0.15)	1.41	110.16	0.19	1.31	43.09	M
7	0.73 (0.06)	0.56 (0.20)	1.29	100.78	0.17	1.30	43.41	M
8	0.60 (0.17)	0.56 (0.18)	1.15	90.04	0.04	1.08	48.16	M
	I3as%=55.81	ΣTL=12.82	TLG=1.6	R3=1.78	$A_{2(3)}$=0.19			

Table 5. Morphometric data within the population 26/10 (2n=18) of *Trifolium subterraneum* L. in Algeria.

Ch p	L (µm) (±SD)	S (µm) (±SD)	TL (µm)	RL‰	d	r	Ci %	Ct
1	1.36 (0.49)	1.25 (0.36)	2.61	160.10	0.11	1.09	47.94	m-sat
2	1.22 (0.43)	1.04 (0.41)	2.26	138.20	0.18	1.17	46.01	M
3	1.25 (0.58)	0.90 (0.33)	2.15	131.45	0.35	1.38	41.96	M
4	1.14 (0.50)	0.85 (0.39)	1.99	121.50	0.29	1.34	42.75	M
5	1.00 (0.52)	0.75 (0.43)	1.75	107.40	0.25	1.33	42.94	M
6	0.91 (0.38)	0.70 (0.28)	1.61	98.97	0.21	1.30	43.50	M
7	0.82 (0.16)	0.68 (0.23)	1.50	92.08	0.14	1.20	45.42	M
8	0.77 (0.30)	0.71 (0.25)	1.48	90.55	0.06	1.09	47.88	M
9	0.56 (0.05)	0.47 (0.02)	1.03	62.48	0.09	1.20	45.15	M
	I4as%=55.07	ΣTL=16.38	TLG=1.82	R4=2.54	$A_{2\ (4)}$=0.26			

Ch p: chromosome pair, L: long arm, S: short arm, LT: total length of chromosome, LR (‰) : relative length, d : long arm - short arm ; r : long arm / short arm, Ic : centromeric index, Ct : chromosome type, Ias% : asymmetry index, R : longest / shortest pair, **Σ**TL : total lenght of diploid set, TLG : average of total length, A2: interchromosomal asymmetry index, (SD) : standard deviation, sat: satellites.

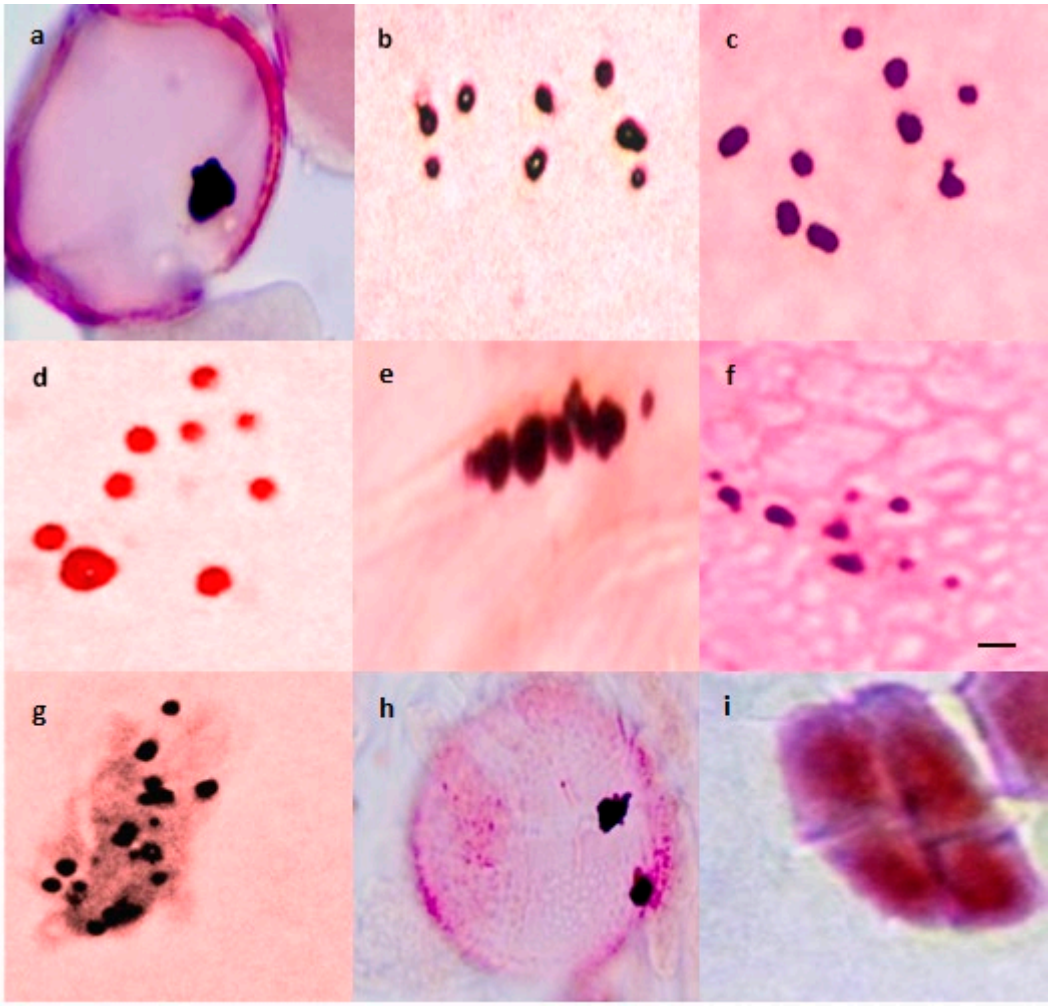

Figure 4. Pollen meiosis in some natural populations of *Trifolium subterraneum* L. in Algeria L. (a) pollen cell ; (b) Diakinesis (population 22/10, n=x=8) ; (c) Diakinesis (22/10, n=x=9) ; (d) Diakinesis (population 23/10, n=x=8) ; (e) Metaphase I (population 23/10, n=x=8) ; (f) Metaphase I (population 23/10 n=x=9) ; (g) Anaphase I ; (h) Telophase I ; (i) Tetrade. Bar: 2 µm.

anaphases I (Figure 4). This allowed us to authenticate the basic haploid number (x = 8) for the populations (12/10; 13/10; 19/10; 20/10; 33/10). Likewise, it confirms the presence of the two chromosome numbers (2n = 16 and 18) detected in mitosis, within the four populations (22/10; 23/10; 25/10; 26/10), through the appearance of two basic haploid numbers (x = 8) and (x = 9).

DISCUSSION

In this study, the chromosome numbers, karyogram, idiogram and karyotype asymmetry of naturel populations of *Trifolium subterraneum*, were determined. Mitotic metaphases showed both the same chromosome number (2n=16) in all studied populations. This number was previously reported by several authors within different ecotypes and varieties from several areas (Senn 1938; Angelo 1975, 1977, 1983; Zohary and Heller 1984; Hezamzadeh Hijazi and Ziaeinasab 2006; Vizintin et al. 2006; Falistocco et al. 1987; Falistocco et al. 2013), considering x=8, as being the ancestral basic chromosome number of the species. Meanwhile, four populations presented two numbers of chromosome (2n=16 and 18) within the cells of the same individual, and also in different individuals of the same population.

The number of chromosomes, as one of the genetic variations, is extremely variable ranging from low numbers to relatively high numbers (Eroğlu and Per 2016). A change in the basic chromosome number of a species represents dysploidy (Yakovlev 1996). According to the same author, this change can occur either in the direction of an increase (ascending dysploidy) or a decrease (downward dysploidy). In plants, this last case seems to be the most frequent, it results from the simultaneous or successive action of several cytogenetic mechanisms (robertsonian translocation, deletion …) (Yakovlev 1996).

Contandriopoulos (1978) reports 2n = 30, 32 and 34 for *Sideritis libanotica* Labill. This author notes that dysploidy still seems anarchic and has not succeeded to form populations with stable karyotypes having their own geographical distribution and a particular morphological differentiation. In such case, according to the same author, it would seem more judicious to speak about hyper and hypoaneuploidy. Aneuploidy may present the beginning of the mechanism leading to dysploidy, provided that the individuals carrying the aneuploid number are able to multiply then impose itself in the population (Contandriopoulos 1978).

Yakovlev (1996) considers that a variable chromosome number within the same population is both an aneuploidy and dysploidy phenomenon, witch is difficult to draw the line between these two phenomena, especially when it is polyploid taxa. An Intra-specific dysploidy represents a transitional step towards a definitive change in the basic chromosome number (Yakovlev 1996). The populations in which such change has occurred and fixed represent, well probably, the direct ancestors of future dysploïde species (Yakovlev 1996).

In the genus *Trifolium*, many variations of the nombre de chromosomes (2n = 16, 14, 12, and 10) characterize different diploid species, and in some instances cytological variants occur within the same species (Falistocco et al. 2013).

Brock (1953) counted two different chromosome numbers (2n = 12 and 16) in the species *Trifolium subterraneum* growing in various regions. This author suggested that the difference could be the result of a chromosomal rearrangement without loss of genetic material.

In the same genus, two basic numbers (X = 8 and 9) were highlighted within the populations of two species of *Trifolium: T. ornithopodiodes* from the British Isles (Rutland 1941; Muñoz-Rodríguez 1995), and also in *T. montanum* var. *montanum.* of Iberian Peninsula (Bleier 1925a; Muñoz-Rodríguez 1995). Issolah and Abdelguerfi (1999b), evenly showed the presence of two basic chromosomes numbers (x = 5 and 6) in the Algerian populations of *Trifolium scabrum*.

According to Pritchard (1969) and Zohary and Heller (1984), the dysploidy is consistently linked to the annual species, and are most common within sections that are at a more advanced stage of evolution, such as *Trifolium* and *Tricocephalum*, in which all the four basic numbers (x =8,7,6 and 5) may be found. Uslu (2012) has shown that taxa in the *Trifolium* section, growing in Turkey, have three numbers (x = 6, 7 and 8).

Within the tribe *Trifolieae*, Darlington and Jamaki (1945) and Darlington and Wylie (1945) reported three basic numbers (x = 7, 8, and 9). The last basic number (x = 9) was detected in Europe in *Trigonella ornithopodiodes* L. (DC) (Darlington and Wylie 1945). This species was reclassified later, for taxonomic reasons, in the *Trifolium* genus (Allen and Allen 1981).

Within the *Fabaceae* family, several cases, observing more than one basic chromosome number, have been reported in different genera including *Onobrychis*, with x = 7 and x= 8 (Hejazi et al. 2010, Arslan et al. 2012) and *Genista* where the most common number of chromosomes is 2n = 48, with the exception of the aneuploid number (2n = 44) revealed in *Genista ovina* (Bacchetta et al. 2012). The same process was detected in species of the genus *Hedysarum*, among which, *H. pallidum* (2n = 16 and 18) (Benhizia et al. 2003); *H. coronarium* (2n =

16 and 2n = 18) (Issolah et al. 2006) and *H. perrauderianum* (2n = 32 and 18) (Benhizia et al. 2013).

In the *Poaceae* family, dysploidy was observed in *Lygeum spartum* L., whose cytogenetic study revealed two basic chromosome numbers, in two Algerian populations of different origins (2n = 16 and 40) (Abddaim-Boughanmi et al. 2009). According to the same authors, the population (2n = 40), also presented a variability of the chromosome number within the same individual.

Yakovlev et al. (2017) have shown that constitutive heterochromatin, DNA GC rich and rRNA are involved in chromosomal rearrangements during the change in basic chromosome numbers in Mediterranean species of the genus *Reichardia* Roth. (*Asteraceae*). These species are characterized by three basic chromosome numbers (x = 9, 8 and 7), which have contributed to the evolution of the genus in the Mediterranean region (Yakovlev et al. 2017).

Concerning chromosome size, our results (1.02-3.1µm) seem to be relatively inferior to those found by Falistocco et al. (2013) on Italian accessions of *Trifolium subterraneum* (2.5-3.5µm). But then, this size appears to be very similar to that recorded in *T. lappaceum* species of Iran (3.03 µm), but smaller than the sizes reported in other *Trifolium* species of Iran (*T. angustifolium:* 14.56 µm, *T. leucanthum:* 12.32 µm, *T. tumens:* 11.09 µm) (Alimardani et al. 2014). Our data are also close to those found within some *Trifolium* species in Turkey, such as *T. echinatum* (1.41-2.74 µm) and *T. phleoides* (1.73-2.78 µm) (Uslu 2012), and appear to be superior to those recorded by kiran et al. (2010) in *T. speciosum* Willd. (0.99-1.64 µm) and *T. campestris* Scherb (1.13-1.73 µm).

Within the same family (*Fabacaea*), the size of *T. subterraneum* chromosomes, found during our study, is relatively close to those reported for some species of the genera *Hedysarum*, *Astragalus* and *Asparagus* studied in Algeria (Benhizia et al. 2003 ; Issolah et al. 2006, Benhizia et al. 2013; Baaziz et al. 2014 and Boubetra et al. 2017).

Our observations highlighted satellites at the first pair of chromosomes. The presence of satellites and their location on the first chromosome pair joins the result found by Falistocco et al. (2013) on Italian accessions. According to Falistocco et al. (1987) and Falistocco et al. (2013), these satellites are present in the three subspecies of *T. subterraneum* (*subterraneum*, *brachycalycinum*, *yanniniccum*), and their size can be used for discriminating the three subspecies. The satellites are more important in *yanninicum* and medium in the other two subspecies (Falistocco et al. 1987).

In all populations, the chromosomes are median. This confirm the results of Falistocco et al. (2013) on Italian accessions, characterized also by median chromosomes, whereas, Angelo et al. (1983) have described two chromosomes types (median and submedian) for Spanish ecotypes. Moreover, two types of karyotypes were identified for the Iranian accessions: the first consists on eight median pairs; the second karyotype is composed by six median pairs and two submedian pairs (Hezamzadeh Hijazi and Ziaeinasab 2006).

Karyotype asymmetry is an important parameter in karyological studies (Eroğlu 2015). In our case, the karyotype (2n=16) of Algerian populations of *Trifolium subterraneum* is very symmetrical. This seems to be a common trait with Italian populations of *T. subterraneum* karyotype (Falistocco et al. 2013), but differs from the Iranian ones. The latter populations of *T. subterraneum* (2n = 16) are characterized by low intrachromosomal symmetry (Hezamzadeh Hijazi and Ziaeinasab 2006).

On the other hand, the karyotype of the population 2n = 18 is considered relatively symmetrical because of the high value of interchomosomal asymmetry. Thus, Muñoz-Rodríguez (1995) does not consider the karyotype of the species *Trifolium ornithopodioides* (2n=18) as asymmetrical, despite the high value of the asymmetry index A2 (0.20). The author noticed this, because of the more or less uniform sizes of the chromosome pairs, except for the first pair, which was larger than the others (Muñoz-Rodríguez 1995).

In the species *Reichardia picroides* (*Asteraceae*), Yakovlev (1986) has suggested that this is a case of secondary symmetry due to chromosomal rearrangements.

The analysis of pollen meiosis confirmed the results obtained in mitosis. At the end of these results we have found that the Algerian populations of *T. subterraneum* are characterized by two chromosomal formulas. The first, (2n = 2x = 16m) (median) usually reported by previous authors, and the second (2n = 2x = 18m) revealed for the first time in this species throughout our present work. It is important to note that the new formla (2n = 2x = 18m) is observed particularly in populations sampled from high altitude sites (800-1110 m), belonging to the same biogeographic area and characterized by a high rainfall (700-900 mm). Consequently, the variation in the chromosome number observed in the populations of this species and the appearance of a new chromosome pair seems to be influenced by these two ecological factors (altitude and rainfall).

Meanwhile, the same populations considered through our study have been the subject of previous work on the ecological characterization of the natural habitat of *T. subterraneum* in Algeria (Issolah et al. 2015). Thus, the results of this latest study have shown that the variation of the edaphic, climatic, and topographic characteristics of the origin sites of these popu-

lations influences the distribution of this species in the North-Est Algeria (Issolah et al. 2015). Significant relationships were found between altitude and rainfall and the physico-chemical parameters of the soils of these populations, and the effect of altitude was relatively more pronounced notably on the nitrogen, clay, pH and C / N ratio (Issolah et al. 2015). Abdelguerfi et al. (2006) indicate that *T. subterraneum* is more prevalent in heavily watered and moist regions. Rossiter and Collins (1988a, 1988b) and Cocks (1992) also observed greater variability of subterranean clover populations in high rainfall areas in Australia.

Various studies have shown that differences in the origin's areas of populations and the variation of the environmental factors of the natural habitat may explain the intra-specific differences. Thus, they can affect the variation of chromosome numbers, ploidy level, chromosome structure, and asymmetry of karyotype in certain species belonging to the genera: *Trifolium* (Issolah and Abdelguerfi, 1999b, Issolah 2006); *Hedysarum* (Issolah et al. 2006, Benhezia et al. 2013); *Bellevalia* and *Muscari* (Azizi et al. 2016); *Asparagus* (Boubetra et al. 2017). Environmental factors also, influenced karyotype parameters in *Aegilops* (*Poaceae*) species (Baik et al. 2017). Significant relationships were found between Altitude, total lengths chromosome set and interchromosomal asymmetry on the one hand and, on the other hand, between rainfall and intrachromosomal asymmetry (Baik et al. 2017).

According to Hayward and Breese (1993), natural habitats are rarely, if ever, uniform in space and time and can encompass several distinct micro-niches or go through large seasonal fluctuations. Although *Trifolium subterraneum* is a self-pollinating species, Allard and Adams (1969) and Hayward and Breese (1993), report that fluctuations and variation in edaphic conditions at the site of origin trigger in self-pollinated species, a disruptive selection that produces and maintains high levels of variability in wild populations.

In Italy, a relationship between many morphological characteristics and the ecological factors of the environment of origin (altitude and rainfall) has been determined in several populations of *T. subterraneum* from Sicily (Piano et al.1993, Pecetti and Piano 1998).

In a large collection of subsp. *subterraneum* germplasm of Sardinia, Piano et al. (1996, 2002) found that the level of complexity for various traits varied greatly among populations and was influenced by the climatic characteristics of the collection sites.

Within the genus *Trifolium*, interesting relationships have been found between many morphological characteristics and some ecological factors (altitude and rainfull) of the environment of origin of several spontaneous Algerian populations belonging to various species (*T. campestre*, *T. glomeratum*, *T. tomontosum*, *T. resupinatum*, *T. scrabrum*, *T. lampaceum*, *T. spumosum*) (Issolah and Abdelguerfi 1993, 1995, 2003 ; Issolah 2006). In addition, Medoukali et al. (2015), do not report any significant relationship between the morphological characteristics and the environment of origin of populations belonging to several *Trifolium* species (*T. angustifolium*, *T. lappaceum*, *T. resupinatum*, *T. tomentosum*, *T. scabrum*, *T. campestre*, *T. fragiferum*, *T. pallidum*, *T. pallescens*, *T. squarrosum*, *T. glomeratum*, *T. cherleri*, *T. stellatum*, *T. repens* and *T. spumosum*). Nevertheless, a large genetic variation of isoenzymes has been observed (Medoukali et al. 2015).

Although the species is self-pollinated with cleistogamous flowers (Katznelson and Morley 1965), there is a possibility of occasional cross breeding, and this exceptional rarefaction could be of great importance for the evolution of *T. subterraneum*. Marshall and Broué (1973) estimated the cross-pollination rate of the Australian clover populations at 0.15%. Variation released by occasional hybridization can then be fixed by selfing and made available to natural selective pressures (Cocks 1992b). According to Piano (1984), natural populations of subterranean clover were formed by clusters of several genetically distinct strains. This would probably explain the chromosomal variation observed in this study within and between populations. As a result, the different populations of *T.subterrarenum* would have been crossed.

Meanwhile, four populations from the same region exhibited the same somatic behaviour (2n = 16 and 18) (within the same individual and between different individuals) and meiotic (n = x = 8 and n = x = 9). These populations would probably be evolved in time, since they belong to a species of the "*Trichocephaleum*" section considered**,** according to Zohary and Heller (1984), as the most evolved section compared to other sections of the genus *Trifolium*. This section is therefore composed of species, whose interaction, with the various ecological characteristics of the natural habitat, would affect the chromosomal rearrangements and evolutionary trends of the populations within *T. subterraneum* species.

CONCLUSION

This study permitted to identify and analyse the intraspecific diversity of the chromosome numbers and karyotypes within nine natural populations of *Trifolium subterraneum,* originating from the different areas of the north eastern Algeria. Two chromosome numbers

are distinguished in this species: 2n=16 (x=8) and 2n=18 (x=9). The first number (2n=16), is widely detected by previous authors, while the second one (2n=18) is newly observed in algerian populations of this species. The latter number (2n=18) is frequently met in populations coming from the high altitude areas. The ecological conditions of the origin's environment of the populations would have an effect on the changes in the genetic and karyological structure, particularly the altitude factor. This karyological approach provides new information that will help researchers to elucidate and complete the systematics and the nature of diversity within *Trifolium subterraneum* species. However, thorough investigations of the morphological and molecular aspects of these natural populations would be necessary, to determine the limits of dysploidy. Furthermore, comparative analysis with other populations from different origins would help to understand more about the genome evolution process of *T. subterraneum* populations in their environment of origin. This would permit to valorize and develop this plant genetic resource in the Mediterranean area, especially in Algeria.

REFERENCES

Allen O N, Allen E.K.1981. *The leguminoseae*, Macmillon.C.O, London.

Abdeddaim-Boughanmi k and Kaid-Harche M. 2009. Structure, ultrastructure of the Anther pollen microsporogenesis and morphology of pollen grains of two populations of *Lygeum spartum* L. in Algeria**.** Americ J. Agric. and Biol Sci. 4 (3) 201-205.

Abdelguerfi A, AbdelguerfI–Laouar M, M'hammedi Bouzina M, Guittonneau GG, Huguet T, Abbas K, Mebarkia A, Aouani M E and Madani T. 2006. Distribution et écologie de quelques Fabaceae spontanées d'intérêt pastoral et / ou fourrager en Algérie. Workshop international sur la Diversité des fabacées fourragères et de leurs symbiotes : Applications biotechnologiques, agronomiques et environnementales. Alger, 19-22 Février 2006: 27-36.

Alimardani F, Torabi S, Naghavi R, Ebrahimi A. 2014. Study of cytological among some *Trifolium* species of Iran. Interciencia. 39 (4) 147– 151.

Allard RW. 1965. Genetic systems associated with colonizing ability in predominantly self-pollinated species. In: Baker H.G. and Stebbins G.L. (Eds), Proc. First International Union of Biological Sciences Symp. Academic Press, New York, pp. 49– 75.

Allard RW, Adams J. 1969. Population studies in predominantly self-pollinating species. XII. Intergenotypic competition and population structure in barley and wheat. Am. Nat. 103: 621– 645.

Angulo MD, Sanchez de Rivera A.M. 1975. Studies on *Trifolium subterraneum* ecotypes. Cytologia, 40: 415–423.

Angulo MD, Sanchez de Rivera.1977. Comparative chromosomal study of Spanich ecotyes and Autralien cultivars of *Trifolium Subterraneum* L. Cytologia 42: 473-482.

Angulo MD, Sanchez de Rivera.1983. Karyological studies on spanich taxa of *Trifolium subterraneum* L. Cytologia 48: 305-312.

Arano H, Saito H. 1980. Cytological studies in family Umbelliferae.V. Karyotypes of seven species in subtribe *Seselinae*. Chromosoma. 2 (17): 471–480.

Arslan E, Ertuğrul K, Tugay O, Dural H. 2012. Karyological studies of the genus Onobrychis Mill. and the related genera *Hedysarum* L. and Sartoria Boiss. & Heldr. (*Fabaceae, Hedysareae*) from Turkey. Caryologia. 65 (1): 11–17.

AxioVision 1999- 2009. By Carl Zeiss. Release 4.8.1.

Azizi N, Amirouche R, Amirouche N. 2016. Karyological investigations and new chromosome number reports in *Bellevalia* Lapeyrouse, 1808 and *Muscari* Miller 1758 (*Asparagaceae*) from Algeria. Comp Cytogen 10: 171-187. doi : 10.3897/CompCytogen.v10i1.6445.

Bacchetta G, Brullo S, Velari TC, Chiapella LF, Kosovel V. 2012. Analysis of the Genista ephedroides group (*Fabaceae*) based on karyological, molecular and morphological data. Caryologia. 65(1):47–61.

Baaziz K, Benamara-Bellagha M, Pustahija F, Brown CS, Siljak-Yakovlev S, Khalfallah N. 2014. First karyotype analysis, physical rDNA mapping and genome size assessment in four North African *Astragalus* taxa (Fabaceae). Turkish J. Bot., 38: 1248–1258. doi: 10.3906/bot-1405-40.

Baik N, Maamri F, Bandou H. 2017. Karylogical styd y and meiotic analysis of four species of *Aegilops* (*Poaceae*) in Algeria. Carylologia.70 (4) : 324-337. Doi.org/10.1080/00087114.2017.1387340.

Benhizia H, Benhizia Y, Ghernoub L, Siljak-Yakovlev S, Khalfallah N. 2013. Meiotic behaviour and karyotype features of endangered endemic fodder species *Hedysarum perrauderianum* (*Fabaceae*) in some populations from Algeria.Caryologia _Firenze. doi: 10.1080/00087114.2013.821838.

Benhizia H, Rached-Mosbah O, Benhizia Y, Kouachi A, KhalfallahN. 2003. Etude cytogenetique d'*Hedysarum pallidum* Desf. Espece endemique Nord-africaine, tolerante a l'antimoine. Universite de Constantine. Sciences et Technologie C. 20: 7–13.

Boubetra K, Amirouche N, Amirouche R. 2017. Comparative morphological and cytogenetic study of

five *Asparagus* (*Asparagaceae*) species from Algeria including the endemic *A. altissimus* Munby. Turk J Bot. 41: 588-599. doi: 10.3906/bot-1612-63

Bleier, H. 1925 b. Chromosomenzahlen und Kern volumina in der Gattung *Trifolium. Ber.* Deutsch Bot. Ges. 43(5): 236-238.

Britten E. 1963. Chromosome number in the genus *Trifolium*. Cytologia, 28: 428-449.

Brock RD.1953. Species formation in *Trifolium subterraneum*. Nature, 171:939. doi 10.1038/171939a0. PMID: 13054785.

Cocks, P.S. 1992b. Evolution in sown populations of subterranean clover (*Trifolium subterraneum* L.) in South Australia. Aust. J. Agric. Res. 43:1583–1595.

Contandriopoulos J. 1978. Contribution à l'étude cytotaxinomique des *Sideritis* section *Empedoclea (Labiatae)*. Plant Syst. Evol. 129(4): 277-289.

Darlington CD, Janaki Ammal, E.K. 1945. Chromosome Atlas of cultivated plants. Allen and Unwin, London.

Darlington CD, Wylie AP. 1945. Chromosome Atlas for flowring plants, George Allen and Unwin Ltd., London.

Dyer AF. 1963. The use of lactopropionic orcein in rapid squash methods for chromosome preparations. Stain. Technol. 38: 85–90.

Ellison NW, Liston A, Steiner JJ, Williams WM, Taylor NL. 2006. Molecular phylogenetics of the clover genus (*Trifolium–Leguminosae*), Mol. Phylogenet. Evol. 39 (2): 688-705.

Eroğlu HE. 2015. Which chromosomes are subtelocentric or acrocentric? A new karyotype symmetry/asymmetry index. Caryologia. 68: 239- 245.

Eroğlu HE, Per S. 2016. Karyotype analysis of *Zygoribatula cognata* (Oudemans) (Acari: Oribatida: *Oribatulidae*). *Turk Entomol. Derg.* 40: 33-38.

Excel 2007. Windows 8. Microsoft office.

Falistocco E, Piccirilli M, Falcinelli M. 1987. Cytotaxonomy of *Trifolium subterraneum* L. Caryologia. 40: 123–130.

Falistocco E, Marconi G, Falcinelli M. 2013. Comparative cytogenetic study on *Trifolium subterraneum* (2n = 16) and *Trifolium israeliticum* (2n = 12). Genome 56: 307–313.

Gillett J M, Taylor NL. 2001. The World of Clovers. Iowa State University Press, Ames, Iowa, USA.

Gladstones JS, Collins WJ.1983. Subterranean clover as a naturalized plant in Australia. J. Aust. Inst. Agric. Sci. 49: 191–202.

Hayward MD, Breese EL. 1993. Population structure and variability. In: Hayward M.D., Bosemark N.O. and Romagosa I. (Eds), Plant breeding. Principles and Prospects. Chapman & Hall, London, pp. 16–29

Hezamzadeh Hijazi S M, Ziaeinasab M. 2006. Karyological study on some of species *of Trifolium* Genus in Iran. *Iran. J. of Biol.* 19 (3): 299 - 313.

Hejazi H, Mohsen S, Nasab MZ. 2010. Cytotaxonomy of some *Onobrychis* (*Fabaceae*) species and populations in Iran. Caryologia. 63(1):18–31.

Hutton EM, Peak JW. 1954. The Effect of autotetraploidy in five varieties of subterranean clover (*Trifolium subterraneum* L.) J.agrc .Res. 5: 356-364.

Issolah R, Abdelguerfi A. 1999 a. Variability within 31 spontaneous populations of *Trifolium scabrum* L., nature of relations with factors of the site of origin. Cahiers options méditerranéennes, 39: 123-127.

Issolah R, Abdelguerfi A. 1999b. Chromosome numbers within some spontaneous populations of *Trifolium* species in Algeria. *Caryologia,* 52: 151-154.

Issolah R. 2006. Synthese de travaux réalises sur des populations algeriennes de plusieurs espèces du genre *Trifolium* L. Workshop international « Diversité des Fabacees fourrageres et de leurs symbiotes : Applications Biotechnologiques, Agronomiques et Environnementales ». Alger, Algérie. 19-22 Février 2006: 81-83.

Issolah R, Benhizia H, Khalfallah N. 2006. Karyotype variation within some natural populations of Sulla (*Hedysarum coronarium* L., Fabaceae) in Algeria. Genet Resourc Crop. Evol. 53(8):1653– 1664.

Issolah R, Khalfallah N. 2007. Analysis of the morpho-physiological variation within some Algerian populations of Sulla (*Hedysarum coronarium* L.; *Fabaceae*). J. Biol. Sci., 7: 1082-1091.

Issolah R, Tahar A, Derbal N, Zidoun F, Ait Meziane MZ, Oussadi A, Dehiles I, Bradai R, Ailane M, Terki N, Aziez F, Zouahra, A, Djellal L. 2012. Caracterisation ecologique de l'habitat naturel du Sulla (*Fabaceae*) dans le Nord-Est de l'Algérie. *Rev. Ecol. (Terre et Vie)*, 67: 295-304.

Issolah R, Bouazza L, Tahar A, Terki N, Dehiles I, Mansour B, Nagoudi T. 2015. Caracterisation ecologique de l'habitat naturel du trefle souterrain (*Trifolium subterraneum* L., *Fabaceae*) dans le Nord- Est de l'Algerie. Rev. Ecol., 70: 182-193.

Issolah R, Tahar A, Sadi S, Adjebi M, Alane F, Chelling-Siziani, Lebied M. 2016. Analysis of the behaviour and the chemical composition within populations of *Trifolium subterraneum* L. J.Biol.Sci., 16: 148-154. doi:10.3923/jb.2016.148.154.

Jahier J, Chevre AM, Delourme R, Eber F, Tangay AM. 1992. Techniques de cytogénétique végétale. INRA. Paris, pp. 1-184.

Kiran Y, Sahin A, Turkoglu I, Kursat M, Emre I. 2010. Karyology of seven *Trifolium* L. taxa growing in Turkey. Acta Biologica Cracoviensia Series Botanica, 52: 81-85.

Kliphuis E. 1962. Chromosome numbers of some annual *Trifolium* species, occuring in the Netherlands. Acta Bot. Neerland 11: 90-92.

Katznelson J. 1974. Biological flora of Israel. 5. The subterranean clovers of *Trifolium* subsect. *Calycomorphum* Katzn. *Trifolium subterraneum* L. (sensu lato). Isr J Bot 23: 69-108.

Katznelson J, Morley F. 1965 a. Speciation processus in *Trifolium suberraneum* L. Israel J. Bot. 14:15-35.

Levan A, Freda K, Sandberg AA 1964. Nomenclature for centromeric position on chromosomes. Hereditas. 52: 201-220.

Marshall DR, Broue´ P. 1973. Outcrossing rates in Australian populations of subterranean clover. Aust. J. Agric. Res. 24: 863–867.

Masson P. 1997. Des prairies de très longue durée avec des espèces annuelles à ressemis spontané : les pâtures à trèfle souterrain. *Fourrages*, 153: 139-146.

Medoukali I, Bellil I, Khelifi D. 2015. Evaluation of Genetic Variability in Algerian Clover (*Trifolium* L.) Based on Morphological and Isozyme markers. *Czech J. Genet. Plant Breed.* 51(2): 50–61.

Muñoz-Rodríguez AF. 1995. *Trifolium* sect. *Paramesus* and Sect. *Trifoliastrum* in the Iberian Peninsula II. Karyological study. Stud Bot. 14:103–128.

Pecetti L, Piano E. 1998. Leaf size variation in subterranean clover (*Trifolium subterraneum* L. sensu lato). Gene.Res.crop. Evol. 45: 161–165

Pecetti L, Piano E. 2002. Variation of morphological and adaptive traits in subterranean clover populations from Sardinia (Italy). Gene.Res.crop. Evol. 00:0-1.

Piano E. 1984. Preliminary observations on the structure and variability of Sardinia populations of subterranean clover. Genet. Agr. 38: 75–90.

Piano E, Spanu F, Pecetti L. 1993. Structure and variation of subterranean clover populations from Sicily, Italy. Euphytica 68: 43–51.

Piano E, Pecetti L. 1996. Selecting subterranean clover varieties for Mediterranean environments in Italy. In: Parente G., Frame J. and Orsi S. (Eds), Grassland and land use system. Proc 16th EGF Meet. ERSA, Gorizia, pp. 283–286.

Piluzza G, Pecetti L, Bullitta S, Piano E. 2005. Discrimination among subterranean clover (*Trifolium subterraneum* L. complex) genotypes using RAPD markers. Genetic Resources and Crop Evolution 52, 193–199.

Pritchard A J. 1969. Chromosome numbers in some species of *Trifolium*. Austral. J. Agric. Res. 20: 883- 887.

Quezel P, Santa S. 1962. Nouvelle flore de l'Algerie et des régions desertiques meridionales. Tome I. Ed. CNRS, France.

Rossiter RC, Collins WJ. 1988 a. Genetic diversity in old subterranean clover (*Trifolium subterraneum* L.) populations in Western Australia. 1. Pastures sown initially to the Dwalganup strain. Aust. J. Agric. Res. 39: 1051–1062.

Rossiter RC, Collins WJ. 1988 b. Genetic diversity in old subterranean clover (*Trifolium subterraneum* L.) populations in Western Australia. 2. Pastures sown initially to the Mount Barker strain. Aust. J. Agric. Res. 39: 1063–1074.

Romero Zarco C. 1986. A new method for estimating karyotype asymmetry. Taxon 35:526-530.

Rutland J.P. 1941. The menton catalogue. A list of chromosome numbers of British plants. Suppl. 1. New Phytol. 40: 210.

Senn HA. 1938. Chromosome number relationship in the *Leguminosae*. Biblioth. Genet. 7: 175- 336. Siljak-Yakovlev S 1996. La dysploïdie et l'évolution du caryotype. Bocconea. 5: 211–220.

Siljak-Yakovlev S, Godelle B, Zoldos V, Vallès J, Garnatje T , Hidalgo O.2017. Evolutionary implications of heterochromatin and rDNA in chromosome number and genome size changes during dysploidy: A case stydy in *Reichardia* genus. Plosone 12(8): e0182318. doi.org/ 10.1371/ journal. Pone .0182318.

Singh R J. 2018. Practical manual on plant cytogenetics. CRC Press, Boca Raton, Boca Raton, FL 33487-2742 © 2018 by Taylor & Francis Group, LLC, pp 1-347.

Taylor NL. (*Editor*). 1985. Clovers around the world. *In* Clover science and technology. American Society of Agronomy, Madison, Wisc. pp. 1–6.

Uslu E. 2012. Karyology of nine *Trifolium* L. taxa from Turkey. Caryologia. 65(4): 304–310.

Vizintin L, Javornik B, and Bohanec B. 2006. Genetic characterization of selected 15 *Trifolium* species as revealed by nuclear DNA content and ITS rDNA region analysis, 16 Plant. Sci. 170: 859-866.

Yates JJ, Brittan NH. 1952. Cytological studies of subterranean clover (*Trifolium subterraneum* L.). Aust. J. Agric. Res. **3**: 300–304. doi: 10.1071/ AR9520300.

Weselxen H. 1928. Chromosome number and morphology in *Trifolium*. Univ .of Calif. Publ. Agric. Sci.2: 255-376.

Zohary D, Katznelson J. 1958. Two species of subterranean clover in Israel. Aust. J. Bot. 6: 177–182. doi: 10.1071/BT9580177.

Zohary M, Heller D. 1984. The genus *Trifolium*. Israel Academy of Sciences and Humanities. Jerusalem. pp. 1-606.

Caryologia
International Journal of Cytology, Cytosystematics and Cytogenetics

Firenze University Press
www.fupress.com/caryologia

OPEN ACCESS

Citation: C.F. Crane (2019) Megagametophyte Differentiation in *Zephyranthes drummondii* D. Don and *Zephyranthes chlorosolen* (Herb.) D. Dietr. (Amaryllidaceae). *Caryologia* 72(4): 105-119. doi: 10.13128/caryologia-670

Published: December 23, 2019

Data Availability Statement: All relevant data are within the paper and its Supporting Information files.

Competing Interests: The Author(s) declare(s) no conflict of interest.

Megagametophyte Differentiation in *Zephyranthes drummondii* D. Don and *Zephyranthes chlorosolen* (Herb.) D. Dietr. (Amaryllidaceae)

Charles F. Crane

USDA-ARS Crop Production and Pest Control Research Unit, West Lafayette, IN 47907 and Department of Botany and Plant Pathology, Purdue University
*Corresponding author: Charles.Crane@ars.usda.gov; ccrane@purdue.edu

Abstract. Megagametophyte differentiation was examined in cleared ovules from emergent buds and open flowers of *Zephyranthes drummondii* D. Don and *Z. chlorosolen* (Herb.) D. Dietr., two highly apomictic species that exhibit the *Antennaria* type of megasporogenesis and hemigamy. Stages from binucleate megagametophytes through early endosperm divisions were sampled. A large central vacuole appears after the megasporocyte divides mitotically, and this vacuole persists until the endosperm becomes cellular. Upon cellularization of the egg and antipodal apparati, a central column of cytoplasm develops longitudinally across the central vacuole, and both polar nuclei move into it before moving in unison to the chalazal end. The mature megagametophyte is organized conventionally, with one egg, two synergid, two polar nuclei, and three antipodal cells. Endosperm development is helobial, but there are few divisions in the chalazal chamber of the endosperm. The behavior of fertilized and unfertilized ovules was also studied in response to pollination. Although synergids degenerate autonomously, pollination accelerates synergid degeneration in unfertilized as well as fertilized ovules relative to unpollinated flowers of the same age. Tabulation of numerical abnormalities suggests that progressive imprinting is involved in megagametophyte differentiation; the data do not support a strictly zonal specification of nuclear fate, but instead a role for nuclear polarization before mitotic divisions. This study demonstrated the value of cleared ovules in gathering statistically and temporally meaningful observations of megagametophyte differentiation, relating in particular to the movement of polar nuclei and the response of the megagametophyte to pollination.

Keywords. Megagametophyte, embryo sac, apomixis, hemigamy, polar nuclei.

INTRODUCTION

Zephyranthes drummondii D. Don and *Z. chlorosolen* (Herb.) D. Dietr. are two congeneric amaryllid species that share apomictic reproduction and a flowering response to rainfall, hence the common name "rain lilies". The buds differentiate within the bulb for several months and then emerge

in response to wetting of the roots. The flowers open at sunset, most frequently on the fourth day following rainfall. The flowers remain open for one or two days, depending on temperature. In nature, self-pollination usually occurs soon after the anthers dehisce inside the bud at mid-morning on the day of anthesis. The incongruous combination of large, showy, sweetly scented flowers and self-pollination has motivated several studies of reproduction in these species and the related *Habranthus tubispathus* (L'Her.) Traub (Pace, 1913; Brown, 1951; Coe, 1953). These studies indicate obligate apomixis by mitotic megasporogenesis, i.e., the *Antennaria* type (first described in *Antennaria alpina* (L.) Gaertn. by Juel, 1900), and hemigamy (synonym: semigamy; Battaglia, 1945), which is development of the zygote after plasmogamy but without fusion of egg and sperm nuclei within the cytoplasm of the egg cell. Various details of the stages from the free-nuclear embryo sacs through fertilization remain to be documented, such as the path taken by the polar nuclei to reach the chalazal end of the central cell and whether the central cell experiences triple fusion to initiate the endosperm.

Many apomictic species require pollination for seed set, but the mechanisms vary. In *Potentilla* (Gustafsson, 1946, p. 31), the embryo can begin to develop autonomously in unpollinated flowers, and a sperm nucleus fertilizes only the central cell, thus initiating endosperm development. The exact fate of the other sperm nucleus is rarely known; in the *Ranunculus auricomus* species complex it has been reported also to fertilize the central cell frequently (Nogler, 1972), leading to expectedly 6n endosperm with the 2:1 maternal to paternal genome ratio usually found in sexually produced endosperm. Facultative double fertilization of the central cell has also been indicated with flow cytometry in apomictic *Crataegus* (Talent and Dickinson, 2007). In most apomictic panicoid and eragrostoid Poaceae (Brown and Emery, 1957; Voight and Bashaw, 1972), there is but one polar nucleus, and fusion with only one sperm would produce the 2:1 maternal:paternal ratio. Nevertheless, Bashaw and Hanna (1990) reported frequently observing a sperm in the central cell of the panicoid grass *Cenchrus ciliaris* L., but none near the egg, possibly indicating that both sperms usually enter the central cell but only one fuses with the lone polar nucleus. In most species with nucellar (adventitious) embryos, such as apomicts in the genus *Citrus*, the megagametophyte is reduced and sexual fertilization is more or less unaffected; the nucellar embryos then outcompete the sexually produced embryo (Gustafsson, 1946, p. 35; Nygren, 1967, p. 559). As defined above, nearly obligate hemigamy is known in nature only in certain species of *Rudbeckia* (Asteraceae; Battaglia, 1945) and *Habranthus* and *Zephyranthes* (sister genera in the Amaryllidaceae). Also, a dominant, incompletely penetrant hemigamous mutant *Se* has been recovered in cotton (Turcotte and Feaster, 1969); unlike hemigamy in *Zephyranthes*, it readily produces maternal haploid, paternal haploid, and hybrid sectors in chimeric embryos or maternal-paternal twin embryos. Similar behavior has been observed at ca. 1% frequency in wild-type *Theobroma cacao*, where it has been exploited as a source of haploids (Lanaud, 1988).

In contrast to broadly descriptive classical studies, modern research (mostly in *Arabidopsis*) has taken advantage of a battery of transposon insertion mutants, a finished genome sequence, fluorescent reporter molecules, and informatic tools, to accumulate a body of concepts and literature dealing with signaling and gene interactions during fertilization in sexual species (Zhou and Dresselhaus, 2019). No form of apomictic reproduction is understood in comparable detail, although apomictic behaviors can spur insights into aspects of sexual reproduction. For example, the facultative double fertilization of the central cell in *Crataegus* (Talent and Dickinson, 2007) suggests that the polar nuclei briefly remain attractive or receptive to a second sperm nucleus after fusing with the first one, that the central cell can attract both sperm nuclei, and that the egg more strongly attracts one and only one sperm nucleus (else triploids and haploids result); once framed, all three of these hypotheses can be tested experimentally in an amenable species. Unfortunately, to date there apparently is no reported *Arabidopsis* mutant that exactly duplicates the hemigamous behavior seen in *Zephyranthes*.

Previous embryological studies of apomictic *Zephyranthes* and *Habranthus* (Pace, 1913; Brown, 1951; Coe, 1953) have produced limited evidence about megasporogenesis, because this stage occurs within the bulb where the bud length is not visible without destroying the plant and each plant produces zero to five buds per year. The evidence in favor of the *Antennaria* type is mostly negative: dyads expected from first-meiotic restitution (the *Taraxacum* type) or complete omission of the first meiotic division (the *Blumea* type [Chennaveeriah and Patil, 1971] or the syndrome in *Elymus rectisetus* (Nees in Lehm.) A. Love et Connor [Crane and Carman, 1987]) have not been observed, while enlarging, vacuolate, undivided megasporocytes are frequent. The positive evidence is a single image of a mitotic metaphase in an enlarged, vacuolate megasporocyte in *Habranthus tubispathus* (Brown, 1951). Indirect evidence is the occurrence of the ordinary, monosporic *Polygonum* type in sexual *Zephyranthes candida* (Ao et al., 2016), which militates against the occurrence of the *Ixeris* type (mei-

otic first-division restitution in the tetrasporic *Fritillaria* type) in *Zephyranthes*. The present study took advantage of the readily accessible later stages in bud development to understand the maturation of the megagametophyte in two apomictic species of *Zephyranthes*, with particular interest in three processes shared with related sexual species: the movements of polar nuclei, the senescence of the megagametophyte with and without fertilization, and the regulation of nuclear fates as the megagametophyte matures. These are universal aspects of angiosperm reproduction that are easily observed in apomictic *Zephyranthes*.

MATERIALS AND METHODS

The ovules of maturing flowers in *Zephyranthes* are particularly suited for clearing studies. At this stage, the ovules are easily removed from the ovary before fixation, and the cleared ovules are readily pipetted onto a microscope slide. The ovules are flat and thus present the embryo sac in sagittal optical section. The embryo sac is very large and thus the egg apparatus and polar nuclei are not close to the plane of overlying and underlying nucellar cells. The nucellus is free of birefringent calcium oxalate crystals at the stages examined, facilitating differential interference-contrast microscopy. Finally, the refractive index of methyl salicylate is close to optimal to resolve nuclei and yet see through many cell layers, which has not been the case in other species like *Nothoscordum bivalve* (L.) Britton in N.L.Britton & A.Brown (Crane, 1978) and *Elymus rectisetus* (Nees) A.Love & Connor (Crane and Carman, 1987).

Flowers were examined in *Z. drummondii* D. Don and *Z. chlorosolen* (Herb.) D. Dietr. at stages from emergence from the bulb through 48 hours post-anthesis. *Zephyranthes drummondii* was collected from two sites in Austin, Texas: at the intersection of 27th Street and Speedway, and at a hilltop on the east side of Interstate 35 just south of its interchange with U.S. 183. *Zephyranthes chlorosolen* was collected along the entrance ramp of U.S. 183 onto southbound Interstate 35. Excised ovules of both species were fixed overnight in FPA50, which is 37% formalin: glacial propionic acid: 50% ethanol, 1:1:18 v:v:v (Herr, 1971), and dehydrated through 70%, 95%, and absolute ethanol. The ovules were infiltrated with methyl salicylate in three steps: 2:1 absolute ethanol: methyl salicylate, 1:2 absolute ethanol: methyl salicylate, and pure methyl salicylate. The dehydration and infiltration steps were minimally one hour. Ovules were viewed under differential interference contrast (Nomarski) as whole mounts in methyl salicylate with cover slips at the side to support an overlying cover slip. Variations of this method have been used subsequently by Young et al. (1979), Stelly et al. (1984), and Zeng et al. (2007); a recent application appeared in Kwiatkowska et al. (2019).

Buds of *Z. drummondii* were collected during the spring of 1976 at stages from emergence through early endosperm development. Buds of *Z. chlorosolen* were collected in triplicate in seven specific groups from 7 July 1976 through 10 July 1976 after rainfall on 4 July 1976, in order to survey development in pollinated and unpollinated flowers before, during, and shortly after the usual time of self-pollination. The *Z. chlorosolen* groups are detailed in Table 1 (below). All the flowers in the first six rows of Table 1 were emasculated at sunset one or two days before opening. Pollinations were performed within an hour with pollen from opening flowers elsewhere in the population. The stigma was removed from unpollinated flowers to prevent pollination. The stigma was slightly exserted above the anthers in the three flowers of the seventh row in Table 1, and these flowers were self-pollinated upon anthesis. After a delay of 48 to 72

Table 1. Batches of *Z. chlorosolen* flowers used in this study.

Code[a]	Emasculation date	Pollination status	Date of anthesis	Date picked	Age relative to anthesis when picked
-2e+72	7 July	Unpollinated	9 July	10 July	+1 day
-2pol+72	7 July	Pollinated	9 July	10 July	+1 day
-1e+48	7 July	Unpollinated	8 July	9 July	+1 day
-1pol+48	7 July	Pollinated	8 July	9 July	+1 day
-1e+72	7 July	Unpollinated	8 July	10 July	+2 days
-1pol+72	7 July	Pollinated	8 July	10 July	+2 days
0pol+48	8 July	Pollinated	8 July	10 July	+2 days

[a]Codes consist of number of days relative to anthesis (0, -1, -2), pollination status (pollinated or emasculated and unpollinated, and the approximate number of hours after pollination or emasculation when the flower was picked for fixation.

hours, picked flowers were brought indoors, with ovule excision and fixation commencing immediately for the first flower processed. The other two flowers per treatment were held at 4C until earlier flowers had been processed. About 30 of the 50 to 80 total ovules were randomly sampled per flower.

Mature embryo sacs of *Z. chlorosolen* were classified as normal or abnormal on the basis of nuclear and cell count. A normal embryo sac consisted of one egg, two synergids, three antipodals, and a binucleate central cell whose nuclei ultimately fused. Abnormal embryo sacs differed in count, usually as a result of non-division of a nucleus at an earlier stage. Synergids were classified as having a filiform apparatus, which usually coincided with a micropylar-end position of their nucleus and a chalazal-end vacuole. The egg did not have a filiform apparatus and had a chalazal or lateral nuclear position and a micropylar-end vacuole. Free nuclei in the central cell were classified as polar nuclei. Sometimes the antipodal cells resembled a second egg apparatus in nuclear and vacuolar positions, such that one antipodal had a nucleus closer to a polar nucleus. Abnormalities were tabulated in an attempt to discern if there was a pattern of successive determination of nuclear fates. Synergid and egg degeneration were also followed in relation to ageing and pollination. Degeneration was indicated by cytoplasmic collapse, nuclear shrinkage, and general loss of visible cellular content.

RESULTS

Gametophytic maturation in Zephyranthes drummondii

Most fertile ovules had reached the four-nucleate stage as the bud emerged from the neck of the bulb at the soil surface, but a few were still binucleate. The embryo sac was discoid at this stage, and its micropylar end directly abutted the nucellar epidermis. There was a large central vacuole, which persisted throughout further development until the endosperm cellularized in fertilized ovules. A tapering cytoplasmic strand, narrowest at the middle, traverses the vacuole after the first mitosis, but this strand disappears before the second mitosis. A prominent hypostase was fully developed at the chalazal end of the ovule, and it persisted well into endosperm development.

Four-nucleate embryo sacs (Fig. 1A) and eight-nucleate embryo sacs lacked any visible cytoplasmic strands that span the central vacuole. In most ovules, the last mitosis occurred on the third day before flower opening. Mitosis at the chalazal end of a four-nucleate embryo sac was observed to precede mitosis at the micropylar end,

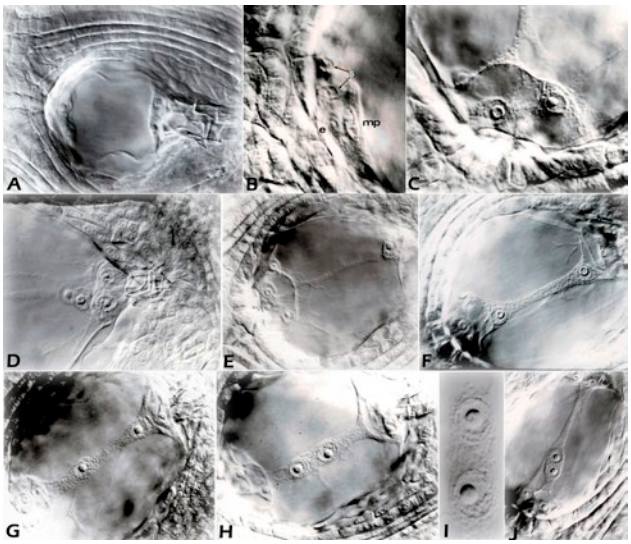

Figure 1. Early development and migration of polar nuclei in *Z. drummondii*. The micropylar end is to the left or down in each picture. A. Tetranucleate embryo sac with nuclei side by side at each end. B. Flattened nuclei soon after telophase at the micropylar end, indicating orthogonal spindles; e, predicted egg nucleus; mp, predicted micropylar polar nucleus; s, predicted synergids, based on frequently occurring positions in the mature egg apparatus. C. More mature, fully cellular egg apparatus with egg nucleus (at left) unusually close to the micropylar end of the egg cell. The filiform apparatus of a synergid (right) appears feltlike or fibrillar. D. Mature antipodal apparatus in contact with the hypostase, whose walls are thickened and birefringent. The migrated but unfused polar nuclei lie immediately to the left. E. Inception of the central column. There are also smaller, variously oriented cytoplasmic strands that appear (with light microscopy) to have intruded into a previously uninterrupted central vacuole. The egg apparatus of this embryo sac appeared in C. F. The central column has reached full thickness. G. The micropylar polar nucleus has entered the central column first. H. Both polar nuclei have entered the central column. I. Striations between the approaching polar nuclei are possibly cytoskeletal elements. J. The polar nuclei can meet near the egg apparatus, or move there temporarily after meeting at the center.

but it is not known if this is generally the case. The post-telophase daughter nuclei at the micropylar end already occupied the positions expected of nuclei in the egg apparatus (Fig. 1B), and their flattened shape indicated that the two mitotic spindles had been perpendicular to each other. The prospective egg nucleus and micropylar polar nucleus were already larger than the prospective synergid nuclei on the second day before flower opening. Meanwhile, the divisions at the chalazal end of the embryo sac were more difficult to see because of the thick, birefringent walls of the hypostase and the presence of up to 20 cell layers in the light path. Nevertheless, the last mitotic spindles there appeared to be mutually perpendicular as they were at the micropylar end,

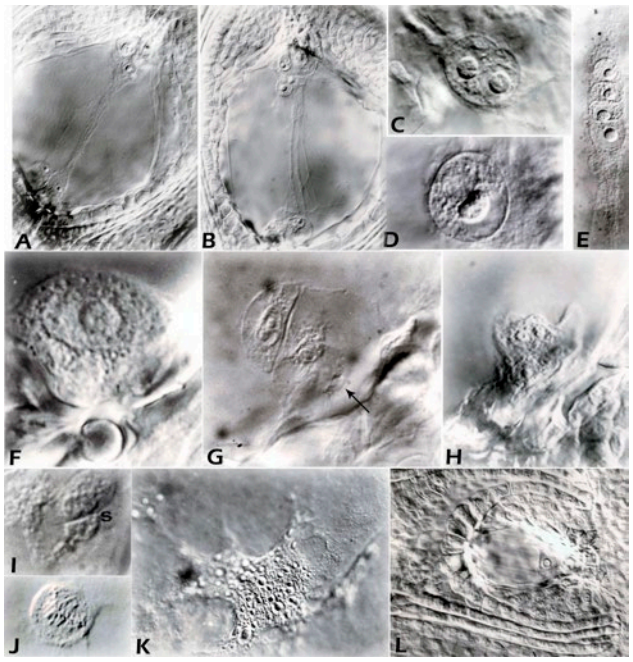

Figure 2. Later development in *Z. drummondii*, except J, which is from *Habranthus robustus* pollinated with *Z. macrosiphon*. A, B. Dissipation of the central column, which splits into parallel strands. C. Appressed polar nuclei next to antipodals. D. Completely fused polar nuclei with fused nucleoli. E. Persistent central column in abnormal embryo sac with four polar nuclei and no synergids. F. Egg cell during or shortly after plasmogamy with a sperm cell. G. Bicellular embryo; one of two sperm-derived daughter nuclei (arrow) lies below the maternal nucleus in *cb*. H. Zygote shrinkage or degeneration. I. Both sperm-derived nuclei (s) have been walled off from *cb* in the same embryo as G. J. Intranuclear metaphase of endosperm nucleus in the micropylar chamber of the helobial endosperm. K. Highly endopolyploid, multinucleolate nucleus in failing endosperm. L. Sterile ovule with uninucleate embryo sac whose nucleus resembles a polar nucleus and occupies the chalazal position of migrated polar nuclei.

and a candidate chalazal polar nucleus was evident farthest from the hypostase before cellularization.

Cellularization occurred by the day before flower opening. The filiform apparatus began to develop (Fig. 1C) in the synergids. The egg nucleolus developed a nucleolar vacuole (Fig. 1C). After cellularization, one of the antipodal nuclei was larger than the other two (Fig. 1D), just as the egg nucleus was larger than the synergid nuclei, and this distinction was even more evident in unfertilized ovules post-anthesis.

The polar nuclei migrated on the day before opening, after the initial cellularization of the egg and antipodal apparati. Before migration, both polar nucleoli had formed a nucleolar vacuole. Thin strands of cytoplasm began to intrude into the central cell vacuole (Fig. 1E), and the central strand soon spanned the vacuole. The central strand continued to thicken and developed a granular appearance (Fig. 1F). The polar nuclei migrated into the central strand; in Fig. 1G the micropylar nucleus has moved first. The polar nuclei approached each other in the strand (Fig. 1H), and faint striations indicated the presence of cytoskeletal elements (microtubules and/or microfilaments) between them (Fig. 1I). Although the polar nuclei could meet relatively near the egg apparatus (Fig. 1J), they finally moved in unison to the chalazal end of the central cell (Fig. 1D). Then the central cytoplasmic strand began to separate into separate strands and disappear (Figs. 2A and 2B; also Fig. 1D) on the day of flower opening. Over time the polar nuclei became appressed (Fig. 2C) and then fused, as indicated by fusion of their nucleoli (Fig. 2D). In one abnormal case with extra polar nuclei in lieu of synergids, all four polar nuclei became trapped within the middle of the central strand and maintained their distinctness through three days past flower opening (Fig. 2E). The abnormality with four trapped polar nuclei was seen several times also in cleared ovules of *Hippeastrum xjohnsoni* (*H. reginae* (L.) Herb. x *H. vittatum* (L'Her.) Herb.).

Fertilization occurred on the second day post-opening. Figure 2F possibly depicts plasmogamy of the egg and sperm cells. Later on the smaller sperm nucleus was visible within the egg, and it could divide before being walled off from cb of the bicellular embryo (Figs. 2G and 2I). Some eggs partially collapsed after plasmogamy (Fig. 2H), but most maintained an expanded, semicircular shape leading to elongation toward the chalaza. The initial division plane was usually transverse. The pollen tube was sometimes visible. In one ovule that had been punctured during excision and handling, where the surrounding synergid debris had been lost, there was an apparent pore at the hooked pollen tube tip where sperms had been released.

Karyogamy appeared to be necessary for endosperm development. In one abnormal instance, karyogamy was incomplete on the tenth day after floral opening, and the partially decondensed, distended sperm nucleus was still appressed to the polar fusion nucleus, which had not divided. In another ovule, the sperm and polar fusion nucleus were close to each other, and both were degenerating. Further evidence for the necessity of karyogamy in hemigamous *Zephyranthes* and *Habranthus* comes from the results of interspecific pollinations, which often result in an increased frequency of endosperm failure and empty seeds. In *H. tubispathus* x *Z. candida* (Lindl.) Herb., for example, all the seeds were empty in spite of seed setting of more than 95%. The primary endosperm nucleus divided transversely and thus produced a small chalazal cell covering the antipodals and a far larger

micropylar cell containing the rest of the volume of the central cell. Free-nuclear divisions ensued in both cells, but no more than five nuclei were observed in the chalazal cell. Abundant free-nuclear mitoses in the micropylar cell resulted in a multinucleate shell that laid down cell walls centripetally as it began to fill in the central vacuole. The first mitoses in the micropylar cell were synchronized and resulted in 2, 4, 8, 16, or 32 nuclei at a time before synchrony broke down, whereas mitoses in the chalazal cell were not synchronized. The early endosperm nuclei were large enough to hold an entire spindle apparatus within the old nuclear membrane (Fig. 2J). The nuclei of mature, fully cellular endosperms were smaller and spherical. Lobate, multinucleolate endosperm nuclei sometimes appeared, but they seemed to be associated with endosperm failure. They appeared to be under traction by attached spindle fibers (Fig. 2K; this example is from *Habranthus robustus* Herb. ex Sweet pollinated with *Z. carinata* Herb.).

The fate of unfertilized embryo sacs was also examined. Neither the egg nucleus nor the fused polar nuclei ever divided. Both synergids usually degenerated one or two days before the egg did. The degenerating egg apparatus lost evident vacuoles as the nuclei faded out. The cytoplasm collapsed, i.e., the egg shrank and its boundary became crenulate. The antipodals degenerated at the about same time as the synergids, and they could be crushed by proliferating nucellar cells near the incompressible hypostase. The central cell nucleus was usually the last nucleus to degenerate in the embryo sac.

From five to 20% of the ovules were sterile, lacking a mature embryo sac. Although both integuments were of normal size, the nucellus was smaller. Sterile ovules fell into four main types: those with a uninucleate embryo sac in a hypodermal position, those with a slightly enlarged megasporocyte in a hypodermal or subhypodermal position, those with no enlarged cells at all, and those with the megasporocyte surrounded by thickened cell walls within the hypostase. Sterile ovules were most frequent toward the base of the ovary, but they could occur anywhere. Figure 2L shows a uninucleate embryo sac with an enlarged nucleus and prominent nucleolar vacuole.

Pollination response and senescence in Zephyranthes chlorosolen

The experimental layout appears in Table 1. Observations centered on timing of fertilization relative to pollination, synergid degeneration, sequence of degeneration of cells in unfertilized embryo sacs, timing of first division in the egg versus the endosperm, frequency of spermatic division in the egg, and numerically abnormal embryo sacs. In total, 796 ovules were examined. They were classified as unfertilized normal, fertilized normal, unfertilized abnormal, or sacless, depending on presence of an embryo sac, number of components in the embryo sac, and evidence of fertilization such as dividing endosperm or presence of a pollen tube at the micropyle or presence of a sperm nucleus within the egg. There were 524 unfertilized normal, 122 fertilized normal, 63 unfertilized abnormal, and 87 sacless ovules in all. Table 2 gives the numbers of instances for all conditions of embryo sacs and their components versus treatment. Supplemental Table 1 gives the same information divided among the 21 individual flowers sampled.

No embryo or endosperm developed in emasculated, unpollinated flowers. Pollen tubes reached the ovules about 48 hours after pollination, but their growth rate depended on the time of pollination, and their arrival continued over a period of many hours. Thus in the "Egg" rows of Table 2, most of the fertilizations occurred between 48 and 72 hours after pollination in buds pollinated the day before natural anthesis, whereas most of the fertilizations had occurred less than 48 hours after pollination in flowers pollinated upon opening. No pollen tubes reached the ovules after pollination two days before opening. In spite of the slower growth rate, pollen tubes reached the ovules sooner after early pollination, as evidenced by the presence of multicellular embryos only after early pollination. At the times sampled, 110 ovules had received one pollen tube, seven had received two, and one had received three; the number was not noted or pollen tubes were not seen in the other evidently fertilized ovules. If only the early pollinated buds collected 72 hours later are considered, these totals became 65, two, and one. When more than one pollen tube had reached an ovule, they followed different paths toward the embryo sac. No instances of two sperm nuclei were seen in undivided egg cells.

The synergids degenerated in both fertilized and unfertilized ovules, but pollination accelerated degeneration (Table 2, "Synergid" rows). At least one of the synergids had begun to degenerate in every fertilized embryo sac, whereas both synergids were intact in a substantial minority of embryo sacs in unpollinated flowers of the same age. Synergids were more degenerated in the unfertilized ovules of pollinated flowers than they were in unpollinated flowers. Although the two synergids generally did not degenerate exactly synchronously, the combination of intact and fully degenerated synergids was relatively uncommon and appeared mostly in fertilized ovules. The independence of degeneration was tested with the chi-squared test. For ovules collected from

Table 2. Classification of *Z. chlorosolen* embryo sacs and their components, merged by time of emasculation, pollination, and collection.

Treatment[a]	-2e	-2pol	-1e	-1pol	-1e	-1pol	0pol			
Hours post	72	72	48	48	72	72	48			
Unfertilized	96	91	94	91	96	22	33			
Fertilized	0	0	0	6	0	70	47			
Abnormal	9	8	15	4	3	7	17			
Sacless	8	13	12	3	9	10	32			
Total	113	112	121	104	108	109	129			
Frac.abnorm.[b]	0.08	0.071	0.124	0.038	0.028	0.064	0.132			
Frac.sacless	0.071	0.116	0.099	0.029	0.083	0.092	0.248			
Frac.(ab+sa)	0.15	0.188	0.223	0.067	0.111	0.156	0.38			
	unf	unf	unf	unf	fert	unf	unf	fert	unf	fert
Egg										
OK	95	89	87	83	5	91	20	59	33	47
Embryo	0	0	0	0	0	0	0	8	0	0
Deging	1	0	2	5	1	4	1	3	0	0
Deg	0	2	5	3	0	1	1	0	0	0
Synergids										
OK-OK	22	16	19	16	0	10	4	0	0	0
OK-+/-OK	4	4	11	8	0	6	2	0	3	0
OK-deging	10	2	2	4	0	7	0	1	1	3
OK-deg	9	13	4	2	0	3	0	9	1	11
+/-OK-+/-OK	3	5	17	11	0	7	0	0	2	1
+/-OK-deging	5	6	6	8	1	5	1	1	4	1
+/-OK-deg	9	7	10	14	2	12	2	9	1	5
Deging-deging	9	10	3	4	0	11	5	2	6	2
Deging-deg	8	4	7	8	1	16	0	14	8	9
Deg-deg	17	24	15	16	2	19	8	34	7	15
Polar nuclei										
OOP	5	8	0	1	0	0	0	0	0	1
Deging	9	10	2	3	0	11	0	1	3	6
Ch appress	63	54	69	69	3	12	2	0	4	7
Ch fusing	14	11	19	13	2	28	6	5	10	5
Ch fused	5	5	4	4	1	45	14	9	15	17
Mult. PEN	0	0	0	0	0	0	0	3	0	5
>=2 endosp	0	0	0	0	0	0	0	50	0	6
1 mc + 1 ch	0	3	0	1	0	0	0	1	1	0
Antipodals										
3: all OK	75	72	59	68	4	47	12	18	9	13
3: all+/-OK	5	1	3	2	0	7	1	7	1	2
3: all deging	2	0	1	2	0	2	3	9	5	4
3: all deg	1	1	0	0	0	3	2	16	4	13
2+/-OK 1deging	3	6	7	7	0	11	3	4	5	4
1+/-OK 2deging	3	1	5	2	0	11	1	9	2	2
5 any	0	1	0	2	0	0	0	0	0	0
4 any	3	4	3	2	1	2	0	1	0	1
2 any	3	3	14	5	0	8	0	3	5	4
1 any	1	0	1	1	1	5	0	3	2	3
none seen	0	2	1	0	0	0	0	0	0	1
Code										
UUUU	16	13	11	9	0	6	3	0	0	0
UDUU	59	56	50	55	5	44	9	13	10	13

Treatment[a]	-2e	-2pol	-1e	-1pol	-1e	-1pol	0pol			
UDUD	9	7	19	11	0	28	7	51	20	27
UDDU	1	7	2	0	0	2	0	0	1	0
UDDD	4	1	0	0	0	7	0	2	1	6
UUUD	2	2	4	5	0	3	1	0	0	0
UUDU	2	1	1	2	0	0	0	0	0	0
UUDD	2	0	0	1	0	1	0	0	1	0
DDUU	1	2	4	8	1	3	0	2	0	0
DUUU	0	0	3	0	0	0	0	0	0	0
DDUD	0	0	0	0	0	2	2	1	0	0

[a]Treatment and "hours post" refer to pollination versus emasculation and the number of hours after either when picked. [b]Left column abbreviations are: Frac.sacless, fraction of all ovules that lacked an embryo sac; Frac.abnorm, fraction of all embryo sacs that were abnormal; Frac.(ab+sa), sum of Frac.sacless and Frac.abnorm.; deg, degenerated; deging, degeneration in progress; OK, intact; OOP, out of position; ch, chalazal; mc, micropylar; mult. PEN, multinucleolate primary endosperm nucleus; appress, appressed; any, any condition. The UD codes follow a system given in the Results section in reference to Table 2.

unpollinated flowers 24 hours after natural opening (the first and third columns of Table 2, "Synergid" rows), there were 76 in which neither synergid had greatly degenerated, 55 in which only one synergid had degenerated, and 59 where both had degenerated. This gave a probability of 0.5447 of not having degenerated versus 0.4553 of having degenerated. If degeneration occurred at random, one would expect 56.373 with neither synergid degenerated, 94.241 with one degenerated, and 39.387 with both degenerated. The resulting chi-squared value was 32.94 with two degrees of freedom, and thus the synergids did not degenerate independently.

The polar nuclei had failed to migrate in six embryo sacs, and they were out of their usual chalazal-end position in 15 more embryo sacs (Table 2, "Polar nuclei" rows). Eighteen of these instances occurred in flowers emasculated two days before opening, even though the flowers were collected at the same age as those emasculated one day before opening. Most polar nuclei were appressed at 24 hours after natural opening. While the polar nuclei were aligned along the long axis of the embryo sac during migration, they assumed other alignments upon reaching the chalazal end, and about a 20:4 ratio of perpendicular to parallel alignments was observed relative to the long axis. Most polar nuclei had begun to fuse or had completely fused, as indicated by complete fusion of their nucleoli, at 48 hours past natural opening. Pollination accelerated nuclear and nucleolar fusion of polar nuclei in both fertilized and unfertilized ovules. The primary endosperm nucleus developed multiple nucleoli before dividing. The large number of multinucleate endosperms after pollination one day early further indicated the earlier time of fertilization in that group.

One or two extra antipodal cells occurred in 18 embryo sacs, but the divisions that produced them were not seen (Table 2, "Antipodal" rows). Fertilization, especially endosperm development, accelerated antipodal degeneration. The unfertilized ovules of pollinated flowers also had more degenerated antipodals than did ovules in unpollinated flowers of the same age. Asynchronous degeneration was more likely to be observed in unpollinated flowers.

The condition of each embryo sac was encoded in Table 2 in four letters, all either U for intact or D for degenerating and degenerated. The letters respectively denoted the egg, synergids, polar nuclei, and antipodals, and any instance of degeneration merited a "D" for synergids and antipodals. Completely intact embryo sacs were most common at 24 hours past natural opening, and pollination two days early did not affect them. Later pollination accelerated synergid and antipodal degeneration. Completely intact embryo sacs were never seen in fertilized ovules, since at least one synergid had degenerated. Antipodal degeneration usually began soon after synergid degeneration had begun. In 20 ovules, the entire egg apparatus was degenerating before the polar nuclei or antipodals began to degenerate. The egg and the polar nuclei were about equally likely to be the last intact component in senescing embryo sacs. However, all possible degeneration sequences were observed multiple times.

Endosperm division clearly preceded egg division (Table 2, ninth column). The egg usually divided after at least eight nuclei existed in the micropylar chamber of the helobial endosperm. In four out of 122 fertilized ovules, the egg degenerated without dividing; this is a typical frequency of mature seeds with plump endosperm but no embryo in *Z. chlorosolen*. The number of sperm nuclei was tabulated in 83 fertilized egg cells. Three of them had experienced division of both sperm

Table 3. Component counts in numerically abnormal embryo sacs in *Z. chlorosolen*[a].

row	N	total	eggs	syn	cent mc	cent ch	antip	inf mc	inf ch
1	7	8	1	2	0	3	2	1	2
2	1	8	0	2	0	3	3	2	1
3	1	8	1	1	0	3	3	2	1
4	1	8	1	1	0	4	2	2	2
5	0	8	1	0	0	4	3	3	1
6	2	7	1	2	0	1	3	0	1
7	1	6	1	0	0	2	3	1	1
8	3	6	1	2	0	2	1	1	1
9	1	6	0	2	0	2	2	1	1
10	6	5	0	0	0	2	3	1	1
11	1	5	1	0	0	1	3	0	1
12	2	5	1	2	0	0	2	0	0
13	1	5	1	0	1	2	1	2	1
14	2	5	1	2	0	1	1	1	0
15	4	4	0	0	0	1	3	0	1
16	2	4	0	0	0	2	2	0	2
17	3	4	1	0	0	2	1	1	1
18	1	4	1	2	0	1	0	1	0
19	2	3	0	0	0	1	2	0	1
20	4	3	0	0	0	3	0	1	2
21	1	3	0	0	0	2	1	1	1
22	1	3	1	0	1	1	0	1	1
23	3	2	0	0	0	1	1	0	1
24	3	2	1	0	0	1	0	1	0
25	1	1	0	0	0	1	0	0	1

[a]syn, synergids; cent mc, free nuclei in micropylar half of the central cell; cent ch, free nuclei in chalazal half of the central cell; antip, antipodal cells; inf mc, inferred to come from the micropylar end of the central cell; inf ch, inferred to come from the chalazal end of the central cell.

and egg nuclei. The remainder contained only one sperm nucleus.

There were 63 embryo sacs that differed from the conventional organization of one egg, two synergids, two polar nuclei, and three antipodals. These are described and enumerated in Table 3, whose columns give the row number in the table, the number of instances observed, the total number of nuclei, the counts of eggs, synergids, free nuclei in the micropylar part of the central cell, free nuclei in the chalazal part of the central cell, and antipodals. Because most of the embryo sacs were examined after the polar nuclei had met and migrated into the chalazal end of the central cell, the last two columns give a best guess as to the numbers of free nuclei at each end of the central cell prior to migration. Most abnormal embryo sacs contained fewer than eight nuclei. The most common abnormalities were misdifferentiation of an antipodal nucleus as a third polar nucleus (row 1), and absence of the egg apparatus (rows 10 and 15). There were 13 embryo sacs with only one antipodal cell, and in four of these (rows 8 and 17) there appeared to be only two chalazal-end nuclei prior to cellularization. The number of functioning polar nuclei ranged from one to four; the latter occurred when both expected synergid nuclei instead became polar nuclei and behaved as in Fig. 2E. Although no instances were observed in *Z. chlorosolen*, four polar nuclei and no synergids (row 5) were seen multiple times in *Hippeastrum xjohnsonii*.

Eight embryo sacs could not be described as combinations of egg, synergids, polar nuclei, and antipodals. In the first, the antipodal nuclei were not walled off from the central cell in an otherwise normal embryo sac. Instead, they remained separate from the two fused polar nuclei. In the second and third, the synergids lacked a filiform apparatus and the polar nuclei were still separate at the ends of the central cell 24 hours after normal anthesis. In the fourth, only the cell walls of the egg apparatus persisted, and all nuclei had degenerated. In the fifth, there was but one antipodal, and it was unusually large. The two polar nuclei flanked this antipodal, and the egg apparatus had degenerated. In the sixth, a transverse partition near the micropylar end divided the sac into two cells, each with four free nuclei seemingly randomly arranged near the partition. In the seventh, the synergid and egg nuclei occupied the same, egglike cell. In the eighth, the egg nucleus had been walled off partially, but then the egg nucleus had migrated to the chalazal end of the central cell as a polar nucleus. The embryo sac was otherwise normal.

DISCUSSION

Development of the embryo sac from the megasporocyte in apomictic *Zephyranthes* is similar to development from the surviving megaspore in *Ornithogalum caudatum* (Tilton and Lersten, 1981). The biggest differences are the larger size and more discoid shape of the embryo sac and its central vacuole in *Zephyranthes*, such that the four-nucleate stage has two nuclei side-by-side at each end, rather than arranged linearly as is usual in *Ornithogalum*. A second difference is the stated movement of only the micropylar polar nucleus through the central column to the chalazal end in *Ornithogalum*, versus migration of both polar nuclei into the column in *Zephyranthes* before migration of both to the chalazal end. Otherwise, Tilton and Lersten (1981) observed the initiation, thickening, and splitting of the column

much as in *Zephyranthes*, although they did not specifically order these stages in time. Tilton and Lersten mentioned other examples of the central column from various taxa, including *Crocus*, *Hordeum*, and in general any species with helobial endosperm. They also cited the notion, from a 1902 paper by Ikeda, that at least one polar nucleus moves through the column. More recently, Zeng et al. (2007) and Hu et al. (2009) also observed in rice the migration of polar nuclei through a transient, de-novo formed cytoplasmic column, where they met at the center and then moved to the micropylar end of the central cell. Tilton and Lersten (1981) suggested that in *Ornithogalum* the second sperm nucleus might reach the fused polar nuclei via the central column, but in *Zephyranthes drummondii* this column has dissipated prior to arrival of the pollen tube at a synergid, and therefore the sperm must take some path through the peripheral cytoplasm of the central cell.

Embryo sac development in emergent buds of *Z. drummondii* and *Z. chlorosolen* is more rapid than in the related *Zephyranthes candida*, at four days in the former and up to seven days in the latter. As in *Z. drummondii*, Ao (2018) reported (on the basis of 10-µm paraffin sections) the formation of a central cytoplasmic column that spanned the central cell and conveyed the micropylar polar nucleus to the chalazal end. However, Ao (2018) reported that the column persisted until fertilization and that sometimes the polar nuclei and sperm nucleus fused within the chalazal part of it, as depicted in his Figure 2D. Ao did not distinguish a stage where both polar nuclei moved into the column and met near its midpoint. Ao (2018, 2019) also noted that the antipodal cells developed callosic walls when the polar nuclei approached them, that the antipodal cells later fused when the callose had disappeared, and that the antipodal nuclei ultimately fused into one. In contrast, in *Z. drummondii* no callose or cellular fusion was observed in the antipodal apparatus before it degenerated. Also, Ao (2019) noted a nuclear endosperm in *Z. candida*, and this in conjunction with the claimed fusion of antipodal cells and claimed increase in antipodal nuclei to nine is consistent with a misinterpretation of a helobial endosperm where the small chalazal chamber has been mistaken for fused antipodal cells.

The inception, thickening, and eventual dissipation of a central column differ markedly from the description of polar-nuclear migration in *Arabidopsis thaliana*. There the polar nuclei are depicted as traveling through a peripheral cytoplasmic shell surrounding the central vacuole, and they migrate while the egg and antipodal apparati form cell walls (Yadegari and Drews, 2004). In rice, the photographs of Zeng et al. (2007) and Hu et al. (2009) were not suitable to detect incipient cell walls, since the nuclei were stained preferentially, but it is possible that the migration began before cellularization began.

The egg apparatus appears to develop complete cell walls in *Zephyranthes*. This is supported by Fig. 1C, which is the egg apparatus from the embryo sac whose pre-migration central cell appears in Fig. 1E. A *Zephyranthes* egg cell tends to maintain its hemispherical shape even when plasmolysis pulls the central cell cytoplasm away from it, which is consistent with a rigid egg-cell wall. Also, Tilton and Lersten (1981) noted the appearance of a complete cell wall around the egg in *Ornithogalum caudatum*, but commented that the chalazal end of the wall might be reticulate at ultrastructural magnification.

Synergid degeneration appears to be autonomous in *Zephyranthes*, but pollination accelerates degeneration in unfertilized as well as fertilized ovules. Degeneration of one synergid is positively correlated with degeneration of the other synergid. Although up to three pollen tubes were observed at the micropyle, there is no evidence in this study that intact synergids attracted pollen tubes. It is possible that penetration necessarily destroyed the receiving synergid. The situation is concordant with the conclusions of Leydon et al. (2015) and cited references therein, that synergids can degenerate autonomously, that approach of a pollen tube promotes synergid degeneration, and that discharge of a pollen tube is observed only in a degenerated synergid.

The embryo-sac abnormalities observed in *Zephyranthes* are not consistent with a random assignment of function at the eight-free-nucleate stage, since combinations such as three egg cells or one synergid and three micropylar-end polar nuclei were not observed. On the other hand, there was insufficient evidence to support a rigidly progressive imprinting of nuclear fate, with consistent defaults for undivided nuclei from each of the three rounds of mitosis. For example, embryo sacs with only one synergid were rare (two out of 63 abnormals), and thus the nuclei that normally become synergid nuclei tended to share the same fate, either becoming synergids or becoming extra, functioning polar nuclei. For this reason, one might conclude that the commitment to becoming synergid nuclei has already happened at the four-nucleate stage of the embryo sac and that it is distinct from the commitment to divide. Yet the combination of no synergids and three polar nuclei was not observed, so the usual fate of an undivided synergid precursor is unclear. For another example, an undivided micropylar end nucleus (one having skipped the second and third mitotic divisions) tended to function

as a polar nucleus, moving to the chalazal end of the central cell upon cellularization. For that matter, even an undivided megasporocyte nucleus could develop the chalazal position and single, large, vacuolated nucleolus typical of migrated polar nuclei (Fig. 2L). In contrast, if the second round of mitosis were skipped, each daughter of the third round could form a polar nucleus and one of something else. Furthermore, failure to wall off one antipodal resulted in an extra free nucleus that was not observed to become appressed to or fuse with the legitimate polar nuclei. Thus very careful, systematic evaluation of a much larger sample of properly timed, abnormal embryo sacs, with attention to the filiform apparatus, nuclear position, and cellular and nucleolar vacuolization, will be needed to establish if the spectrum of abnormalities can support the inference of checkpoints and default fates in differentiating embryo sacs.

The spectrum of abnormalities varies among plant taxa. Yudakova (2009) observed a 10- to 100-fold higher frequency of extra eggs and polar nuclei in embryo sacs of the *Hieracium* type in *Poa chaixii* and *Poa pratensis* than in embryo sacs of the *Taraxacum* (or possibly *Elymus rectisetus*) type in *Poa badensis*. Yudakova (2009) also stated that, "No significant cases of extra polar nucleus formation from the synergid nuclei were recorded among numerous analyzed embryo sacs of the studied bluegrass species, while female gametophytes with additional egg cells instead of synergids occurred in all studied plants." This situation markedly contrasts with the greater frequency of expected synergid nuclei becoming extra polar nuclei in *Zephyranthes* and *Hippeastrum*. In semifertile hybrids of *indica* × *japonica* rice, Zeng et al. (2007) observed a wide range of abnormalities over stages from degenerating megaspores through mature embryo sacs. At maturity, frequent abnormalities included small size, a misplaced (lateral) egg apparatus, absence of the egg apparatus, misplaced (lateral) antipodals, and migration of polar nuclei to the chalazal end (which would be normal in *Zephyranthes*). If the egg apparatus was absent, the micropylar-end polar nucleus was either present or absent. Otherwise, Zeng et al. (2007) did not detail numerical abnormalities in the manner of Table 3.

The failure to observe multiple egg cells in *Zephyranthes* (Table 3) could reflect observational bias, since the filiform apparatus develops over time and is not always clearly visible in whole mounts, and the position of the nucleus varied from lateral to chalazal-end within egg cells. An indirect line of evidence comes from twin embryos. Spontaneous diploid-haploid twins are relatively easily found in *Lilium* (Cooper, 1940) and in grasses, where they are a source of spontaneous haploids apart from *indeterminate gametophyte* mutants. Within *Zephyranthes*, identical (maternal) twins are about 10 times more frequent in *Z. pulchella* J.G. Smith than in *Z. chlorosolen*. An extra egg would be the most facile source of such twins, although postzygotic cleavage is also possible, and experimental distinction would be difficult in an apomictic species. An extra egg could account for frequent maternal haploid production from *indeterminate gametophyte* (*ig*) mutants in maize and rice (Evans, 2007; Zhang et al., 2015), although *ig* maize also produces androgenetic haploids when used as a female parent with other maize genotypes (Kindiger and Hamann, 1993).

Yudakova (2009) followed the four-zone hypothesis of Enaleeva (2002) to account for abnormalities in *Poa* embryo sacs. From the micropylar end, the consecutive zones are synergid, egg, central, and antipodal. Yudakova (2009) conjectured that the zones were established in response to signals from adjacent nucellar cells and that each zone determined the fate of its contained nuclei. Abnormalities would arise when a free nucleus was situated out of its proper zone, and a piece of evidence for this was the prevalence of an extra egg rather than polar nucleus in place of a synergid, since the synergid and central zones are not adjacent. However, in *Zephyranthes* and *Hippeastrum* the relative abundances are reversed, with a tendency of both prospective synergid nuclei to function as extra polar nuclei. Also, in *Zephyranthes*, the egg and synergid nuclei can begin at the same distance from the micropylar extremity of the embryo sac (Fig. 1B). Furthermore, in rice (Zeng et al., 2007) and *Habranthus tubispathus* (Pace, 1913), an otherwise normal egg apparatus sometimes appears on the side of the embryo sac rather than at the micropylar end. A lateral egg apparatus would require that the zones would respond to particular cells or cell groups in the nucellus and that free nuclei would move in response to some attraction from those nucellar cells. Alternatively, a lateral egg apparatus could easily arise from a misoriented spindle of the first mitotic division, if the nuclei move only slightly thereafter.

Nuclear movement seems to occur only at particular times in the differentiation of embryo sacs, first after the division of the megasporocyte (which functions as the surviving megaspore in apomictic *Zephyranthes*), then upon migration of the polar nuclei, then upon fertilization, and finally during the first few rounds of mitosis in the developing endosperm. The nuclei appear to remain nearly stationary apart from these four episodes. The nature of the fertilization block is particularly interesting in *Zephyranthes*, since the sperm nucleus can approach within its own diameter the egg nucleus with-

out fusing with the egg nucleus. Also remarkable is how the other sperm nucleus moves or is moved across more than 100 micrometers of the peripheral cytoplasm of the central cell to reach the fused polar nuclei.

Karyogamy of the sperm and fused polar nuclei appears to be necessary for endosperm development in *Z. drummondii* and *Z. chlorosolen*, as evidenced by an invariably undivided central cell nucleus in unfertilized ovules and the similar types of endosperm failures in interspecific crosses of these species and interspecific crosses of sexual *Z. traubii* (W. Hayw.) Moldenke. However, this necessity contrasts with the situation described by Tandon and Kapoor (1962) in *Zephyranthes* cv. 'Ajax' (*Z. candida* (Lindl.) Herb. x *Z. citrina* Baker), where 4n chromosome counts were reported for 366 out of 430 endosperm metaphases after self-pollination. This suggests that hemigamy also operates in the central cell, assuming that this seed-propagatable cultivar is apomictic like its *Z. citrina* parent (Howard, 1996). Apomictic *Zephyranthes* possibly vary in their requirement for karyogamy for endosperm inception. If so, there is a very unanswered question as to how the usual maternal-paternal imprinting mechanism (endosperm balance number) is circumvented in *Z. citrina* and *Z. pulchella*. The problem merits further investigation with flow cytometry and paternal markers in all of these species.

STUDY LOCATION

The *Z. drummondii* flowers were collected at latitude 30°17'37.5"N, longitude 97°44'11.5"W (30.293736, -97.736538). The *Z. chlorosolen* flowers were collected at latitude 30°20'16.4"N, longitude 97°42'04.4"W (30.337887, -97.701208). Both populations have been destroyed by subsequent building and road construction.

ACKNOWLEDGEMENTS

I performed the experiments in partial fulfillment of the requirements for the Ph.D. degree at the University of Texas at Austin. I thank my now deceased major professor, Walter V. Brown, for stimulation and tolerance of this and related projects during my graduate research. I thank Stefan Kirchanski for suggesting methyl salicylate as a clearing agent. I thank Edwin T. Bingham, David A. Sleper, John G. Carman, David M. Stelly, and Stephen B. Goodwin for support over subsequent decades. Finally, I thank my wife, Yan M. Crane, for reformatting the photomicrographs and for her steadfast support.

DECLARATION

The author declares no conflicts of interest regarding this research.

REFERENCES

Ao, C.Q. 2019. The endosperm development and the variations of structures of embryo sacs: unraveling the low fecundity of *Zephyranthes candida* (Amaryllidaceae). Plant Biosystems. 153: 673-678.

Ao, C.Q. 2018. Double fertilization in *Zephyranthes candida*, with special notes on the second fertilization and the behavior of the primary endosperm nucleus. Phyton. 58: 135-138.

Ao, C.Q., Wang, L.Y., Sun, H., Lin, J.T., Chai, Y., and Chen, C.C. 2016. Megasporogenesis and megagametogenesis in *Zephyranthes candida* (Amaryllidaceae), with special notes on the behavior of the synergids, the central cell and the antipodal cells. Phyton. 56: 91-101.

Bashaw, E. C., and Hanna, W. W. 1990. Apomictic reproduction. In: Chapman GP, ed. *Reproductive versatility in the grasses.* Cambridge, UK: Cambridge University Press, 100–130.

Battaglia, E. 1945. Fenomeni citologici nuovi nella embriogenesi (semigamia) e nella microsporogenesi (doppio nucleo di restituzione) di *Rudbeckia laciniata* L. Nuovo Giorn. Bot. Ital. N. S. 52:34-38.

Brown, W. V. 1951. Apomixis in *Zephyranthes texana* Herb. American Journal of Botany 38: 697-702.

Brown, W. V., and Emery, W. H. P. 1957. Apomixis in the Gramineae, tribe Andropogoneae: *Themeda triandra* and *Bothrochloa ischaemum*. Botanical Gazette 118: 246-253.

Chennaveeriah, M.S., and Patil, R.M. 1971. Apomixis in *Blumea*. Phytomorphology 21: 71-76.

Coe, G. E. 1953. Cytology of reproduction in *Cooperia pedunculata*. American Journal of Botany 40: 335-343.

Cooper, D. C. 1943. Haploid-diploid twin embryos in *Lilium* and *Nicotiana*. American Journal of Botany 30(6): 408-413.

Crane, C. F. 1978. Apomixis and crossing incompatibilities in some Zephyrantheae. Ph.D. dissertation, The University of Texas at Austin.

Crane, C. F., and Carman, J. G. 1987. Mechanisms of apomixis in *Elymus rectisetus* from eastern Australia and New Zealand. American Journal of Botany. 74: 477-496.

Enaleeva, N.K. 2002. On the cytological mechanism of "normal" and "abnormal" cell differentiation in angi-

osperm megagametophytogenesis. Reproduktivnaya biologiya, genetika i selektsiya (Reproductive Biology, Genetics, and Selection). Saratov: Izd-vo un-ta, 2002, p. 47–54.

Evans, M.M.S. 2007. The indeterminate gametophyte1 gene of maize encodes a LOB domain protein required for embryo sac and leaf development. The Plant Cell. 19: 46-62.

Gustafsson, A. 1946. Apomixis in higher plants. I. The mechanism of apomixis. Lunds Universitets Arsskrift 42: 1-67.

Herr, J. M. 1971. A new clearing-squash technique for the study of ovule development in some angiosperms. American Journal of Botany. 58: 785-790.

Howard, T. 1996. Two new *Zephyranthes* species from Mexico. Herbertia. 51: 38-41.

Hu, C. Y., Zeng, Y. X., Lu, Y. G., Li, J. Q., and Liu, X. D. 2009. High embryo sac fertility and diversity of abnormal embryo sacs detected in autotetraploid indica/japonica hybrids in rice by whole-mount eosin B-staining confocal laser scanning microscopy. Plant Breeding 128: 187-192.

Juel, H.O. 1900. Vergleichende Untersuchungen über typische und parthenogenetische Fortpflanzung bei der Gattung *Antennaria*. Kongliga Svenska Vetenskaps-Akademiens Handlingar 33: 1-59.

Kindiger, B., and Hamann, S. 1993. Generation of haploids in maize: a modification of the indeterminate gametophyte (*ig*) system. Crop Science. 33: 342–344.

Kwiatkowska, M., Kadluczka, D., Wedzony, M., Dedicova, B., and Grzebelus, E. 2019.

Refinement of a clearing protocol to study crassinucellate ovules of the sugar beet (*Beta vulgaris* L., Amaranthaceae). Plant Methods 15: 71.

Lanaud, C. 1988. Origin of haploids and semigamy in *Theobroma cacao* L. Euphytica 38: 221-228.

Leydon, A., Tsukamoto, T., Dunatunga, D., Qin, Y., Johnson, M., and Palanivelu, R. 2015. Pollen tube discharge completes the process of synergid degeneration that is initiated by pollen tube-synergid interaction in *Arabidopsis*. Plant Physiology. 169: 485-496.

Nogler, G. 1972. Genetik der Aposporie by *Ranunculus auricomus* s.l. W. Koch. II. Endospermzytologie. Berichte Schweiz. Botanische Gesellschaft. 82:54-63.

Nygren, A. 1967. Apomixis in the angiosperms. In Ruhland, W., ed., Handbuch der Pflanzenphyiologie, vol. 18: 551-596.

Pace, L. 1913. Apogamy in *Atamosco*. Botanical Gazette. 56: 376-394.

Stelly, D.M., Peloquin, S.J., Palmer, R.G, and Crane, C.F. 1984. Mayer's hemalum-methyl salicylate: A stain-clearing technique for observations within whole ovules. Stain Technology 59: 155-161.

Talent, N., and Dickinson, T.A. 2007. Endosperm formation in aposporous *Crataegus* (Rosaceae, Spiraeoideae, tribe Pyreae): parallels to Ranunculaceae and Poaceae. New Phytologist 173: 231-249.

Tandon, S.L, and Kapoor, B.M. 1962. Contributions to the cytology of endosperm in some angiosperms -- I. *Zephyranthes Ajax* Sprenger. Caryologia. 15: 21-41.

Tilton, V. R., and Lersten, N. R. 1981. Ovule development in *Ornithogalum caudatum* (Liliaceae) with a review of selected papers on angiosperm reproduction. III. Nucellus and megagametophyte. New Phytologist 88: 477-504.

Turcotte, E.L, and Feaster, C.V. 1969. Semigametic production of haploids in Pima cotton. Crop Sci. 9: 653-655.

Voight, P.W., and Bashaw, E.C. 1972. Apomixis and sexuality in *Eragrostis curvula*. Crop Science 12: 843-847.

Yadegari, R., and Drews, G.N. 2004. Female gametophyte development. The Plant Cell. 16: S133-S141.

Young, B.A., Sherwood, R.T, and Bashaw, E.C. 1979. Cleared-pistil and thick-sectioning techniques for detecting aposporous apomixis in grasses. Canadian Journal of Botany. 57: 1668-1672.

Yudakova, O.I. 2009. Abnormalities of female gametophyte development in apomictic bluegrass forms. Russian Journal of Developmental Biology 40: 150–156.

Zeng, Y. X., Hu, C. Y., Lu, Y. G., Li, J. Q., and Liu, X. D. 2007. Diversity of abnormal embryo sacs in *indica/japonica* hybrids in rice demonstrated by confocal microscopy of ovaries. Plant Breeding 126: 574-580.

Zhang, J., Tang, W., Huang, Y., Niu, X., Zhao, Y., Han, Y., and Liu, Y. 2015. Down-regulation of a *LBD*-like gene, *OsIG1*, leads to occurrence of unusual double ovules and developmental abnormalities of various floral organs and megagametophyte in rice. Journal of Experimental Botany 66: 99-112.

Zhou, L.Z., and Dresselhaus, T. 2019. Friend or foe: Signaling mechanisms during double fertilization in flowering seed plants. Current Topics in Developmental Biology 131: 453-496.

Supplemental Table 1. Classification of *Z. chlorosolen* embryo sacs and their components, itemized in columns by individual flower. Codes appear as in Table 2, except FIXD, which is time of day when ovules were fixed.

COND	-2e72	-2e72	-2e72	-2p72	-2p72	-2p72	-1e48	-1e48	-1e48	-1p48	-1p48	-1p48	-1e72	-1e72	-1e72	-1p72	-1p72	-1p72	0p48	0p48	0p48								
FIXD	20:00	22:00	1:00	21:00	0:00	2:00	22:00	22:00	23:00	22:00	23:00	-	20:00	23:00	1:00	21:00	23:00	1:00	23:00	-	-								
UNFE	33	33	30	28	30	33	32	31	31	33	31	27	31	33	32	11	8	3	12	7	14								
FERT	0	0	0	0	0	0	0	0	0	0	1	5	0	0	0	21	22	27	7	23	17								
ABNO	5	3	1	5	3	0	5	6	4	0	0	4	1	2	0	1	6	0	9	4	4								
SACL	4	1	3	7	4	2	2	4	6	2	1	0	4	1	4	4	4	2	15	8	9								
TOTA	42	37	34	40	37	35	39	41	41	35	33	36	36	36	36	37	40	32	43	42	44								
FRAB	0.119	0.081	0.029	0.125	0.081	0	0.128	0.146	0.098	0	0	0.111	0.028	0.056	0	0.027	0.15	0	0.209	0.095	0.091								
FRSC	0.095	0.027	0.088	0.175	0.108	0.057	0.051	0.098	0.146	0.057	0.03	0	0.111	0.028	0.111	0.108	0.1	0.062	0.349	0.19	0.205								
FRAS	0.214	0.108	0.118	0.3	0.189	0.057	0.179	0.244	0.244	0.057	0.03	0.111	0.139	0.083	0.111	0.135	0.25	0.062	0.558	0.286	0.295								
	unf	unf	unf	unf	unf	unf	unf	unf	unf	unf	unf	fert	unf	fert	unf	unf	unf	unf	fert	unf	fert	unf	fert	unf	fert	unf	fert	unf	fert
Egg																													
INTA	33	33	29	27	29	33	30	31	26	31	29	1	23	4	29	31	31	9	18	8	21	3	20	12	7	7	23	14	17
EMBR	0	0	0	0	0	0	0	0	0	0	0	0	0	0	0	0	0	0	2	0	0	0	6	0	0	0	0	0	0
DEGI	0	0	1	0	0	0	1	0	1	2	1	0	2	1	1	2	1	1	1	0	1	0	1	0	0	0	0	0	0
DEGE	0	0	0	1	1	0	1	0	4	0	1	0	2	0	1	0	0	1	0	0	0	0	0	0	0	0	0	0	0
Synergids																													
ITIT	5	10	7	3	7	6	14	2	3	6	3	0	7	0	0	2	8	0	0	3	0	1	0	0	0	0	0	0	0
ITPI	1	3	0	1	3	0	2	5	4	5	1	0	2	0	0	4	2	1	0	1	0	0	0	2	0	0	0	1	0
ITDN	3	6	1	0	2	0	0	1	1	2	0	0	2	0	2	2	3	0	0	0	1	0	0	1	0	0	1	0	2
ITDG	0	6	3	5	4	4	0	1	3	0	0	0	2	0	1	0	2	0	0	0	7	0	2	0	2	1	7	0	2
PIPI	1	1	1	1	2	2	3	6	8	2	6	0	3	0	3	0	4	0	0	0	0	0	0	0	2	0	0	0	1
PIDN	4	1	0	6	0	0	4	2	0	3	4	0	1	1	0	3	2	1	1	0	0	0	0	3	0	0	0	1	1
PIDG	4	2	3	1	4	2	1	6	3	6	6	1	2	1	6	4	2	0	2	2	2	0	5	0	1	0	2	1	2
DNDN	6	3	0	3	3	4	1	1	1	1	0	0	3	0	3	6	2	5	1	0	0	0	1	0	1	3	1	3	0
DNDG	5	1	2	2	1	1	3	4	0	4	3	0	1	1	9	5	2	0	8	0	3	0	3	3	1	2	6	3	2
DGDG	4	0	13	6	4	14	4	3	8	4	8	0	4	2	7	7	5	4	9	2	9	2	16	1	2	1	6	5	7
Polar nuclei																													
OOPO	2	0	3	4	0	4	0	0	0	0	0	0	1	0	0	0	0	0	0	0	0	0	0	0	1	0	0	0	0
DEGI	3	5	1	4	3	3	2	0	0	2	1	0	0	0	3	6	2	0	0	0	0	0	1	2	1	1	5	0	0
CAPP	17	23	23	14	25	15	22	27	20	25	26	0	18	3	4	3	5	1	0	1	0	0	0	2	0	1	6	1	1
CFUS	7	4	3	3	2	6	7	4	8	4	3	1	6	1	11	7	10	2	0	2	4	2	1	4	0	2	1	4	4
CFUD	4	1	0	1	0	4	1	0	3	2	0	0	2	1	13	17	15	8	4	5	2	1	3	4	4	2	1	9	12
MPEN	0	0	0	0	0	0	0	0	0	0	0	0	0	0	0	0	0	0	1	0	1	0	1	0	1	0	4	0	0
END2	0	0	0	0	0	0	0	0	0	0	0	0	0	0	0	0	0	0	15	0	15	0	20	0	0	0	6	0	0
MCCH	0	0	0	2	0	1	0	0	0	0	1	0	0	0	0	0	0	0	1	0	0	0	0	0	0	1	0	0	0
Antipodals																													

3INT	24	29	22	22	22	28	17	22	20	20	26	1	22	3	16	12	19	4	2	7	11	1	5	5	1	0	4	4	8
3PIP	1	3	1	1	0	0	1	0	2	1	0	0	1	0	0	3	4	1	3	0	1	0	3	0	0	0	1	1	1
3DGN	1	0	1	0	0	0	1	0	0	1	0	0	1	0	1	1	0	2	5	1	3	0	1	4	0	0	3	1	1
3DEG	1	0	0	1	0	0	0	0	0	0	0	0	0	0	2	1	0	1	7	0	3	1	6	1	2	2	10	1	1
2PDN	1	0	2	2	1	3	2	3	2	3	3	0	1	0	6	2	3	2	1	0	0	1	3	1	1	2	1	2	2
1PDN	2	1	0	1	0	0	4	0	1	2	0	0	0	0	1	7	3	1	3	0	2	0	4	1	1	0	0	1	1
5ANY	0	0	0	0	1	0	0	0	0	1	0	0	1	0	0	0	0	0	0	0	0	0	0	0	0	0	0	0	0
4ANY	2	0	1	0	2	2	0	1	2	1	1	0	0	1	2	0	0	0	0	0	1	0	0	0	0	0	0	0	1
2ANY	0	0	3	1	2	0	5	5	4	3	1	0	1	0	3	3	2	0	0	0	1	0	2	0	0	2	3	3	1
1ANY	1	0	0	0	0	0	1	0	0	1	0	0	0	1	0	4	1	0	0	0	0	0	3	0	1	1	1	1	1
UNSE	0	0	0	0	2	0	1	0	0	0	0	0	0	0	0	0	0	0	0	0	0	0	0	0	1	0	0	0	0
Status																													
UUUU	3	8	5	2	6	5	7	2	2	1	2	0	6	0	0	1	5	0	0	3	0	0	0	0	0	0	0	0	0
UDUU	22	18	19	15	18	23	9	23	18	18	23	1	14	4	17	11	16	4	1	4	9	1	3	4	1	2	4	4	8
UDUD	5	2	2	5	1	1	7	6	6	7	3	0	1	0	9	14	5	5	19	1	11	1	21	6	4	4	14	10	9
UDDU	0	1	0	4	1	2	2	0	0	0	0	0	0	0	0	1	1	0	0	0	0	0	0	1	0	0	0	0	0
UDDD	1	2	1	0	0	1	0	0	0	0	0	0	0	0	3	3	1	0	0	0	1	0	1	0	1	1	5	0	0
UUUD	0	0	2	1	0	1	4	0	0	3	0	0	2	0	0	0	3	0	0	0	0	1	0	0	0	0	0	0	0
UUDU	0	2	0	0	1	0	1	0	0	1	1	0	0	0	0	0	0	0	0	0	0	0	0	0	0	0	0	0	0
UUDD	2	0	0	0	0	0	0	0	0	1	0	0	0	0	0	1	0	0	0	0	0	0	0	1	0	0	0	0	0
DDUU	0	0	1	1	1	0	0	0	4	2	2	0	4	1	1	1	1	0	1	0	1	0	0	0	0	0	0	0	0
DUUU	0	0	0	0	0	0	2	0	1	0	0	0	0	0	0	0	0	0	0	0	0	0	0	0	0	0	0	0	0
DDUD	0	0	0	0	0	0	0	0	0	0	0	0	0	0	1	1	0	2	0	0	0	0	1	0	0	0	0	0	0

Finito di stampare da
Logo s.r.l. – Borgoricco (PD) – Italia

OPEN ACCESS POLICY

Caryologia provides immediate open access to its content. Our publisher, Firenze University Press at the University of Florence, complies with the Budapest Open Access Initiative definition of Open Access: By "open access" , we mean the free availability on the public internet, the permission for all users to read, download, copy, distribute, print, search, or link to the full text of the articles, crawl them for indexing, pass them as data to software, or use them for any other lawful purpose, without financial, legal, or technical barriers other than those inseparable from gaining access to the internet itself. The only constraint on reproduction and distribution, and the only role for copyright in this domain is to guarantee the original authors with control over the integrity of their work and the right to be properly acknowledged and cited. We support a greater global exchange of knowledge by making the research published in our journal open to the public and reusable under the terms of a Creative Commons Attribution 4.0 International Public License (CC-BY-4.0). Furthermore, we encourage authors to post their pre-publication manuscript in institutional repositories or on their websites prior to and during the submission process and to post the Publisher's final formatted PDF version after publication without embargo. These practices benefit authors with productive exchanges as well as earlier and greater citation of published work.

PUBLICATION FREQUENCY

Papers will be published online as soon as they are accepted, and tagged with a DOI code. The final full bibliographic record for each article (initial-final page) will be released with the hard copies of *Caryologia*. Manuscripts are accepted at any time through the online submission system.

COPYRIGHT NOTICE

Authors who publish with *Caryologia* agree to the following terms:

- Authors retain the copyright and grant the journal right of first publication with the work simultaneously licensed under a Creative Commons Attribution 4.0 International Public License (CC-BY-4.0) that allows others to share the work with an acknowledgment of the work's authorship and initial publication in Caryologia.
- Authors are able to enter into separate, additional contractual arrangements for the non-exclusive distribution of the journal's published version of the work (e.g., post it to an institutional repository or publish it in a book), with an acknowledgment of its initial publication in this journal.
- Authors are permitted and encouraged to post their work online (e.g., in institutional repositories or on their website) prior to and during the submission process, as it can lead to productive exchanges, as well as earlier and greater citation of published work (See The Effect of Open Access).

PUBLICATION FEES

Open access publishing is not without costs. *Caryologia* therefore levies an article-processing charge of € 150.00 for each article accepted for publication, plus VAT or local taxes where applicable.

We routinely waive charges for authors from low-income countries. For other countries, article-processing charge waivers or discounts are granted on a case-by-case basis to authors with insufficient funds. Authors can request a waiver or discount during the submission process.

PUBLICATION ETHICS

Responsibilities of *Caryologia*'s editors, reviewers, and authors concerning publication ethics and publication malpractice are described in *Caryologia*'s Guidelines on Publication Ethics.

CORRECTIONS AND RETRACTIONS

In accordance with the generally accepted standards of scholarly publishing, *Caryologia* does not alter articles after publication: "Articles that have been published should remain extant, exact and unaltered to the maximum extent possible".

In cases of serious errors or (suspected) misconduct *Caryologia* publishes corrections and retractions (expressions of concern).

Corrections

In cases of serious errors that affect or significantly impair the reader's understanding or evaluation of the article, *Caryologia* publishes a correction note that is linked to the published article. The published article will be left unchanged.

Retractions

In accordance with the "Retraction Guidelines" by the Committee on Publication Ethics (COPE) *Caryologia* will retract a published article if:

- there is clear evidence that the findings are unreliable, either as a result of misconduct (e.g. data fabrication) or honest error (e.g. miscalculation)
- the findings have previously been published elsewhere without proper crossreferencing, permission or justification (i.e. cases of redundant publication)
- it turns out to be an act of plagiarism
- it reports unethical research.

An article is retracted by publishing a retraction notice that is linked to or replaces the retracted article. *Caryologia* will make any effort to clearly identify a retracted article as such.

If an investigation is underway that might result in the retraction of an article *Caryologia* may choose to alert readers by publishing an expression of concern.

COMPLYNG WITH ETHICS OF EXPERIMENTATION

Please ensure that all research reported in submitted papers has been conducted in an ethical and responsible manner, and is in full compliance with all relevant codes of experimentation and legislation. All papers which report in vivo experiments or clinical trials on humans or animals must include a written statement in the Methods section. This should explain that all work was conducted with the formal approval of the local human subject or animal care committees (institutional and national), and that clinical trials have been registered as legislation requires. Authors who do not have formal ethics review committees should include a statement that their study follows the principles of the Declaration of Helsinki

ARCHIVING

Caryologia and Firenze University Press are experimenting a National legal deposition and long-term digital preservation service.

ARTICLE PROCESSING CHARGES

All articles published in *Caryologia* are open access and freely available online, immediately upon publication. This is made possible by an article-processing charge (APC) that covers the range of publishing services we provide. This includes provision of online tools for editors and authors, article production and hosting, liaison with abstracting and indexing services, and customer services. The APC, payable when your manuscript is editorially accepted and before publication, is charged to either you, or your funder, institution or employer.

Open access publishing is not without costs. *Caryologia* therefore levies an article-processing charge of € 150.00 for each article accepted for publication, plus VAT or local taxes where applicable.

FREQUENTLY-ASKED QUESTIONS (FAQ)

Who is responsible for making or arranging the payment?

As the corresponding author of the manuscript you are responsible for making or arranging the payment (for instance, via your institution) upon editorial acceptance of the manuscript.

At which stage is the amount I will need to pay fixed?

The APC payable for an article is agreed as part of the manuscript submission process. The agreed charge will not change, regardless of any change to the journal's APC.

When and how do I pay?

Upon editorial acceptance of an article, the corresponding author (you) will be notified that payment is due.

We advise prompt payment as we are unable to publish accepted articles until payment has been received. Payment can be made by Invoice. Payment is due within 30 days of the manuscript receiving editorial acceptance. Receipts are available on request.

No taxes are included in this charge. If you are resident in any European Union country you have to add Value-Added Tax (VAT) at the rate applicable in the respective country. Institutions that are not based in the EU and are paying your fee on your behalf can have the VAT charge recorded under the EU reverse charge method, this means VAT does not need to be added to the invoice. Such institutions are required to supply us with their VAT registration number. If you are resident in Japan you have to add Japanese Consumption Tax (JCT) at the rate set by the Japanese government.

Can charges be waived if I lack funds?

We consider individual waiver requests for articles in Caryologia on a case-by-case basis and they may be granted in cases of lack of funds. To apply for a waiver please request one during the submission process. A decision on the waiver will normally be made within two working days. Requests made during the review process or after acceptance will not be considered.

I am from a low-income country, do I have to pay an APC?

We will provide a waiver or discount if you are based in a country which is classified by the World Bank as a low-income or a lower-middle-income economy with a gross domestic product (GDP) of less than $200bn. Please request this waiver of discount during submission.

What funding sources are available?

Many funding agencies allow the use of grants to cover APCs. An increasing number of funders and agencies strongly encourage open access publication. For more detailed information and to learn about our support service for authors.

APC waivers for substantial critiques of articles published in OA journals

Where authors are submitting a manuscript that represents a substantial critique of an article previously published in the same fully open access journal, they may apply for a waiver of the article processing charge (APC).

In order to apply for an APC waiver on these grounds, please contact the journal editorial team at the point of submission. Requests will not be considered until a manuscript has been submitted, and will be awarded at the discretion of the editor. Contact details for the journal editorial offices may be found on the journal website.

What is your APC refund policy?

Firenze University Press will refund an article processing charge (APC) if an error on our part has resulted in a failure to publish an article under the open access terms selected by the authors. This may include the failure to make an article openly available on the journal platform, or publication of an article under a different Creative Commons licence from that selected by the author(s). A refund will only be offered if these errors have not been corrected within 30 days of publication.

2019
Vol. 72 – n. 4

Caryologia

International Journal of Cytology, Cytosystematics and Cytogenetics

Table of contents

€ 25,00